ISSN 0021-9673

SHED
LY

VOL. 237 NO. 1 MARCH 5, 1982

RNAL OF

CHROMATOGRAPHY

ERNATIONAL JOURNAL ON CHROMATOGRAPHY, ELECTROPHORESIS AND RELATED METHODS

ELSEVIER SCIENTIFIC PUBLISHING COMPANY
AMSTERDAM

JOURNAL OF CHROMATOGRAPHY

Scope. The *Journal of Chromatography* publishes papers on all aspects of chromatography, electrophoresis and related methods. Contributions consist mainly of research papers dealing with chromatographic theory, instrumental development and their applications. The section *Biomedical Applications*, which is under separate editorship, deals with the following aspects: developments in and applications of chromatographic and electrophoretic techniques related to clinical diagnosis (including the publication of normal values); screening and profiling procedures with special reference to metabolic disorders; results from basic medical research with direct consequences in clinical practice; combinations of chromatographic and electrophoretic methods with other physicochemical techniques such as mass spectrometry. In *Chromatographic Reviews*, reviews on all aspects of chromatography, electrophoresis and related methods are published.

Submission of Papers. Papers in English, French and German may be submitted, in three copies. Manuscripts should be submitted to: The Editor of *Journal of Chromatography*, P.O. Box 681, 1000 AR Amsterdam, The Netherlands, or to: The Editor of *Journal of Chromatography, Biomedical Applications*, P.O. Box 681, 1000 AR Amsterdam, The Netherlands. Reviews are invited or proposed by letter to the Editors and will appear in *Chromatographic Reviews* or *Biomedical Applications*. An outline of the proposed review should first be forwarded to the Editors for preliminary discussion prior to preparation. Submission of an article is understood to imply that the article is original and unpublished and is not being considered for publication elsewhere. For copyright regulations, see below.

Subscription Orders. Subscription orders should be sent to: Elsevier Scientific Publishing Company, P.O. Box 211, 1000 AE Amsterdam, The Netherlands. The *Journal of Chromatography* and the *Biomedical Applications* section can be subscribed to separately.

Publication. The *Journal of Chromatography* (incl. *Biomedical Applications*, *Chromatographic Reviews* and *Cumulative Author and Subject Indexes*, *Vols. 221–230*, *231–240* and *241–250*) has 25 volumes in 1982. The subscription prices for 1982 are:

J. Chromatogr. (incl. *Chromatogr. Rev.* and *Cum. Indexes Vols. 221–230, 231–240 and 241–250*) + *Biomed. Appl.* (Vols. 227–251):
Dfl. 3625.00 plus Dfl. 500.00 (postage) (total *ca.* US$ 1650.00)

J. Chromatogr. (incl. *Chromatogr. Rev.* and *Cum. Indexes Vols. 231–240* and *241–250*) only (Vols. 234–251):
Dfl. 2826.00 plus Dfl. 360.00 (postage) (total *ca.* US$ 1274.50)

Biomed. Appl. (incl. *Cum. Indexes Vols. 221–230*) only (Vols. 227–233):
Dfl. 1050.00 plus Dfl. 140.00 (postage) (total *ca.* US$ 476.00).

Journals are automatically sent by air mail to the U.S.A. and Canada at no extra costs, and to Japan, Australia and New Zealand with a small additional postal charge. Back volumes of the *Journal of Chromatography* (Vols. 1 through 226) are available at Dfl. 156.00 (plus postage). Claims for issues not received should be made within three months of publication of the issue. If not, they cannot be honoured free of charge. For customers in the U.S.A. and Canada wishing additional bibliographic information on this and other Elsevier journals, please contact Elsevier Science Publishing Company Inc., Journal Information Center, 52 Vanderbilt Avenue, New York, NY 10017. Tel.: (212) 867-9040.

Abstracts/Contents Lists published in Analytical Abstracts, Biochemical Abstracts, Biological Abstracts, Chemical Abstracts, Chemical Titles, Current Contents/Physical, Chemical & Earth Sciences, Current Contents/Life Sciences, Index Medicus, and Science Citation Index.

See page 3 of cover for Publication Schedule, Information for Authors, and information on the News Section and Advertisements.

Printed in The Netherlands

VOL. 237, NO. 1 JOURNAL OF CHROMATOGRAPHY MARCH 5, 1982

CONTENTS

(Abstracts/Contents Lists published in Analytical Abstracts, Biochemical Abstracts, Biological Abstracts, Chemical Abstracts, Chemical Titles, Current Contents/Physical, Chemical & Earth Sciences, Current Contents/Life Sciences, Mass Spectrometry Bulletin, Index Medicus and Science Citation Index)

(Continued overleaf)

Contents (continued)


HAMILTON
GC Syringes
without caprices.
Series 800 and 1800
Microliter® syringes
Hamilton's 800 Series syringes and their new gas-tight versions of the 1800 Series pose none of the problems with which you are sadly familiar: plunger bending, heat transfer from hand to samples and repair of defective needles are things of the past. A special integrated stop prevents plunger blow-out in high pressure applications.
All syringe parts, including glass barrel, needles and plunger guide, are replaceable in the field.
Threaded needles as well as accessories such as reproducibility control devices, plus the well-known needles for Rheodyne and Waters injection systems, are also available.
Try one of these syringes – its performance will delight you.
Write for a copy of our special leaflet!
Hamilton Bonaduz AG,
P.O.B. 26, CH-7402 Bonaduz,
Switzerland.
HAMILTON
Switzerland
800

JOURNAL OF CHROMATOGRAPHY

VOL. 237 (1982)

JOURNAL *of* CHROMATOGRAPHY

INTERNATIONAL JOURNAL ON CHROMATOGRAPHY, ELECTROPHORESIS AND RELATED METHODS

ELSEVIER SCIENTIFIC PUBLISHING COMPANY
AMSTERDAM

J. Chromatogr., Vol. 237 (1982)

Printed in The Netherlands

Journal of Chromatography, 237 (1982) 1–14
Elsevier Scientific Publishing Company, Amsterdam — Printed in The Netherlands

CHROM. 14,410

MEASUREMENT OF DIFFUSION COEFFICIENTS BY REVERSED-FLOW GAS CHROMATOGRAPHY INSTRUMENTATION

N. A. KATSANOS* and G. KARAISKAKIS
Physical Chemistry Laboratory, University of Patras, Patras (Greece)
(First received July 7th, 1981; revised manuscript received September 28th, 1981)

SUMMARY

A method is reported for measuring mutual diffusion coefficients in gases. It is a gas chromatographic method, but not a broadening technique. Two short empty columns are placed perpendicular to one another: a diffusion column through which no carrier gas flows, and a chromatographic column. The carrier gas which flows through the latter carries over to the detector the diffusion flux established in the diffusion column. Analysis of the concentration–time curve recorded gives the value of the diffusion coefficient of an injected solute into the carrier gas. More reliable results are obtained by the so-called "chromatographic sampling", *i.e.* reversing the direction of flow of the carrier gas at definite known times. The analytical mathematical expression, describing the elution curves when the gas flow is reversed, is derived and used to determine diffusion coefficients for fifteen gas pairs. The results are of high precision, and comparison with the theoretical values shows that they have also high accuracy.

INTRODUCTION

The measurement of diffusion coefficients of a gas A into another gas B by gas chromatography has been reviewed by Maynard and Grushka[1]. It has been solely based on zone broadening by diffusion of a narrow pulse of component A (the solute) introduced into a long empty chromatographic column, through which component B continuously flows as a carrier gas. Obviously, these methods use the superposition of two fluxes in the same direction x: one diffusional flux, $-D(\partial c/\partial x)$, which is added to a much higher "chromatographic" flux, vc. This addition results in two undesirable features. First, long columns are required to make the diffusional flux manifest itself in the chromatographic signal, and second, the precision of the method is relatively low. It occurred to us that both can be improved if the two fluxes are separated by placing them perpendicular to one another, as shown schematically in Fig. 1. The component B enters at point D_2 and meets the detector at D_1, or *vice versa*, flowing continuously through the "chromatographic column" $l' + l$, either in direction F (forward) or in direction R (reverse). It does not flow, however, through the "diffusion column", length L, at the closed end of which the solute A is introduced, as a gas or vapour, in the form of a pulse (by means of a syringe or a gas valve).

0021-9673/82/0000–0000/$02.75

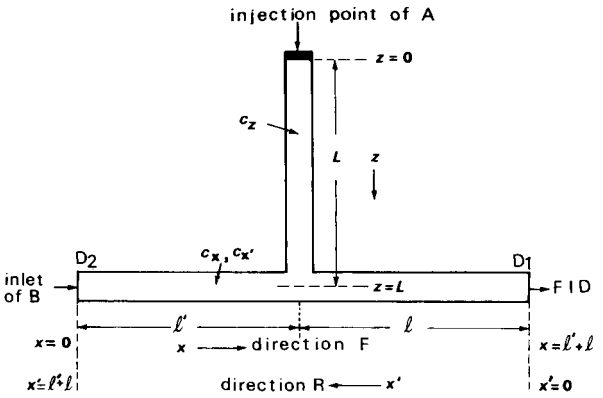

Fig. 1. Schematic representation of the diffusion (L) and the chromatographic ($l' + l$) columns for determining diffusion coefficients by the reversed-flow method.

A pure diffusion flux of A into B is set up inside column L and the result of this at $z = L$ is carried over to the detector by the carrier gas B, being recorded there as a concentration–time curve. Analysis of this curve permits calculation of the diffusion coefficient D_{AB}. Even more precise results are obtained by repeatedly sampling the chromatographic column and recording the amount of A entering it at $z = L$ within a small time interval t_M. This sampling is accomplished by repeatedly reversing the direction of the flow of B at definite known times.

It must be noted that the arrangement of Fig. 1 is free of "secondary flow" phenomena due to coiled tubes, since the diffusion column L is relatively short (0.5–1 m) and can be made straight.

EXPERIMENTAL

Apparatus

The experimental set-up for the application of the reversed-flow method is very simple. A conventional gas chromatograph with a high-sensitivity detector, *e.g.* a flame-ionization detector (FID) is modifed as shown diagrammatically in Fig. 2. The solute A is injected into the diffusion column L (61 cm × 4 mm I.D.) while the carrier gas B flows through the chromatographic column $l' + l$ (40 + 40 cm × 4 mm I.D.), either entering at D_2 with the detector placed at D_1 or *vice versa*. The reversing of the flow direction is effected by means of valve S (four-port or six-port with two alternate ports connected through a small piece of 1/16 in. tube). A restrictor can be placed at H to increase the pressure within the whole system.

Materials

The carrier gases used (nitrogen, hydrogen, helium) were of gas chromatographic grade (Linde, or Aga Chropei, $\geqslant$ 99.99% purity). The various solutes injected were purchased either from Matheson Gas Products (methane 99.99, ethylene 99.98, propylene 99.7%), or from Fluka (ethane puriss grade, *n*-butane practical grade).

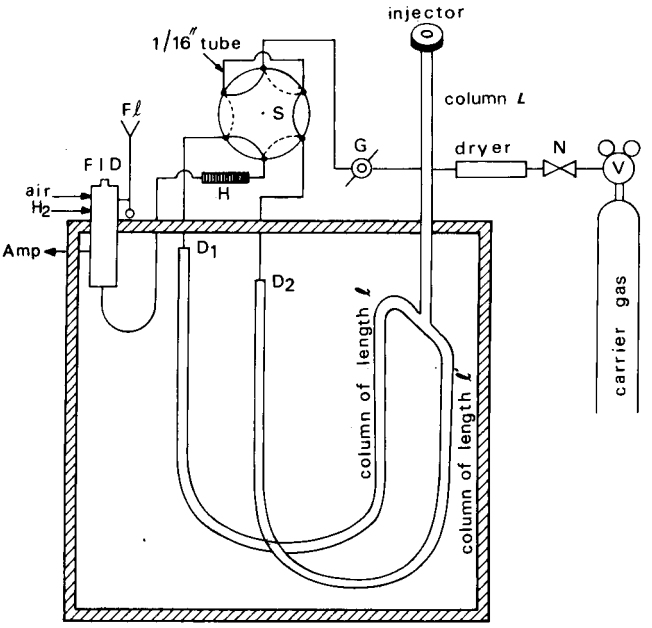

Fig. 2. Gas lines and important connections for measuring diffusion coefficients by reversed-flow gas chromatography. V = two-stage reducing valve and pressure regulator; N = needle valve; G = gas flow controller for minimizing variations in the gas flow-rate; S = six-port gas sampling valve with a short 1/16 in. tube connecting two alternate ports; H = restrictor, which can be omitted; Fl = bubble flow meter; Amp = signal to amplifier.

Procedure

While carrier gas B is flowing through the chromatographic column in direction F (Fig. 2, valve S in position indicated by the solid lines), a small amount of solute A (usually 0.5 cm^3 of gas at atmospheric pressure) is injected into the diffusion column L. After a certain time, during which no signal is noted, an asymmetric concentration–time curve for the solute is recorded, which rises slowly and then decays even more slowly. At a time (measured from the moment of injection) greater than the gas hold-up time in the column length l, the direction of the carrier gas is reversed by switching valve S to the other position (dotted lines). After a certain dead time, when no signal is recorded by the detector, the chromatographic elution curve rises steeply, then slowly and finally returns abruptly to the original concentration–time curve (Fig. 3, R-peak). After a time (from the moment of reversal) greater than the total gas hold-up time in the total column length $l + l'$, the carrier gas is again turned to the direction F. This is followed by a new extra signal (Fig. 3, F-peak). The procedure is repeated several times, until a whole series of peaks is obtained. If the two column lengths l and l' are equal, no distinction can be made between peaks obtained in direction F or R.

The pressure drop along the whole column $l' + l$ was negligible, and the diffusion coefficients were considered to have been determined at that pressure, which was measured at the injection point, by means of an open mercury manometer.

No temperature regulation was made, and the temperature reported in the

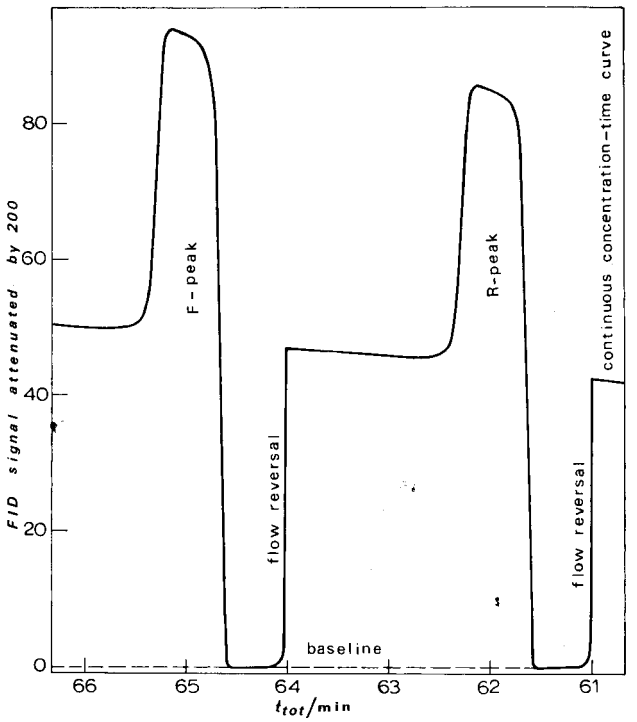

Fig. 3. A reversed-flow chromatogram for measuring the diffusion coefficient of C_2H_6 (0.5 cm^3) into N_2 ($\dot{V}$ = 0.267 cm^3 sec^{-1}) at 293°K and 1.99 atm.

results was the ambient temperature, the variation of which was small during each experiment.

THEORETICAL ANALYSIS

The analytical mathematical expressions which describe the concentration–time curve of the solute A at the detector, as well as the elution curves of peaks resulting from the reversal of the flow (R- and F-peaks, Fig. 3) are derived by reference to Fig. 1, under the following assumptions:

(a) Radial diffusion in all columns is negligible.

(b) Axial diffusion of A along coordinate x or x', *i.e.* in the chromatographic column, is negligible. This seems reasonable for a high enough flow-rate of B.

(c) The solute A is introduced in an very small section of column L, so that its total mass m is concentrated initially in the plane $z = 0$.

Notation

a = cross sectional area of the columns (cm^2)

c_b = concentration defined by the last term of eqn. 32 (mol cm^{-3})

c_x, $c_{x'}$ = concentrations of the solute vapour A in the chromatographic column with the carrier gas B flowing in direction F or R, respectively (mol cm^{-3})

c_z = concentration of the solute vapour A in the diffusion column L (mol cm^{-3})

$\bar{c}_x$ = Laplace transform of c_x with respect to t'
$\bar{\bar{c}}_x$ = double Laplace transform of c_x with respect to t' and t
$C_{x'}$, C_z = Laplace transforms of $c_{x'}$ and c_z with respect to t_0
$\bar{C}_{x'}$ = double Laplace transform of $c_{x'}$ with respect to t_0 and t'
$D \equiv D_{AB}$ = mutual diffusion coefficient of A and B ($cm^2\ sec^{-1}$)
f = area under the curve of F- and R-peaks (mol)
h = height above the baseline defined by eqn. 36 ($mol\ cm^{-3}$)
l, l' = lengths of the two sections of the chromatographic column depicted in Fig. 1 (cm)
L = length of diffusion column depicted in Fig. 1 (cm)
m = mass of injected solute A (mol)
N = constant defined by eqn. 13
p_0, p', p = transform parameters with respect to t_0, t' and t, respectively
q = parameter defined by eqn. 3
t_0 = time measured from the injection of solute A (sec)
t_{tot} = total time passed from the injection of A to the last reversal of the gas flow (sec)
t, t' = time measured from the last reversal of the gas flow, in direction F or R, respectively (sec)
t_M, t'_M = gas hold-up time of column section l or l', respectively (sec)
v = linear velocity of the carrier gas B in the chromatographic column ($cm\ sec^{-1}$)
$\dot{V}$ = volume flow-rate of carrier gas ($cm^3\ sec^{-1}$)
x, x', z = distance coordinates defined in Fig. 1 (cm)
θ, θ' = time parameters defined by eqns. 16 and 22, respectively (sec)
τ, τ' = time measured from the last reversal of the flow diminished by the gas hold-up time in the flow direction, eqns. 31 and 27 (sec).

The problem will be considered separately in the chromatographic columns, in which the concentrations of A as functions of time and distance are determined by certain differential equations with certain initial and boundary conditions.

Diffusion column L

The concentration in this column $c_z(z, t_0)$ obeys the diffusion equation (Fick's second law):

$$\frac{\partial c_z}{\partial t_0} = D \frac{\partial^2 c_z}{\partial z^2} \tag{1}$$

Laplace transformation with respect to t_0 of this equation, under the initial condition $c_z(z,0) = (m/a)\delta(z)$, where $\delta(z)$ is the Dirac delta function, gives the linear second-order equation

$$\frac{d^2 C_z}{dz^2} - q^2 C_z = -\frac{m}{aD}\delta(z) \tag{2}$$

where

$$q^2 = p_0/D \tag{3}$$

Eqn. 2 can be solved by using z Laplace transformation and, after taking the inverse transform, replacing sinh (qz) and cosh (qz) by exponential functions, and collecting terms with the same exponential, one obtains:

$$C_z = \left[C_z(0) - \frac{C_z'(0)}{q} + \frac{m}{aDq}\right]\frac{\exp(-qz)}{2} + \left[C_z(0) + \frac{C_z'(0)}{q} - \frac{m}{aDq}\right]\cdot \frac{\exp(qz)}{2} \tag{4}$$

where $C_z(0)$ and $C_z'(0)$ is the t_0 transform of the concentration c_z and its first z derivative, respectively, at $z = 0$. For the approximation of a semi-infinite cylinder, the pre-exponential factor in brackets [...] of the last term would normally be set equal to zero, to assure that $C_z = 0$ as $z \to \infty$. However, this approximation is not needed here, since there are two boundary conditions at $z = L$ or $x = l'$, by means of which the relation between $C_z(0)$ and $C_z'(0)$ can be found. These conditions, in the form of their t_0 Laplace transforms, are

$$(C_z)_{z=L} = (C_x)_{x=l'} \tag{5}$$

and

$$-D\left(\frac{\partial C_z}{\partial z}\right)_{z=L} = v(C_x)_{x=l'} \tag{6}$$

By combining eqns. 4, 5 and 6, one finds

$$C_z = \left[\frac{m}{aDq} - \frac{C_z'(0)}{q}\right]\cdot \frac{(1 + v/Dq)\exp(-qz) + (1 - v/Dq)\exp[-q(2L - z)]}{(1 + v/Dq) - (1 - v/Dq)\exp(-2qL)} \tag{7}$$

With $v = 0$, *i.e.* no flux across the boundary $z = L$ (*cf.* also eqn. 6), eqn. 7 is multiplied by the volume element $a\,dz$ and integrated between the limits 0 and L, the result being $m/p_0 - C_z'(0)aD/p_0$. Since this integration must yield m/p_0, *i.e.* the t_0 Laplace transform of the total mass of A injected, it follows that $C_z'(0) = 0$. Using this in eqn. 7, and the approximation of neglecting $\exp(-2qL)$ compared to 1 in the denominator (this is justified for not too short diffusion columns and not too long times), the above equation becomes

$$C_z = \frac{m}{aDq}\exp(-qz) + \frac{m}{aDq}\exp[-q(2L-z)]\left(\frac{2}{1 + v/Dq} - 1\right) \tag{8}$$

This equation provides a simple way to find the solution of the diffusion equation in a cylinder of *finite* length L, without the need of using reflections on boundaries, superpositions etc. It is done by putting $v = 0$, when the last term in pa-

rentheses becomes unity, and inverse Laplace transformation with respect to p_0 gives c_z as a function of time and distance:

$$c_z = \frac{m}{a(\pi D t_0)^{\frac{1}{2}}} \exp\left(-\frac{z^2}{4Dt_0}\right)\left\{1 + \exp\left[-\frac{L(L-z)}{Dt_0}\right]\right\} \tag{9}$$

For $L \to \infty$ the last exponential vanishes and eqn. 9 reduces to the well-known expression for a semi-infinite cylinder, as expected. At $t_0 = 0$ eqn. 9 vanishes everywhere except at $z = 0$, where it becomes infinite, in agreement with assumption (*c*).

Finally, eqn. 8 with $z = L$ gives $(C_x)_{x=l'}$, according to condition 5:

$$(C_x)_{x=l} = \frac{2m}{aDq} \cdot \frac{\exp(-qL)}{1 + v/Dq} \tag{10}$$

which, for high enough flow-rates, becomes

$$(C_x)_{x=l'} = \frac{2m}{\dot{V}} \exp(-qL) \tag{11}$$

since then $v \gg Dq$ and 1 can be omitted from the denominator of eqn. 10. Inverse Laplace transformation of eqn. 11 gives

$$(c_x)_{x=l'} = \frac{N \exp(-L^2/4Dt_0)}{t_0^{3/2}} \tag{12}$$

where

$$N = mL/\dot{V}(\pi D)^{1/2} \tag{13}$$

Chromatographic column $l' + l$

If the carrier gas B flows in the direction F, the concentration of A at $x = l'$, as given by eqn. 12, spreads out in the column section l towards the detector at D_1 (Fig. 1) according to the following mass balance equation, under assumption (b):

$$\frac{\partial c_x}{\partial t_0} = -v \frac{\partial c_x}{\partial x} + v(c_x)_{x=l'} \delta(x-l') \tag{14}$$

where $\delta(x-l')$ is the Dirac delta function.

Taking the t_0 Laplace transform of eqn. 14, with the initial condition $c_x(x,0) = 0$, we find an ordinary differential equation for C_x as a function of x. This can be integrated by means of its x Laplace transform, the result being

$$C_x = (C_x)_{x=l'} \exp(-p_0\theta) \cdot u(x-l') \tag{15}$$

where

$$\theta = (x-l')/v \tag{16}$$

and $u(x-l')$ is the Heaviside unit step function, which equals 0 for $x < l'$ and 1 for $x \geqslant l'$. At the detector, *i.e.* at $x = l' + l$, $u(x-l')$ becomes $u(l) = 1$ for $l > 0$, and 0 becomes $l/v = t_M$, *i.e.* the gas hold-up time in the column section l. Thus eqn. 15 reduces to

$$C_x = C_x(l', p_0) \exp(-p_0 t_M) \tag{17}$$

and, according to a well known property of Laplace transformations ("translation"), the inverse transform of eqn. 17 for $t_M \geqslant 0$ is

$$c_x = c_x(l', t_0 - t_M) \cdot u(t_0 - t_M)$$

Using eqn. 12 for $c_x(l', t_0)$, one finds for the concentration–time curve at the detector

$$c_x = \frac{N \exp\left[-L^2/4D\,(t_0 - t_M)\right]}{(t_0 - t_M)^{3/2}} \cdot u(t_0 - t_M) \tag{18}$$

From this curve the diffusion coefficient can be computed if the height of the detector signal h (which is proportional to c_x) is multiplied by $(t_0 - t_M)^{3/2}$ and the logarithm of this product is plotted against $1/(t_0 - t_M)$. According to eqn. 18, this plot should be linear with a slope equal to $-L^2/4D$, from which D is found. An example of this type of plot is shown in Fig. 4.

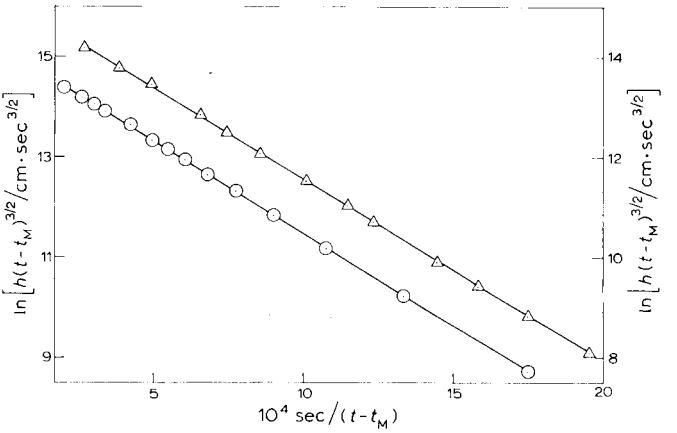

Fig. 4. Examples of plotting eqn. 18 (△, right-hand ordinate) and eqn. 36 (○, left-hand ordinate) for the diffusion of CH_4 (0.5 cm^3) into He ($\dot{V} = 0.283$ cm^3 sec^{-1}), at 296°K and 2.03 atm.

The above method based on eqn. 18, however, presupposes that: (1) a negligible distortion of the concentration–time curve due to longitudinal diffusion along the column l takes place, and (2) the baseline of the recording system is precisely adjusted and corrected during each determination, so that nothing is added or subtracted from c_x. It is not always easy to substantiate the above requirements, and another version free of these is based on what we term "chromatographic sampling" at known times. This is very simply done by reversing the direction of the flow of B at definite

times. Each reversion of the flow takes the amount of solute A which has entered the chromatographic column at $z = L$ from the diffusion column between the times $t_{tot} - t_M$ and t_{tot}, and exhibits it as an extra peak on the otherwise continuous chromatographic signal (see Fig. 3). This is predicted by the mathematical analysis which follows.

Chromatographic sampling

While the carrier gas is flowing in direction F giving the curve described by eqn. 18, its flow is reversed to the direction R at a time $t_0 > t_M$. The time measured from the moment of reversal is called t'. The distance co-ordinate x is now changed to x' defined by the relation

$$x' = l' + l - x \tag{19}$$

and the concentration $c_{x'}(x', t')$ in this time interval is given by the following equation, analogous to eqn. 14:

$$\frac{\partial c_{x'}}{\partial t'} = -v \cdot \frac{\partial c_{x'}}{\partial x'} + v(c_{x'})_{x'=l}\delta(x'-l) \tag{20}$$

As with eqn. 14, one proceeds by taking Laplace transforms of this equation with respect to time, but now the t_0 transform is taken first, followed by the t' transform. The initial condition for the latter is the expression

$$C_{x'}(x', p_0, 0) = C_{x'}(l, p_0, 0) \cdot \exp(p_0\theta') \, [1 - u(x'-l)] \tag{21}$$

obtained from eqn. 15 by writing $C_{x'}(l, p_0, 0)$ for $(C_x)_{x=l'}$, substituting $1 - u(x'-l)$ for $u(x-l')$ and replacing θ, as defined by eqn. 16, by its equivalent

$$\theta = (l-x')/v = -(x'-l)/v = -\theta' \tag{22}$$

The result of the above double Laplace transformation is

$$\frac{d\bar{C}_{x'}}{dx'} + \frac{p'}{v} \cdot \bar{C}_{x'} = \frac{C_{x'}(l, p_0, 0)}{v} \cdot \exp(p_0\theta') \cdot [1 - u(x'-l] + \bar{C}_{x'}(l, p_0, p') \cdot \delta(x'-l) \tag{23}$$

This ordinary differential equation is easily integrated by using x' Laplace transforms, giving $\bar{C}_{x'}(x', p_0, p')$:

$$\bar{C}_{x'} = \frac{C_{x'}(l, p_0, 0)}{p' + p_0} \{\exp(p_0\theta') \, [1 - u(x'-l)] + \exp(-p'\theta') \cdot u(x'-l) +$$

$$-\exp[-(p_0 l + p'x')/v]\} + \bar{C}_{x'}(l, p_0, p') \cdot \exp(-p'\theta') \cdot u(x'-l) \tag{24}$$

At the detector, *i.e.* for $x' = l' + l$, $u(x'-l)$ becomes $u(l') = 1$ for $l' > 0$, and θ' becomes $l'/v = t'_M$, *i.e.* the gas hold-up time in the column section l'. Then eqn. 24

simplifies to

$$\bar{C}_{x'} = \frac{C_{x'}(l,p_0,0)}{p' + p_0}\{\exp(-p't_M) - \exp[-p'(t'_M + t_M)]\cdot\exp(-p_0t_M)\} + \bar{C}_{x'}(l,p_0,p')\exp(-p't'_M) \quad (25)$$

Taking now the inverse transforms, first with respect to p' and then with respect to p_0, one finds $c_{x'}$ at the detector as a function of t' and t_0:

$$c_{x'} = c_{x'}(l,t_0-\tau')\cdot[u(\tau') - u(\tau'-t_M)]\cdot u(t_0-\tau') + c_{x'}(l,t_0+\tau')\cdot u(\tau') \quad (26)$$

where

$$\tau' = t' - t'_M \quad (27)$$

The behaviour of eqn. 26 for various values of τ' is interesting. For $\tau' < 0$, *i.e.* for $t' < t'_M$, $c_{x'} = 0$ and no signal is recorded by the detector, until the gas hold-up time t'_M is reached, when $u(\tau') = 1$ and the chromatographic signal rises abruptly to $c_{x'}(l,t_0-\tau') + c_{x'}(l,t_0+\tau')$. It falls again to $c_{x'}(l,t_0+\tau')$ when $\tau' \geqslant t_M$, *i.e.* when $t' \geqslant t'_M + t_M$, because the square function in braces [ ] becomes zero. Then the $u(t_0-\tau')$ factor remains unity in the above interval on account of the condition that the flow is reversed at $t_0 > t_M$. Thus, the function described by eqn. 12, *i.e.* the concentration of A at $x = l'$ or $x' = l$ (*cf.* Fig. 1) which can be denoted by $c_x(l',t_0)$ or $c_{x'}(l,t_0)$, is shifted in time on reversing the flow direction. This time-shift takes place in two opposite directions, "forwards" to $c_{x'}(l,t_0+\tau')$ and "backwards" to $c_{x'}(l,t_0-\tau')$. The first shift starts at $t' = t'_M$ and continues uninterrupted. It is nothing more than the continuation of eqn. 18 at the other end of the chromatographic column. The backward shift is barred in the interval $0 \leqslant \tau' \leqslant t_M$ or $t'_M \leqslant t' \leqslant t'_M + t_M$, and therefore starts with the concentration $c_{x'}(l,t_0)$ and ends with that of a preceding time, namely $c_{x'}(l,t_0-t_M)$. This extra signal (R-peak) adds to the forward shift and constitutes the "chromatographic sampling" signal. Thus, the experimental behaviour exhibited in Fig. 3 is predicted.

At a time $t' > t'_M + t_M$ the carrier gas flow is again turned to the direction F, the time from this moment being denoted by t. The distance coordinate is changed from x' back to x, according to eqn. 19, and the concentration $c_x(x,t)$ is again described by eqn. 14 with t substituted for t_0. To solve this equation by the method of Laplace transformations, we need the initial condition at $t = 0$. This, in the form of its t' transform, is obtained from the last term of eqn. 24, since all other terms of this equation disappear at $\tau' > t_M$. The remaining term, after taking the p_0 inverse transform, changing θ' to $-\theta$ and $u(x'-l)$ to $1 - u(x-l')$, gives the desired condition at $t = 0$ as

$$\bar{c}_x(x,t_0,p',0) = \bar{c}_x(l',t_0,p',0)\cdot\exp(p'\theta)\,[1 - u(x-l')] \quad (28)$$

The rest of the solution in the t interval follows the same procedure as that outlined for eqn. 20, namely the t' Laplace transform is taken first, then the t transform with initial condition eqn. 28. This leads to a differential equation in x similar to eqn. 23,

which in turn gives the equivalent of eqn. 24, and finally the counterpart of eqn. 25 is obtained as

$$\bar{\bar{c}}_x = \frac{\bar{c}_x(l',t_0,p',0)}{p+p'} \{\exp(-pt_M) - \exp[-p(t_M+t'_M)] \cdot \exp(-p't'_M)\} + \\ + \bar{\bar{c}}_x(l',t_0,p',p) \cdot \exp(-pt_M) \tag{29}$$

Successive inverse transformations with respect to p and p' then give the c_x value at the detector:

$$c_x = c_x(l',t_{tot}-\tau) \cdot [u(\tau) - u(\tau-t'_M)] \cdot u(t'-\tau) + c_x(l',t_{tot}+\tau) \cdot u(\tau) \tag{30}$$

where

$$\tau = t - t_M \tag{31}$$

and $t_{tot} = t_0 + t'$.

This equation is symmetrical with eqn. 26 and its behaviour is analogous. It predicts that $c_x = 0$ for $\tau < 0$, and at $\tau > 0$ two functions are recorded as a sum. One is given by eqn. 12 with the total time t_{tot} in place of t_0 and shifted forwards by τ. This continues uninterrupted as the last term of eqn. 30 shows. In the other function the t_{tot} is shifted backwards by τ and this function vanishes when $\tau \geqslant t'_M$. Thus, an extra signal (F-peak) appears in the interval $0 \leqslant \tau \leqslant t'_M$ "sitting" on the otherwise continuing chromatographic curve. The function $u(t'-\tau)$ in eqn. 30 is kept at unity in the above interval on account of the condition that the new reversal was at $t' > t'_M + t_M$.

Repeating the reversal of the carrier gas flow in the direction R for a second time at $t > t_M + t'_M$, then in the direction F for a third time at $t' > t'_M + t_M$, and so on, two series of peaks are produced. The R-peaks are described by eqn. 26 with t_{tot} in place of t_0, while the F-peaks are given by eqn. 30. Since the definitions "forward" and "reverse" are arbitrary, and the two above equations have the same form, one of them suffices to describe both kinds of peaks. In what follows we make use only of eqn. 30. This can be written explicitly using eqn. 12 in place of $c_x(l',t_{tot}-\tau)$ and $c_x(l',t_{tot}+\tau)$, the resulting expression describing the concentration–time curve at the detector:

$$c_x = \frac{N \exp[-L^2/4D(t_{tot}-\tau)]}{(t_{tot}-\tau)^{3/2}} \cdot [u(\tau) - u(\tau-t'_M)] + \\ + \frac{N \exp[-L^2/4D(t_{tot}+\tau)]}{(t_{tot}+\tau)^{3/2}} \cdot u(\tau) \tag{32}$$

Here, N is given by eqn. 13, t_{tot} is the total time passed from the injection of A to the *last* reversal of the gas flow, τ the time measured *from* the last reversal of the flow diminished by the gas hold-up time in the direction of the flow (*cf.* eqns. 27 and 31) and t'_M the hold-up time in the opposite direction of the flow. The function $u(t'-\tau)$ in eqn. 30 has been assumed unity, because the time elapsing between any two

successive reversals is greater than the total hold-up time $t_M + t'_M$, as mentioned before.

Two other relations are useful. The first is that which gives the area under the F- and R-peaks, taking the last term of eqn. 32 as baseline. For this purpose one can use eqn. 25 and the well known relation

$$\mathscr{L}_{t_0} f = \int_0^\infty C_{x'} \, dV = \dot{V} \int_0^\infty C_{x'} \, dt' = \dot{V} \lim_{(p' \to 0)} (\bar{C}_{x'}) \tag{33}$$

where in place of $\bar{C}_{x'}$ we use only the first term on the right-hand side of eqn. 25, the last term giving rise to the baseline. The result is

$$\mathscr{L}_{t_0} f = \dot{V} \cdot \frac{C_{x'}(l,p_0,0)}{p_0} \cdot [1 - \exp(-p_0 t_M)] \tag{34}$$

The area under the peaks is simply found by substituting eqn. 11 for $C_{x'}(l,p_0,0)$ and taking the p_0 inverse transform:

$$f = 2m \left[\operatorname{erfc} \frac{L}{2D^{1/2} t_0^{1/2}} - \operatorname{erfc} \frac{L}{2D^{1/2}(t_0 - t_M)^{1/2}} \cdot u(t_0 - t_M) \right] \tag{35}$$

A second useful relation is that giving the height of the F- or R-peaks above the continuous chromatographic signal (the latter being taken as baseline) at $\tau = t'_M$, which is the maximum value of τ before returning to the baseline. Denoting by c_b the last term of eqn. 32 (baseline), one finds for this height

$$h \equiv (c_x - c_b)_{\tau = t'_M} = \frac{N \exp(-L^2/4D(t_{tot} - t'_M))}{(t_{tot} - t'_M)^{3/2}} \tag{36}$$

Thus, the plotting of $\ln[h(t_{tot} - t'_M)^{3/2}]$ against $1/(t_{tot} - t'_M)$ should result in straight lines with slope $-L^2/4D$. Knowing L, D can be calculated. An example of such a plot is shown in Fig. 4.

RESULTS AND DISCUSSION

Using eqn. 36, values for the diffusion coefficient of five gaseous hydrocarbons in three carrier gases have been determined and are collected in Table I. The values and their standard errors found by regression analysis using standard least-squares procedures, are reduced to 1 atm after multiplication by the pressure of the experiment. This pressure is given in Table I, so that one can find the actual values determined from the ratio D/p. For the pair ethylene–nitrogen the diffusion coefficient was determined at three different pressures, and for the pair methane–helium at two pressures. In both cases the variation of the results with small changes in pressure (and in $\dot{V}$) was small.

The precision of the method, defined as the relative standard deviation (%), can be judged from the data given for methane–helium. From the five values quoted, a precision of 0.9% is calculated.

TABLE I

DIFFUSION COEFFICIENTS OF VARIOUS SOLUTES INTO THREE CARRIER GASES AT AMBIENT TEMPERATURES AND REDUCED TO 1 atm PRESSURE

The actual values found at the pressure of the experiment, p, are simply D/p. All errors given are "standard errors", calculated by regression analysis.

Carrier gas	*Solute gas*	T (°K)	$\dot{V}$ ($cm^3\ sec^{-1}$)	p (atm)	$10^3\ D$ ($cm^2\ sec^{-1}$)			*Accuracy**** (%)
					Present work	*Calcd.*	*Lit.*[ref.]	
N_2	CH_4	296.0	0.260	1.96	272 ± 4	214	–	21.3
	C_2H_6	293.0	0.267	1.99	142 ± 0.03	144	148[2]	1.4 (2.7)
	n-C_4H_{10}	295.5	0.300	2.15	98 ± 0.2	98.6*	96[2]	0.3 (2.7)
	C_2H_4	296.0	0.120	1.49	168 ± 2	156	163[2]	7.1 (4.3)
		292.0	0.268	2.00	156 ± 0.4			0
		292.0	0.538	2.71	161 ± 0.4			3.1
	C_3H_6	298.0	0.260	1.96	124 ± 0.4	120*	–	3.2
H_2	CH_4	293.0	0.287	1.70	699 ± 3	705	730[3]	0.9 (3.4)
	C_2H_6	297.0	0.267	1.56	548 ± 5	556	540[3]	1.5 (3)
	n-C_4H_{10}	296.0	0.273	1.60	386 ± 3	373	400[3]	3.4 (6.8)
	C_2H_4	293.0	0.300	1.75	525 ± 5	559	602[2]	6.5 (7.1)
	C_3H_6	296.0	0.273	1.60	485 ± 3	486	–	0.2
He	CH_4	295.7	0.250	1.78	527 ± 3	669	–	26.9
		295.0	0.283	2.03	520 ± 1			28.7
		296.0	0.283	2.03	522 ± 1**			28.2
		296.0	0.283	2.03	514 ± 0.2			30.2
		296.7	0.283	2.03	522 ± 3			28.2
	C_2H_6	295.6	0.300	2.15	518 ± 3	507	–	2.1
	n-C_4H_{10}	290.0	0.283	2.03	333 ± 3	330	364[4]	0.9 (9.3)
	C_2H_4	296.0	0.283	2.03	558 ± 4	544	–	2.5
	C_3H_6	291.0	0.283	2.03	412 ± 4	440	–	6.8

* The necessary parameters σ and ε/k were obtained from ref. 6.

** This value was determined by using eqn. 18, without reversing the flow.

*** This is defined by eqn. 38. Numbers in parentheses are the accuracies of the respective literature values.

The values of the present work are compared in Table I with those calculated theoretically by the equation[5].

$$D_{AB} = 0.0018583\ T^{3/2} \left(\frac{1}{M_A} + \frac{1}{M_B} \right)^{1/2} \Big/ p\sigma_{AB}^2 \Omega_{D,AB} \tag{37}$$

where M_A and M_B are molar masses, and $\Omega_{D,AB}$ is a dimensionless function of the temperature and of the intermolecular potential field for one A and one B molecule. Combining the Lennard–Jones parameters σ and ε/k of A and B, as given in Table B-1 of ref. 5, σ_{AB} and ε_{AB}/k are found:

$$\sigma_{AB} = (\sigma_A + \sigma_B)/2 \text{ and } \frac{\varepsilon_{AB}}{k} = \left(\frac{\varepsilon_A}{k} \cdot \frac{\varepsilon_B}{k} \right)^{1/2}$$

From this kT/ε_{AB} is calculated and then Table B-2 of ref. 5 gives the $\Omega_{D,AB}$ value.

The calculated values in Table I are for the temperature of the experiment, while the literature values refer to temperatures which differ from those of the present work by not more than 5°C. The accuracy given in the last column of Table I is a

measure of the deviation of the present values from the calculated ones, defined as

$$\text{Accuracy } (\%) = \frac{|D_{\text{found}} - D_{\text{calcd}}|}{D_{\text{found}}} \cdot 100 \tag{38}$$

With the exception of two pairs containing methane as solute, this accuracy is better than 7.1% in all cases and in 8 out of the 15 pairs is better than 2.5%. The high deviation of the experimental from the calculated values for the pairs methane–nitrogen and methane–helium, in spite of the fact that the precision is 0.9% as mentioned before, is probably due to the approximations used in the calculated values. Finally, the accuracies of the present values can be compared with the accuracies of the respective literature values, given in parentheses in Table I and defined again by eqn. 38 with D_{lit} in place of D_{found}. This comparison leads to the conclusion that, with the exception of ethylene–nitrogen, the values of diffusion coefficients determined by the method reported here are closer to the theoretical calculated values than are the experimental values found in the literature, under similar conditions of temperature and pressure.

One final remark is that the D values determined by the present method are very sensitive to the precision with which L is measured, since D is proportional to L^2. Instead of measuring directly the length L, one can use a solute–carrier gas pair of accurately known diffusion coefficient, and carry out a calibration experiment for L. The value of L so calculated can now be used to estimate unknown diffusion coefficients. In the results reported in Table I, however, the actual length L was used, without any calibration.

In conclusion, with the aid of simple gas chromatography instrumentation, precise and accurate mutual diffusion coefficients in gases can be determined. The method has certain instrumental similarities with a technique reported by Desty *et al.*[7]. They used the diffusion of vapour from a liquid surface through a stagnant column of gas in a capillary tube, to maintain constant low concentrations of the vapour in a gas stream, in order to study the performance of a flame-ionization detector. They also described how to determine the rate of diffusion from the open end of the capillary by measuring the distance between this end and the liquid meniscus as a function of time.

ACKNOWLEDGEMENTS

The authors acknowledge the help of Mrs. Anna Sinou-Karahaliou and Mrs. M. Barkoula.

REFERENCES

1 V. R. Maynard and E. Grushka, *Advan. Chromatogr.*, 12 (1975) 99.
2 C. A. Boyd, N. Stein, V. Steingrimsson and W. F. Rumpel, *J. Chem. Phys.*, 19 (1951) 548.
3 P. Fejes and L. Czaran, *Hung. Acta Chim.*, 29 (1961) 171.
4 G. L. Hargrove and D. T. Sawyer, *Anal. Chem.*, 39 (1967) 244.
5 R. B. Bird, W. E. Stewart and E. N. Lightfoot, *Transport Phenomena*, Wiley, Chichester, New York, 1960, p. 511.
6 J. O. Hirschfelder, C. F. Curties and R. B. Bird, *Molecular Theory of Gases and Liquids*, Wiley, Chichester, New York, 1964, p. 1213.
7 D. H. Desty, C. J. Geach and A. Goldup, in R. P. W. Scott (Editor), *Gas Chromatography 1960*, Butterworths, London, 1960, p. 46.

Journal of Chromatography, 237 (1982) 15–23
Elsevier Scientific Publishing Company, Amsterdam — Printed in The Netherlands

CHROM. 14,440

"BAND BROADENING IN SPACE" AND THE "RETENTION GAP" IN CAPILLARY GAS CHROMATOGRAPHY

K. GROB, Jr.
Kantonales Labor, P.O. Box, CH-8030 Zürich (Switzerland)
(Received October 6th, 1981)

SUMMARY

Peaks may be broadened, distorted or even split if the sample components are spread out in the column inlet by large amounts of condensed solvent. This "band broadening in space" occurs during splitless injections with the solvent effect and cold on-column sampling. The features of the band broadening in space are summarized. Peak distortion is often found to be less pronounced than would be expected from the length of the flooded column section. It is assumed that this is due to partial transport of the solvent within the flooded zone by the vapour phase. Minor temperature gradients in the column inlet may greatly influence the peak distortion.

The "retention gap" is proposed as a method of eliminating peak distortion caused by band broadening in space. The retention in the column inlet (the approximate length of the flooded zone) is reduced to accelerate the migration of the spread sample components and to reconcentrate them at the beginning of the regular film of the stationary phase. The peak broadening is reduced by a factor corresponding to the reduction of the film thickness in the retention gap zone compared with the remainder of the column. For the routine analysis of free sterols it is shown that the retention gap completely eliminates the peak distortion and, at the same time, greatly reduces problems caused by by-products of the sample which disturb or degrade the stationary phase in the flooded zone of the column inlet.

INTRODUCTION

In a previous paper[1] we described the phenomenon of "band broadening in space". We also investigated its origin when it occurs associated with splitless injections with the solvent effect or cold on-column sampling. These two injection techniques create large amounts of condensed solvent in the column inlet and the thick layer of liquid is not stable. The rapid stream of carrier gas drives the liquid further into the column, flooding 20–60 cm of the column inlet. When the liquid is spread out as a thin, stable film, the expansion stops and the solvent evaporates. In splitless injection a considerable proportion and in cold on-column injection all of the sample material is dissolved in the flooding liquid. Hence it becomes spread out into the column as far as the flowing liquid reaches. The resulting bands are sufficiently broad

0021-9673/82/0000–0000/$02.75

to cause severe peak broadening at least for short to medium sized columns. Commonly peaks are not only broadened, but are also distorted or split into two maxima, which is due to the uneven distribution of the sample material over the flooded section of the column. We used the expression "band broadening in space" because the parameter that is common to the bands of all sample components is the geographical distribution in the column. This distinguishes it from the "band broadening in time" where the bands of the different components do not have the same local extension within the column. The latter bands expand by gas chromatographic migration during a fixed period of time, resulting in a geographically more extended band for a rapidly migrating substance than for a highly retained substance.

Typical features of the band broadening in space are as follows:

(1) Peaks eluting up to 40°C above the column temperature during the injection are not distorted. Distortion increases with increasing elution temperature for the range of compounds chromatographed within the following *ca.* 50°C and is the most drastic for solutes eluted at elevated column temperatures.

(2) For splitless injections only the peak is distorted which is related to the proportion of sample having reached the flooded zone. Various amounts of the sample components (depending on their volatility) are trapped in the warm, bottom part of the vaporizing injector and may elute as a separated, undistroted peak.

(3) The pattern of the peak distortion (the shape of the peak or its splitting) is very similar for all components of a sample. Above the critical temperature where band broadening in space becomes active, all peaks are affected.

(4) The broadening effect on the peaks as measured, *e.g.*, in millimetres on the chart paper is proportional to the retention of the peak. In isothermal runs the distortion of the peaks increases with retention; in temperature programming the peaks are more drastically affected if slow programming rates are applied.

(5) The effects of the band broadening in space are the more pronounced the shorter is the column, because the distortion of the peaks and the reduction of the separation efficiency are directly related to the proportion of the flooded column compared with the total length of the capillary.

(6) The distortion increases with increasing sample volume because the larger amount of liquid extends the flooded zone. In cold on-column sampling peaks are commonly broadened only when the sample volume is below about 0.8 μl. They are usually split for sample sizes exceeding 1 μl.

The decrease in the separation efficiency due to the band broadening in space may be massive. For a cold on-column injection of 1 μl of sample into a 15-m column, the separation efficiency may be reduced by a factor of about two in terms of resolution (determined, *e.g.*, as separation number, TZ) or by a factor of four in terms of theoretical plates.

OCCURRENCE OF BROADENING IN SPACE

Peak broadening is often less drastic than expected on the basis of the length of the capillary inlet section, which becomes wet during the injection. In splitless injection this may be due to the fact that the proportion of the sample components which are trapped in the bottom of the injector is so dominating that the broadened prepeak of the material spread in the flooded zone is hardly visible, which is a dangerous source of error for quantitative analyses.

In cold on-column sampling no peak broadening may be observed during a series of chromatograms, whereas under apparently identical conditions strongly distorted peaks may result another time. According to our experience, band broadening in space is seldom visible to its full extent if the solvent is pentane or hexane. On the other hand, it is always evident if the solvent is more polar such as acetone, diethyl ether or an alcohol. The fact that the sample components are often spread out less far than to the front of the zone with condensed solvent leads us to conclude that the transport of the solvent occurred at least partially through the vapour phase. If the liquid expands by evaporation and recondensation the sample components are not carried along, and hence their bands are not broadened. A minor proportion of transport through the vapour phase is sufficient to block the expansion of the sample components.

The proportion of the liquid transferred through the liquid and the vapour phase seems to depend on the evaporation energy of a solvent. Further, it depends on minor details of the conditions, which is also the reason for the often poor reproducibility of the extent and the pattern of the peak distortion. We noted that minor temperature gradients in the inlet section of the column are very important. The distortion was changed by turning the column into another position in the gas chromatographic (GC) oven, as illustrated in Fig. 1. The same mixture of *n*-alkanes

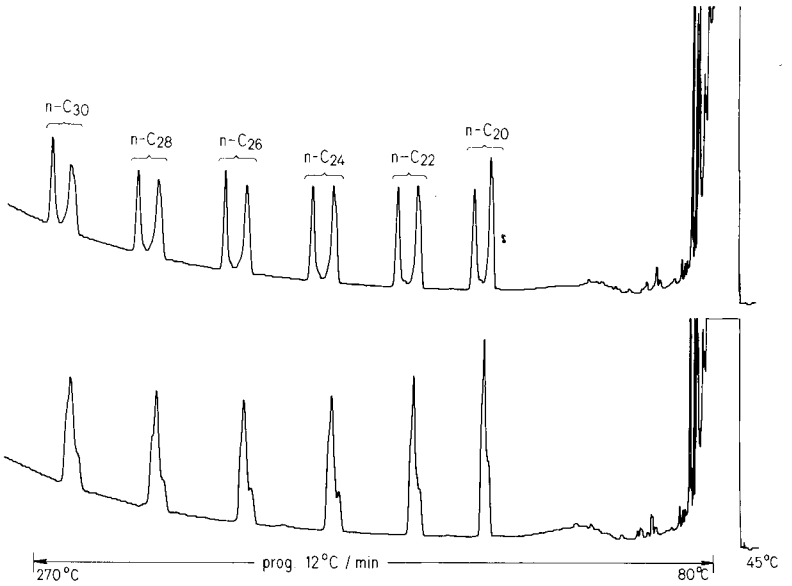

Fig. 1. Comparison of the distortion pattern of peaks in two chromatograms run under identical conditions except for the position of the column inlet in the GC oven. Volumes of 2 μl of the even-carbon C_{20}–C_{30} *n*-alkanes diluted 1:50,000 in acetone; cold on-column injection at 45°C into a 5 m × 0.30 mm I.D. glass capillary coated with 0.6 μm of OV-73 with a fully coated inlet section; temperature programme, 10°C/min from 80 to 270°C. For the upper chromatogram the column turned from the injector towards the centre, and for the lower chromatogram towards the corner of the GC oven. The distortion pattern shows that the alkanes were distributed differently within the flooded zone. The materials were located at the ends of the flooded zone in the upper chromatogram and remained together in the lower chromatogram. We assume that these differences are due to different proportions of solvent transported through the vapour phase.

dissolved in acetone was injected twice. All analytical conditions were kept constant except that the column was turned by about 60° about the straightened inlet section. Instead of going from the injector towards a corner, the column turned towards the centre of the oven. The distribution of the sample material within the flooded zone changed completely. In one instance the material was split into two portions located near the ends of the flooded zone. In the other position of the column the materials remained together, thus producing a single, although distorted, peak.

We assume that the phenomenon of band broadening in space may not only be observed as a result of the flooding solvent as described up to now. We expect that certain types of peak tailing behave in the same way and that some undesirable solvent effects producing distorted peaks might be better understood when relating them to this kind of band broadening. However, these subjects need to be explored further.

THE RETENTION GAP

Band broadening in space cannot be corrected by the conventional reconcentration techniques used to eliminate the effects of the band broadening in time, *i.e.*, cold trapping and the solvent effect[2]. Band broadening in space is in fact even an undesirable side-effect of the solvent effect. The reconcentration of the bands resulting from band broadening in time requires a temporary increase in the retention in the column inlet. However, GC retention does not hinder the sample spreading out in the liquid phase.

The concept of the reconcentration of the bands broadened in space calls for the opposite: instead of an increase in the retention it requires a retention gap, *i.e.*, an inlet section of the column with a negligible retention compared with the separating major part of the column. The retention gap accelerates the migration of the sample components and allows them to be reconcentrated on the beginning of the regular film of the stationary phase. The length of the retention gap zone has to include the complete flooded zone. Hence about 60 cm should be sufficient for sample volumes up to 1.5 μl.

The mechanism of reconcentration by the retention gap may be described differently for temperature-programmed and isothermal runs. Both explanations have their benefits. They might appear to be different just because of the simplifications involved.

Assuming that a wash of the column inlet extracted 90% of the stationary phase, the sample components migrate through this section of the capillary at a temperature decreased by about 50°C. In temperature-programmed runs the components move at relatively low temperature through the column inlet as far as to the beginning of the regular coating of the stationary phase, where they are focused by the increasing retention. As they have to "wait" there, the front and rear ends of the broadened band nearly meet each other. The components wait until the column temperature is sufficiently increased to allow their chromatography.

In isothermal GC a reduced retention in the column inlet increases the speed of the migration of the sample components. The acceleration is approximately proportional to the reduction of the film thickness of the stationary phase (phase ratio). Thus a 90% extraction of the stationary phase accelerates chromatography by a factor of

ten. As a consequence, the sample arrives at the beginning of the regular film within a time shortened by a factor of ten, *i.e.*, the original width of the band is reduced by 90%. Alternatively, looking at the front and rear ends of the band, the front of the band migrates on the regular coating by a tenth of the speed of the rear end until the latter also reaches the regular film. Thus the rear end is able to reduce its delay to the front by 90%.

The retention gap does not completely eliminate the effects of the band broadening in space because "retention gap" never means "zero retention". However, as in most instances it is easy to reduce the retention in the column inlet by a large factor, the peak broadening rapidly becomes negligible.

Fig. 2 and Table I show some experimental data on the depth of the retention gap required to render peak distortion negligible. We used a capillary with an extremely thick coating (2 μm of OV-73) and varied the retention of its inlet section. First, the column was 7 m long and coated throughout the inlet (end-section straightened electrically under nitrogen[3]). Then 1 m of the column was replaced with 1-m pieces of other columns with a known, lower film thickness, reducing the film thickness stepwise by factors of two. The stationary phase of all columns was immobilized[4] to prevent phase stripping. The effects on peak broadening were determined by cold on-column injections of 1.5 μl of the even-carbon C_{20}–C_{30} *n*-alkanes diluted 1:50,000 in acetone. The chromatogram on the bottom of Fig. 2 shows the full effect of the band broadening in space as obtained by the column inlet coated with the 2 μm film. The peaks are split and broadened by a factor exceeding four. The chromatogram next to the bottom was obtained from the 6-m column with a 2-μm coating attached to a 1-m inlet section with a 1-μm film (using shrinkable PTFE tubing). Peak splitting and broadening were strongly reduced but were still severe. The next chromatogram was obtained from the configuration with an inlet section of a quarter of the film thickness of the main column. Peak splitting disappeared, but peaks were still noticeably distorted and broadened. The top chromatogram was made on a column attached to a 1-m persilanized but uncoated inlet section. In this chromatogram the peaks were no longer distorted and their width corresponded to a chromatogram made by a split injection.

Table I lists the peak widths at half-height obtained from chromatograms as shown in Fig. 2 (although the widths at half-heigth have to be considered as rough approximations when peaks are distorted or even split). The broadening effect due to band broadening in space was calculated by subtraction of the peak width of the capillary with the uncoated pre-column from the peak widths of the columns with coated inlets. The data show that the broadening effect is halved when the thickness of the coating of the pre-column is halved. This is in agreement with the mechanism of the retention gap as described above; the sample components are accelerated by the same proportion as the film thickness (phase ratio) of the inlet section is reduced. If the two maxima of the split peak reach the beginning of the stationary phase in half the time, the distance between the two maxima is also halved.

The data in Table I are based on moderately extreme conditions; the column was short (6 m) and the sample volume was fairly large (1.5 μl), using acetone, which provides the virtually complete realization of the broadening effect. Under these still realistic conditions a decrease in the film thickness in the retention gap area by a factor of ten still gave considerable peak broadening (a decrease in separation ef-

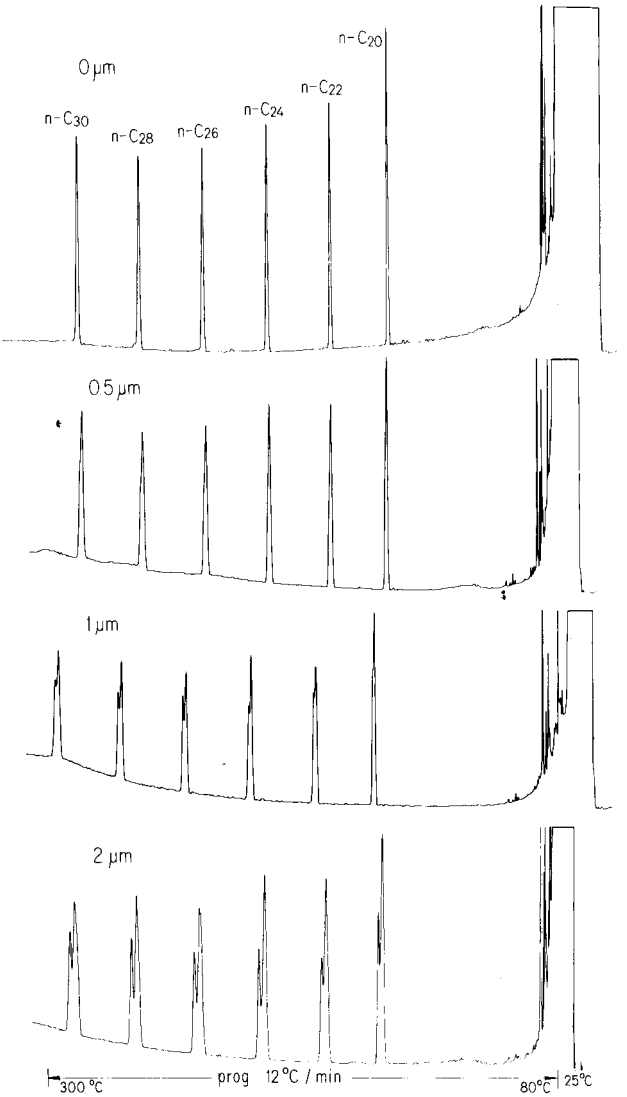

Fig. 2. Effect of the film thickness in the column inlet on the peak distortion by the band broadening in space. The bottom chromatogram was made on a 7-m column coated with 2 μm of OV-73. For the chromatograms above, 1 m of the column inlet was replaced with 1 m of column coated with only 1 and 0.5 μm of the same stationary phase. For the top chromatogram the column inlet consisted of persilanized but uncoated tubing. Volumes of 1.5 μl of the indicated *n*-alkanes, diluted 1:50,000 in acetone, were injected with an open oven door by cold on-column injection; 0.1 atm of hydrogen as carrier gas; temperature programme 12°C/min from 80 to 300°C, started 20 sec after the injection. The broadening effect is halved for each reduction of the film thickness in the column inlet by a factor of two. The top chromatogram with the uncoated pre-column gave the same peak width as a split injection. Peak widths and broadening effects, listed in Table I, indicate that a retention gap to render peak distortion negligible requires a reduction of the film thickness in the retention gap zone by a factor of 50–100. Under conditions creating less distortion by the band broadening in space, a smaller reduction is sufficient.

TABLE I

PEAK WIDTHS AT HALF-HEIGHT AND BROADENING EFFECTS FOR C_{22}, C_{26} and C_{30} *n*-ALKANES WHEN 2 μl OF THEIR ACETONE SOLUTION WERE INJECTED INTO A 6-m COLUMN COATED WITH 2 μm OF OV-73 WITH ATTACHED 1-m INLET SECTIONS COATED WITH VARIOUS FILM THICKNESSES

Film thickness of inlet (μm)	*Peak width (mm)*			*Broadening effect (mm)*		
	n-C_{22}	*n*-C_{26}	*n*-C_{30}	*n*-C_{22}	*n*-C_{26}	*n*-C_{30}
2	4.8	5.0	5.2	3.2	3.8	4.0
1	2.4	2.8	3.2	1.4	1.6	2.0
0.5	1.8	2.2	2.3	0.8	1.0	1.1
0.25	1.3	1.7	1.8	0.3	0.5	0.6
0.08	1.1	1.2	1.3	0.1	0	0.1
0	1.0	1.2	1.2	–	–	–

ficiency in terms of separation number, TZ, of about 40%). A retention gap to reduce the peak broadening to a negligible level required a reduction in the retention by a factor of 50–100. However, for longer columns and smaller sample volumes a reduction in the retention by a factor of 10 is sufficient.

The model considering the mechanism of the retention gap in isothermal runs is useful as it allows correct predictions. However, if the chromatogram is run isothermally at the column temperature during the injection, band broadening in space does not occur. The conditions creating broadened and distorted peaks always involve steps which resemble temperature programming. For an analysis above the boiling point of the solvent, the column temperature during sampling must be decreased. As soon as the sampling process is finished, the column temperature is rapidly increased to the temperature of the analysis. Thus even isothermal analyses include in fact a (controlled or uncontrolled) step of temperature programming.

It may be objected that an uncoated section of the column behaves as a dead volume because it allows diffusion processes to broaden the bands, but it does not contribute to the separation. However, this holds true in only a single case: if the column is used isothermally at the temperature during the injection and if the sample is introduced by a split injection. Even in this instance, the broadening is small because the residence time of the sample in this column section is short. As the components are virtually not retained, the residence time is just a fraction of the dead time of the column which is equal to the proportion of the retention gap on the total length of the column. For a retention gap of 1-m length in a 10-m column and for a component eluted with a capacity factor $k = 5$, the peak is estimated to be broadened by 2%. Under the usual working conditions it is even less. As soon as temperature programming is involved, the re-concentration on the beginning of the regular film of the stationary phase, eliminates the broadening effect. In splitless or cold on-column injection the broadening effect is reduced by the solvent effect if working isothermally or again is completely eliminated as soon as a substantial temperature increase after the injection is involved.

Fig. 3 gives an example of a routine analysis where the retention gap is a prerequisite for reasonable chromatography. Sterols, *e.g.*, from fats, margarines or

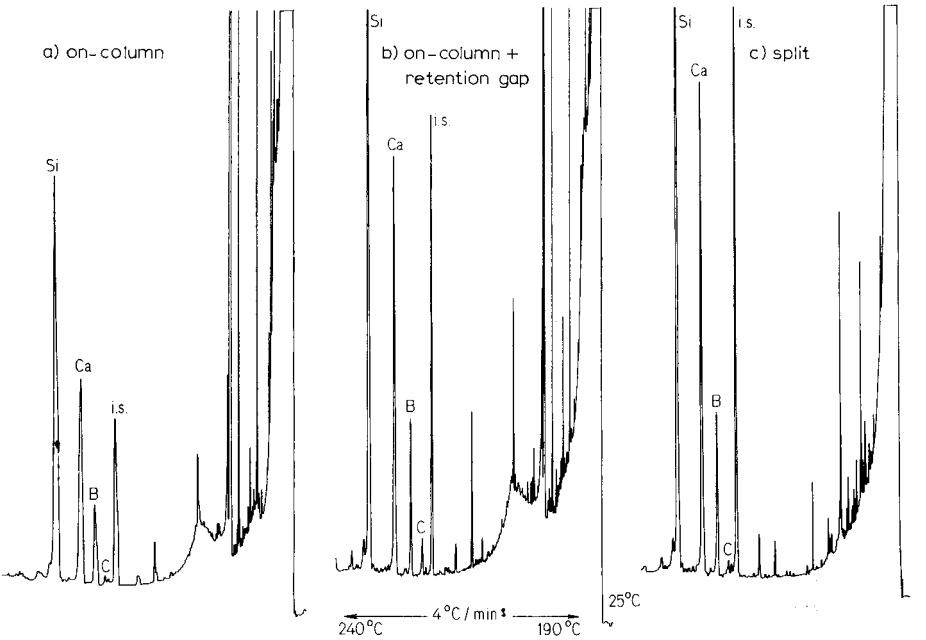

Fig. 3. Analysis of free sterols (from rapeseed oil) as an application of the retention gap. (a) Cold on-column injection of 0.7 μl of an ethereal solution at 25°C; 15 m × 0.32 mm I.D. glass capillary, coated with 0.15 μm of OV-73 throughout the column; 0.3 atm of hydrogen as carrier gas; temperature programme 4°C/min from 190 to 240°C. Peaks: i.s. = internal standard (*n*-triacontane); C = cholesterol; B = brassicasterol; Ca = campesterol; Si = sitosterol. All peaks are distorted by the band broadening in space. (b) As (a) but a 60-cm length of a persilanized, uncoated capillary was linked to the column inlet to serve as a retention gap. Peak widths are now the same as in (c) for a vaporizing split injection. Cold on-column sampling is preferable to split sampling because of the accuracy of the results.

similar foodstuffs, are easily analysed in their underivatized form on a moderately well deactivated capillary column. For several applications an accuracy of the results in the range 2–5% is required. The large amount of the material available would allow a vaporizing split injection, the most rapid and most convenient injection technique for this application. However, unless the conditions are well optimized and quantitation is based on carefully designed calibration procedures, the required accuracy is not guaranteed. The sterols enter the column by a smaller proportion than the internal standard (an *n*-alkane), and this proportion is difficult to reproduce. For split injection the use of the alkali-stable coprostanol as an internal standard is preferable, but it still gives high deviations. Accuracy is no problem when using cold on-column sampling. However, as chromatogram A in Fig. 3 shows, the band broadening in space requires attention. This chromatogram was obtained by an injection of 0.7 μl of an ethereal solution of the unsaponifiable material of rapeseed oil on a 15 m × 0.30 mm I.D. glass capillary coated with 0.15 μm of OV-73. Thus conditions did not favour band broadening in space as the sample volume was relatively small and for many purposes a third of the column length would have done the separation just as well.

The use of a 60-cm long persilanized and uncoated pre-column (connected by shrinkable PTFE tubing) solves two problems with this analysis simultaneously. It

serves as a retention gap, completely eliminating the peak broadening effects as shown by the comparison of chromatograms B and C, representing cold on-column injection with a retention gap and vaporizing split injection, respectively. Second, the empty pre-column greatly reduces the problems with the by-products extracted from the strongly alkaline aqueous solution. In routine practice we neither wash the ethereal solution intensively to remove the alkali, nor do we dry it. In particular, basic salts rapidly destroy the silicone phases. As alkaline salts are not volatile, they are deposited exclusively in the flooded inlet section on the column. The absence of stationary phase in this section of the column prevents the resulting bleeding and peak tailing due to accumulated degradation products.

CONCLUSIONS

Band broadening in space hinders analyses of certain injection techniques as long as it is not recognized and understood. However, the introduction of a retention gap by keeping the column inlet free from stationary phase is so easy that band broadening in space cannot be considered a problem.

We have recommended the use of capillary inlets free from stationary phase for many years, although for another reason. Most problems with capillary columns during their use are due to deficiencies in the inlet sections. The replacement of the inlet section, either by breaking it off or by replacing a pre-column, renovates most used columns[5,6]. However, the absence of stationary phase in the inlet section avoids these problems to a large extent. Hence the use of columns with an empty inlet section now has another advantage due to the retention gap.

The retention gap may be introduced in many ways, but in to our experience most of them have limitations. These technical aspects will be discussed in a forthcoming paper.

REFERENCES

1 K. Grob, Jr., *J. Chromatogr.*, 213 (1981) 3.
2 K. Grob and K. Grob, Jr., *J. High Resolut. Chromatogr. Chromatogr. Commun.*, 1 (1978) 57.
3 K. Grob, G. Grob, B. Brechbühler and P. Pichler, *J. Chromatogr.*, 205 (1981) 1.
4 K. Grob, G. Grob and K. Grob, Jr., *J. Chromatogr.*, 211 (1981) 243.
5 K. Grob, Jr., *J. High Resolut. Chromatogr. Chromatogr. Commun.*, 1 (1978) 307.
6 F. Berthou and Y. Dreano, *J. High Resolut. Chromatogr. Chromatogr. Commun.*, 2 (1979) 251.

Journal of Chromatography, 237 (1982) 25–39
Elsevier Scientific Publishing Company, Amsterdam — Printed in The Netherlands

CHROM. 14,453

ADSORPTION–THERMAL DESORPTION AS A METHOD FOR THE DETERMINATION OF LOW LEVELS OF AQUEOUS ORGANICS

JAMES F. PANKOW* and LORNE M. ISABELLE
Department of Environmental Science, Oregon Graduate Center, 19600 N.W. Walker Road, Beaverton, OR 97006 (U.S.A.)
(First received August 3rd, 1981; revised manuscript received October 20th, 1981)

SUMMARY

Adsorption followed by thermal desorption (ATD) with Tenax GC is an effective analytical tool for the preconcentration–analysis of water samples containing μg/kg quantities of the three United States Environmental Protection Agency (U.S. EPA) "Priority Pollutants" *p*-dichlorobenzene, hexachloro-1,3-butadiene, and 2-chloronaphthalene. A centrifugation method allows the removal of all but 80 μl of water from a glass cartridge packed with 0.75 g Tenax GC. A 10-min follow-up vacuum-desiccation step will reduce the residual water to ≈ 5 μl. A new procedure is presented for conducting recovery tests with sparingly soluble compounds and for the desorption of loaded cartridges. The recovery efficiencies for the three compounds showed little dependence upon the sample flow-rate in the range 0.25–2.0 ml/sec. One cartridge adsorbed ≈ 80% of these compounds at all flow-rates, and a second cartridge in series recovered the remaining ≈ 20%.

INTRODUCTION

Several analytical procedures have been developed for the analysis of trace organics in water, including purge and trap[1], "Grob stripping"[2], solvent extraction[3], and adsorption onto a solid support, such as the Amberlite XAD resins, followed by solvent extraction[4]. A fifth technique, adsorption from aqueous solution onto a solid support followed by thermal desorption (ATD), although very promising for certain types of analyses[5–10], has not been studied extensively. Three conclusions may be drawn:

(1) The inert gas purging methods are effective for many of the volatile organic compounds.

(2) Solvent-extraction-based methods do not allow equal ease of determination for compounds of relatively low volatility.

(3) ATD presents an attractive method for the analysis of compounds of low to intermediate volatility. It does not require solvents, and provides for maximum sensitivity since all of the adsorbed organics may be desorbed onto the analytical gas chromatographic (GC) column.

0021-9673/82/0000–0000/$02.75

Rationale for the development of ATD with Tenax GC

The fact that ATD has not developed into an accepted analytical technique for aqueous samples is due to the difficulties experienced during early research with:

(1) The extremely high blank levels associated with the thermal desorption of resin adsorbents such as the styrene-divinylbenzene polymer Amberlite XAD-2[11]. (Modified XAD-4 polymers can be synthesized which have lower blank levels[6].)

(2) The tendency for the activated charcoal adsorbents to retain many organics and catalyze their degradation[12].

(3) The relatively low specific surface area (10–30 m^2/gram[13,14]) of the adsorbent Tenax GC.

(4) The retention of water in the inter-particle void volume of the cartridge as well as within the particles of adsorbent, and the problems which this water poses for columns and detectors (*e.g.*, the flame ionization detector (FID) and the mass spectrometer (MS)).

The use of Tenax GC as the adsorbent in aqueous ATD alleviates the first and second problems. This material, poly(2,6-diphenyl-paraphenylene oxide)[15] is stable up to temperatures of 350°C, exhibits very low blank levels on thermal desorption[11,15], and has been used extensively in the ATD analysis of the atmospheric environment[16–18]. Problems posed by water on the adsorbent may be circumvented by drying the cartridge prior to desorption. Versino *et al.*[8] have shown that storage of Tenax GC cartridge tubes over the desiccant P_2O_5 at 10 Torr for 24 h is an effective drying procedure which gives 99% recoveries at the μg level, even for volatile compounds such as benzene. If the cartridge is thermally desorbed directly onto a capillary column which is at sub-0°C temperatures, this type of thorough desiccation will be required to avoid plugging the column with ice. If focussing at such low temperatures is not required, complete desiccation may not be necessary as fused silica columns are now available which are reportedly stable to repeated loadings of low μl amounts of water[19].

At 19–30 m^2/g (refs. 13 and 14), Tenax GC does not have as high a specific surface area as desired in an adsorbent, and it probably has a lower capacity for most organics than do the styrene–divinylbenzene polymers XAD-2 (290–330 m^2/g)[20] and XAD-4 (750 m^2/g)[21]. Nevertheless, in studies using solvent extraction as the recovery step, Leoni and co-workers[22,23] have found Tenax GC to be very retentive of pesticides such as γ-BHC and DDT as well as the polychlorinated biphenyls (PCBs) and several polynuclear aromatic hydrocarbons (PAHs). Therefore, although Tenax GC is both thermally stable at elevated temperatures as well as adsorptive of non-polar, aqueous organics, the potential of ATD with this material has not been developed beyond the preliminary investigations carried out by earlier workers[8,10].

The three compounds *p*-dichlorobenzene, hexachloro-1,3-butadiene, and 2-chloronaphthalene have been chosen as model compounds. Chlorinated organics are often found as contaminants in drinking waters[24]; these compounds are of particular interest since they are among the "base–neutrals" in the U.S. EPA Priority Pollutant List and in many cases must be determined by solvent extraction procedures. This paper will demonstrate the applicability of ATD with Tenax GC to the preconcentration–analysis of compounds such as these.

EXPERIMENTAL APPROACH

Recovery tests

Many organic pollutants of interest have solubilities in the low ppm range, and those of *p*-dichlorobenzene, hexachloro-1,3-butadiene, and 2-chloronaphthalene are 79[25], 2[26], and 7 ppm[27], respectively. (The solubilities of the other organic Priority Pollutants have recently been compiled by Callahan *et al.*[27]). In the determination of the efficiency of solvent extraction or inert gas purging procedures, one may simply spike the solution to be assayed. Material which is lost to the vessel walls may be recovered during the execution of the method. In the examination of cartridge adsorption efficiencies, however, such wall losses will not be recovered. We have adopted a method which circumvents this problem. It involves injecting a small volume ($\approx \mu$l) of water-miscible solvent containing μg quantities of the analytes into a stream of water which then passes on to the cartridge. While this approach does not simulate what occurs when the same overall volume of water containing the same amount of dissolved analyte(s) is passed through a cartridge, it will provide a *lower* bound on the retention efficiencies since: (1) the analytes flow on in one slug and the adsorbent is then washed by analyte-free water; and (2) the small amount of solvent injected may tend to help retain some portion of the analyte(s) in solution as the slug passes through the resin bed. We included a cartridge of tightly packed glass wool between the first Tenax GC cartridge and the injection port to retain any particles of analyte which might precipitate during this injection process. Their rapid re-solubilization would then take place in a manner similar to what occurs in the "generator columns" recently conceived for the preparation of low-level aqueous standards of sparingly soluble PAHs[28]. The occurrence of irreversible adsorption on the glass wool may be ruled out if all of the analyte materials are recovered from the cartridges.

Cartridge desiccation

While the 24-h vacuum desiccation of Versino *et al.*[8] appeared to be too time-consuming, the simple passage of a high velocity stream of nitrogen through the cartridges to dislodge the water as done by other workers seemed incapable of providing adequate desiccation. We have investigated a two-step desiccation procedure. The first step utilizes centrifugation to remove the bulk of the water, and the second step involves evacuating the cartridge for a 10–20 min period of time.

Cartridge desorption

Many methods and devices have been proposed in the literature for the desorption of sorbent cartridges into GC systems. A considerable amount of this work has been carried out by researchers involved in the analysis of trace organics in air. The simplest approach has been to insert a loaded sorbent cartridge before the GC column using compression fittings such as those marketed under the tradename Swagelok (Crawford Fitting, Solon, OH, U.S.A.)[5,10,11,31,33,36]. After a suitable purge time for the removal of any oxygen which may have entered the system, the cartridge is flash desorbed by thermal means. Resistively heated wire and tape[31] and ovens which slide over the cartridge[10,11,36] provide the heat. Although this interfacing method is simple, it is cumbersome in practice due to the nut loosening, nut tightening, and leak testing required.

A second class of desorption device utilizes a capped injector-type chamber[16,29,30] maintained at the desorption temperature. The cartridge is inserted, and a flow of carrier-gas transfers the analytes onto either an intermediate trap (a second sorbent bed or a cooled capillary line) for focussing[16,29,30] or directly onto the head of the analytical column. The disadvantages are: (1) no provision is made for purging oxygen from the cartridge prior to its desorption; (2) the cartridge does not make a positive seal in the chamber to the carrier gas supply, therefore close tolerances must be maintained in order that the majority of the desorption flow passes through the cartridge in a reproducible manner from cartridge to cartridge, and not merely via the annular space between the cartridge and the chamber; and (3) contaminants on the outside of the cartridge may enter the analytical column via whatever flow is passing through this annular space.

The desorption apparatus which we have constructed does not suffer from these deficiencies. The exchange of one cartridge for another does not require the removal of ferrule type fittings, and yet a positive seal is made between the cartridge and the analytical column. Furthermore, provision is made for the removal of oxygen from the cartridge prior to desorption.

EXPERIMENTAL

Cartridge preparation

The cartridges were of Pyrex glass (Corning Glass, Corning, NY, U.S.A.). The bed length, I.D., and O.D., were 7.0, 0.9, and 1.25 cm, respectively. A 1.5-cm piece of 2.0 mm I.D., 6.4 mm (0.25 in.) O.D. glass tubing was fused to each end of this main body. The overall length of a cartridge was 10.0 cm. The cartridges were packed with approximately 0.75 g of 35–60 mesh Tenax GC obtained from Alltech Assoc. (Los Altos, CA, U.S.A.). The Tenax GC was held in place with silanized glass wool (Supelco, Bellefonte, PA, U.S.A.). After passing a 20-ml/min flow of nitrogen (precleaned with charcoal and molecular sieve 5A (Chemical Research Services, Addison, IL, U.S.A.)) for 60 min to remove oxygen, the cartridges were conditioned for 60 min at 280°C. They were then cooled quickly, removed from the nitrogen flow, and sealed with 1/4-in. Swagelok end caps with TFE Teflon® ferrules.

Recovery tests

The apparatus used in recovery tests is presented in Fig. 1. The water used to fill the reservoir was obtained from a Millipore (Bedford, MA, U.S.A.) Super-Q water purification system. This system contains an activated carbon bed in addition to ion-exchange beds. The gases occupying the cartridge void volumes were first removed by setting the peristaltic pump at a fast flow-rate ($\approx$ 4–5 ml/sec) for approximately one min. The flow-rate for a given experiment was then set, and 4 μl of the 0.5-μg/μl standard (in acetone) was injected through the septum. After the passage of the first liter of water, the second Tenax GC cartridge was replaced with an identical cartridge and a second liter of water was passed through the system. Two more liters of water were then passed only through the first cartridge. All three of the cartridges were then desiccated and analyzed.

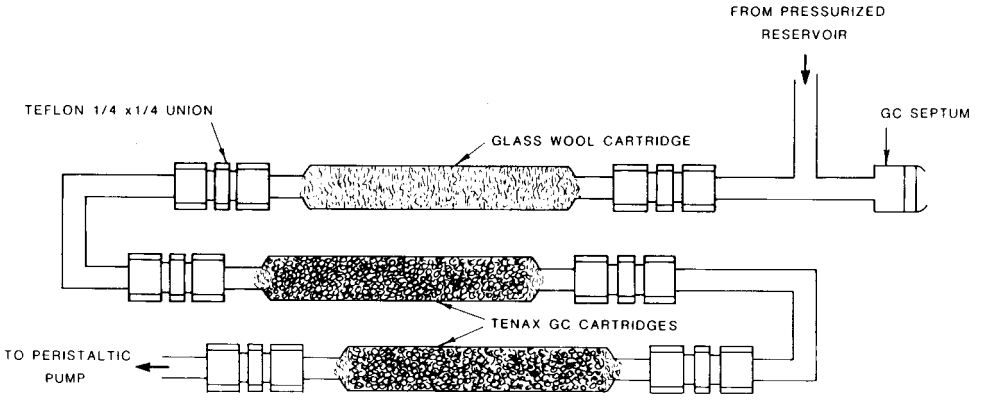

Fig. 1. Apparatus used for recovery tests.

Cartridge desiccation

A wet cartridge was first spun at 3500 rpm for 10 min in a screw cap Pyrex culture/centrifuge tube previously cleaned by heating to 500°C in a muffle furnace. The screw cap liner and a set of two supporters were TFE Teflon (see Fig. 2). In some cases, additional water was removed with the apparatus presented in Fig. 3. The liquid nitrogen (LN_2) trap was included to protect the pump as well as to protect the cartridge from contaminants in the vacuum line. With both values closed, the cap was removed and the cartridge inserted. The valve on the vacuum line was then opened. After desiccation, this snap valve was again closed and the vacuum within the apparatus relieved via the second snap valve.

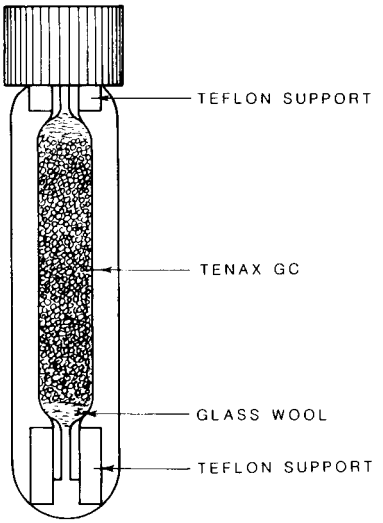

Fig. 2. Assembled culture tube for 3500 rpm centrifugation desiccation of adsorbent cartridges. Cap liner and cartridge supporters are of TFE Teflon®.

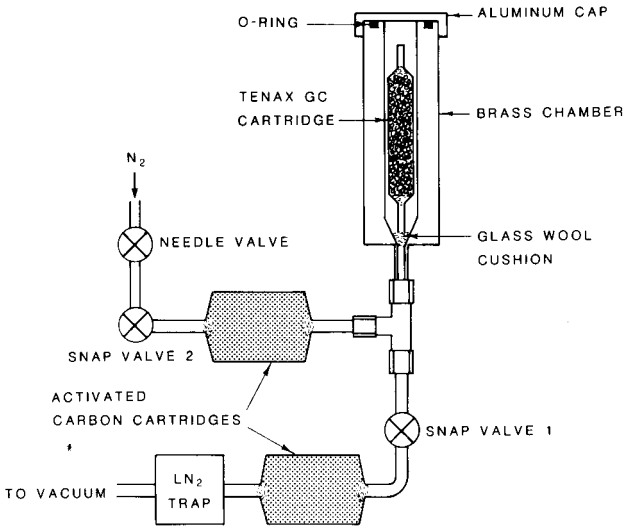

Fig. 3. Vacuum desiccation apparatus.

Cartridge desorption

The desorption apparatus which we have developed is presented in Fig. 4. This apparatus possesses several positive design features. They are:

(1) One gasket provides all necessary sealing. This gasket is made by punching out a 0.50-in. diameter hole from the center of a 0.75-in. diameter Teflon-backed Type F-174 GC septum obtained from Canton Bio-Medical Products (Boulder, CO, U.S.A.).

(2) Near all-brass construction provides for rapid heat conduction during thermal desorption.

(3) Cartridge and GC column may be butted up against one another.

(4) Upper and lower "septum" sweep lines prevent bleed contamination from septum sealing gasket. Upper sweep line also removes contaminants desorbed from exterior walls of cartridge.

(5) The desorbed analytes need not pass through any heated valving.

The following standard operation procedure (SOP) describes the use of this apparatus:

Step		*Comments*	
(1)	Turn off GC fan.	(1)	Helps to maintain high temperature in section of desorption apparatus which extends into GC oven.
(2)	Unscrew top knob, lift off brass desorption chamber, and remove previously desorbed cartridge.	(2)	–
(3)	Close snap-valve on line D.	(3)	Prevents carrier gas flow out of top of cartridge. This would occur if line D were left open and until such time that the brass desorption chamber had become pressurized.

(4)	Insert new cartridge and reverse step 2.	(4)	–
(5)	Purge cartridge 10 min with nitrogen. Flows: line A, 30 ml/min line B, 3 ml/min line C, 3 ml/min line D, 0 ml/min for first 3 min, then 5 ml/min line E, 0 ml/min	(5)	Removes O_2 from cartridge and column.
(6)	Open snap-valve on line D 3 min into O_2 purge time. (See step 5.)	(6)	Returns lower septum sweep flow and ensures that all desorption flow is on column.
(7)	Lower oven for 15 min. Flows same as in step 5.	(7)	Desorption.
(8)	Raise oven. Flows: line A, 0 ml/min line B, 3 ml/min line C, 3 ml/min line D, 5 ml/min line E, 30 ml/min	(8)	Carrier flow returned directly to column. Note continued upper septum sweep flow due to back flushing of cartridge.
(9)	Start temperature program GC run.	(9)	–

Gas chromatography

The oven top of a model 5700 Hewlett-Packard (Avondale, PA, U.S.A.) gas chromatograph was modified to accept the desorption apparatus. A 1.5 m × 2 mm I.D. glass GC column packed with 35–60 mesh Tenax GC was connected directly to the desorption apparatus with a graphite/vespel ferrule (Alltech Assoc.). During a GC analysis, the carrier gas, hydrogen, and air flow rates were 29 ml/min, 30 ml/min, and 240 ml/min, respectively. The detector temperature was 300°C. The column was at ambient temperature during the desorption of the cartridge. Following a desorption, the GC run was carried out using a temperature program run from 60° to 250°C at 16°/min. Chromatograms were recorded and peaks integrated with a Model 4100 Spectra-Physics (Santa Clara, CA, U.S.A.) computing integrator.

RESULTS AND DISCUSSION

Cartridge desiccation–centrifugation step

The cartridge desiccation procedure used for the bulk of the analyses involved only the centrifugation step. The amount of water remaining after this step was generally in the vicinity of 80 μl. This caused the formation of visible amounts of condensation within the packed column. Upon the initiation of the temperature program, this water did not extinguish the FID, nor did it interfere with these analyses since the first of the compounds to elute, *p*-dichlorobenzene, appeared in the temperature program at approximately 150°C. This is after all of the water had vaporized and left the column, and therefore we experienced no difficulty with this water interfering with the detector response for these compounds. The evaporative loss of the analyte compounds during the centrifugation step was also not a problem.

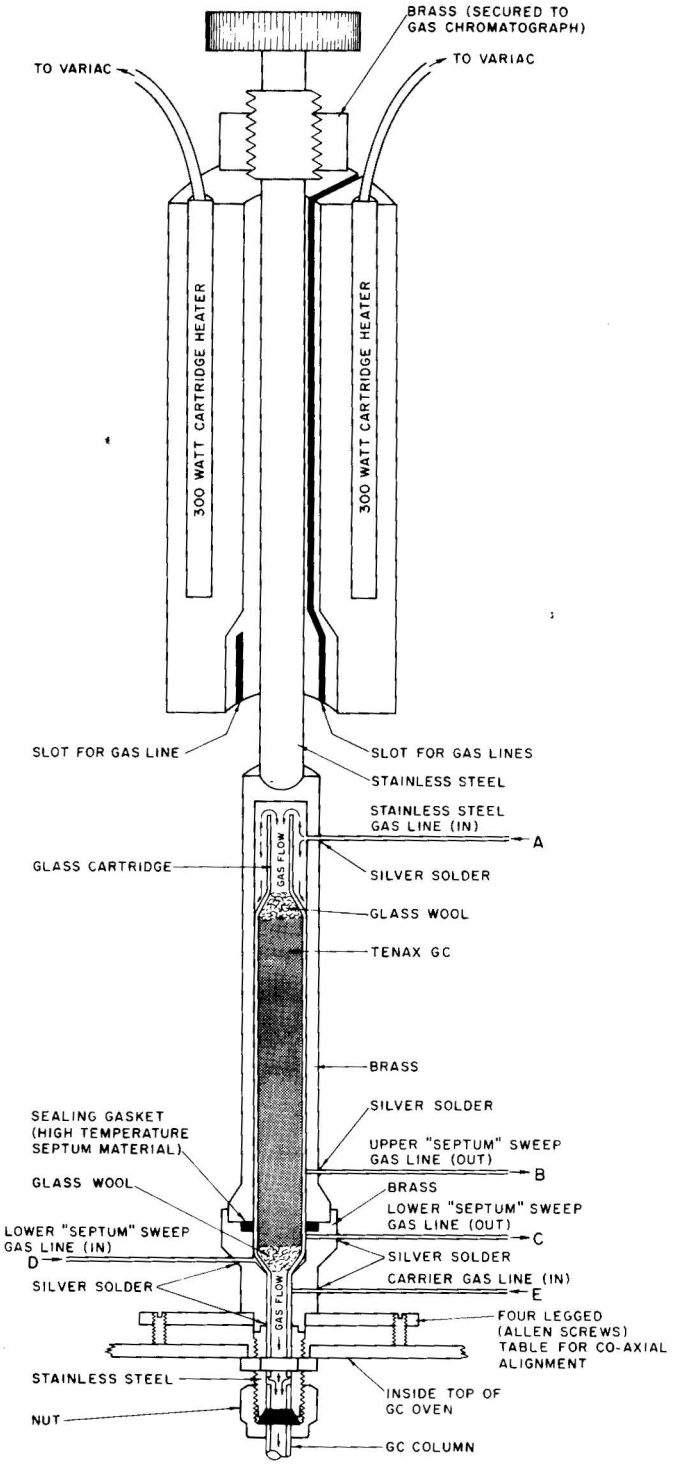

Fig. 4. Cartridge desorption apparatus. Desorption temperature is 280°C.

TABLE I

WEIGHT LOSS FROM A PRE-WETTED, CENTRIFUGE-DESICCATED TENAX GC CARTRIDGE SUBJECTED TO VACUUM DESICCATION

Time (min)	*Cartridge weight (g)*	*Cartridge weight change (g)*	*Water remaining (μl)*
0	10.6530	–	79.7
2	10.6355	0.0175	62.2
4	10.6129	0.0226	39.6
6	10.5981	0.0148	24.8
8	10.5871	0.0110	13.8
10	10.5784	0.0087	5.1
12	10.5746	0.0038	1.3
14	10.5743	0.0003	1.0
16	10.5742	0.0001	0.9
After thermal desorption at 280°C	10.5733	0.0009	0.0

Peak areas for runs in which a standard was injected directly onto fully wetted cartridges which were then centrifuge-desiccated and analyzed were found to be equal, within experimental error, to the peak areas obtained when the same amount of standard was placed onto pre-wetted, pre-centrifuge-desiccated cartridges.

Cartridge desiccation–evacuation step

Not all compounds of interest are retained on a Tenax GC column at temperatures exceeding the boiling point of water. Moreover, not all packed-column stationary phases are stable to μl amounts of water, and certainly 80 μl would preclude the use of capillary columns. An experiment was conducted to determine the rate at which a vacuum will remove the residual water. A centrifuge-desiccated cartridge containing 79.7 μl of water was vacuum-desiccated for a succession of 2-min periods (Table I). Approximately 94% of the ≈80 μl is removed in 10 min. We therefore chose 10 min as the standard desiccation period in a series of experiments designed to determine whether vacuum desiccation would cause a range of compounds to be lost from the Tenax GC cartridges.

Table II presents the percent recoveries observed for 2 μg of each of the compounds loaded onto pre-wetted, centrifuge-desiccated, then vacuum-desiccated cartridges. The desorptions were performed as discussed in the experimental section. These data indicate that vacuum desiccation does not cause significant loss for a variety of compound classes. They are also in agreement with the results of Versino *et al.*[8] (24 h evacuation) as well as research in the analysis of organics in air where Tenax GC has shown good retention properties during cartridge storage. The slight "losses" observed for tetracosane and methyl eicosanoate reflect a need for a longer cartridge desorption time with high molecular weight compounds.

The combination of centrifugation and vacuum desiccation is an effective procedure for the desiccation of fully-wetted cartridges. For packed-column work, a 10-

TABLE II

RECOVERY EFFICIENCIES FOR VARIOUS COMPOUNDS LOADED ONTO PRE-WETTED, CENTRIFUGE-DESICCATED TENAX GC CARTRIDGES

Compound			*Recovery (%)*
Aromatics	Benzene	C_6H_6	98 ± 1
	Toluene	C_7H_8	98 ± 1
	Xylene	C_8H_{10}	97 ± 1
Chlorinated hydrocarbons	*p*-Dichlorobenzene	$C_6H_4Cl_2$	95 ± 2
	Hexachlorobutadiene	C_4Cl_6	96 ± 1
	2-Chloronaphthalene	$C_{10}H_7Cl$	96 ± 1
Alkanes	Decane	$C_{10}H_{22}$	103 ± 0.5
	Tetradecane	$C_{14}H_{30}$	100 ± 0.5
	Hexadecane	$C_{16}H_{34}$	100 ± 0.5
	Docosane	$C_{22}H_{46}$	100 ± 1
	Tetracosane	$C_{24}H_{50}$	92 ± 5
Methyl esters of fatty acids	Methyl octanoate (methyl caprylate)	$C_9H_{18}O_2$	100 ± 1
	Methyl hendecanoate (methyl undecanoate)	$C_{12}H_{24}O_2$	100 ± 1
	Methyl tetradecanoate (methyl myristate)	$C_{15}H_{30}O_2$	100 ± 1
	Methyl octadecanoate (methyl stearate)	$C_{19}H_{38}O_2$	100 ± 1
	Methyl eicosanoate (methyl arachidate)	$C_{21}H_{42}O_2$	96 ± 1

min evacuation period is adequate if 1 to 5 μl of water may be tolerated. For capillary column work, a longer evacuation period may be required, particularly if sub-0°C focussing is needed.

Desorption efficiencies

Standards in acetone were used to place amounts ranging between 0.2–2.0 μg per component into the upper ends (as viewed in the desorption apparatus) of pre-wetted, centrifuge-desiccated cartridges. These cartridges were then desorbed and analyzed (Fig. 5). The fact that each of the plots is linear with a slope close to one indicates that: (1) the desorption efficiencies are linear across the mass range studied; and (2) a linear–linear plotting of the data would indicate zero response for zero mass.

When the desorption apparatus was first put into regular use, we felt that when the oven was first lowered, the ballistic temperature rise might caused the water remaining on the cartridge to volatilize so rapidly that the gas flow would back up in the cartridge and that a portion of the analyte(s) might thereby be lost to the surrounding brass enclosure. Since the cartridges analyzed in this series had been spiked on their upper ends, and since the analyses of spiked dry cartridges gave the same area/μg response factors, this was not problematic with the compounds studied. The fact that we saw little difference in the peak areas for cartridges which were spiked on

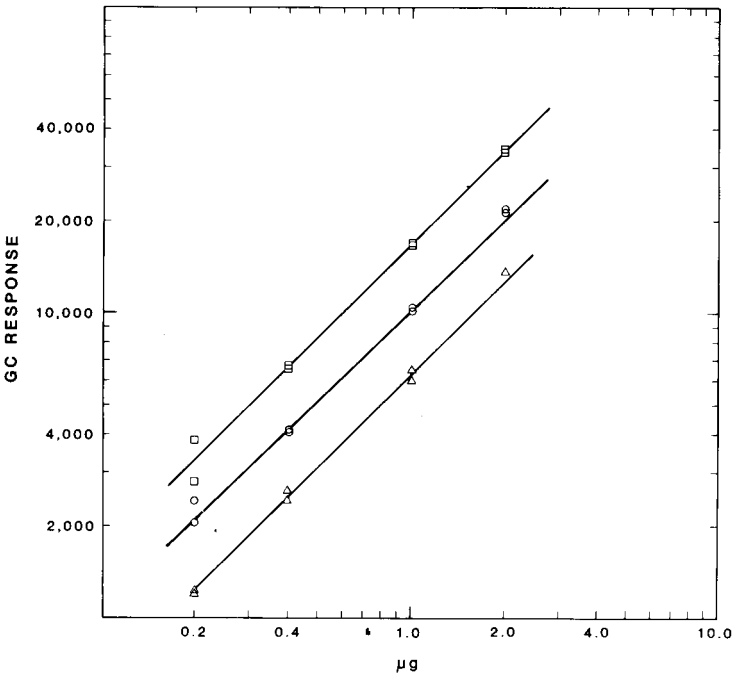

Fig. 5. Calibration plots for the desorption of varying amounts of *p*-dichlorobenzene (○), hexachloro-1,3-butadiene (△), and 2-chloronaphthalene (□). Plots are linear with slopes close to one.

the top *vs.* those spiked on the bottom indicates that desorption occurs equally well regardless of the physical distribution of the analyte(s) on the cartridges.

Recovery tests from water

A series of experiments was carried out at flow-rates of 0.25, 0.50, 1.0, and 2.0 ml/sec. A 4.0-μl volume of an acetone solution containing 0.5 μg/μl of each of the model compounds was injected at time zero. Fig. 6a–c are GC chromatograms from an experiment carried out at a flow-rate of 1.0 ml/sec. Fig. 6a is for the primary cartridge after 4 l had passed through. Fig. 6b is for the secondary cartridge, which was exposed to only the first of these 4 l, and Fig. 6c is for the secondary cartridge which was exposed to only the second of these 4 l. Fig. 7 is for the direct desorption of 4.0 μl of the acetone standard placed on the bottom of a pre-wetted, centrifuge-desiccated cartridge. The broad solvent peak is a result of the inability of the Tenax GC to retain the acetone at the head of the column during the desorption step. The retention times of the model compounds *p*-dichlorobenzene, hexachloro-1,3-butadiene, and 2-chloronaphthalene were approximately 9.5, 10.8, and 12.8 min, respectively. The relative magnitudes of the peak areas in Fig. 7 demonstrate the effects of chlorination on FID response factors. A variety of other peaks due to contaminants in the water and in the acetone are also present.

An examination of Figures 6a-c indicates that portions of these analytes escape the first cartridge and are retained on the second. However, this loss does not continue during the passage of the second liter (Fig. 6c) and seems related to the initial

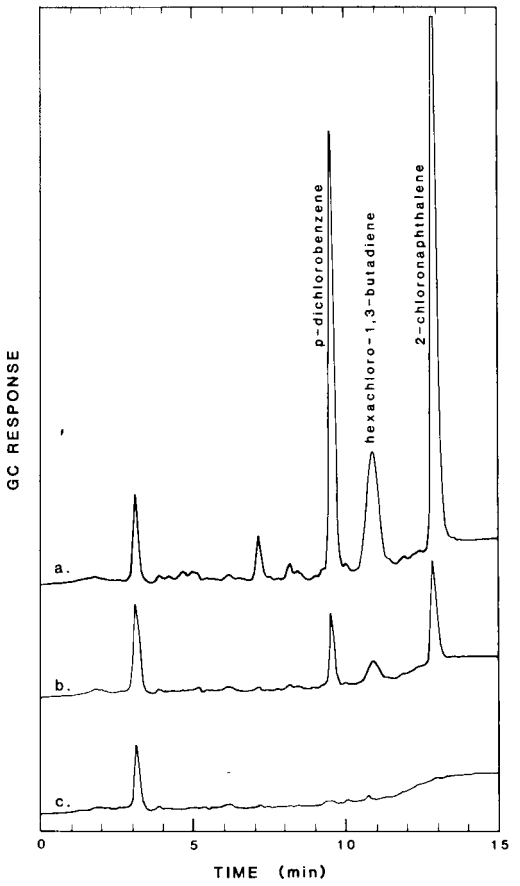

Fig. 6. Recovery from water of *p*-dichlorobenzene, hexachloro-1,3-butadiene, and 2-chloronaphthalene at 1.0 ml/sec. Attenuation = 128, or 128 × 5 × 10^{-12} A full scale for chromatogram a. a: Primary cartridge after 4 l. b: Secondary cartridge exposed to first of 4 l passing through primary cartridge. c: Secondary cartridge exposed to second of 4 l passing through primary cartridge.

injection. Remarkably, as Table III indicates, the percentage recovery (based on the desorption of a wet cartridge spiked on the bottom) did not appear to be a strong function of flow-rate. The recoveries based on the primary cartridge alone hover very near to 80%, and the recoveries including that retained on the first secondary cartridge are generally close to 100%.

CONCLUSIONS

The results obtained with a new type of desorption apparatus indicate that Tenax GC can retain non-polar organics of intermediate molecular weight very well even when substantial amounts (*e.g.*, 4 l) of water pass through the cartridges. Since flow-rates of ≈2 ml/sec are possible, a liter of water may be processed in only 8 min. This method is therefore simple, sensitive, and expedient, and will be applicable in the analysis of a wide variety of aqueous organic compounds.

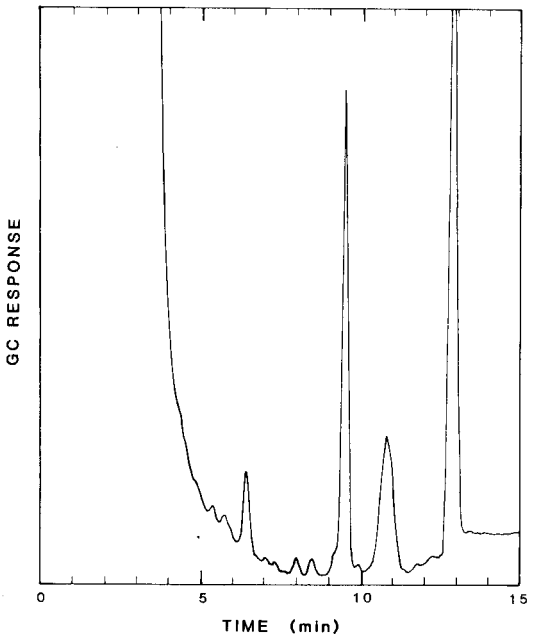

Fig. 7. Desorption of 4.0 μl acetone solution (containing 0.5 μg/μl per component) placed directly on bottom of pre-wetted and centrifuge-desiccated cartridge. Note solvent peak from acetone as for typical GC injection. This solvent peak is absent in Fig. 6. Attenuation = 128, or 128 × 5 × 10^{-12} A full scale for this chromatogram.

TABLE III

RECOVERY EFFICIENCIES AS A FUNCTION OF FLOW-RATE FOR *p*-DICHLOROBENZENE, HEXACHLORO-1,3-BUTADIENE, AND 2-CHLORONAPHTHALENE

Flow-rate (ml/sec)	*Compound*	*Recoveries (%)*	
		$\frac{\text{Primary cartridge}}{\text{Standard run}} \times 100$	$\frac{\text{Primary + first secondary cartridge}}{\text{Standard run}} \times 100$
0.25	*p*-Dichlorobenzene	86	101
	Hexachloro-1,3-butadiene	87	105
	2-Chloronaphthalene	81	98
0.5	*p*-Dichlorobenzene	76	87
	Hexachloro-1,3-butadiene	77	92
	2-Chloronaphthalene	83	99
1.0	*p*-Dichlorobenzene	80	92
	Hexachloro-1,3-butadiene	90	105
	2-Chloronaphthalene	78	91
2.0	*p*-Dichlorobenzene	81	100
	Hexachloro-1,3-butadiene	82	102
	2-Chloronaphthalene	74	94

ACKNOWLEDGEMENTS

This work was financed in part with federal funds from the United States Environmental Protection Agency (U.S. EPA) under Cooperative Agreement Identification Number 807898. The contents do not necessarily reflect the views and policies of the U.S. EPA nor does mention of trade names or commercial products constitute endorsement or recommendation for use. The authors thank Dr. John Glaser of the U.S. EPA Environmental Monitoring Support Laboratory, Cincinnati, OH, for helpful discussions during the course of this study. The authors also thank Ms. Toni Kristensen for her assistance in conducting a portion of the analytical work.

REFERENCES

1 T. Bellar and J. J. Lichtenberg, *J. Amer. Water Works Assn.*, 66 (1974) 739.
2 K. Grob and F. Zürcher, *J. Chromatogr.*, 117 (1976) 285.
3 W. A. Hoffman, Jr., *Anal. Chem.*, 50 (1978) 2158.
4 P. van Rossum and R. Webb, *J. Chromatogr.*, 150 (1978) 381.
5 J. P. Mieure and M. W. Dietrich, *J. Chromatogr. Sci.*, 11 (1973) 559.
6 J. P. Ryan and J. S. Fritz, *J. Chromatogr. Sci.*, 16 (1975) 488.
7 R. G. Melcher and V. J. Caldecourt, *Anal. Chem.*, 52 (1980) 875.
8 B. Versino, H. Knöppel, M. DeGroot, A. Peil, J. Poelman, H. Schauenburg, H. Vissers and F. Geiss, *J. Chromatogr.*, 122 (1976) 373.
9 M. Dressler, *J. Chromatogr.*, 165 (1979) 167.
10 S. N. Chesler, B. H. Gump, H. S. Hertz, W. E. May, S. M. Dyszel and D. P. Enagonio, *Trace Hydrocarbon Analysis: The NBS Prince William Sound/Northwestern Gulf of Alaska Boseline Study; NBS Tech. Note, No. 889*, NBS, Washington, DC, 1976.
11 W. E. May, S. N. Chesler, S. P. Cram, B. H. Gump, H. S. Hertz, D. P. Enagonio and S. M. Dyszel, *J. Chromatogr. Sci.*, 13 (1975) 535.
12 C. D. Chriswell, R. C. Chang and J. S. Fritz, *Anal. Chem.*, 47 (1975) 1325.
13 K. Sakodynskii, L. Panina and N. Klinskaya, *Chromatographia*, 7 (1974) 339.
14 E. D. Pellizzari, J. E. Bunch, R. E. Berkeley and J. McRae, *Anal. Lett.*, 9 (1976) 45.
15 R. van Wijk, in A. Zlatkis (Editor), *Advances in Chromatography 1970*, Chromatography Symposium, Houston, TX, 1970, pp. 122–124.
16 A. Zlatkis, H. A. Lichtenstein and A. Tishbee, *Chromatographia*, 6 (1973) 67.
17 E. D. Pellizzari, J. E. Bunch and B. H. Carpenter, *Environ. Sci. Technol.*, 9 (1975) 552.
18 T. Tanaka, *J. Chromatogr.*, 153 (1978) 7.
19 *1980 Products Catalog*, J&W Scientific, Rancho Cordova, CA, 1980.
20 *Technical Bulletin, Amberlite XAD-2*, Rohm & Haas, Philadelphia, PA, Nov., 1978.
21 *Technical Bulletin, Amberlite XAD-4*, Rohm & Haas, Philadelphia, PA, Feb., 1978.
22 V. Leoni, G. Puccetti and A. Grella, *J. Chromatogr.*, 106 (1975) 119.
23 V. Leoni, G. Puccetti, R. J. Colombo and A. M. D'Ovidio, *J. Chromatogr.*, 125 (1976) 399.
24 I. H. Suffet, L. Brenner and P. R. Cairo, *Water Research*, 14 (1980) 853.
25 K. Verscheueren, *Handbook of Environmental Data on Organic Chemicals*, Van Nostrand-Reinhold Press, New York, 1977.
26 C. R. Pearson and G. McConnell, *Proc. Royal Soc. London B*, 189 (1975) 305.
27 M. A. Callahan, M. W. Slimak, N. W. Gabel, I. P. May, C. F. Fowler, J. R. Freed, P. Jennings, R. L. Durfee, F. C. Whitmore, B. Maestri, W. R. Mabey, B. R. Holt and C. Gould, *Water Related Environmental Fate of 129 Priority Pollutants, Vols. I and II, Document Nos. 440/4-79-029 a and b*, U.S. EPA, Washington, DC, 1979.
28 W. E. May, J. M. Brown, S. N. Chesler, F. Guenther, L. R. Hilpert, H. S. Hertz and S. A. Wise, *Trace Organic Analysis: A New Frontier in Analytical Chemistry; Special Publication 579*, NBS, Washington, DC, 1979, p. 219.
29 W. Bertsch, R. C. Chang and A. Zlatkis, *J. Chromatogr. Sci.*, 12 (1974) 175.

30 E. D. Pellizzari, B. H. Carpenter and J. E. Bunch, *Environ. Sci. Technol.*, 9 (1975) 556.
31 J. W. Russell, *Environ. Sci. Technol.*, 9 (1975) 1175.
32 W. V. Ligon, Jr. and R. L. Johnson, Jr., *Anal. Chem.*, 48 (1976) 481.
33 J. P. Ryan and J. S. Fritz, *J. Chromatogr. Sci.*, 16 (1978) 488.
34 H. Peterson, G. A. Eiceman, L. R. Field and R. E. Sievers, *Anal. Chem.*, 50 (1978) 2152.
35 W. K. Fowler, C. H. Duffey and H. C. Miller, *Anal. Chem.*, 51 (1979) 2333.
36 J. P. Conkle, W. W. Lackey and C. L. Martin, *U.S. Patent*, 4,170,901 (1979).

Journal of Chromatography, 237 (1982) 41–48
Elsevier Scientific Publishing Company, Amsterdam — Printed in The Netherlands

CHROM. 14,424

SAMPLING TECHNIQUES IN THE GLASS CAPILLARY GAS CHROMATOGRAPHY OF FATTY ACIDS OF RAPE-SEED

R. HILTUNEN*
School of Pharmacy, University of Helsinki, Fabianinkatu 35, SF-00170 Helsinki 17 (Finland)
I. LAAKSO
School of Pharmacy, University of Helsinki (Finland)
S. HOVINEN
Plant Breeding Institute, Hankkija, Hyrylä (Finland)
and
J. DEROME
Finnish Forest Research Institute, Helsinki (Finland)
(Received August 13th, 1981)

SUMMARY

The development of erucic acid-free varieties of rape-seed presupposes highly-accurate determinations of fatty acids in rape-seed oil. Comparison of sampling techniques (split, splitless and on-column) indicated that the on-column technique gives the best results. Regular analyses carried out over a long period of time were found to be unreliable, especially if only small samples are taken from biologically very heterogeneous seed material.

INTRODUCTION

Impending legislation concerning the growing of erucic acid-free varieties of rape in Finland has resulted in the need for accurate and reliable fatty acid analyses in the breeding of suitable varieties of rape. As the varieties must be genetically pure as regards the formation of erucic acid, *i.e.* none of the multiple alleles controlling erucic acid synthesis must be present, very low levels of erucic acid may frequently have to be determined during the plant-breeding stage and subsequent monitoring of commercial crops grown from these varieties.

The correlation between the major and minor fatty acid components of rape-seed oil is high. For example, the presence of eicosenic acid in rape-seed oil indicates that the alleles controlling erucic acid synthesis are present. Hence reliable analytical determinations of minor fatty acids, which are of little significance in themselves, are of great importance for plant breeders in characterizing plant genotypes.

Nowadays, gas chromatography is the most common analytical method used in the determination of fatty acids. Very high accuracy and reproducibility can be achieved in gas–liquid chromatographic (GLC) analysis using present-day techniques

0021-9673/82/0000–0000/$02.75

and methods. The relative standard deviation (S_{rel}) for fatty acids, for instance, varies from 1 to 5% in repeated analyses, the precision of course depending on the relative proportions of the different components and their separability. However, such a high reproducibility does not always give a true picture of the reliability of this method because the S_{rel} values frequently presented in the literature have been obtained by repeating the analyses a number of times at short intervals, often within the course of a single day. In plant-breeding studies, on the other hand, one is forced to analyse, almost without exception, large sample lots over very long periods of time. In such cases, the columns almost invariably have to be changed at some time or other during the course of the trial, with the subsequent risk of changes occurring in the overall characteristics of the analytical set-up properties.

In capillary chromatography, the splitting conditions often have to be altered owing to the variation in the concentrations of the components in the samples being analysed. In addition, the instrument itself may have been replaced during the course of the experiment. In order to improve the reliability of the results, the different sources of error inherent in the analytical method have to be identified and an attempt made to estimate the magnitude of these errors for each component in the mixture.

As the greatest problem in GLC, and above all in capillary GLC, is nowadays no longer the choice of a suitable column or its quality, the sampling method and the instrument itself represent the most important sources of error.

The aim of this study was to determine the effect of variations in the splitting ratio and sample size on the reproducibility and accuracy of fatty acid analyses. Furthermore, the split, splitless and on-column methods are compared in connection with fatty acid analyses.

The results obtained by these different methods are compared with each other and with results obtained during the analysis of a large biological sample. In addition, the results of fatty acid analysis on the same selection line, carried out during 3 years, are compared with analyses made on the same line at short intervals.

EXPERIMENTAL

Materials

The cruciferous seed material (Spring turnip rape, *Brassica campestris* L. var. *annua*) used in this work was obtained from the Plant Breeding Institute of Hankkija, Hyrylä, Finland. A selected line (line 43.2) with a low erucic acid content was chosen as the representative sample. Seeds were also taken from a total of 486 plants of the lines (M_1 and M_2) obtained by crossing line P-7622 and line P-7629 for purposes of comparison. The oil from 10–15 seeds was extracted and the methyl esters of the components were prepared by esterification as described earlier[1].

Instrumentation

Gas chromatographic analyses were carried out with a Carlo Erba Fractovap 2300 gas chromatograph using either a split or splitless technique. On-column analyses were performed on a Dani 3200 gas chromatograph. Both instruments were equipped with a flame-ionization detector (FID). In addition, the Dani 3200 was also fitted with an on-column injector and secondary cooling system.

In the split and splitless trials a free fatty acid phase (FFAP) glass capillary

column (25 m × 0.35 mm I.D.) was used under the following conditions: carrier gas, hydrogen at 0.3 kg/cm^2 (flow-rate 2.9 ml/min), injector temperature 250°C, oven temperature 200°C (isothermal). The splitting ratio was either kept constant at 15:1, or else varied from 500:1, 200:1, 70:1, 15:1, 8:1, 7:1 to 3:1 when testing the effect of the splitting ratio. The sample size was either a constant 0.5 μl, or else varied from 0.1, 0.3, 0.6, 1.2 to 2.4 μl when determining the effect of increasing sample size. The number of successive analyses carried out in the different trials are shown in Tables I–IV.

A longer FFAP column (45 m × 0.35 mm I.D.) was used in the on-column analyses. Nitrogen was used as the carrier gas at 0.9 kg/cm^2 (flow-rate 1.8 ml/min).

Peak areas were measured with Infotronics CRS-208 (for the Carlo Erba gas chromatograph) and Hewlett-Packard 3390 A (for the Dani gas chromatograph) peak integrators.

The standard deviations, coefficients of variation and variances were used as measures of dispersion. The dispersion between the test groups were compared using variances and the *F*-test. Quantitative differences between the groups were tested by Student's *t*-test using the split sampling results as the basis of comparison.

RESULTS AND DISCUSSION

When comparing different methods of sample introduction or their modifications, two basic aspects, namely precision and accuracy, have to be taken into account.

Factors affecting the accuracy of a determination include, in addition to be integrator error, also the changes taking place during the vaporization of the sample, adsorption, decomposition, sample size and the splitting ratio[2–5].

Under constant volume, temperature and pressure, different-sized samples produced momentary changes in pressure in the vaporization chamber, resulting in short-term eddy currents. Such an explosive change in pressure results in the situation in which back pressure in the capillary column prevents the volatilized sample from entering the column[5,6].

If the splitting ratio is large, an appreciable proportion of those incompletely volatilized components of low volatility in the sample will escape through the split before the flow conditions in the system have stabilized[6]. The composition of the vapour entering the column is thus changed. This could be called "discrimination through volatility". Discrimination also takes place when a constant splitting ratio is used as the size of the sample is increased[4,7]. As well as affecting the quantitative results, the sample size also affects the precision of sample series and thus the comparison between different members of the same series. The results of analyses of the methyl esters of fatty acids obtained using the constant splitting ratio method and other methods are compared in Table I.

It can be seen from Table I that there are very significant ($p < 0.01$) and highly significant ($p < 0.001$) quantitative differences between the different methods. In addition, the dispersions of the results of the different sampling methods were either very significantly or highly significantly different in the case of certain components. The mean precision (coefficient of variation, C.V. = 2.3%) for the on-column technique was the best, the mean values for the split and splitless techniques being of

TABLE I

COMPARISON OF SAMPLING TECHNIQUES IN GLC ANALYSIS OF FATTY ACIDS IN RAPE-SEED OIL

Fatty acid	*Split (n = 10)*			*Splitless (n = 6)*			*On-column (n = 6)*		
	Relative peak area (%)	*S.D. (%)*	*C.V. (%)*	*Relative peak area (%)*	*S.D. (%)*	*C.V. (%)*	*Relative peak area (%)*	*S.D. (%)*	*C.V. (%)*
16:0	3.0	0.06	2.1	2.9***,§	0.03	0.9	3.0	0.08	2.7
18:0	1.6	0.04	2.4	1.5	0.15***,§§	10.2	1.4***	0.03	2.3
18:1	58.6	0.19	0.3	58.5	0.19	0.3	57.6***	0.07**	0.1
18:2	20.2	0.10	0.5	20.7***	0.07	0.4	20.7***	0.11	0.5
18:3	12.7	0.07	0.5	12.8**	0.10	0.8	13.0***	0.03	0.3
20:0	0.5	0.04	8.1	0.4**	0.03	7.1	0.4***	0.01**	1.8
20:1	1.7	0.11	6.7	1.5	0.16	10.7	1.8*	0.04**	2.2
20:2	0.2	0.03	21.6	0.1***	0.01***	5.2	0.2	0.01**	5.2
22:0	0.3	0.05	14.1	0.2**	0.04	18.2	0.2***	0.01**	4.7
22:1	1.3	0.10	7.8	1.4	0.09	6.6	1.7***	0.06**	3.5

* $p < 0.05$.
** $p < 0.01$.
*** $p < 0.001$.
§ Student's *t*-test.
§§ *F*-test.

TABLE II

COMPARISON OF DIFFERENT MODIFICATIONS OF THE SPLIT-SAMPLING TECHNIQUE

Fatty acid	*Varying split (n = 7)*			*Varying sample size (n = 5)*			*"Hot-needle"-technique (n = 6)*		
	Relative peak area (%)	*S.D. (%)*	*C.V. (%)*	*Relative peak area (%)*	*S.D. (%)*	*C.V. (%)*	*Relative peak area (%)*	*S.D. (%)*	*C.V. (%)*
16:0	3.6**·§	0.48***·§§	13.4	3.4	0.51***·§§	14.9	3.1	0.29***·§§	9.2
18:0	1.5	0.12***	8.3	1.4**	0.07	5.1	1.6	0.01*	0.8
18:1	58.6	0.18	0.3	58.7	0.31	0.5	58.8	0.27	0.5
18:2	20.5**	0.16	0.8	20.3**	0.06	0.3	20.4*·	0.16	0.1
18:3	12.7	0.13	1.1	12.7	0.06	0.5	12.8	0.16*	1.2
20:0	0.4*	0.07	16.1	0.4**	0.03	7.7	0.4	0.07	15.6
20:1	1.4**	0.17	12.3	1.7	0.18*	16.6	1.5	0.22	15.0
20:2	0.1***	0.10	19.1	0.1	0.03	18.8	0.1***	0.02	21.1
22:0	0.2**	0.07	33.6	0.2***	0.02	10.4	0.2**	0.06	27.9
22:1	0.9**	0.23	24.4	1.1	0.23*	23.3	1.1	0.33**	30.9

* $p < 0.05$.
** $p < 0.01$.
*** $p < 0.001$.
§ Student's *t*-test.
§§ *F*-test.

similar magnitude (C.V. 6.4 and 6.0%). The dispersion of certain compounds varied considerably (*e.g.* $C_{20:2}$ and $C_{22:0}$ in the split mode and $C_{18:0}$, $C_{20:1}$ and $C_{22:0}$ in the splitless technique).

The split-sampling technique is most commonly used because of its ease of operation and, above all, because it avoids overloading and contamination of the column, thus lengthing column life. The split conditions in extended series of experiments may change as a result of changes taking place in the column and flow pressure. In addition, the sample concentrations may vary and so either the splitting ratio or sample size have to be frequently changed. Such changes may have a considerable effect on the results. In order to determine the possible significance of these changes, the effect of varying the splitting ratio and sample size on the results were compared using the split method. In addition, the differences between the so-called hot-needle injection and conventional cold-needle techniques were compared.

The results of the analysis shown in Table II were compared with the results obtained using the constant-split method (Table I). Significant differences were found between both the relative peak area and the dispersions of certain compounds in comparison with the corresponding results for the constant split method.

The considerable variation in the amounts of behenic and erucic acids are of particular interest (*cf.* also Table III). In the case of the varying-split method, the high levels of palmitic acid and low levels of erucic acid can be explained by the fact that larger sample sizes and, on average, smaller splitting ratios were used. The corresponding feature in the results for the varying sample size method were caused by larger sample sizes than those used with the other methods, on average.

The results for methyl palmitate and methyl erucate obtained using different sampling methods and modifications of these methods are presented in Table III.

TABLE III

EFFECT OF SAMPLE SIZE AND SPLITTING RATIO ON RELATIVE PEAK AREA OF METHYL PALMITATE AND METHYL ERUCATE COMPARED WITH RESULTS OBTAINED WITH SPLITLESS AND ON-COLUMN TECHNIQUES

Sampling	*Sample size (μl)*	*Splitting ratio*	*Relative peak area*		*Peak-area ratio*
			$C_{16:0}$	$C_{22:1}$	$(C_{16:0}/C_{22:1})$
Split	0.5	15:1	3.0	1.3	2.3
Split "hot-needle"	1.0*	15:1	3.1	1.1	2.8
	0.1	15:1	2.9	1.4	2.1
	0.2	15:1	3.4	1.3	2.6
	2.4	15:1	4.3	0.7	6.1
	1.0	200:1	3.2	1.3	2.5
	1.0	70:1	3.3	1.1	3.0
	1.0	8:1	3.6	0.9	4.0
	1.0	3:1	4.2	0.7	6.0
Splitless	0.3**	–	2.9	1.4	2.1
On-column	1.0**	–	3.0	1.7	1.8

* 1.0 μl sample + 1.0 μl *n*-hexane.

** Diluted: 1:100.

It is evident that the proportion of methyl palmitate increased, and that of methyl erucate decreased as the sample size was increased or the splitting ratio decreased. These relative quantitative changes can be attributed to the effect of discrimination through volatility (see above). It is apparent that sample sizes of greater than 1 μl, or splitting ratios of less than 15:1, give very unreliable results for these components. This is further borne out by the results for peak ratios. However, a splitting ratio of 70:1 resulted in a relative decrease in the peak-area ratio for erucic acid. This is without doubt a result of interaction between the splitting ratio and sample size. The peak-area ratio of 1.8 obtained with the on-column technique proved to be the correct one after a prepared mixture of these two compounds had been analysed.

As the same sample (line 43.2) was used in all these runs, the sum of variances of all ten components in the different methods can be used as a measure of the differences between the different methods. Sources of variation, number of observations, variances and their share out of the total variance, as well as coefficients of variation for comparison purposes, are presented in Table IV.

The corresponding values for the material consisting of six samples, taken from the same selection line (line 43.2) over a period of 3 years, are shown in Table IV. The analyses were carried out by the split method under conditions which correspond to the constant-split method used elsewhere in this study. Despite the fact that a number of different columns were used during this period, the same liquid stationary phase (FFAP) was used. The source of variance shown in Table IV includes the variation caused by the fact that a small sample (10–15 seeds) only was selected from the seed material, which had a large degree of biological variation. In addition, the selection variance includes the variation arising from the isolation, transesterification and of course GLC analysis of the fatty acids. As well as the earlier mentioned sources of variance, the 3-year term variance also includes the variance arising from replacement of the column and slight adjustments to the carrier gas flow-rate. The total variance presented in Table IV has been estimated from the total variance of the two selection line crosses (M_1 and M_2).

It is evident from Table IV that the selection and the 3-year term variances are the only sources of variance as far as the sum of the variances of the ten fatty acids is

TABLE IV

VARIANCES AND COEFFICIENTS OF VARIATION IN FATTY ACID ANALYSIS

Source of variance	*n*	*Variance*	*Percentage of total variation*	*C.V. (%)*
Split:				
Constant	10	0.082	0.6	6.4
Varying split	5	0.420	2.8	12.9
Varying sample size	7	0.507	3.4	9.8
"Hot needle"	7	0.373	2.5	12.3
3-year term	6	4.512	30.3	11.3
Splitless	6	0.111	0.7	6.0
On-column	6	0.029	0.2	2.8
Selection	20	4.364	29.3	13.6
Total variation	486	14.902	100.0	–

concerned. On the other hand, the proportion of the sum of the variances arising from the GLC method (0.2–3.4%) are negligible and appear to be of no practical importance in plant breeding studies if the size of the sample is kept sufficiently large. However, methodological errors are important in the determination of certain components. The variances for palmitic acid in the case of the varying split in the varying sample size methods are 0.23 and 0.26, the corresponding values for the constant-split method varying in the biological materials (M_1 and M_2) from 0.10 to 0.23 (*cf.* also Table III).

CONCLUSIONS

It was found in the study that the analysis of fatty acids by different sampling methods gave results which differed significantly from each other as regards both precision and accuracy. The on-column technique (C.V. 2.8%) gave the most reliable results, the sum of variances of all ten different components being in this case only 0.2% of the total variation. The largest source of error proved to be selection combined with analyses carried out over a long period of time (*ca.* 30% of the total variation). This can be mainly attributed to the fact that only 10–15 seeds were analysed from the biologically very heterogeneous material. However, it should be remembered that the variance also includes the variation due to transesterification.

The sample size and splitting ratio proved, in the case of palmitic and erucic acids, to be highly critical. The most reliable results in the case of the split technique were obtained with small sample sizes (0.1–0.5 μl) and a splitting ratio of 15:1.

REFERENCES

1 R. Hiltunen, A. Huhtikangas and S. Hovinen, *Acta Pharm. Fenn.*, 88 (1979) 31.
2 G. Schomburg, H. Behlau, R. Dielmann, F. Weeke and H. Husmann, *J. Chromatogr.*, 142 (1977) 87.
3 K. Grob, Jr. and H. P. Neukom, *J. High Resolut. Chromatogr. Chromatogr. Commun.*, 2 (1979) 15.
4 K. Grob, Jr. and H. P. Neukom, *J. Chromatogr.*, 189 (1980) 109.
5 M. Galli and S. Trestianu, *J. Chromatogr.*, 203 (1981) 193.
6 G. Schomburg, H. Husmann and R. Rittmann, *J. Chromatogr.*, 204 (1981) 85.
7 M. J. Hartigan and L. S. Ettre, *J. Chromatogr.*, 119 (1976) 187.

Journal of Chromatography, 237 (1982) 49–56
Elsevier Scientific Publishing Company, Amsterdam — Printed in The Netherlands

CHROM. 14,421

POLISH DIATOMACEOUS SUPPORTS FOR GAS CHROMATOGRAPHY.

II.* SOLID STRUCTURE INVESTIGATIONS BY HYDROGEN CHLORIDE GAS PURIFICATION

Z. SUPRYNOWICZ and E. TRACZ*
Maria Curie-Sklodowska University, Institute of Chemistry, Pl. Marii Curie-Sklodowskiej 3, 20-031 Lublin (Poland)
(Received September 1st, 1981)

SUMMARY

The changes in geometric and crystallographic structures of Polish diatomaceous supports and Chromosorb P after washing with hydrogen chloride gas at elevated temperatures in connection with chemical composition changes were examined. The results of X-ray diffraction spectroscopy and microanalysis together with scanning electron microscopic and transmission electron microscopic investigations are presented.

INTRODUCTION

The most important properties of gas chromatographic supports are adsorptivity and catalytic properties as well as chemical purity and homogeneity of the surface, all of which determine the ability of the support to achieve uniform coverage with liquid stationary phase with low mass transfer and good selectivity.

In practice, ideal diatomaceous supports do not exist and much research has been carried out to improve their chromatographic performance. The presence on the surface of supports of metals such as aluminium, iron and titanium as well as their oxides causes adsorptive and catalytic activity. In an earlier paper[1] we concluded that the percentage of the metals removed from the supports is highly dependent on the chemical form of the metal, *e.g.* oxide, silicate or halide. This depends on the origin of the deposits from which the raw material for the supports comes, as well as on the mineralogical form of that material. Therefore, it was interesting to determine how the mineralogical form of a support influences its cleaning-up ability using the gas-phase method described by Aue *et al.*[2] and how this procedure influences the geometric and crystallographic structure of the supports. Both these effects are clearly visible after bonding of Carbowax 20M and checking of the chromatographic properties of the support-bonded phase, described in the previous paper[1].

* For Part I, see ref. 1.

0021-9673/82/0000–0000/$02.75

EXPERIMENTAL

Supports

Polish diatomite supports of the type Polsorb B and C[7] (Permedia, Lublin, Poland) and Chromosorb P (Johns-Manville, Denver, CO, U.S.A.) were employed.

Methods

To evaluate the surface properties of the supports the following methods were used: X-ray diffraction spectroscopy, microanalysis, scanning electron microscopy (SEM) and transmission electron microscopy (TEM).

Apparatus

A Dron-2 diffractometer, a JEOL JXA-5-CMD microprobe, a Cambridge S4-10 scanning electron microscope and a JEM 100 B transmission electron microscope were employed.

Preparation of samples

Samples for X-ray microanalysis were prepared using the following procedure. The support grains, submerged in epoxy resin, were polished with diamond powder and covered with a gold layer in a vacuum. Single grains were examined for their homogeneous surface parts as well as parts with various intrusions. Linear and facial distributions of elements such as aluminium, titanium, iron and silicon were recorded using a photographic method.

Changes in the shape of the support grains were studied using SEM (200× magnification); the primary and secondary structure was observed using 1000× magnification[3]. A relatively small magnification for surface research was used owing to the fact that sponge-like diatoms are particulary difficult subjects for SEM studies.

These difficulties are connected with electrification of the electron beam even after covering the specimens with an insulating layer. To diminish this effect saturation of the surface with osmium tetraoxide and covering with carbon and gold layers was used. The Pt–C direct replica method using TEM was employed while studying the secondary and tertiary structure of the diatom at magnification 70,000×. After a five-fold photographic blow-up, the final magnification was 350,000×.

RESULTS AND DISCUSSION

The X-ray microanalyser (electron microporobe) gives information about each chosen area of the specimen, while X-ray diffraction makes confirmation of the presence of particular crystallographic phases possible, and X-ray spectroscopy describes how these crystallographic phases are located in the single grain. It is also possible to determine the composition and size of the crystals.

Both methods yield useful information and supplement each other. We have found that in Polsorb C, silica is present in the form of α-quartz, after gas washing more than half of which is converted into α-crystobalite. In the case of Polsorb B and Chromosorb P we have found two forms of silica, α-crystobalite and α-quartz. Washing with hydrogen chloride gas did not give any changes in this case.

Amorphous silica, present in the diatom, changes partially into α-crystobalite

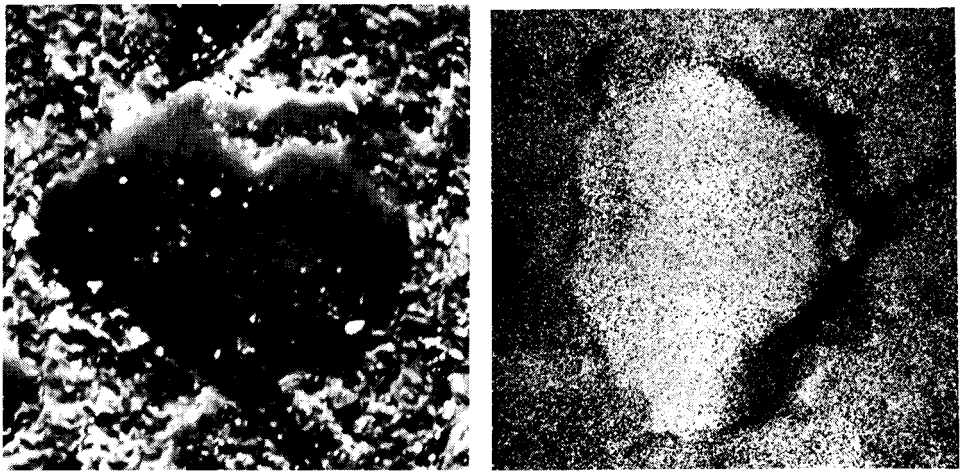

Fig. 1. Surface of commercial Polsorb C, large crystalline form of silica: topological picture (415×).

Fig. 2. As Fig. 1: facial distribution of silica.

(low-temperature form, 180–270°C) or into α-quartz (573–870°C) in the production process of commercial supports. As a result of our investigations it may be concluded that commercial as well as gas-washed supports consist of silica in both amorphous and crystalline forms. These two forms show different surface properties. The critical surface tension of the two forms traditionally coated by a liquid stationary phase may be different and may also influence the support bonding process due to a different distribution of OH groups on the surface. Pink supports such as Chromosorb P and Polsorb C, compared with white supports, contain more crystalline forms of silica, aluminosilicates, iron and titanium compounds as well as having larger crystals. The

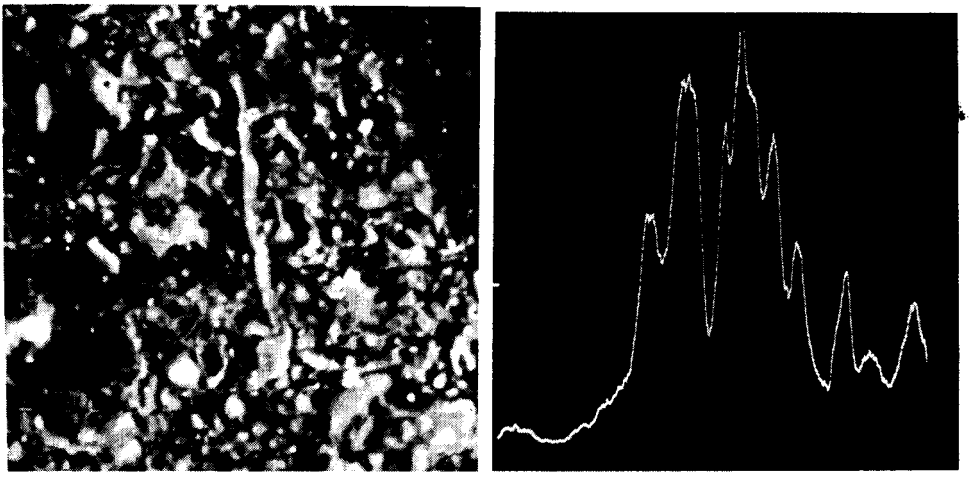

Fig. 3. Surface of commercial Polsorb B, small crystalline form of silica: topological picture (415×).

Fig. 4. As Fig. 3: linear distribution.

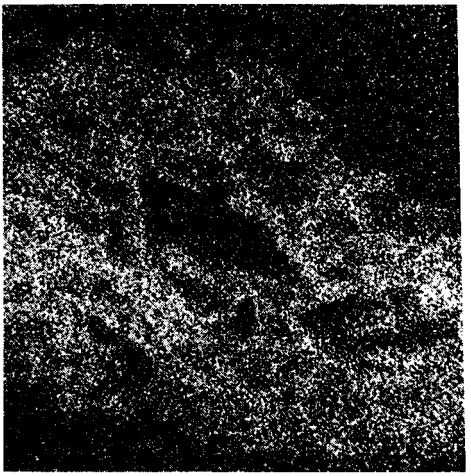

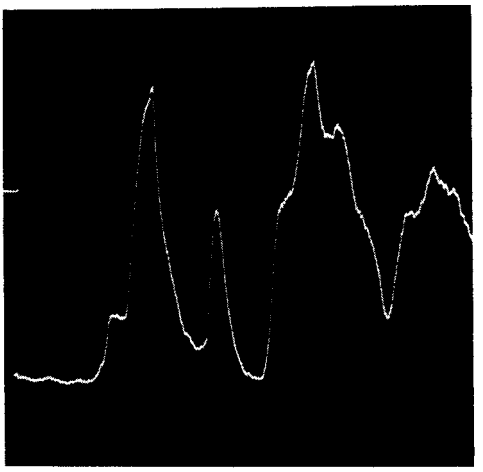

Fig. 5. Distribution of alumina in commercial supports: facial distribution.

Fig. 6. As Fig. 5: linear distribution.

differrence in size is due to the different composition of the raw material: the mean size of the crystals in the pink material is 50 μm (Figs. 1 and 2) while that for the white ones is smaller (10 μm) (Figs. 3 and 4).

All the commercial supports, according to our X-ray diffraction examination, contain illite, an aluminosilicate, as a separate crystalline form. The gas-washing procedure has no influence on the form in Polsorb B and Chromosorb P while in Polsorb C, illite is converted into sillimanite.

Sillimanite, a polymorphous variety of $AlSiO_5$, represents the highest energy of the crystal network. The above-mentioned property is probably responsible for the

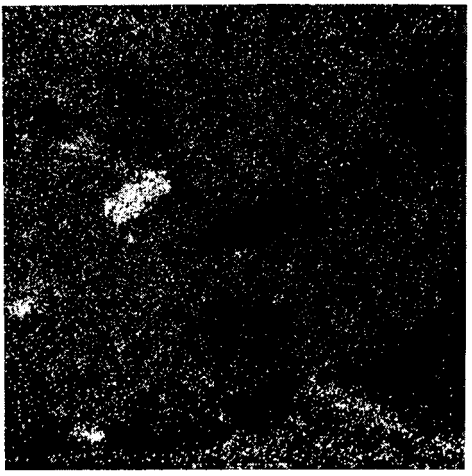

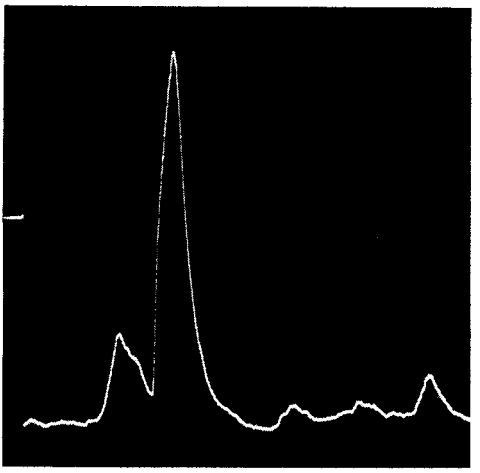

Fig. 7. Distribution of alumina in supports after gas washing: facial distribution.

Fig. 8. As Fig. 7: linear distribution.

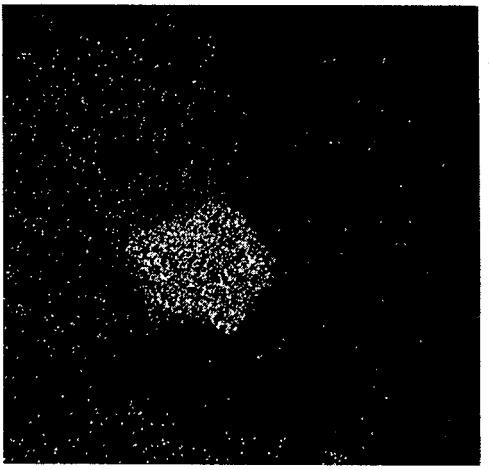

Fig. 9. Distribution of iron and titanium: topological picture (415 ×).

Fig. 10. As Fig. 9: facial distribution of Ti.

difficulties in removing the Polsorb C alumina compared with Chromosorb P and Polsorb B.

Elemental analyses are listed in Table I from ref. 1, from which it can be seen that gas-washed Polsorb C contains 6.61 % Al, even more than commercial Polsorb B (5.5 % Al). This relatively high content in the gas-washed supports did not affect the bonding procedure of Carbowax 20M, unlike for commercial products such as Chromosorb P and Polsorb B and C. Commercial supports show a higher contents of alumina in crystalline intrusions (Figs. 5 and 6).

Gas-washed supports generally show a lower alumina content (Fig. 7). Linear analysis of the concentration of this element showed a sharp peak only in places

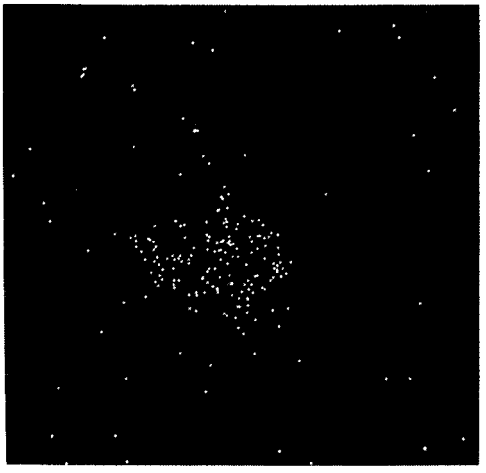

Fig. 11. As Fig. 9: facial distribution of Fe.

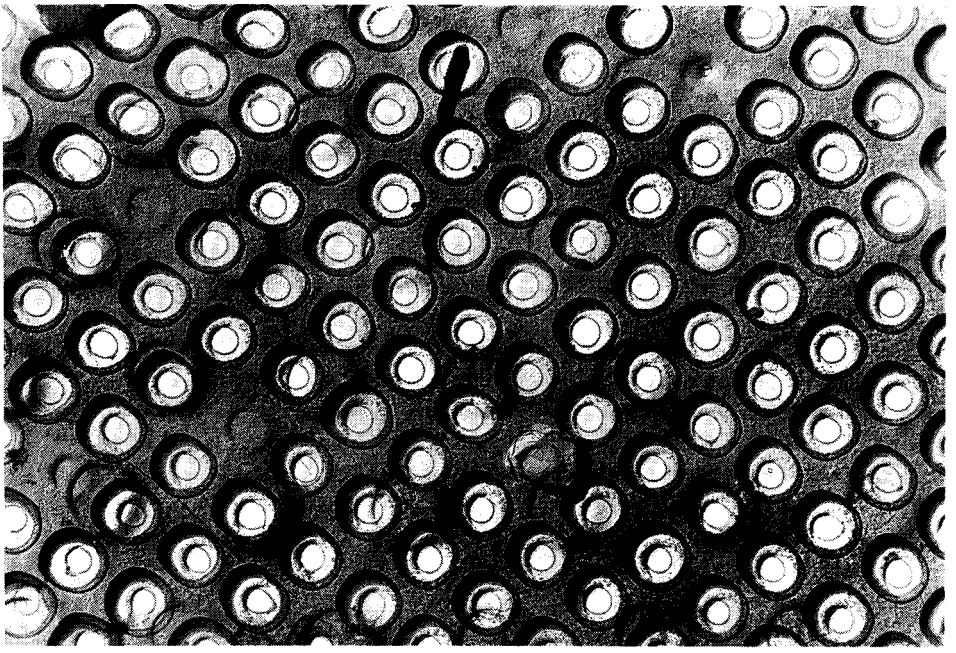

Fig. 12. External topology of commercial supports: macropores of selections of diatom (TEM, 8100 ×).

Fig. 13. As Fig. 12: macropores created by production process (SEM, 5940 ×).

Fig. 14. As Fig. 12: "flat" surface of support, namely quartz (TEM, 5940 ×).

where alumina–silicate intrusions were present (Fig. 8). This phenomenon clearly indicates that removal of the aluminium present in the supports as aluminosilicates is impossible while the other elements may be easily removed. Iron and titanium are present in commercial supports in crystalline forms (Fig. 9), *e.g.* rutile as a crystalline form of TiO_2 in Polsorb C.

Figs. 10 and 11 show an unequal distribution of iron and titanium. Such plases, as well as aluminosilicate intrusions, may disturb not only the bonding of Carbowax 20M but also, owing to their crystallographic activity, generally diminish the chromatographic performance of the support. After the gas-washing procedure the iron and titanium content is low, being undetectable even using X-ray spectrometry. The gas-washed supports are thus silica with small aluminosilicate intrusions.

Aue and co-workers[1–4] have stated that the chemical composition and the method of preparation of the supports play crucial roles in the bonding of the Carbowax 20M layer. However it seems to be important to take into consideration the external topology of the support grains. The topology of the commerical supports is shown in Figs. 12–14. It may be characterized by the presence in the diatom skeleton of micropores (Fig. 12) and macropores created by the production process (Fig. 13), and "flat" surfaces, namely quartz (Fig. 14).

After gas-washing the surface appears different. There is no diatom skeleton and the macropores and the surface have become fused and sponge-like (Figs. 15 and 16). Aluminosilicates present on the surface are in macro-crystal forms (Fig. 17).

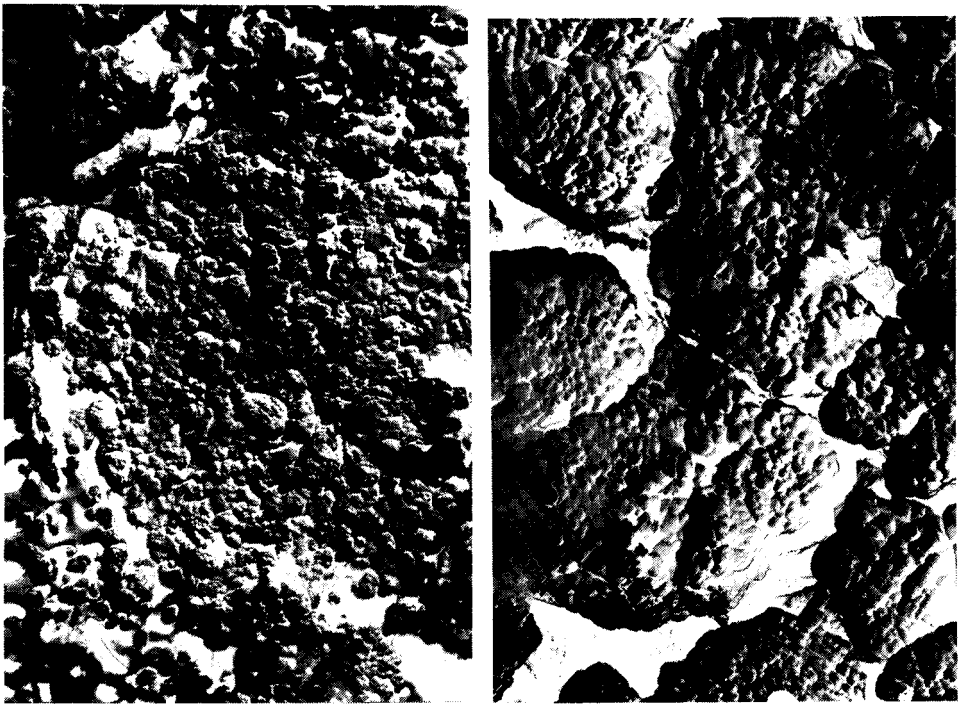

Fig. 15. Sponge-like surface of support after gas washing (TEM, 5940 ×).

Fig. 16. As Fig. 15.

Fig. 17. Macro-crystal forms of aluminosilicate on the surface of support after gas washing (SEM, 5940 ×).

Even after gas-washing, the supports are chemically pure although their external topology is far from the ideal macroporous structure. Thus it can be concluded that the surface, after coating with a liquid stationary phase, represents a mean value for the structures of different geometry and topology, with the additional influence of the spots with different chemical composition. It thus seems that the model assumptions of Giddings[5] and Sepinet[6] regarding distribution of the liquid stationary phase are of limited value, being applicable only to gas-washed and not commercial supports. The phenomenon of statistically uneven coatings of the liquid stationary phase on the support grains, especially in the case of non-polar phases, may be of great importance, particularly with only low percentages of the stationary phase.

REFERENCES

1 E. Tracz, Z. Suprynowicz and M. Daniewski, *Chem. Anal.*, in press.
2 W. A. Aue, M. M. Daniewski, E. E. Pickett and P. R. Mc. Cullongh, *J. Chromatogr.*, 111 (1957) 37.
3 D. M. Ottenstein, *J. Gas Chromatogr.*, 4 (1963) 1.
4 M. M. Daniewski and W. A. Aue, *J. Chromatogr.*, 130 (1978) 506.
5 J. C. Giddings, *Anal. Chem.*, 34 (1962) 458.
6 J. Serpinet, *J. Chromatogr.*, 119 (1973) 483.

Journal of Chromatography, 237 (1982) 57–63
Elsevier Scientific Publishing Company, Amsterdam — Printed in The Netherlands

CHROM. 14,443

CHROMATOGRAPHY OF ORGANOMETALLIC AND ORGANOMETALLOIDAL DERIVATIVES OF AMINO ALCOHOLS

III. DIALKANOLAMINE DERIVATIVES

V. D. SHATZ*, V. A. BELIKOV, I. P. URTANE, G. I. ZELCHAN and E. LUKEVICS
Institute of Organic Synthesis, Latvian S.S.R. Academy of Sciences, Riga (U.S.S.R.)
(Received October 6th, 1981)

SUMMARY

The retention behaviour of 25 derivatives of dialkanolamines and diethylene glycol on Apiezon L and OV-225 has been investigated. It was found that organosilicon derivatives have no transannular N → Si bond under gas–liquid chromatographic conditions. As in the case of atranes, the chromatographic behaviour of boron-containing derivatives of diethanolamine indicates a stronger transannular interaction when compared with the silicon compounds. It is shown by quantum-chemical calculations that the charge distribution in derivatives of dialkanolamines is similar to that observed in atranes. This indicates that the strong solute–sorbent interaction of atranes is due mainly to a specifically favourable conformation which facilitates the attraction of oxygen atoms to alternatively charged centres on the stationary phase.

INTRODUCTION

Previous publications in this series[1,2] discussed the chromatographic properties of atranes, triethanolamine derivatives of boron, silicon, germanium and tin. The chromatographic behaviour of these compounds failed to agree with the simple additive scheme and the difference between the calculated and experimental values of retention indices ($\delta I_{N \rightarrow M}$) could be indicative of a transannular bond between the nitrogen atoms and the element in atrane existing under gas–liquid chromatographic (GLC) conditions.

Information is available that diethanolamine derivatives may or may not have such a transannular N → M bond depending on the substituent[3,4]. This bond tends to be less strong than in the corresponding derivatives of triethanolamine. Several organosilicon derivatives of diethanolamine have been shown to occur in solution as an equilibrium of two forms, one of which has the intra-complex N → Si bond, whereas the other fails to do so[4]. It was therefore of interest to study the gas chromatographic properties of dialkanolamine derivatives on Apiezon L and OV-225, which is the subject of this paper.

0021-9673/82/0000–0000/$02.75

TABLE I

RETENTION PARAMETERS OF COMPOUNDS OF GENERAL FORMULA

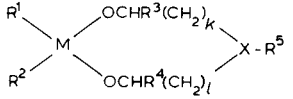

No.	*M*	*X*	*k*	*l*	R^1	R^2	R^3	R^4	R^5	*I*		*ΔI*	$\delta I_{X \to M}$	
										*A**	*C**		*A**	*C**
1	Si	O	1	1	C_6H_5	CH_3	H	H	–	1557	2127	560	80	60
2	Si	O	1	1	C_6H_5	C_3H_7	H	H	–	1700	2232	532	20	−30
3	Si	O	1	1	C_6H_5	C_6H_5	H	H	–	2110	2838	728	50	0
4	Si	N	1	1	CH_3	CH_3	H	H	C_6H_5	1724	2247	523	150	140
5	Si	N	1	1	C_6H_5	CH_3	H	H	CH_3	1632	2160	528	60	50
6	Si	N	1	1	C_6H_5	CH_3	H	H	C_6H_5	2260	3020	760	110	130
7	Si	N	1	1	C_6H_5	CH_3O	H	H	CH_3	1701	2370	669	10	140
8	Si	N	1	1	C_6H_5	C_2H_5O	H	H	CH_3	1711	2289	578	−80	−40
9	Si	N	1	1	C_6H_5	C_2H_5O	H	H	CH_3	2182	3015	833	30	45
10	Si	N	1	1	C_6H_5	C_6H_5	H	H	CH_3	2179	2921	742	30	30
11	Si	N	1	1	C_6H_5	C_6H_5	H	H	C_2H_5	2219	2957	738	−30	−30
12	Si	N	1	1	C_6H_5	C_6H_5	H	H	C_3H_7	2277	2986	709	−70	−100
13	Si	N	1	1	C_6H_5	C_6H_5	H	H	C_4H_9	2357	3076	719	−90	−115
14	Si	N	1	1	C_6H_5	C_6H_5	H	H	$C(CH_3)_3$	2353	3066	713	0	20
15	Si	N	1	1	C_6H_5	C_6H_5	H	H	C_6H_5	2750	3649	899	20	−20
16	Si	N	1	1	C_6H_5	C_6H_5	H	H	NH_2	2179	3098	919	−80	−90
17	Si	N	1	1	*p*-CH_3-C_6H_4	*p*-CH_3-C_6H_4	H	H	CH_3	2350	3081	731	0	−10
18	Si	N	1	1	C_6H_5	CH_3	CH_3	H	CH_3	1609	2089	480	0	−40
19	Si	N	1	1	C_6H_5	C_6H_5	CH_3	H	CH_3	2148	2842	694	−40	−70
20	Si	N	1	1	C_6H_5	C_6H_5	CH_3	CH_3	CH_3	2127	2755	628	−100	−170
21	B	N	1	1	C_6H_5	–	H	H	CH_3	1943	3313	1370	470	1303
22	B	N	1	1	C_6H_5	–	H	H	$C(CH_3)_3$	1944	3076	1132	270	906
23	B	N	1	1	C_6H_5	–	CH_3	CH_3	CH_3	1886	3141	1255	340	1091
24	B	N	1	2	C_6H_5	–	H	H	CH_3	2061	3330	1269	490	1220
25	B	N	2	2	C_6H_5	–	H	H	CH_3	2054	3253	1199	380	1043

* A = Apiezon L; C = OV-225.

EXPERIMENTAL

The measurement of retention indices were conducted on a Chrom-4 chromatograph at 200°C as described earlier[1,2], using Apiezon L and OV-225 as stationary phases, 80–100-mesh Chromosorb W HP as the solid support and 1.2 m × 3 mm I.D. glass columns. The quantum-chemical calculations were carried out using the CNDO 2 program[5]. Compounds 1–3 (Table I) were obtained by reaction of the corresponding diorganyldiethoxysilanes with diethylene glycol. Similarly, compounds 4–20 were obtained by the reaction of diethoxy- or dimethoxysilanes and diethanolamines, whereas compounds 24–25 were synthesized by reaction of dialkanolamines with phenylboric acid in dioxan solution.

RESULTS AND DISCUSSION

The title compounds have the general formula

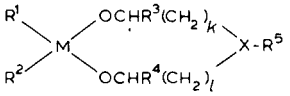

where R^1 = alkyl, aryl; R^2 = alkyl, alkoxyl, aryl; R^3,R^4 = H, methyl; R^5 = H, alkyl, phenyl; M = Si, B; X = O, N; and k,l = 1 or 2.

Their retention parameters are summarized in Table I. Unlike the trialkanolamine derivatives studied earlier, organosilicon derivatives of dialkanolamines are characterized by low, sometimes negative, values of $\delta I_{X\rightarrow M}$. This provides evidence that the above compounds in the chromatographic system appear to possess no intra-complex bond. This conclusion is supported by the comparison of $\delta I_{X\rightarrow M}$ values in organosilicon derivatives of dialkanolamines and the corresponding diethylene glycol derivatives (compounds 1–3), which have been shown to have no bond of this type.

It can be assumed that the intra-complex N → Si bond is stabler at low temperatures[6,7]. So, if this gain in stability is appreciable, the values of $\delta I_{N\rightarrow Si}$ are expected to increase with decreasing temperature. We estimated $\delta I_{N\rightarrow Si}$ values for compound 10 at various temperatures. The transannular bond in this compound, existing both as crystals and in solution, is due to the electron-donor character of the methyl group on the nitrogen atom and the electron-acceptor properties of phenyl radicals[3,4]. Nevertheless, the data presented in Table II demonstrate that with decreasing temperature (down to 160°C) the values of $\delta I_{N\rightarrow Si}$ fail to increase, and a slight decrease in the values is even observed. These data suggest that diethanolamine derivatives during GLC at 160–250°C exist in the form without an intra-complex bond.

Boron derivatives, unlike the organosilicon derivatives of dialkanolamines, are characterized by high values of $\delta I_{N\rightarrow M}$ comparable to those of boratranes. The relationship of these values to the number of six-membered rings in the molecule is roughly the same for the derivatives of di- and trialkanolamines (Fig. 1). Organoboron derivatives of dialkanolamines resemble boratranes with respect to other physico-chemical properties, *e.g.*, melting points and solubility in organic solvents. The high melting points are apparently responsible for the asymmetric peaks observed in these compounds despite the fact that the temperature of the injection port

TABLE II

RETENTION INDICES OF $(C_6H_5)_2Si(OCH_2CH_2)_2$-$NCH_3$ AS A FUNCTION OF TEMPERATURE

Temperature (°C)	*I*	*δI/10°C*	$\delta I_{N\rightarrow Si}$
250	2521		70
		10.2	
200	2470		20
		12.0	
180	2446		0
		11.5	
160	2423		−30

of the chromatograph was kept at 350–400°C and the samples were injected as dilute solutions.

The replacement of a secondary with a tertiary amino group usually brings about an increase in retention indices by 70–150 units, depending on the polarity of the stationary phase used. Our experimental conditions provided a reliable identification of compounds with retention indices up to 4000. However, our attempts to perform chromatographic analyses of boron compounds with R^5 = H were unsuccessful. The explanation probably lies in the low thermal stability of these compounds, as evidenced by experiments using a short column (50 cm).

Thus, as with atranes, the chromatographic behaviour of boron-containing derivatives of diethanolamine indicates a stronger transannular interaction than with silicon compounds, apparently because the migration of the unshared electron pair on the nitrogen atom to the *p* orbital of boron is preferred to the *d* orbital of silicon.

An analysis of retention data in earlier publications suggests that the association of atranes with the stationary phase molecules involves oxygen atoms of the atrane backbone. It is to be expected that if the steric hindrances for various derivatives are roughly similar, the solute–sorbent association will be determined primarily by the atoms carrying the greatest absolute charge. To test this assumption, quantum-chemical calculations were conducted for several compounds (Table III). The results obtained show that the charges are most conspicuous on the silicon atom and the oxygen atoms directly bound to it. It should be noted, however, that the silicon atom

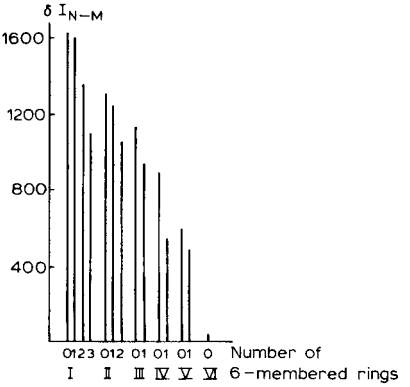

Fig. 1. Relationship between $\delta I_{N\rightarrow M}$ and number of 6-membered rings in the molecule. I = B derivatives of triethanolamine; II = B derivatives of diethanolamine, $R^1 = C_6H_5$; III = Ge derivatives of triethanolamine, $R^1 = C_6H_5$; IV = Si derivatives of triethanolamine, $R^1 = C_6H_5$; V = Si derivatives of triethanolamine, $R^1 = CH_3$; VI = Si derivatives of diethanolamine, $R^1 = R^5 = CH_3$, $R^2 = C_6H_5$.

TABLE III

CHARGE DISTRIBUTION IN ATRANE MOLECULES ACCORDING TO QUANTUM-CHEMICAL CALCULATIONS

Compound	*Charge*		
	Si	*O*	R_1
$HSi(OCH_2CH_2)_3N$	+0.478	−0.296 −0.296 −0.296	−0.121
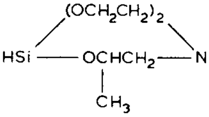	+0.472	−0.302 −0.290 −0.290	−0.118
$HSi(OCHCH_2)_3N$ with CH_3 on each CH	+0.468	−0.310 −0.309 −0.307	−0.124
$HSi(OCHCH_2)_3N$ with CH_3 on each CH	+0.463	−0.302 −0.302 −0.302	−0.120
$CH_3Si(OCH_2CH_2)_3N$	+0.440	−0.291 −0.291 −0.291	−0.058
$C_2H_5Si(OCH_2CH_2)_3N$	+0.438	−0.288 −0.288 −0.291	−0.054
$CH_2=CHSi(OCH_2CH_2)_3N$	+0.438	−0.293 −0.293 −0.293	−0.067
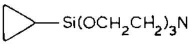	+0.435	−0.289 −0.293 −0.293	−0.057
$CH_3OSi(OCH_2CH_2)_3N$	+0.576	−0.291 −0.294 −0.294	−0.195
$(CH_3)_2Si(OCH_2CH_2)_2NCH_3$	+0.522	−0.281 −0.281 −0.279	−0.032
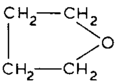	+0.522 (C′)	−0.236	

is strongly shielded by other atoms and is therefore unlikely to participate directly in the formation of an associate. At the same time, a certain contribution is provided by the substituent on the silicon atom, which explains our attempts to relate the charge values over sterically accessible atoms to chromatographic characteristics:

$$\Delta I_{OV\text{-}225} = -4404 + 2772q_{R_1} + 5837q_O \ (r = 0.98;\ \sigma = 39)$$
$$\delta I_{N\rightarrow Si} = -9882 + 2232q_{R_1} + 11936q_O \ (r = 0.96;\ \sigma = 83)$$

where q_{R_1} and q_O are the charges on the R_1 and oxygen atoms, respectively.

Further, as evidenced by quantum-chemical calculations, the charges on all remaining atoms in the estimated molecules show little dependence on the character of

the substituent on the silicon atom. It is evident, therefore, that they cannot be responsible for the different chromatographic behaviour of particular compounds and therefore were neglected.

The present model for explaining the chromatographic properties of compounds appears to be more general in character than the models proposed in our earlier work[1]. It permits, for instance, the assessment of the sequence of elution for diastereoisomeric atranes as well as the calculation of $\delta I_{N \to Si}$ values for 1-hydrosilatrane, which cannot be achieved with previously proposed equations.

Nevertheless, the quantum-chemical calculations applied to a diethanolamine derivative gave a charge distribution pattern in the molecule (Table III) similar to that observed in atranes. Dialkanolamine derivatives are characterized by small $\delta I_{N \to M}$ values, suggesting that the strong solute–sorbent association in the case of atranes in due mainly to the charges on the oxygen atoms being in a specifically favourable environment to participate in intermolecular interactions. Unlike organosilicon derivatives of diethanolamine, atrane molecules exhibit enhanced conformational rigidity. In the molecules carrying a transannular bond, oxygen atoms are incorporated in the 5- and 6-membered rings, forming a constant protrusion which facilitates their attraction by the alternatively charged centres of the stationary phase. On the other hand, molecules without a transannular bond permit a variety of energetically equivalent conformations, only some of which are suitable for the specific intermolecular interaction.

This interpretation of the strong chromatographic retention is supported by a certain similarity between the atrane system and the corresponding cyclic ethers. The excessive negative charge on the oxygen atom in tetrahydrofuran is only slightly lower than that on the oxygen atom in atranes (Table III). The additive scheme can be useful for the calculation of retention indices in the hypothetical system, the carbon analogue of 1-methylsilatrane. The retention index of tetrahydrofuran on OV-225 is about 830 at 200°C; hence for the 1-methylsilatrane analogue it should be 830 + (2 · 630) + 100 = 2190, which is in good agreement with the experimental value[1].

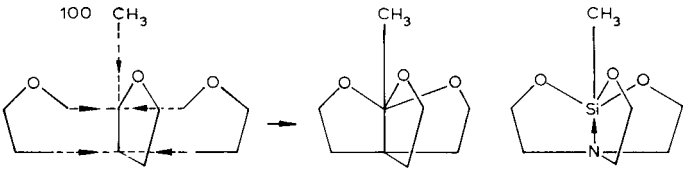

We therefore think that the high $\delta I_{N \to M}$ values found for intra-complex ethers are due mainly to the formation of 5- and 6-membered oxygen-containing heterocycles having a conformation that is favourable for intermolecular interactions. If such a conformation predominates, other (secondary) factors come into play, *e.g.*, the electron density distribution and the steric environment of the oxygen atoms.

ACKNOWLEDGEMENT

The authors acknowledge their indebtedness to Dr. M. A. Shokhen for his helpful cooperation in conducting quantum-chemical calculations and for discussion of the results.

REFERENCES

1 V. D. Shatz, V. A. Belikov, G. I. Zelchan, I. I. Solomennikova and E. Lukevics, *J. Chromatogr.*, 174 (1979) 83–95.
2 V. D. Shatz, V. A. Belikov, G. I. Zelchan, I. I. Solomennikova, N. P. Yerchak, O. A. Pudova and E. Lukevics, *J. Chromatogr.*, 200 (1980) 105–114.
3 A. Kemme, J. Bleidelis, I. Urtane, G. Zelchan and E. Lukevics, *J. Organomet. Chem.*, 202 (1980) 115–121.
4 E. Liepins, Yu. Popelis, I. Birgele, I. Urtane, G. Zelchan and E. Lukevics, *J. Organomet. Chem.*, 201 (1980) 113–121.
5 J. A. Pople and D. L. Beveridge, *M.O. Approximate Theory*, McGraw-Hill, New York, 1970.
6 Quang Shen and R. L. Hildebrandt, *J. Mol. Struct.*, 64 (1980) 257–262.
7 L. Párkányi, L. Bihátsi and P. Hencsei, *Cryst. Struct. Commun.*, 7 (1978) 435–440.

Journal of Chromatography, 237 (1982) 65–78
Elsevier Scientific Publishing Company, Amsterdam — Printed in The Netherlands

CHROM. 14,452

INFLUENCE OF WATER CONTENT OF THE MOBILE PHASE ON CHROMATOGRAPHIC PERFORMANCE IN ADSORPTION CHROMATOGRAPHY*

L. SZEPESY**, C. COMBELLAS, M. CAUDE* and R. ROSSET
Laboratoire de Chimie Analytique de l'École Supérieure de Physique et de Chimie Industrielles de la Ville de Paris, 10 Rue Vauquelin, 75231 Paris Cedex 05 (France)

(First received May 12th, 1981; revised manuscript received October 20th, 1981)

SUMMARY

Silicas (LiChrosorb Si 60 and Si 100) and aluminas (Alox T, Woelm, A5Y Spherisorb) with different specific surface areas were investigated with chloroform and dichloroethane as mobile phases containing various amounts of water in the range 0–600 ppm. The water content of the eluent was adjusted by adding a measured amount of water and was determined by the Karl Fisher method. Measurements were carried out with different mobile phase velocities and reduced plate heights were determined. From the measured data, the capacity ratio (k'), selectivity (α), number of theoretical plates (N_{max}) and resolution (R_S) were determined and plotted as a function of the water content of the mobile phase.

It was established that in order to evaluate the influence of the water content of the mobile phase on the chromatographic performance of an adsorbent packing, not only changes in the capacity ratios but also the changes in the selectivities and efficiencies and from these data the changes in resolution should be determined.

INTRODUCTION

It has been long recognized that retention on active stationary phases such as silica and alumina with non-polar and moderately polar eluents is strongly influenced by the water content of the eluent[1,2]. Water is often added to the eluent in adsorption chromatography to improve isotherm linearity and column efficiency[3–10]. These investigations have shown that the different adsorbents can be adjusted to defined activity levels by changing the water content of the eluent.

The above studies, however, were directed mainly to investigations of the change in capacity ratio (k') as a function of the water content of the mobile phase. Some indications were given of the variation of relative retention, *i.e.*, selectivity, by

* Presented at the *5th International Symposium on Column Liquid Chromatography, Avignon, May 11–15, 1981*. The majority of the papers presented at this symposium has been published in *J. Chromatogr.*, Vol. 218 (1981).

** On leave from the Technical University of Budapest, Hungary.

0021-9673/82/0000–0000/$02.75

changing the water content[4–6,8–10], but no definite conclusions were drawn. It was generally stated that on increasing water content of the mobile phase the column efficiency increases[1,2,4,6]; even an optimum range was indicated[8], but the values given in the literature are contradictory and not supported by experimental evidence. No systematic evaluation of the influence of water content on the chromatographic performance, *i.e.*, the resolving power of the different adsorbent packings, has yet appeared. For this reason we investigated the influence of the water content of the mobile phase on the resolution of columns packed with silicas and aluminas with different characteristics.

EXPERIMENTAL

Equipment

A Varian Aerograph Model 5000 liquid chromatograph equipped with a Valco injector valve (10-μl loop) and an LDC SpectroMonitor III UV detector were used.

The water content of the eluent was determined by means of a coulometric Karl Fischer titrator (Automate Bizot et Constant, Prolabo, Paris).

Columns

The column tubes used were 15 cm × 4.6 mm I.D. for each packing. Table I summarizes the main physical characteristics of the packings used. The silicas were activated at 180°C for 6 h and the aluminas at 400°C for 12 h. The columns were filled by the slurry technique. For silica packings the suspending solvent was a mixture of carbon tetrachloride (90%) and methanol (10%), forming a dilute suspension (2 g of silica per 20 ml of solvent).

For alumina packings, the slurry for the balanced-density technique was prepared by using a mixture of 3 g of alumina and 20 ml of solvent. Different solvents were tried (acetone, methanol, ethylene glycol–acetone, ethylene glycol–dioxane, triethylene glycol–acetone, glycerol–methanol, tetrabromoethane–dioxane). The best results were obtained by using 80% tetrabromoethane–20% dioxane, giving a mixture of density equal to that of the alumina (balanced-density slurry): With the other

TABLE I

CHARACTERISTICS OF THE INVESTIGATED PACKINGS

Packings	*Particle size (μm)*	*Mean particle size (μm)*	*Particle shape*	*Surface area (m^2/g)*	*Producer**
LiChrosorb Si 60	5–7	6	Irregular	482	Merck
LiChrosorb Si 100	4–7	5	Irregular	309	Merck
Alox T	5–7	6	Irregular	68	Merck
Alumina Woelm N 3-6	3–6	5	Irregular	145	Woelm
Spherisorb A5Y	3–7	5	Spherical	110	Phase Separations

* Merck, Darmstadt, G.F.R.; Woelm, Eschwege, G.F.R.; Phase Separations, Queensferry, Great Britain.

solvents indicated no stable suspensions were obtained; on the other hand, by using high-viscosity solvents (glycols, glycerol) the packing procedure became much slower, resulting in a poorer column efficiency.

Ethanol was used as the supporting liquid for both silicas and aluminas. After packing, the columns were flushed with 300–400 ml of ethanol to eliminate the slurry liquid.

Reagents

Chloroform and 1,2-dichloroethane of LiChrosolv quality (Merck, Darmstadt, G.F.R.) were used as eluents.

The solutes used were of analytical-reagent grade and had different polarities in order to cover a broad enough range of capacity factors for each adsorbent.

Procedures

The filled columns were conditioned by eluting them with 300–400 ml of chloroform.

The measurements were started at a low water content with solvents dried over molecular sieve 5Å. The water content of the solvent was then adjusted by adding a measured amount of water and equilibrated overnight by recycling the eluent. The water content of the eluent was subsequently determined by the Karl Fischer method at different intervals during the measurements. In addition, the capacity ratios were measured and checked for constancy.

The solutes were dissolved in the mobile phase and 10-μl samples were injected with the sampling valve. In all experiments toluene was used as the unretained component.

Measurements with a given water content of the eluent were carried out on the same day; then the water content was adjusted for the next measurements and equilibrated as described above.

RESULTS AND DISCUSSION

Water adsorption isotherms

For the silica gels and aluminas used water adsorption isotherms were available, having been determined in our laboratory. The mobile phase (solvent + water) is percolated in a closed circuit into a chromatographic column connected to two small columns containing a weighed adsorbent mass. When equilibrium is attained (solute retention times are constant) the mobile phase is removed with a syringe through a septum and then the two small columns are removed from the circuit. The water contents of the mobile and stationary phases are then determinated by Karl Fischer titration. This dynamic method gives a rapid equilibrium owing to good contact between the two phases[11,12]. In this work we tried to evaluate and interpret the influence of the water content of the mobile phase on the chromatographic characteristics of the different adsorbents on the basis of the shapes and characteristics of the water adsorption isotherms.

The water adsorption isotherms are shown in Fig. 1. The amount of water adsorbed is given by the number of moles of water adsorbed per unit weight of the sorbent (nH_2O) and the weight percentage of water in the sorbent; the ab-

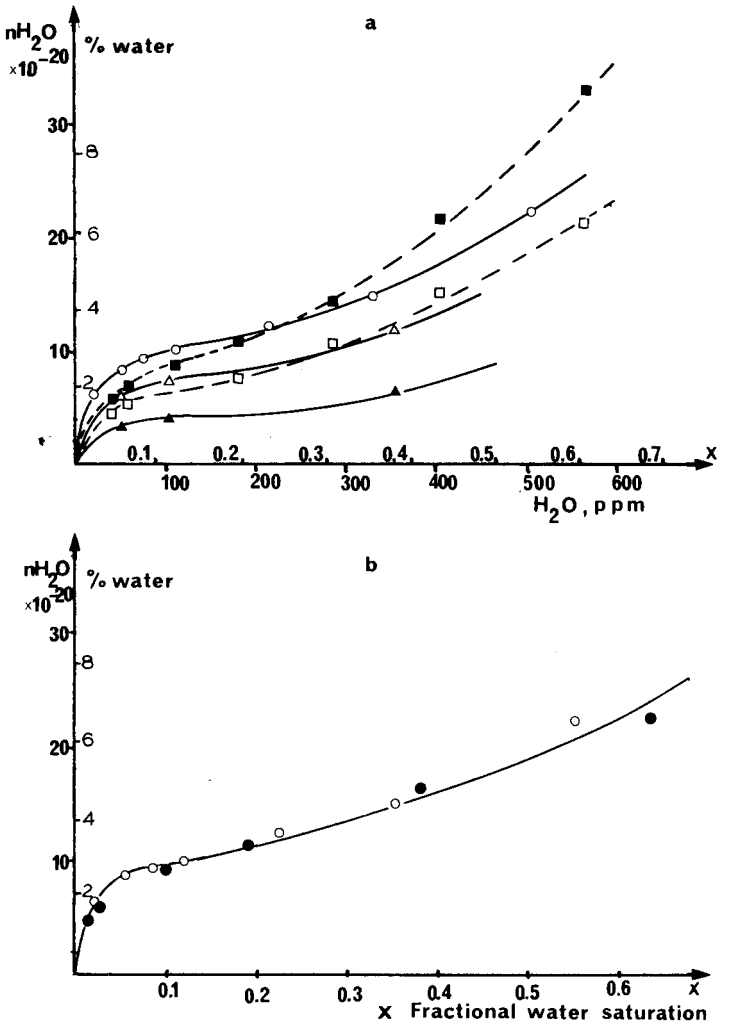

Fig. 1. Water adsorption isotherms. (a) On different adsorbents in chloroform as solvent: □, Si 100; ■, Si 60; ○, Woelm alumina; ▲, Alox T; △, A5Y. (b) On Woelm alumina: ○, in chloroform; ●, in dichloroethane.

scissas indicate the water content of the mobile phase (Fig. 1a) and the fractional water saturation (Fig. 1b). Fig. 1a shows that each isotherm consists essentially of two distinct ranges. At low water contents, a concave part can be observed, which can be linearized with the Langmuir equation[11]; at higher water contents a convex part characteristic of multilayer adsorption can be distinguished. The transition from the concave to the convex curve occurs at about 120 ppm of water in chloroform and 220 ppm of water in dichloroethane, corresponding to monomolecular coverage. Corresponding to the difference between the surface areas, the amount of water adsorbed on Si 60 is much higher than that adsorbed on Si 100. For the alumina packings the water adsorption isotherms also reflect the differences in the surface areas as given in Table I.

By comparing the water adsorption isotherms in Fig. 1a it can be seen that at low water contents the amounts of water adsorbed on the aluminas are much higher than those obtained on the silicas in spite of the lower surface areas, indicating a more pronounced activity of the alumina surface. At higher water contents the amount of water adsorbed increases more rapidly for the silicas than for the aluminas.

In Fig. 1b the water adsorption isotherms measured for Woelm alumina in chloroform and in dichloroethane are represented as a function of the fractional water saturation (X) of the solvents:

$$X = \frac{\text{ppm } H_2O \text{ (acutal)}}{\text{ppm } H_2O \text{ (saturation)}}$$

The saturation values were found to be 930 ppm for chloroform and 1860 ppm for dichloroethane at 20°C. In Fig. 1b it can be seen that the points of the isotherms measured in the two solvents are practically on the same curve, indicating that the quality of these two similar solvents has no influence on the amount of water adsorbed at the same fractional water saturation. The limit of the validity of the Langmuir equation was determined to be about $X = 0.12$ in both solvents, corresponding to monomolecular coverage of the adsorbent by water.

Thomas *et al.*[9] studied these conditions and defined isohydric solvents for improving reproducibility in liquid–solid chromatography.

Influence of water content on retention

In order to investigate the influence of the water content on retention the capacity ratios (k') of different solutes were determined. The results are shown in Figs. 2 and 3.

In Fig. 2a the capacity ratios determined on the silica packings are shown as a function of the water content in chloroform. At low water contents there is a steep decrease in the k' values corresponding to a small increase in the water content. This effect has also been observed by other workers[4,8,10]. By increasing the water content a quasi-linear slower decrease can be observed. The two parts of the curves can be approximated by straight lines, indicating a transition at about 120 ppm of water corresponding to the validity of the Langmuir equation, *i.e.*, to the formation of a monolayer of water on the silica surface.

In Fig. 2b the k' values determined on aluminas A5Y and Alox T are shown. Corresponding to the higher activity of the alumina surface and the shape of the water isotherm at low water contents, the decrease in k' values is much steeper than on silica. There are considerable differences among the capacities of the aluminas investigated in accordance with the differences in the specific surface areas. It is interesting that at higher water contents (above 300–400 ppm) these differences become very small, indicating a more uniform surface activity due to the larger amount of water adsorbed.

In Fig. 3 the effect of the solvent on the capacity ratios can also be observed. As the amount of water adsorbed is the same at a given fractional water saturation for both solvents, the influence of the solvent strength can be studied under these "isohydric" conditions. It can be seen that the k' values obtained in the "weaker" chloroform are much higher than those obtained in dichloroethane. The curves in Figs. 2

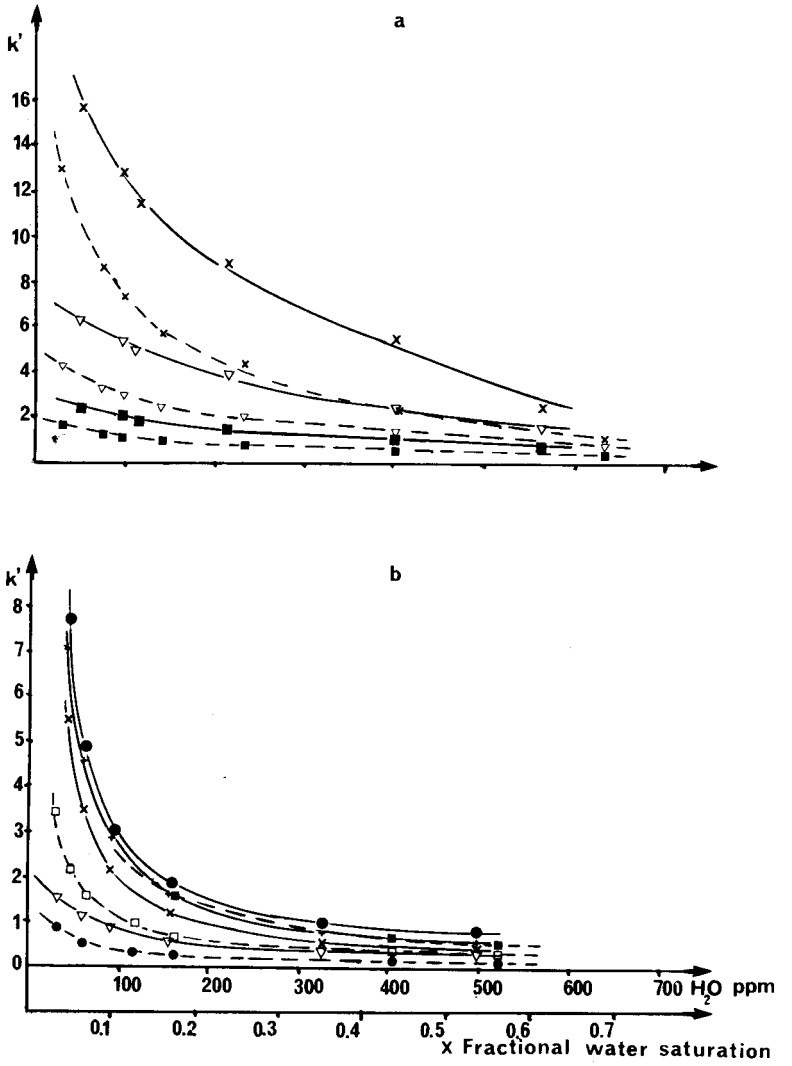

Fig. 2. Changes in capacity ratios as a function of the water content of chloroform. (a) On silica packings: ———, Si 60; – – –, Si 100; ■, ethyl benzoate; ▽, acetophenone; ×, dibutyl phthalate. (b) On alumina packings: ———, A5Y; – – –, Alox T; ▽, acetophenone; ×, dibutyl phthalate; +, diethyl phthalate; ●, dimethyl phthalate; □, *o*-nitroaniline; ■, *p*-nitroaniline.

and 3 demonstrate the importance of controlling the water content at low water contents in order to obtain the reproducibility required for the determination of k' values. The results obtained at higher water contents indicate, however, that in spite of the steep increase in the water adsorption isotherms, *i.e.*, the amount of water adsorbed in this range, the activity of the surface of all of the adsorbents investigated hardly decreases for the different solutes investigated, resulting in a very small decrease in the k' values with increasing water content of the mobile phase.

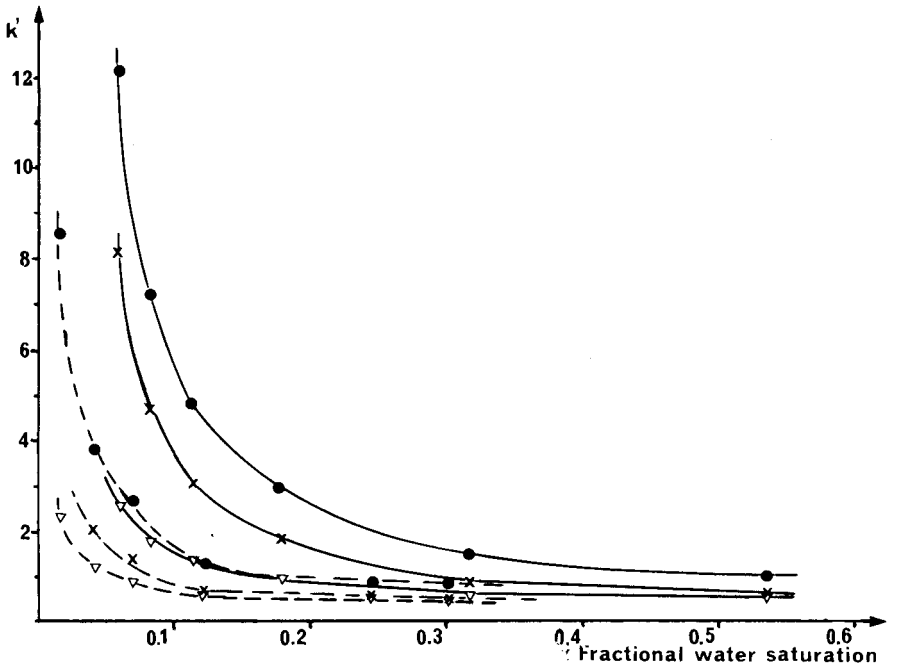

Fig. 3. Changes in capacity ratios as a function of the wate. content of the mobile phase on Woelm alumina. — —, Chloroform; – – –, dichloroethane; ▽, acetophenone; ×, dibutyl phthalate; ●, dimethyl phthalate.

Influence of water content on selectivity

In the literature, some general comments can be found on the influence of the water content of the mobile phase on the relative retention, *i.e.*, selectivities of different solutes[1–4,7–10]. It was generally observed that the retentions of different solutes vary differently on increasing the water content, sometimes resulting in a considerable change in selectivity (α). For a given pair of solutes even variations in the order of elution are possible[1,10]. However, no systematic investigation of the variation in selectivity has been published. As the selectivity has a considerable effect on the resolution, *i.e.*, the chromatographic performance of the column, the influence of the water content on the selectivity is of paramount importance for selecting the optimum conditions of the separation.

In Figs. 4 and 5 relative retentions, *i.e.*, selectivity values are shown for different pairs of solutes. In Fig. 4a the α values determined on silica packings are shown. As with the curves obtained for the capacity ratios, two parts of the curves can be distinguished. At low water contents there is a steeper decrease in the α values corresponding to a small increase in the water content of the chloroform. Again, the two parts of the curves can be approximated by straight lines, indicating a transition at about 120 ppm of water, corresponding to the formation of a monolayer of water on the silica surface. For the solutes investigated the α values always decrease with increasing water content of the chloroform.

In Fig. 4b the selectivities determined on A5Y and Alox T alumina packings are shown. In accordance with the shapes of the curves obtained for the k' values, the

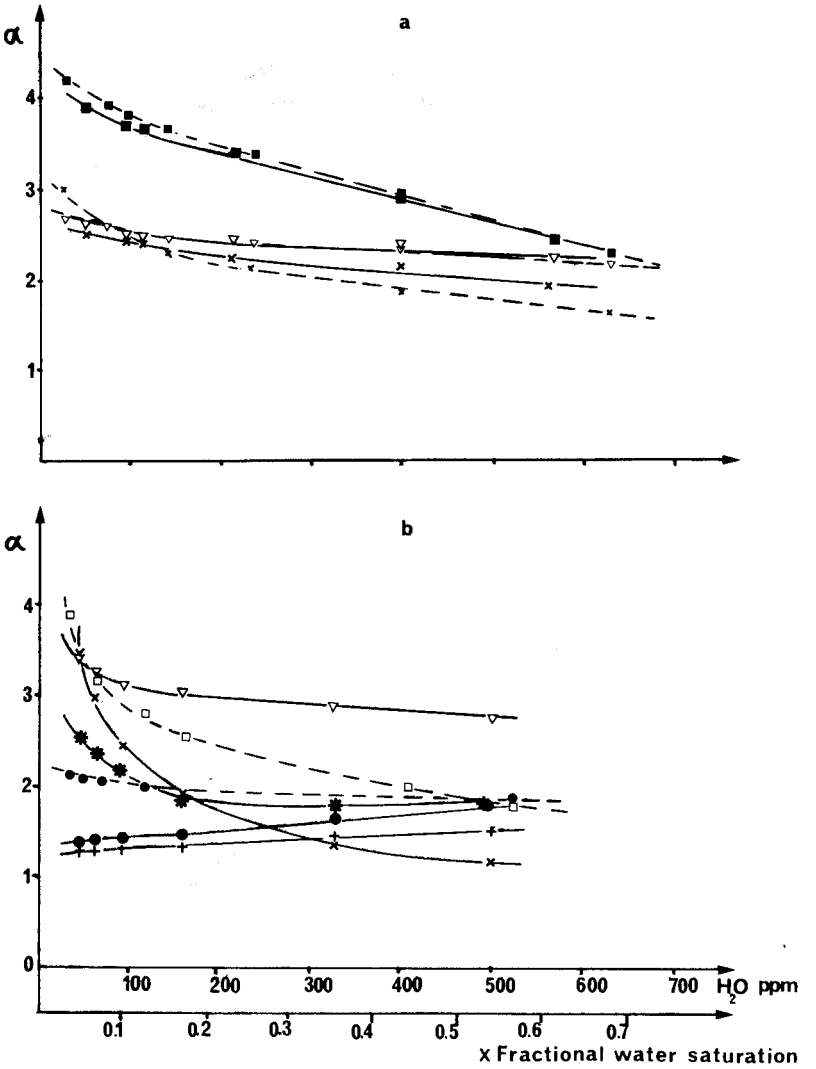

Fig. 4. Changes in selectivities as a function of the water content of chloroform. (a) On silica packings: ——, Si 60; – – –, Si 100; ■, ethyl benzoate–nitrobenzene; ▽, acetophenone–ethyl benzoate; ×, dibutyl phthalate–acetophenone. (b) On alumina packings: ——, A5Y; – – –, Alox T; ▽, acetophenone–nitrobenzene; ×, dibutyl phthalate–acetophenone; +, diethyl phthalate–dibutyl phthalate; ●, dimethyl phthalate–dibutyl phthalate; ★, acetophenone–benzonitrile.

decrease in the α values is much more significant at low water contents than that on the silicas. On the aluminas, however, the change in selectivity with increasing water content is ambiguous. For some pair of solutes (phthalic acid esters) a small but continuous increase in the selectivity can be observed with increasing water content. This indicates a special mechanism of phase exchange for these compounds on the alumina surface covered partly or completely with adsorbed water. Again, at higher water contents the decrease in selectivity becomes negligibly small, indicating a nearly

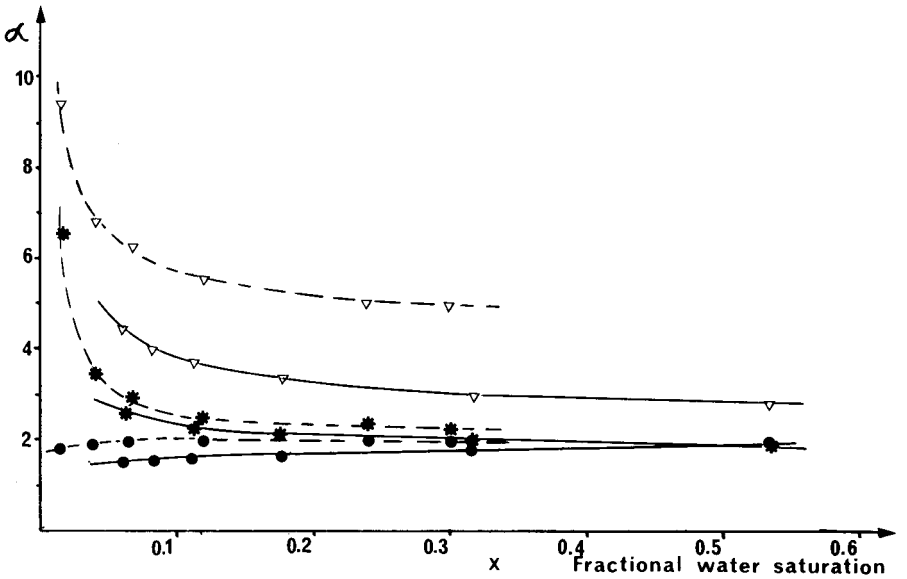

Fig. 5. Changes in selectivities as a function of the water content of the mobile phase on Woelm alumina. ——, Chloroform; – – –, dichloroethane; ▽, acetophenone–nitrobenzene; ●, dimethyl phthalate–dibutyl phthalate; ★, acetophenone–benzonitrile.

constant activity of the surface covered with adsorbed water.

In Fig. 5 the α values determined in chloroform and dichloroethane are shown as a function of the fractional water saturation (X) of the mobile phase. The considerable differences in the α values measured in the two solvents are interesting. Surprisingly, for most of the pairs of solutes investigated, higher selectivities were obtained with the stronger dichloroethane eluent. This finding emphasizes the necessity for further investigations on the influence of the eluent on selectivities in liquid–solid chromatography.

Influence of water content on efficiency

Very few experimental data, and some contradictory observations could be found in the literature on the influence of the water content on column efficiency. It is generally accepted that with a "dry" mobile phase, *i.e.*, at low water contents, much lower efficiencies can be obtained because of the strong active sites of the adsorbent surface, leading to slow adsorption-desorption kinetics[1,4,8,13]. The variation in efficiency as a function of the water content of the mobile phase was studied by El Rassi *et al.*[8] on different silica packings using dichloromethane as eluent, but only for one solute, linuron. The HETP values given show a flat minimum in each instance but at widely different and fairly high water contents for the three silicas investigated (Si 60, Si 100, Partisil 5). In another study column efficiency was found to be virtually independent of the composition of the mobile phase[14].

In our study, column efficiency was investigated by determining the number of theoretical plates at different water contents. The measurements of efficiency were carried out at different mobile phase velocities and with high chart speeds in order to

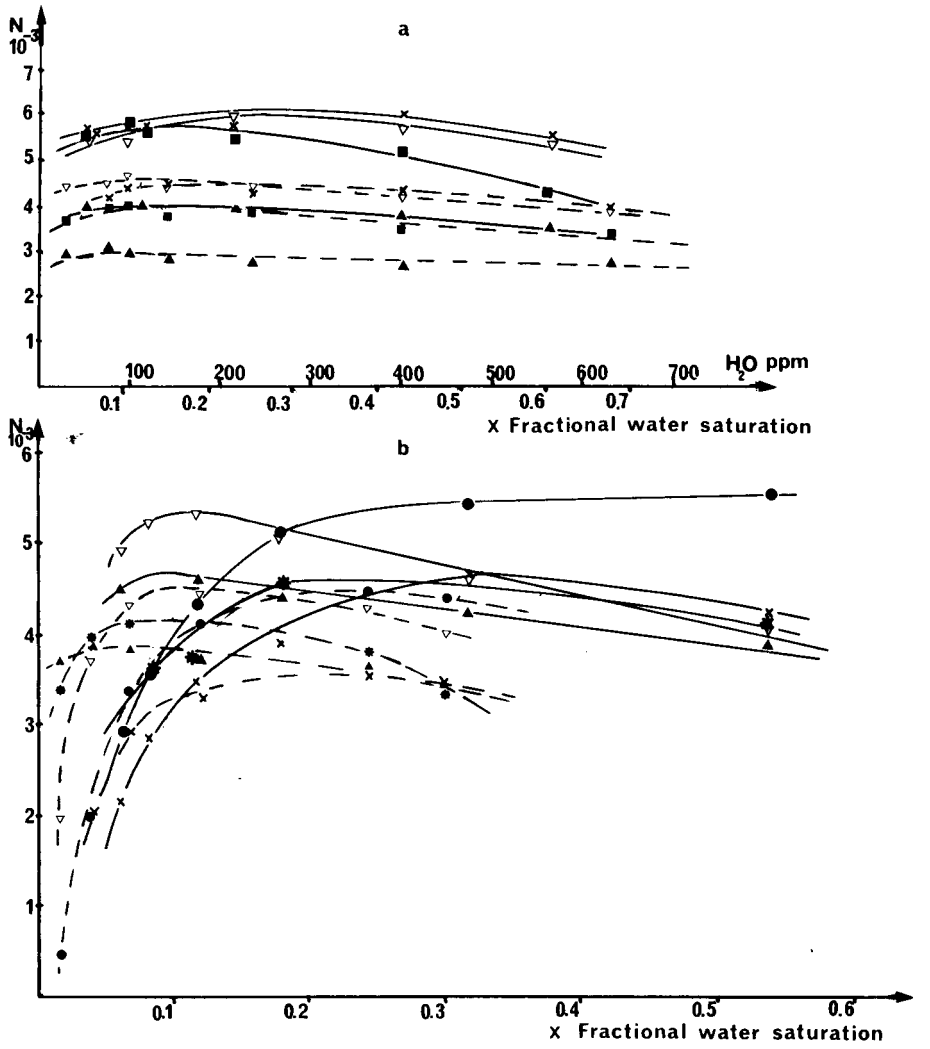

Fig. 6. Changes in number of theoretical plates as a function of the water content of the mobile phase. Flow-rate, 0.5 ml/min. (a) On silicas in chloroform: ———, Si 60; – – –, Si 100; ▲, nitrobenzene; ■, ethyl benzoate; ▽, acetophenone; ×, dibutyl phthalate. (b) On Woelm alumina: – – –, chloroform; – – –, dichloroethane; ▲, nitrobenzene; ★, benzonitrile; ▽, acetophenone; ×, dibutyl phthalate; ●, dimethyl phthalate.

permit the reliable determination of peak characteristics. Peak widths measured at half-height were used for the calculation of the number of theoretical plates, N. It should be noted that N values were calculated by using the actual peak parameters and no correction was made for external effects. N_{max} values are shown in Fig. 6 as a function of the water content of the mobile phase. Depending on the success of the filling procedure, the columns investigated showed some differences in efficiency, but this had no influence on the trends observed.

For the silica packings, the curves in Fig. 6a show flat maxima in the range

100–200 ppm of water, *i.e.*, at about the formation of a monolayer. It can also be seen that there is not much difference in efficiency in the range investigated.

The results obtained for the alumina packings were very different. Fig. 6b shows N values measured on Woelm alumina in the two solvents. At low water contents considerable peak broadening and consequently very low efficiency can be observed for nearly all of the solutes investigated. On increasing the water content the curves pass through maxima in the range 0.08–0.3 of fractional water saturation, except for dimethyl phthalate. At higher water contents the decrease in efficiency is generally slight and almost linear. The same types of N curves also were obtained on A5Y and Alox T aluminas.

Fig. 6b shows the effect of the viscosity of the eluent on column efficiency. For the less viscous chloroform (η = 0.57 cP) much higher efficiencies can be achieved than for dichloroethane (η = 0.79 cP) on the same column.

It can be concluded that peak broadening and consequently column efficiency may be different for the different solutes and different eluents and no *a priori* prediction of these values can be made. The very low and rapidly changing values at low

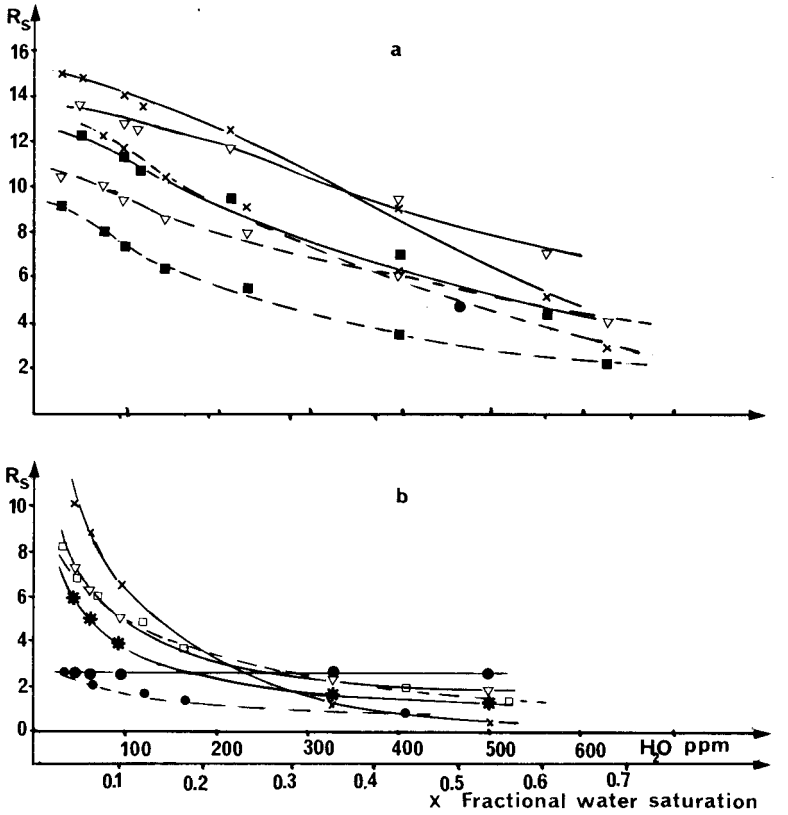

Fig. 7. Changes in R_s as a function of the water content of chloroform. (a) On silica packings: ———, Si 60; – – –, Si 100; ■, ethyl benzoate–nitrobenzene; ▽, acetophenone–ethyl benzoate; ×, dibutyl phthalate–acetophenone. (b) On alumina packings: ———, A5Y; – – –, Alox T; ▽, acetophenone–nitrobenzene; ×, dibutyl phthalate–acetophenone; ●, dimethyl phthalate–dibutyl phthalate; ★, acetophenone–benzonitrile; □, *o*-nitroaniline–dimethyl phthalate.

water contents again indicate the necessity for selection and control of the water content in the mobile phase.

Influence of water content on resolution

In every chromatographic separation the object is to separate the components of a mixture, and this separation is characterised by the resolution of two peaks (R_S). In the literature different equations are used for the determination of peak resolution. It was found that the peak resolutions determined from the chromatograms were best fitted by the values calculated by the following equation[15]:

$$R_S = \frac{\bar{N}^{1/2}}{2} \cdot \frac{\alpha - 1}{\alpha + 1} \cdot \frac{\bar{k}'}{1 + \bar{k}'}$$

where $\bar{N}$ and $\bar{k}'$ are the arithmetic mean values of the plate numbers and capacity ratios, respectively, measured for the two components being evaluated.

For this reason, eqn. 1 was used for the calculation of the R_S values shown in Figs. 7 and 8. No study has appeared in the literature on the influence of the water content of the mobile phase on peak resolution. As the terms in eqn. 1 change in different manners with changes in the basic characteristics (N,α,k'), obviously the superposition of these variations will give the variation of R_S with varying water content.

In Fig. 7a the influence of the water content on the resolution determined for the silica packings is shown. In accordance with the shape of the curves given for the basic characteristics in Figs. 2, 4 and 6, roughly two parts can be distinguished on the curves in Fig. 7a. At low water contents the decrease in the resolution is more pronounced than at higher water contents. The change in the shape of the curves at very

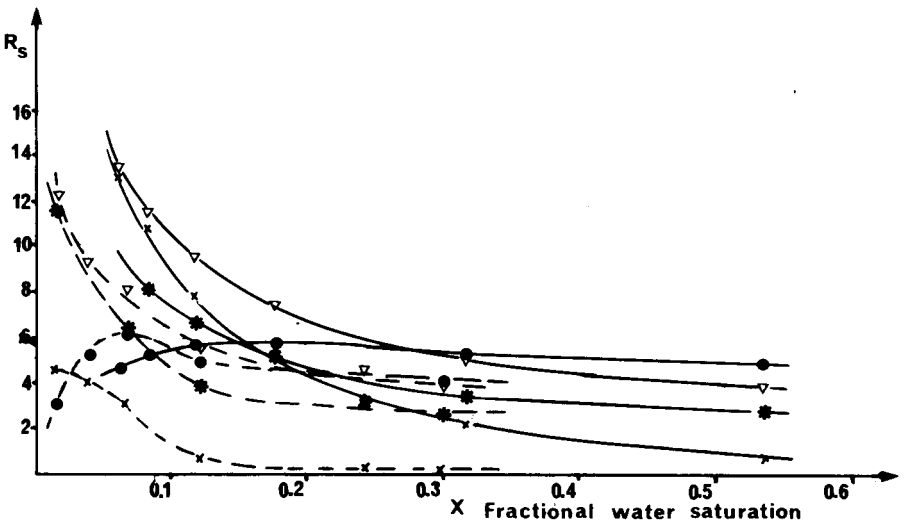

Fig. 8. Changes in R_S as a function of the water content of the mobile phase on Woelm alumina. ———, Chloroform; – – –, dichloroethane; ▽, acetophenone–nitrobenzene; ×, dibutyl phthalate–acetophenone; ●, dimethyl phthalate-dibutyl phthalate; ★, acetophenone–benzonitrile.

low water contents can be explained by the decreasing column efficiency in this region.

In Fig. 7b the resolutions obtained on A5Y and Alox T aluminas are compared. In accordance with the steep decrease in the k' and α values with increasing water content at low water contents, for most of the compounds investigated the decrease in R_S is more pronounced with increasing water content than with the silica packings. On the other hand, above a certain water content (about 200–300 ppm) the resolution decreases only very slightly.

Corresponding to the anomalous shape of the α curves obtained for some pairs of solutes (phthalic acid derivatives) and the low efficiencies obtained at low water contents, a very slight decrease, or even an increase, in resolution can also be observed with increasing water content.

The shape of the resolution curves shown in Fig. 8, obtained on Woelm alumina, reveal similar changes in resolution to those obtained on the other alumina packings. The different effects of the two eluents on the k', α and N values result in a higher resolution for the chloroform eluent.

CONCLUSION

In order to evaluate the influence of the water content of the mobile phase on the chromatographic performance of an adsorbent packing, not only changes in the capacity ratios but also changes in the selectivities and efficiencies and from these data the changes in resolution should be determined.

The changes in the chromatographic characteristics with increasing water content of the mobile phase can be explained qualitatively on the basis of the water adsorption isotherms measured on the different adsorbents.

For silica packings and the solutes investigated, an increase in the water content of the mobile phase results in a decrease in the k' and α values and flat maxima of the N values. In accordance with these variations, R_S decreases continuously with increasing water content but this decrease is more pronounced at low than at higher water contents. The transition occurs at about 120 ppm of water in chloroform, corresponding to the formation of a monolayer on the adsorbent surface. On the alumina packings investigated, in accordance with the higher activity of the alumina surface, k' and α values decrease more rapidly with increasing water content and for the α values reversed effects can also be observed. The plate numbers are very poor at low water contents and pass through flat maxima at higher water contents.

Corresponding to these effects, for most of the compounds investigated the decrease in R_S is more pronounced with increasing water content than that on silica packings, but beyond a certain limit R_S decreases only very slightly. For some pairs of solutes a very slight decrease, or even an increase, in resolution can also be observed with increasing water content.

The results obtained with two different solvents on Woelm alumina indicate the influence of the solvent on the chromatographic characteristics. The choice of the best solvent for a given separation is still a hardly exploited area in high-performance liquid chromatography. The effect of the water content on the chromatographic characteristics of different solutes may be quite different, indicating a possible diversity of mechanisms and the necessity for further investigations with a broad range of solutes.

The results of this study also reveal some possibilities of practical importance. Adsorbent packings with moderately polar solvents and a properly adjusted water content can be used advantageously for the separation of polar compounds. At higher water contents both the variation in the water content and the effect of this variation on the chromatographic performance are much less important, in many instances negligible, than at the low water contents generally applied in adsorption chromatography.

ACKNOWLEDGEMENT

L.S. gratefully acknowledges a research grant from the Scientific Exchange Agreement (SEA) Foundation.

REFERENCES

1 L. R. Snyder, *Principles of Adsorption Chromatography*, Marcel Dekker, New York, 1968.
2 J. J. Kirkland, *Modern Practice of Liquid Chromatography*, Wiley, New York, 1971.
3 H. Halpaap, *J. Chromatogr.*, 78 (1973) 63.
4 H. Engelhardt and H. Wiedemann, *Anal. Chem.*, 45 (1973) 1641.
5 G. Cavina, G. Moretti and A. Cantafora, *J. Chromatogr.*, 80 (1973) 89.
6 H. Engelhardt, J. Asshauer, V. Neue and N. Weigand, *Anal. Chem.*, 46 (1974) 336.
7 L. V. Berry and H. Engelhardt, *J. Chromatogr.*, 95 (1974) 27.
8 Z. El Rassi, C. Gonnet and J. L. Rocca, *J. Chromatogr.*, 125 (1976) 179.
9 J. P. Thomas, A. Brun and J. P. Bounine, *J. Chromatogr.*, 139 (1977) 21.
10 W. Boehme and H. Engelhardt, *J. Chromatogr.*, 133 (1977) 67.
11 M. Thibert, M. Caude and R. Rosset, *Analusis*, 7 (1979) 454.
12 C. Combellas, M. Caude and R. Rosset, *J. Chromatogr.*, in preparation.
13 L. R. Snyder, *Anal. Chem.*, 39 (1967) 698.
14 J. E. Paanakker, J. C. Kraak and H. Poppe, *J. Chromatogr.*, 149 (1978) 111.
15 L. R. Snyder and J. J. Kirkland, *Introduction to Modern Liquid Chromatography*, Wiley, New York, 1974.

Journal of Chromatography, 237 (1982) 79–88
Elsevier Scientific Publishing Company, Amsterdam — Printed in The Netherlands

CHROM. 14,496

AMBERLITE XAD-2 AND XAD-4 AS CATION-EXCHANGE RESINS OF LOW CAPACITY

AN INVESTIGATION USING AN ATOMIC FLUORESCENCE DETECTOR DIRECTLY COUPLED TO A LIQUID CHROMATOGRAPH

D. J. MACKEY
Division of Oceanography, CSIRO Marine Laboratories, P.O. Box 21, Cronulla, NSW 2230 (Australia)
(Received October 20th, 1981)

SUMMARY

A four-channel atomic fluorescence detector, directly coupled to the output of a chromatography column, has been used to monitor the adsorption of magnesium, iron, zinc and copper by Amberlite XAD resins and the subsequent elution of these metals by disodium dihydrogenethylenediamine tetraacetate or ammonia. All the metals can be adsorbed from aqueous solution at pH 2.5 but the adsorption of iron is strongly pH dependent and this influences the adsorption of the other metals since iron forms the strongest complexes in the pH range 1.5–2.5. The adsorption capacity of XAD-4 is approximately halved by washing with methanolic hydrochloric acid and evidence is presented for the existence of a number of different, but unknown, impurity sites on these resins. These results are of special significance to the use of these resins for studying trace metal speciation in natural waters.

INTRODUCTION

The chemical speciation of trace metals in seawater and other natural waters has been the subject of much discussion. It is generally agreed that biologically important metals such as copper, zinc and iron exist mostly in forms other than the simple cations, but the actual chemical species present are unknown. While there is undoubtedly some metal present as inorganic complexes or as inorganic or organic colloidal material, there is increasing evidence that significant amounts of these metals may exist in natural waters as metal–organic complexes. The donor groups of any ligating organic compound are probably hydrophilic moieties such as –COOH, –OH and $-NR_2$ and hence the metal–organic compounds would tend to be more hydrophobic than the parent organic molecules and should be more readily adsorbed on hydrophobic resins. The Amberlite XAD resins have been widely used for extracting organic compounds from nautral waters and in some cases metal organic complexes have been extracted. Thus Mantoura *et al.*[1] used XAD-2 resin to extract humic substances from natural waters and found that the humic compounds contained trace

0021-9673/82/0000–0000/$02.75

metals and Riley and Taylor[2] found that added vitamin B_{12} could be quantitatively removed from seawater by adsorption onto Amberlite XAD-1. These studies are not directly relevant to trace metal speciation in seawater since, in the first case, the seawater was acidified to pH 2.2 to remove the humic compounds and this could change the speciation significantly while, in the second case, the seawater was spiked with vitamin B_{12} at a concentration about three orders of magnitude higher than occurs naturally.

Sugimura *et al.*[3,4] used XAD-2 resin to extract trace metals from seawater and Lyons *et al.*[5] used XAD-2 to extract iron from anoxic nearshore sediment pore fluids. These authors assumed that any metal adsorbed by these resins was in the form of organic complexes since it had been reported[2–7] that simple inorganic cations were not adsorbed. Recent experiments[8] have shown that this is not the case and that Amberlite XAD-1 and XAD-2 adsorb significant amounts of iron, copper and zinc from distilled deionized water spiked with simple cations of these metals. This adsorption of simple cationic species of copper and zinc was presumed to be the reason that these metals could not be reproducibly extracted from seawater by XAD-1[8].

The Amberlite resins (XAD-1, XAD-2 and XAD-4) are all made by the polymerization of styrene–divinylbenzene mixtures and differ primarily in pore size and effective surface area. In principle, they contain no functional groups that can coordinate trace metals, although Puon and Cantwell[10] found that XAD-2 was capable of adsorbing 1 μmole H_3O^+ or 0.2 μmole OH^- per gram of resin depending on pH. The acrylic ester resins (XAD-7 and XAD-8) have been reported as possessing a very low ion-exchange capacity —in the order of 10 μmole g^{-1} in the case of XAD-8[11]— but these authors also reported that the cross-linked polystyrene resins (XAD-1, XAD-2 and XAD-4) possessed no ion-exchange capacity and it is possible that there could be batch to batch variations in these resins. The manufacturer of these resins was unable to provide any information as to the nature or concentration of potential impurity sites.

In a previous paper[9] the adsorption of trace metals from water by XAD-2 was studied by means of a multichannel atomic fluorescence detector (AFD) coupled directly to the output of a chromatographic column packed with the resin. The measurements on XAD-2 are extended in this paper under more rigorously controlled conditions and the results are compared with similar experiments on the chemically identical resin XAD-4.

EXPERIMENTAL

Standard solutions containing 1 g l^{-1} of metal were made by dissolving analytical-reagent grade metal sulphates (ammonium-ferric-alum in the case of iron) in distilled deionized water (DDW) from a Milli-Q system. The stock solution was made by diluting 10 ml each of these solutions to a litre and contained 10 mg l^{-1} of magnesium, iron, zinc and copper. This solution gradually precipitated ferric hydroxide and was acidified drop wise with analytical-reagent grade sulphuric acid until the precipitate disappeared. The final pH was 2.50. A subsample of this stock solution was acidified to pH 1.50 and another subsample was adjusted to the same pH in the presence of $10^{-2}M$ analytical-reagent grade acetic acid. The solutions used for eluting the columns were 10^{-3} M analytical-reagent grade disodium dihydrogenethylenediamine tetraacetate (H_2Y^{2-}) and 5% Aristar-grade ammonia (NH_3). DDW was used in all cases.

The chromatographic equipment was the same as described previously[9] and was of the Cheminert type manufactured by Laboratory Data Control. A CMP-3K pump was used and the chromatography columns were 6 mm I.D. and contained about 4 ml of resin. Two columns, containing XAD-2 and methylated XAD-2 respectively, were the same columns as used previously[9]. The third column was packed with XAD-4 resin that had been soxhlet extracted for 16 h with methanol and 8 h with acetonitrile.

The AFD has been described earlier[9] but the magnesium lamp was operated at 5mA rather than 20 mA. Careful alignment of the optics had resulted in much stronger fluorescence signals for all metals and at higher lamp currents the magnesium fluorescence was so intense that it interfered severely with the iron and copper signals. Under the conditions used in this paper, there was no interference between the separate channels.

The general experimental procedure consisted of injecting 500 μl of stock solution (containing 5 μg each of magnesium, iron, zinc and copper) onto the column with DDW at a flow-rate of 100 ml h^{-1}. The effluent from the column passed directly into the variable nebulizer of the AFD and the nebulizer was adjusted so that the uptake rate was identical to the flow rate through the column. Any adsorption by the column resulted in a reduced signal from the detector. Even allowing for a reduction in the maximum concentration in the effluent due to band broadening and/or adsorption, the peak concentration was generally higher than the linear region of the fluorescence versus concentration calibration curve. This saturation effect is less important for iron than for copper and zinc and previous experiments[9] showed that significant departures from linearity occur at concentrations of 600 $\mu g\, l^{-1}$ (Zn), 1000 $\mu g\, l^{-1}$ (Cu) and $\geqslant$ 1600 $\mu g\, l^{-1}$ (Fe). Thus a small decrease in the copper or zinc fluorescence signal corresponds to considerable adsorption of these ions by the resin. Saturation effects were not apparent for magnesium which is surprising since Larkins[12], using similar equipment, reported non-linear effects at concentrations above 400 $\mu g\, l^{-1}$ (Mg), 300 $\mu g\, l^{-1}$ (Zn) and 2000 $\mu g\, l^{-1}$ (Fe). No attempt was made to quantify the amounts of trace metal in the effluent from the column since this is difficult using the AFD at the concentrations involved and the main interest was in comparing the adsorption properties as a function of resin type, pH, number of loadings etc. The fluorescence signals were compared by measuring the peak heights and half-widths. The "tailing" of the peaks was determined by measuring the width at one tenth of peak height. The fluorescence signals for iron and, particularly, zinc and copper are generally truncated due to saturation effects. Hence the experimentally determined half-width is actually the width at a much lower fraction of the maximum signal intensity. Any reduction in the concentration of copper and zinc (and to a lesser extent iron) initially leaves the peak height almost constant but the line shape changes as the truncation effect is reduced. This leads to an apparent decrease in the experimentally determined half-width. However, any interaction with the column will also cause line broadening and the resultant line width is a compromise between these two opposing tendencies. The concentrations of metal in the H_2Y^{2-} and NH_3 eluates were usually much lower than in the column effluents and the metal concentrations should be roughly proportional to peak height.

After the fluorescence signals in the effluent returned to background levels, the columns were eluted at 100 ml h^{-1} with H_2Y^{2-} or NH_3 and the eluate was monitored

by the AFD. All washing and preconditioning of the columns was done at a flow-rate of 500 ml h^{-1}. The columns were also eluted after two, three and five successive injections of stock solution.

The iron, zinc and copper fluorescence signals were recorded on a three-pen recorder and the magnesium fluorescence on a separate recorder. The recorder traces shown in this paper were made by superimposing the signals from both recorders. The traces have been offset slightly for clarity.

RESULTS AND DISCUSSION

XAD-2

Five successive samples of stock solution at pH 2.50 were injected onto a column of XAD-2 and the fluorescence signals in the effluent are shown in Fig. 1a. The recorder traces for the last four injections are identical but the first injection is distinguished by a slightly diminished copper peak while the tailing is a little more pronounced for the iron peak and a little less pronounced for the zinc peak. The differences are small but are reproducible. Figs. 1b–e show the elution peaks when the column was eluted with H_2Y^{2-} after separate experiments where the column was loaded with 5, 3, 2 and 1 injection of stock solution, respectively. The small magnesium fluorescence in all the elutions and the zinc fluorescence after 5 and 3 injections may be due to insufficient time being allowed for all the stock solution to pass through the column before the elution with H_2Y^{2-}.

Inspection of the elution peaks in Figs. 1b–e reveals that the four metals interact quite differently with XAD-2. In the presence of iron, copper and zinc, the adsorption and subsequent elution of magnesium is negligible. The amount of zinc adsorbed by the resin decreases markedly on the second injection and becomes negligible after

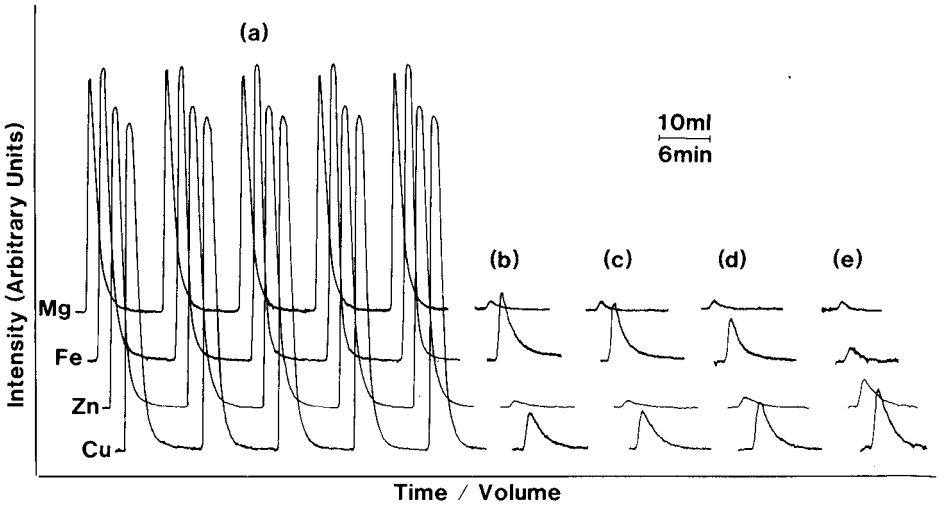

Fig. 1. (a), Atomic fluorescence signals from the effluent from a column of XAD-2 resin after five successive loadings of 500 μl of stock solution at pH 2.50. (b)–(e), Atomic fluorescence signals from the eluent when the column was eluted with H_2Y^{2-} after 5, 3, 2 and 1 loading, respectively.

the third injection. A decrease in the amount of adsorbed copper is also observed but the decrease is much less marked and the amount adsorbed appears to be approaching some equilibrium value. The amount of iron adsorbed by the resin increases on successive injections and it is apparent that iron is able to completely displace adsorbed zinc and partially displace adsorbed copper. The strength of interaction of these four metals decreases in the sequence $Fe^{3+} > Cu^{2+} > Zn^{2+} > Mg^{2+}$.

Although there is significant adsorption of zinc on the first injection, the peak height of the zinc fluorescence in the effluent is indistinguishable from the peak height on the second injection when zinc is actually being added to the effluent due to the displacement of zinc by iron. This is caused by the saturation of the zinc fluorescence signal but it appears that zinc is rapidly adsorbed on the first injection since the effluent band is slightly narrowed. Iron obviously reacts more slowly with the resin since the total amount of adsorbed iron increases steadily with successive additions and this gives rise to a broader signal with more pronounced tailing on the first injection. The rate of adsorption of copper appears to be somewhat between the rates for iron and zinc with the net result that the line shape of the effluent peak remains unaltered although the peak height increases slightly after the first addition.

The adsorption of these metals by methylated XAD-2 resin[9] closely parallels the behaviour of the unmethylated resin. The same small differences exist between the fluorescence signals of the effluent from the first injection relative to all subsequent injections and the fluorescence signals are essentially indistinguishable from those of the unmethylated resin as shown in Fig. 1a. The amount of iron, copper and zinc eluted from the column by H_2Y^{2-} is about 20% less than for the untreated resin and this reduction in adsorption capacity is independent of the number of injections of stock solution. This implies that the functional groups that had been methylated were representative of the donor sites on the resin and did not have a special affinity for any of the metals studied.

When stock solution at pH 1.50 was injected onto the column of XAD-2, the fluorescence signals of the effluent solution were similar to those obtained at pH 2.50. The effluent peaks after a single injection were also different from those of subsequent loadings and in addition to the slight differences observed at pH 2.50, it was found that both the half-width and tailing of the copper signal were slightly larger for the first peak relative to all subsequent peaks. However, the total amount of metal adsorbed onto the resin at pH 1.50 was less than half the amount adsorbed at pH 2.50 although the general pattern was similar with negligible adsorption of magnesium and little adsorption of zinc which was displaced from the resin after the second injection of stock solution. The displacement of copper by iron was much less pronounced at the lower pH and after five loadings, the final iron and copper signals in the H_2Y^{2-} eluate were approximately the same whereas, at pH 2.50, the iron fluorescence was approximately double that of copper (Fig. 1b).

The column of XAD-2 was also loaded by successive injections of a stock solution at pH 1.50 in the presence of 10^{-2} *M* HOAc and the results are indistinguishable from those obtained in the absence of acetic acid. The stock solution had a total metal concentration of $9 \cdot 10^{-4}$ *M* and was also 10^{-2} *M* in undissociated acetic acid and $3 \cdot 10^{-2}$ *M* in hydrogen ions and one would expect at least some adsorption of undissociated acetic acid onto the resin. If the complexing sites on XAD-2 were similar to isolated carboxyl groups, there should be increased adsorption of trace

metals by the resin in the presence of acetic acid. Since this does not occur, either a negligible amount of acetic acid is adsorbed or else the impurity donor sites are different from simple carboxylate groups.

In order to confirm that the results obtained above were not due to adsorbed ethylenediamine tetraacetic acid, the column of XAD-2 was extensively washed with NH_3 solution and DDW and the previous experiment was repeated. The results after this treatment were identical to those obtained prior to washing with ammonia.

XAD-4

The adsorption of trace metals by XAD-4 at pH 1.50 is comparable to that of XAD-2 at the same pH and, as found earlier, the presence of 10^{-2} *M* acetic acid has no effect. The traces for successive loadings and elutions are shown in Fig. 2. The copper fluorescence signal in the first column effluent is much less truncated than is found in subsequent effluents while tailing effects are more pronounced. The copper in the effluent has been spread out over a larger volume with a subsequent decrease in the maximum concentration. This implies a significant interaction between copper and XAD-4. A similar but less pronounced effect is observed for iron after the first addition even though negligible iron is removed from the resin on elution with H_2Y^{2-} (Fig. 2e). However, the resin is capable of adsorbing iron as is apparent from Fig. 2b where iron is found in the H_2Y^{2-} eluate after the column had been loaded five times. As before, this adsorption of iron occurred at the expense of copper and zinc. The desorption peaks from XAD-4 (Figs. 2b–e) are broader than those from XAD-2 (Figs. 1b–e) and it seems that H_2Y^{2-} is a less effective eluent in the former case. In agreement with this, it was found that reproducible behaviour could only be obtained if the column was extensively washed between experiments. The washing time could be reduced by including an ammonia wash between the H_2Y^{2-} and DDW elutions.

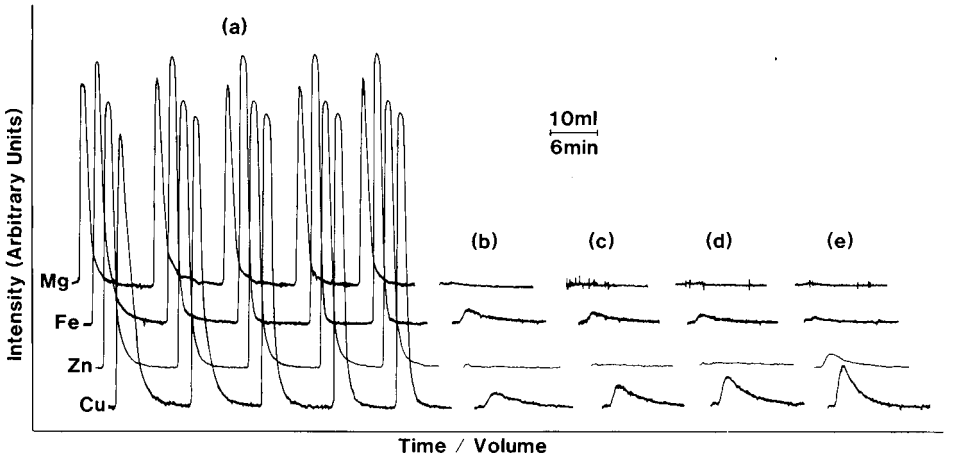

Fig. 2. (a), Atomic fluorescence signals from the effluent from a column of XAD-4 resin after five successive loadings of 500 μl of stock solution at pH 1.50 in the presence of 10^{-2} *M* acetic acid. (b)–(e), Atomic fluorescence signals from the eluent when the column was eluted with H_2Y^{2-} after 5, 3, 2 and 1 loading, respectively.

In the previous experiments, the total amount of metal in each 500 μl injection (450 nmol) exceeded the adsorption capacity of the resin and the competition between the metals for the available coordination sites excluded significant adsorption of zinc and magnesium. The larger surface area of XAD-4 (725 $m^2 g^{-1}$) compared to XAD-2 (300 $m^2 g^{-1}$) would be expected to give rise to a greater adsorption capacity by XAD-4 and although this was not observed at pH 1.50, the results at pH 2.50 are very different from those described previously since the adsorption capacity of the resin becomes comparable to the amount of metal in each injection. Under these conditions, the effluent and elution peaks become quite different since on the first injection even magnesium is strongly adsorbed and all the effluent peaks are reduced in height and show no evidence of truncation due to saturation effects (Fig. 3a). The strong interaction between the resin and iron, copper and zinc gives rise to pronounced tailing although this is not apparent for magnesium. The kinetics of adsorption and desorption of magnesium may be more rapid than for the other metals. On elution with H_2Y^{2-}, strong signals are observed for copper, zinc and magnesium with

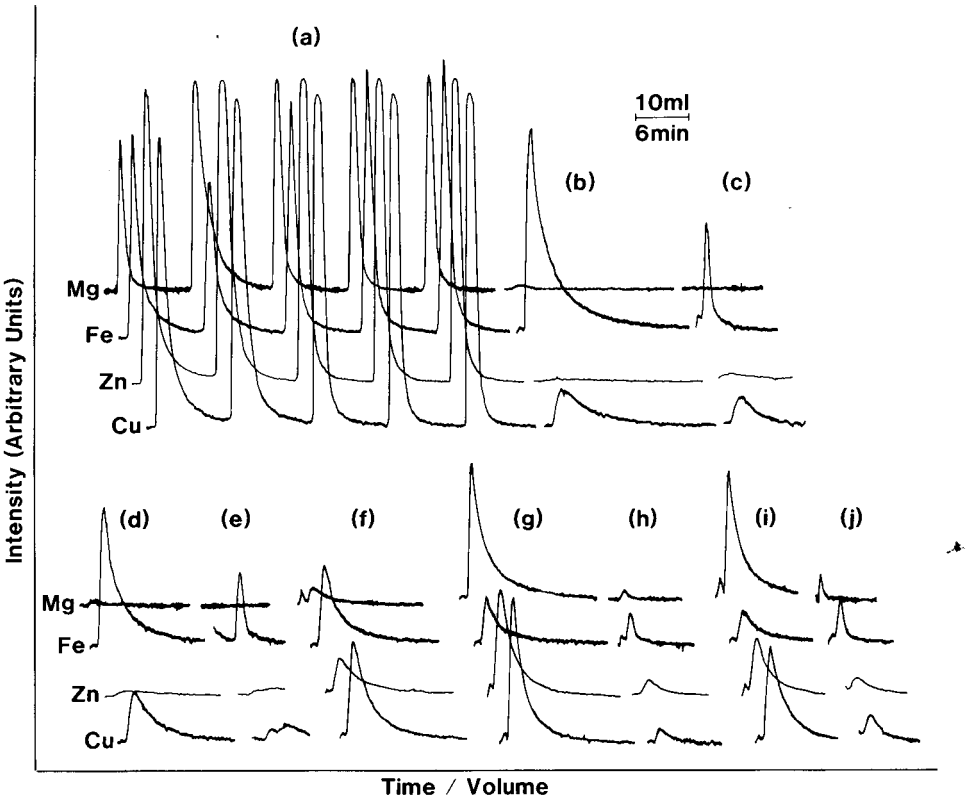

Fig. 3. (a) Atomic fluorescence signals from the effluent from a column of XAD-4 resin after five successive loadings of 500 μl of stock solution at pH 2.50. (b)–(j), Atomic fluorescence signals from the eluents under the following conditions: five loadings and elution with (b) H_2Y^{2-} followed by (c) NH_3; three loadings and elution with (d) H_2Y^{2-} followed by (e) NH_3; two loadings and elution with (f) H_2Y^{2-}; one loading and elution with (g) H_2Y^{2-} followed by (h) NH_3; one loading (at 25 ml h^{-1}) and elution with (i) H_2Y^{2-} followed by (j) NH_3.

a weaker iron signal (Fig. 3g). The elution peaks are broad and asymmetric and subsequent elution with NH_3 gives rise to broad, weak copper and zinc signals, a small, sharp iron signal and a negligible magnesium signal (Fig. 3h).

On further injections of stock solution, the copper and zinc concentrations in the effluent increase until the fluorescence signals in the second effluent are nearly equal to those in the third and subsequent effluents although there is slightly more tailing. The second magnesium effluent peak is much greater than the third and subsequent peaks while the iron peak is even smaller than the first. It is apparent that iron is being strongly adsorbed at the expense of magnesium and from Fig. 3f it is seen that the iron elution peak is much stronger and there is very little magnesium eluted from the column. On the third and subsequent injections, the iron effluent peaks increase but iron is still being strongly adsorbed as is evidenced by the lack of saturation effects and by increasingly strong iron fluorescence in the H_2Y^{2-} elutions (Figs. 3f, d, b). After five injections, only iron and copper remain on the column and the H_2Y^{2-} elution peaks are very broad and asymmetric. Subsequent elutions with NH_3 produced broad copper signals and much sharper iron signals (Figs. 3c, e, h) and the significance of this is discussed later.

The minimum in the iron effluent concentration on the second injections means that iron is more readily adsorbed by the resin on the second injection and hence that the resin was preconditioned by the first loading. There are two ways in which this could occur. Firstly the stock solution had a higher acidity (pH 2.50) than the DDW used to wash the column and the first loading could have protonated impurity groups that existed in their basic form prior to the initial loading. If such protonated groups are still present on the resin when the second loading occurs, and if ferric ions react more readily with such groups, then iron would be more readily adsorbed on the second injection. Alternatively, ferric ions could react more readily with sites coordinated to magnesium and hence the second loading would give rise to an increased adsorption or iron (relative to the first loading) with a concomitant release of magnesium as is observed. It is possible that both processes occur and the chances of observing such an enhancement in adsorption require a serendipitous choice of pH, metal concentrations and resin adsorption capacity.

Iron appears to be absorbed more slowly than magnesium (Fig. 3) and kinetic effects were investigated by loading the column of XAD-4 with one injection of stock solution (pH 2.50) at 25 ml h^{-1}. The column was then eluted with H_2Y^{2-} and NH_3 in the usual way and the results are shown in Figs. 3i and j. The traces are qualitatively the same as obtained when the column was loaded at 100 ml h^{-1} (Figs. 3g and h), although it is difficult to explain why there is less iron, copper and zinc adsorbed at the slower flow rate. However, the important fact is that the relative affinity of XAD-4 for these metals is not affected by changing the loading rate by a factor of four.

In order to get further information on the binding between trace metals and XAD-4, the column was loaded with a single injection of stock solution (pH 2.50) and eluted successively with H_2Y^{2-} and NH_3 (Fig. 4a). The experiment was repeated with the NH_3 elution preceding the H_2Y^{2-} elution and the results are shown in Fig. 4c. As observed earlier (Figs. 3c, e, h and j) iron, copper and zinc can still be eluted by NH_3 even after extensive washing with H_2Y^{2-}. When the elution order is reversed, there is a ready release of copper and zinc, presumably as $M(NH_3)_4^{2+}$. Magnesium and iron do not form ammonia complexes in aqueous solution and any metal liberated from

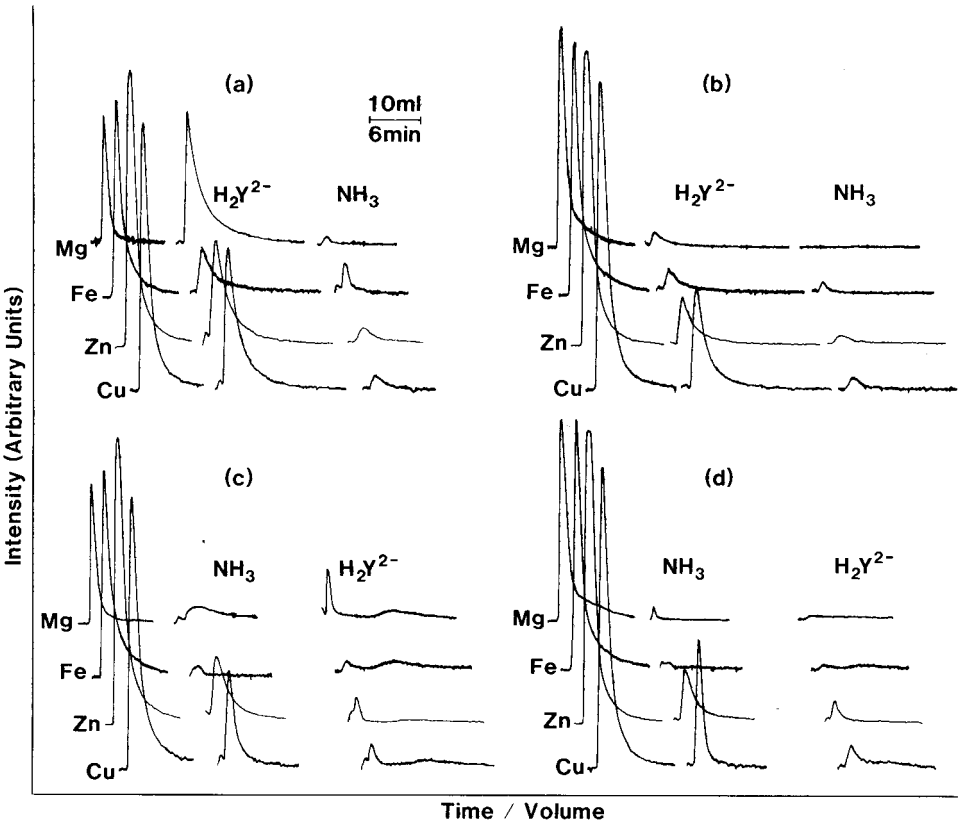

Fig. 4. Atomic fluorescence signals from the effluent from a column of XAD-4 after a single loading of stock solution at pH 2.50 followed by elution with (a) H_2Y^{2-} then NH_3 and (c) NH_3 then H_2Y^{2-}. The resin was then washed with methanolic HCl and the experiments repeated giving the traces shown in (b) and (d).

the resin would be converted into insoluble hydroxides which pass slowly through the column giving rise to rather broad featureless elution bands. On subsequent elution with H_2Y^{2-}, small amounts of copper and zinc are desorbed while magnesium and iron both give rise to two elution bands. The broad weak second bands are probably due to slow dissolution of iron and magnesium hydroxides by H_2Y^{2-}. The origin of the initial sharper peaks is not quite so clear and two possibilities arise: (a) the peaks could be due to the rapid release of iron and magnesium bound to impurity sites on the resin that do not readily release these metals to NH_3, or (b) mixed hydroxy/ethylenediamine tetraacetate complexes may be formed which are more readily eluted due to an increase in the negative charge on the complex. Using tabulated stability constants[13] it can readily be shown that the iron complex $FeY(OH)^{2-}$ is not stable in dilute ammonia (pH $\approx$ 11) but at the interface between ammonia and H_2Y^{2-} (pH 4.5) suitable conditions might exist. Such an explanation could also account for the strong sharp elution peaks of iron when the column was eluted with ammonia in earlier experiments (Figs. 3c and e).

When the column was eluted with NH_3 prior to elution with H_2Y^{2-} the resin required extensive cleaning to remove the precipitated hydroxides of iron and magnesium although the original characteristics of the column could ultimately be reproduced. After all the previous experiments had been completed, the column was

washed at 100 ml h^{-1} with 400 ml of 10% methanolic HCl (Merck Suprapure) followed by 125 ml of DDW (500 ml h^{-1}). This procedure had a substantial effect on the adsorption capacity of the resin and comparison of Figs. 4a and b reveals that the column is no longer capable of adsorbing magnesium under the conditions used while the amount of iron, copper and zinc in the eluates is reduced by at least one third. There is also a suggestion that the relative affinity of metals for the resin is altered since the ammonia elution peak for copper (Fig. 4c) is smaller than that observed after the resins had been treated with methanolic HCl (Fig. 4d) contrary to the results for all other elution peaks. It is apparent that some of the functional groups have either been hydrolysed by the methanolic HCl or else have been methylated with a subsequent reduction in Lewis basicity.

In experiments involving only copper and zinc[9] it was found that the adsorption of these metals by XAD-1 and XAD-2 was not strongly dependent on pH. This is not the case where iron is also present since Fe^{3+} forms stronger complexes than zinc or copper and the adsorption of Fe^{3+} is pH dependent. This is of great importance to any investigation of natural waters since iron is generally more abundant than either copper or zinc. Mackey[9] also found evidence for more than one type of impurity donor site on XAD-1 and XAD-2 and the present results on XAD-4 tend to support that idea since some of the adsorbed trace metal is more readily eluted by H_2Y^{2-} than NH_3 while the reverse holds for some adsorbed metal and a significant amount is readily desorbed by either eluant although the desorption is generally slower for XAD-4 than for XAD-2.

The kinetics of adsorption by these resins is interesting and there is no obvious reason for the gradual increase in the amount of iron adsorbed on successive injections nor for the fact that magnesium can be adsorbed from solution even though the column effluent still contains large amounts of iron, copper and zinc (Figs. 3g, 3i and 4a). However, the fact that magnesium can be adsorbed by XAD-4 (and presumably XAD-2), under certain conditions should be borne in mind if these resins are used for speciation studies on seawater where the magnesium concentration may be six orders of magnitude greater than that of the trace metals of interest.

Since iron seems to displace magnesium very readily, this adsorption of magnesium may catalyse the uptake of iron from seawater. In any case, adsorption of trace metals by XAD-2 from natural waters acidified to approximately pH 2.50 cannot be taken as evidence for the existence of organically associated metals in those waters[3–5].

REFERENCES

1 R. F. C. Mantoura, A. Dickson and J. P. Riley, *Estuarine Coastal Mar. Sci.*, 6 (1978) 387.
2 J. P. Riley and D. Taylor, *Anal. Chim. Acta*, 46 (1969) 307.
3 Y. Sugimura, Y. Suzuki and Y. Miyake, *J. Oceanogr. Soc. Jap.*, 34 (1978) 93.
4 Y. Sugimura, Y. Suzuki and Y. Miyake, *Deep-Sea Res.*, 25 (1978) 309.
5 W. B. Lyons, H. E. Gaudette and P. B. Armstrong, *Nature (London)*, 282 (1979) 202.
6 Y. Sakai, *Talanta*, 27 (1980) 1073.
7 A. K. Burnham, G. V. Calder, J. S. Fritz, G. A. Junk, H. J. Svec and R. Willis, *Anal. Chem.*, 44 (1972) 139.
8 D. J. Mackey, *Mar. Chem.*, (1982) in press.
9 D. J. Mackey, *J. Chromatogr.*, 236 (1982) 81.
10 S. Puon and F. F. Cantwell, *Anal. Chem.*, 49 (1977) 1256.
11 G. R. Aiken, E. M. Thurman, R. L. Malcolm and H. J. Walton, *Anal. Chem.*, 51 (1979) 1799.
12 P. L. Larkins, *Spectrochim. Acta, Part B*, 26 (1971) 477.
13 L. G. Sillén and A. E. Martell, *Stability Constants of Metal Ion Complexes, Special Publication No. 25*, Chemical Society, London, 1971, p. 623.

Journal of Chromatography, 237 (1982) 89–97
Elsevier Scientific Publishing Company, Amsterdam — Printed in The Netherlands

CHROM. 14,427

CHROMATOGRAPHIC SEPARATION OF ISOTHIOCYANATO COMPLEXES OF CHROMIUM(III) BY USE OF A SEPHADEX GEL COLUMN

KAZUHISA YOSHIMURA* and TOSHIKAZU TARUTANI
Department of Chemistry, Faculty of Science, Kyushu University 33, Hakozaki, Higashiku, Fukuoka 812 (Japan)
(Received September 29th, 1981)

SUMMARY

The separation of inert successive complexes of chromium(III) with thiocyanate was achieved by adsorption chromatography using Sephadex gels. The separation may be due to the hydrophobic interaction of thiocyanate groups in the complexes with the gel matrix. The more the complex species contains thiocyanate as ligand, the later it emerges from the column. The geometric isomers of bis- and tris(isothiocyanato)chromium(III) could be separated.

INTRODUCTION

Gel chromatography using Sephadex gels has been employed as a means of separation of inorganic compounds[1–3]. Sephadex gels are composed of dextran cross-linked by epichlorohydrin, and adsorption, partition, and/or ion exchange participate in the separation of inorganic compounds.

It has been shown in the previous papers[4,5] that borate and vanadate(V) are adsorbed selectively on Sephadex G-25 gel at different pH ranges and desorbed reversibly with acidic solutions. This characteristic was utilized for the spectrophotometric determination of boron and vanadium in natural waters and rocks. Oxo-anions of boron, vanadium(V)[6], molybdenum(VI)[7] and tungsten(VI)[8] are considered to form chelate complexes with hydroxyl groups of glucose units in the gel matrix. On the other hand, simple inorganic anions such as iodide, perchlorate and thiocyanate are adsorbed on to the gel, mainly because of hydrophobic interactions between the solutes and the gel matrix[9,10]. Kura *et al.*[11] have separated some metal ions in the thiocyanate media by use of Sephadex G-15 gel as an anion exchanger in the thiocyanate form.

Inert successive complexes relating to these anions mentioned above may have different affinities with the gel matrix. If a long time is taken to reach complexation equilibrium at room temperature, each successive complex can be separated by column chromatography. In this study, the chromium(III)–isothiocyanato complex system was investigated.

0021-9673/82/0000–0000/$02.75

EXPERIMENTAL

Chemicals

All the reagents used were of analytical-reagent grade.

$Cr(ClO_4)_3 \cdot 9H_2O$ and $K_3[Cr(NCS)_6] \cdot 4H_2O$ were prepared by the methods of Weinland and Enograber[12] and Roester[13], respectively.

The mixture of successive isothiocyanato complexes of chromium(III) was prepared by heating 50 ml of solution containing $Cr(ClO_4)_3 \cdot 9H_2O$ (1.28 g) and potassium thiocyanate (0.73 g) at 95°C for 3 h. After the solution was cooled, $Cr(ClO_4)_3 \cdot 9H_2O$ (0.26 g) and $K_3[Cr(NCS)_6] \cdot 4H_2O$ (0.30 g) were added to the solution. The solution was stored in a refrigerator and the precipitate of potassium perchlorate was removed by filtration.

Sephadex G-10, G-15 and G-25 (Medium) gels (Pharmacia, Uppsala, Sweden) were used.

Elution procedure

In a glass column (45 × 1.0 cm I.D.), a gel suspended in water was packed as described in the literature[14]. The sample solution (1 ml) was loaded on to the top of the column, and then eluted. The effluent was collected with an automatic fraction collector. The chromium content in each fraction was determined by atomic-absorption spectrophotometry with a Nippon Jarrell-Ash Model AA-781 instrument.

Another column techhique was employed for the preparation of solutions containing the complex species corresponding to bands V–VIII in Fig. 1. A poly(ethylene chloride) column (50 × 0.8 cm I.D.) was packed with 23 ml of Sephadex G-15 gel; 2 ml of the sample solution were loaded and then eluted with 0.1 *M* perchloric acid solution. After the complex species corresponding to band IV in Fig. 1 had been eluted from the column, the column was cut and four portions of purple bands were taken out. Then, each complex species was eluted with 0.1 *M* perchloric acid solution.

Determination of ratios of thiocyanate to chromium(III)

The value of the SCN/Cr ratio of each complex separated was determined by analysis of chromium and thiocyanate. Chromium was determined by atomic-absorption spectrophotometry. Thiocyanate was determined absorption spectrophotometrically as iron(III) complexes after decomposition of the complexes by sodium hydroxide solution[15].

Measurement of distribution ratio for identification of the geometric isomers

To 25 ml of solution containing the chromium complex corresponding to band III or IV in Fig. 1 and various amounts of perchloric acid, 1 g of AG 50W-X8 (H^+, 100–200 mesh) cation-exchange resin was added. After equilibration at 20°C (15 min), the resin was allowed to settle and then the absorbance of the supernatant solution was measured at 300 nm with a Hitachi Model EPS-2U. The distribution ratio, *D*, of the chromium complex species was calculated by

$$D = \frac{\text{mmol Cr(III) adsorbed/g of air-dried resin}}{\text{mmol Cr(III)/ml of solution}}$$

Measurement of distribution coefficient

To investigate the adsorption of complex species on Sephadex G-10, G-15 and G-25 gels, the distribution coefficient, K_d or K_{av}, was measured at 20°C by a column technique for the chromium species corresponding to bands–IV, and by a batch technique for those corresponding to bands V–VII in Fig. 1 and $[Cr(NCS)_6]^{3-}$ complex species.

For the column technique, the value of K_d or K_{av} is given by

$$K_d = \frac{V_e - V_0}{V_i} \text{ or } K_{av} = \frac{V_e - V_0}{V_t}$$

where V_e, V_0, V_i, and V_t represent the elution void, inner and total bed volumes, respectively[14]. The values of V_0 were determined using sodium polyphosphate for the Sephadex G-10 column[16] and Blue Dextran 2000 (Pharmacia) for the Sephadex G-15 and G-25 columns. V_i is defined as the product of the water regain, W_r, and the weight of dry gel, m; $V_i = W_r \cdot m$. The values of W_r were 1.27 and 2.34 ml/g of dry gel for Sephadex G-15 and G-25, respectively (separate test with Blue Dextran 2000).

For the batch technique, K_d is given by

$$K_d = [(C_i - C_f)V/C_f m\, W_r] + 1$$

when m g of dry gel is added to V ml of solution. C_i and C_f are the initial concentration of the complex species and the concentration of the complex species in the equilibrated solution, respectively. These values were determined by atomic-absorption spectrophotometry or by absorbance measurements at 300 nm.

The value of each parameter is shown in the caption to each figure.

RESULTS AND DISCUSSION

Separation of successive isothiocyanato complexes of chromium(III)

Fig. 1 shows a typical elution curve for the complex species obtained on the Sephadex G-15 gel column using 0.2 *M* sodium perchlorate solution as eluent. In order to prevent the complexes from being hydrolysed, the pH of the eluent was maintained at 2 by addition of perchloric acid. The concentration scales of some bands are different from one another. It can be seen that the chromium species were separated into eight fractions. The elution profiles of Blue Dextran 2000 and thiocyanate ion obtained in separate tests are also shown. The chromium species were all more strongly adsorbed on the gel than thiocyanate ion. As expected, the different affinity of each isothiocyanato complex for the gel matrix facilitates their separation.

Identification of chromium(III) complex species

The ratios of thiocyanate to chromium in the portions of bands I–VIII were tabulated as integers (Table I). The separated species were considered to be successive complexes, $[Cr(NCS)_n(H_2O)_{6-n}]^{(3-n)+}$ (n = 0–6). Band VIII was a mixture of n = 5 and 6. The more the complex species contains thiocyanate as ligand, the stronger is the interaction with the gel matrix.

The complex species of n = 0–2 have already been separated by cation-ex-

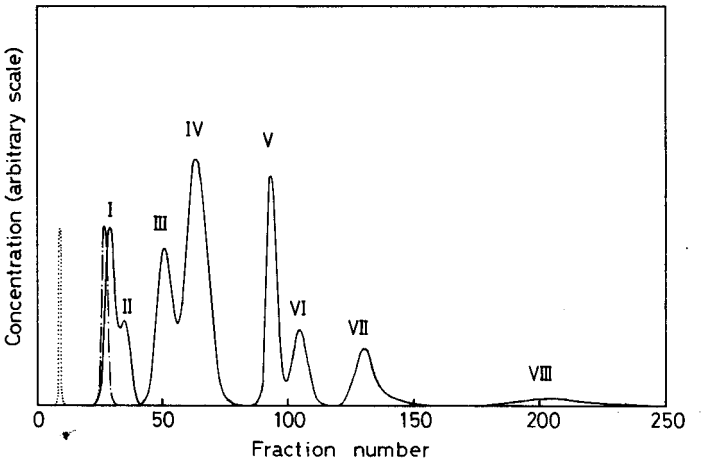

Fig. 1. Chromatographic separation of successive isothiocyanato complexes of chromium(III). Gel: Sephadex G-15, 8 g. Column: 33 × 1.0 cm I.D. Eluent: 0.2 *M* $NaClO_4$ (pH 2). Flow rate: 40 ml/h. Fraction volume: 1–80, 1 ml; 81–110, 5 ml; 111–250, 20 ml. ·····, Blue Dextran 2000; — · —, free thiocyanate ion.

TABLE I

ANALYSIS OF SCN TO Cr RATIO OF EACH BAND IN ELUTION CURVE

Elution band	I	II	III	IV	V	VI	VII	VIII
SCN/Cr ratio	0	1	2	2	3	3	4	5–6

change chromatography[17]. The first two complex species were eluted at the positions of bands I and II shown in Fig. 1, whereas the bis(isothiocyanato) complex obtained as one band by the cation-exchange chromatography was separated into two bands, III and IV, in this study.

The cation-exchange equilibrium for *m*-positive charged species is expressed in the logarithmic form:

$$\log D = \log K + m \log [H^+]_R - m \log [H^+]$$

where K and the subscript R refer to the ion-exchange equilibrium constant between *m*-positive charged species and a proton, and to the resin phase, respectively. At low loading $[H^+]_R$ is almost unchanged, hence the charge of the species can be obtained from the slope of a plot of log D *versus* log $[H^+]$. The loading analysis on the cation-exchange resin for the complex species corresponding to bands III and IV shows that both species are mono-positively charged ions, and the species of band III has a lower affinity for the cation-exchange resin (Fig. 2). As has already been found by King and Walter[18] and by Mori *et al.*[19], a *cis*-isomer is more strongly adsorbed on to cation-exchange resins than the corresponding *trans*-isomer, owing to its relatively larger dipole moment. These results show that the species of band III is *trans*-bis(isothiocyanato)chromium(III) and that of band IV is the *cis*-isomer. Hougen *et*

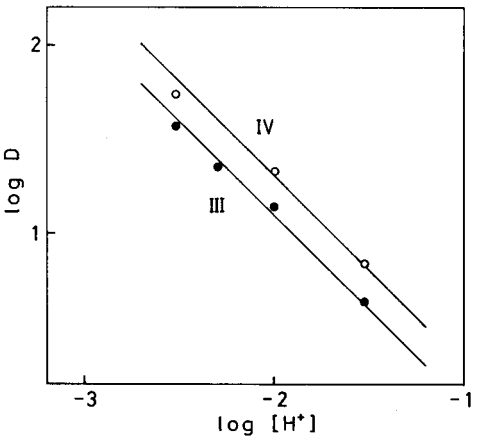

Fig. 2. Determination of the ionic charge of the complexes of SCN/Cr = 2 (III and IV in Fig. 1). Solution: 25 ml ($HClO_4$). Resin: AG 50W-X8 (H^+, 100–200 mesh), 1 g. Time for equilibration: 15 min.

al.[20] have separated the geometric isomers using a cation-exchange resin column of length 240 cm and have found that the *trans*-isomer is more easily eluted than the *cis*. The absorption spectra of the separated isomers were measured. In the ultraviolet region their spectra are in fair agreement with ours, whereas they are not in the visible region. From the experimental evidence of our study, it is concluded that the visible absorption spectrum of the "*cis*-isomer" reported by Hougen *et al.* is that of the *trans*-isomer, and *vice versa*.

The complex species of bands V and VI are geometric isomers, and may be *mer*- and *fac*-tris(isothiocyanato)chromium(III), respectively, from the viewpoint of the dipole moment of the two complexes. The absorption spectra for each complex species will be described elsewhere in detail.

Effect of background electrolytes on the adsorption of complex species

The affinity of the complex species for Sephadex G-15 was measured in 0.2 *M* solutions of the sodium salts of thiocyanate, perchlorate, nitrate, chloride and sulphate. The results are shown in Fig. 3. The affinity of the complex species for the gel increases in the order $SCN^- < ClO_4^- < NO_3^- < Cl^- < SO_4^{2-}$. The order is consistent with the reverse order of affinity of these anions for the gel. The values of K_{av} for these anions are 1.54, 1.45, 0.74, 0.54 and 0.20, respectively[10]. There may be a competitive reaction between the complexes and these anions. Kura *et al.*[11] have pointed out the similar adsorption characteristics of thiocyanate on the G-15 gel and have suggested that the anions which interact more strongly with the gel cause a greater decrease in the amount of thiocyanate ion adsorbed. It can be seen that the adsorbability of complex species with higher ligand numbers is more strongly influenced by the presence of various kinds of electrolytes (Fig. 3). Thiocyanate groups in the complex species may significantly participate in the adsorption.

The effect of the concentration of sodium perchlorate on K_d values was examined over the concentration range 0.1–1 *M*, the pH of the solution being maintained at 2 (Fig. 4). The complex species of $n = 0$–2 were hardly affected in the presence of sodium perchlorate in various concentrations. For those of $n = 3$–6, the

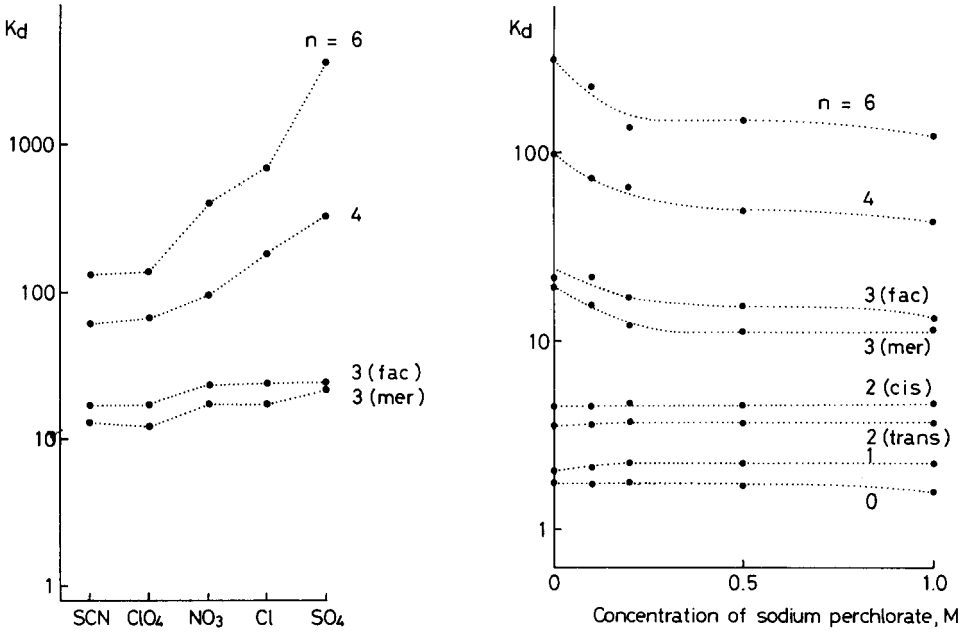

Fig. 3. Effects of co-existing electrolytes on K_d values for the successive complexes, $[Cr(NCS)_n(H_2O)_{6-n}]^{(3-n)+}$ (n = 3–6). Solution: 25 ml (sodium salt, 0.2 *M*, pH 2). Gel: Sephadex G-15 (W_r = 1.27 ml/g dry gel), 0.5 g. Time for equilibration: 30 min.

Fig. 4. Effects of the concentration of sodium perchlorate on K_d values for the successive complexes. n = 0–2: the column method. Gel: Sephadex G-15. Column: 50 × 1.0 cm I.D., V_0 = 13.0 ml, V_i = 15.2 ml. Flow-rate: 14 ml/h. n = 3–6: the batch method. Solution: 25 ml (pH 2). Gel: Sephadex G-15 (W_r = 1.27 ml/g dry gel), 0.5 g. Time for equilibration: 30 min.

degree of affinity for the gel decreased on increasing the concentration of perchlorate. It can be seen that thiocyanate or perchlorate solution as eluent is efficient for the separation of the respective complex species, but the gradient-elution method may not be effective for the present system.

Effect of the degree of crosslinking of the gel on the adsorption of complex species

The difference of cross-linking of the dextran gel affects the adsorption behaviour of the complex species. Fig. 5 shows the K_{av} values of the complex species (n = 0–2) on Sephadex G-10, G-15 and G-25 gels. The K_{av} values are plotted as a function of the concentration of sodium perchlorate. Because it was difficult to obtain the value of V_i for Sephadex G-10, the comparison was carried out using the K_{av} values. All the complex species show the strongest affinity for Sephadex G-10. The Sephadex G-10 system was most influenced by the presence of sodium perchlorate. At lower concentrations of the salt, the ion-exchange mechanism may be present. The separation factors for the bis(isothiocyanato) isomers are 1.07, 1.25 and 1.51 for Sephadex G-25, G-15 and G-10, respectively, and therefore the separation of the isomers may be efficiently carried out by use of a Sephadex G-10 column.

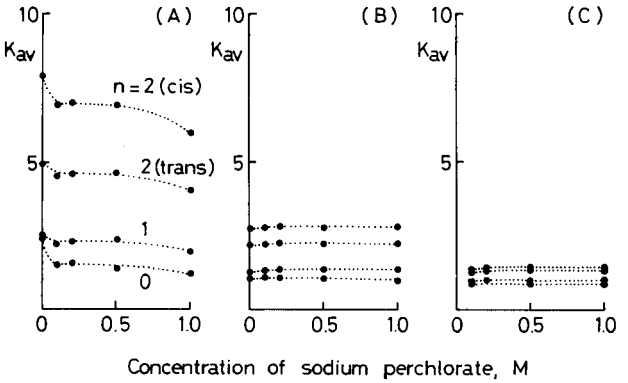

Fig. 5. Effects of the degree of cross-linking on K_{av} values for the cationic complexes. (A) Gel: Sephadex G-10, V_0 = 13.2 ml, V_t = 35.7 ml. (B) Gel: Sephadex G-15, V_0 = 13.0 ml, V_t = 38.1 ml. (C) Gel: Sephadex G-25, V_0 = 15.1 ml, V_t = 37.4 ml.

Comparison with other methods

Bjerrum has investigated the chromium(III)–isothiocyanato complex system by the precipitate-formation and solvent-extraction methods and has reported stability constants of the successive complexes[21]. However, he failed to separate mono- and bis(isothiocyanato) complexes and also pentakis- and hexakis(isothiocyanato) complexes. The cation-exchange method made it possible to separate the cationic complex species[17,20]; bis(isothiocyanato) complexes are eluted with 0.15 *M* perchloric acid, mono(isothiocyanato) complex witn 1 *M* perchloric acid and hexa-aqua species with 5 *M* perchloric acid. As anionic complexes are so strongly adsorbed by polystyrene-type anion-exchange resins, they cannot be eluted. Kaufman and Keyes[22] have succeeded for the tetrakis(isothiocyanato) complex with the cellulose anion exchanger and 1 *M* perchloric acid as eluent. However, pentakis- and hexakis(isothiocyanato) complexes could not be eluted without the decomposition occurring.

The present method makes it possible to separate successive complexes of n = 0–4 by use of a single column under mild conditions and to separate geometric isomers of a tris(isothiocyanato) complex for the first time. Complex species with various charges are separated from one another without concentration-gradient elution. However, the later the complexes are eluted, the more the samples are diluted. It is convenient, in this case, to use the poly(ethylene chloride) tube method, as mentioned in the Experimental section. Alternatively, it can be seen from Figs. 3 and 5 that the selection of gel and eluent may give a relatively rapid and complete separation method for the complexes concerned. Complete separation of complexes of n = 0–2 was accomplished by use of the Sephadex G-10 gel column (Fig. 6a). Group separation of the successive complexes can be almost completely and rapidly separated by a combination of the Sephadex G-25 gel column and 0.2 *M* sodium chloride–sodium perchlorate solution as eluent (Fig. 6b).

The present method may be utilized to separate preparatively many inert complexes containing thiocyanate as ligand, and may be available for investigation of complexation equilibrium in solution.

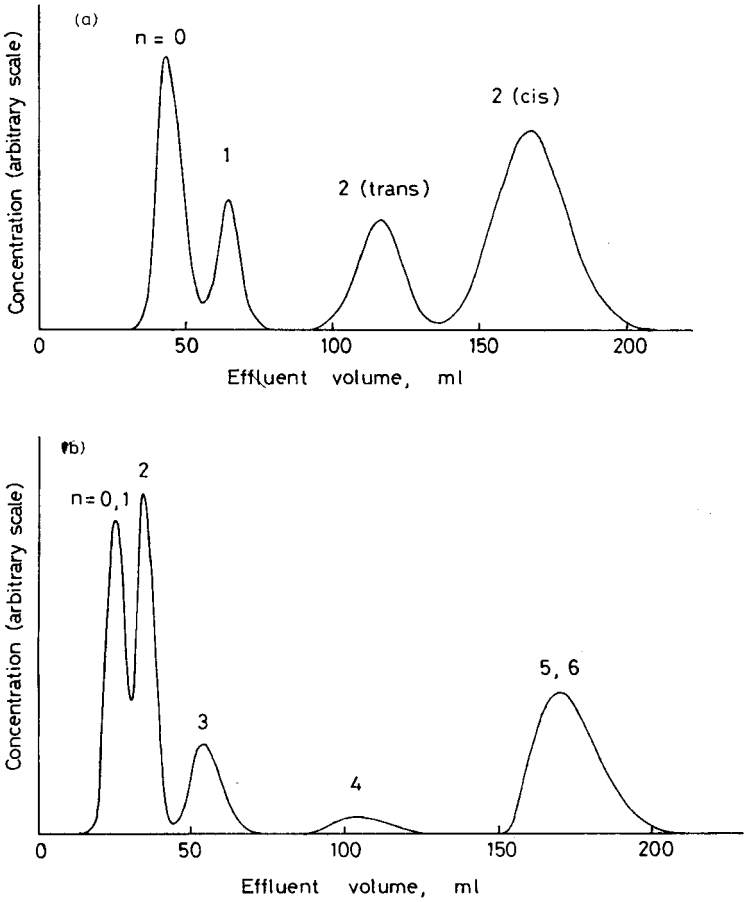

Fig. 6. (a) Chromatographic separation of the cationic isothiocyanato complexes of chromium(III). Gel: Sephadex G-10. Column: 46 × 1.0 cm I.D. Eluent: 0.1 *M* $HClO_4$. Flow-rate: 19 ml/h. (b), Chromatographic group separation of successive complexes. Gel: Sephadex G-25 (Fine). Column: 41 × 1.0 cm I.D. Eluent: 0–125 ml, 0.2 *M* NaCl (pH 2); 125–350 ml; 0.2 *M* $NaClO_4$ (pH 2). Flow-rate: 39 ml/h.

REFERENCES

1 S. Ohashi, N. Yoza and Y. Ueno, *J. Chromatogr.*, 24 (1966) 300.
2 P. A. Neddermeyer and L. B. Rogers, *Anal. Chem.*, 41 (1969) 94.
3 N. Yoza, *J. Chromatogr.*, 86 (1973) 325.
4 K. Yoshimura, R. Kariya and T. Tarutani, *Anal. Chim. Acta*, 109 (1979) 115.
5 K. Yoshimura, H. Kaji, E. Yamaguchi and T. Tarutani, *Anal. Chim. Acta*, 130 (1981) 345.
6 H. M. Ortner and H. Dalmonego, *J. Chromatogr.*, 89 (1974) 287.
7 S. Karajannis, H. M. Ortner and H. Spitzy, *Talanta*, 19 (1972) 903.
8 H. M. Ortner, *Anal. Chem.*, 47 (1975) 162.
9 V. Di Gregorio and M. Sinibaldi, *J. Chromatogr.*, 129 (1976) 407.
10 T. Deguchi, A. Hisanaga and H. Nagai, *J. Chromatogr.*, 133 (1977) 173.
11 G. Kura, A. Koyama and T. Tarutani, *J. Chromatogr.*, 144 (1977) 245.
12 R. F. Weinland and F. Enograber, *Z. Anorg. Chem.*, 84 (1913) 353.
13 J. Roester, *Justus Liebigs Ann. Chem.*, 14 (1867) 185.
14 L. Fischer, *An Introduction of Gel Chromatography*, North-Holland, Amsterdam, 1969.

15 E. B. Sandell, *Colorimetric Determination of Traces of Metals*, Interscience, New York, 1959.
16 Y. Ueno, N. Yoza and S. Ohashi, *J. Chromatogr.*, 52 (1970) 469.
17 E. L. King and E. B. Dismukes, *J. Amer. Chem. Soc.*, 74 (1952) 1674.
18 E. L. King and R. R. Walter, *J. Amer. Chem. Soc.*, 74 (1952) 4471.
19 M. Mori, M. Shibata and K. Hori, *Bull. Chem. Soc. Jap.*, 34 (1961) 1809.
20 J. T. Hougen, K. Schug and E. L. King, *J. Amer. Chem. Soc.*, 79 (1957) 519.
21 N. Bjerrum, *Z. Anorg. Allg. Chem.*, 119 (1921) 179.
22 S. Kaufman and L. S. Keyes, *Anal. Chem.*, 36 (1964) 1777.

Journal of Chromatography, 237 (1982) 99–105
Elsevier Scientific Publishing Company, Amsterdam — Printed in The Netherlands

CHROM. 14,442

DETERMINATION OF CHROMIUM IN ORCHARD LEAVES BY REVERSED-PHASE HIGH-PERFORMANCE LIQUID CHROMATOGRAPHY

JAMES D. WILLETT and MARGARET M. KNIGHT*
Department of Chemistry, University of Idaho, Moscow, ID 83843 (U.S.A.)
(Received October 6th, 1981)

SUMMARY

Chromium, as chromium acetylacetonate, was determined in nitric acid digested samples of NBS Standard Reference Material 1571, Orchard Leaf by reversed-phase high-performance liquid chromatography on μBondapak C_{18} using 36% acetonitrile in water. The determined value was 2.4 ± 0.1 ppm. The limits of detection for this method are 1 ng on-column injection. By standard microchemical enrichment techniques parts-per-billion analyses can be achieved.

INTRODUCTION

Gas chromatography and, more recently, high-performance liquid chromatography (HPLC) have been used with increasing frequency for the separation of metal complexes since their separation by gas chromatography was first reported in 1959[1–3]. The extraction of metals by chelating agents in organic solvents is a well established procedure. By carefully selecting ligand, solvent, pH of the aqueous phase, and sequestering agents, one can enhance or modulate the preferential extraction of a specific metal or group of metals from a complex matrix. Efficient chromatographic separation coupled with selective solvent extraction of metal complexes from matrices of interest provides a system capable of rapid, simultaneous multi-element analysis of the trace or ultratrace level. Advantages of the use of chromatography of metal complexes over other methods capable of trace metal analysis such as atomic absorption, emission spectrometry, and neutron activation analysis include the possibility of distinguishing among oxidation states of a given metal and distinguishing free versus bound metals in various matrices. The decreased expense of chromatographic analysis relative to at least some of the alternatives may prove advantageous in some instances.

Gas chromatography has been used for the quantitative analysis of a very few metals as metal chelates from biological and inorganic matrices[4–14]. However, the requirements of the gas chromatographic analysis of metal complexes, volatility and thermal stability, are not inherent characteristics of metal complexes themselves.

* Present address: WTC 2D25, Weyerhaeuser Company, Tacoma, WA 98477, U.S.A.

0021-9673/82/0000–0000/$02.75

Even fluorinated β-diketonates, many of which are volatile and thermally stable, undergo on-column hetero-molecular reactions in the complex molecules. These on-column interactions become especially apparent at trace levels[15–17]. HPLC on the other hand, is not dependent upon high volatility or thermal stability for efficient and effective separation. Further, increased selectivity over gas–liquid chromatography can be gained in HPLC by the added partition variable of the solvent mobile phase[16].

The analytical potential of HPLC for metals has been demonstrated. Complexes of Cr(III), Fe(II) and Mn(II)[18] have been investigated as well as tricarbonyl homologues of Cr(III)[19], triphenyl phosphine complexes of rhodium and iridium[20], acetylacetonates and trifluoroacetylacetonates of several transition metals[21,22] and tetradentate β-ketoamine complexes of Co(II), Ni(II), Cu(II), and Pd(II)[23,24]. Heizmann and co-workers[25,26] have separated several metal 1,2-diketobisthiobenzyhydrazones, dialkyldithiocarbamates, 1,2-diketobisthiosemicarbazones, and dithizonates by HPLC. Some of these complexes undergo on-column exchange reactions which create multiple peaks per metal analyzed[16,17]. However, there is a paucity of analytical determinations on real samples using the procedure.

Determinations have been made on standard solutions of diacetylbisthiobenzhydrazonates of Cu(II), Fe(II), Mn(II), Zn(II), Cd(II), and Pb(II) to 10 to 1100 ng[28]. To date, however, application of high-performance liquid chromatography to metal ion analysis in real systems has been limited to the determination of selenium as the naphthalene–2,3-diaminato complex in industrial waste, sewage sludge, and biological materials[29]. We would like to report a method for the determination of chromium in NBS Standard Reference Material 1571, Orchard Leaf, using reversed-phase HPLC. This method allows detection of chromium in biological materials at the parts-per-billion (10^9) level with an on-column detection limit of 1 ng.

EXPERIMENTAL

Liquid chromatograph

A Waters Associates ALC-202 liquid chromatograph was used with a model 6000 pump at a constant flow-rate of 1 ml/min. The chromatograph was equipped with a 254 nm detector.

Columns

Waters Associates μBondapak C_{18} and μPorasil were used.

Injection port

A Precision Sampling Valveseal septumless injector was used.

In-line filter

A removable 2-μm filter was installed between the injector and the column to minimize column plugging.

Syringes

Samples were injected using 10- or 25-μl syringes (Precision Sampling LC212B).

Mobile phase

Eluent was 36% acetonitrile in water.

Reagents

Unless otherwise specified, reagents are Mallinckrodt reagent-grade chemicals. Nitric acid was purified by sub-boiling distillation. All water used was purified with a Millipore Super Q water purification system. The metal chelates were synthesized according to standards methods[30], recrystallized, and characterized by their melting points and mass spectra. Acetylacetone (Aldrich reagent) was redistilled before use.

Glass ware

All glassware was cleaned by soaking overnight in concentrated sulphuric acid saturated with sodium nitrate and then rinsed eight times in purified water.

Analytical procedure

A 250-mg amount of Orchard Leaf was placed in a 10–50-ml round-bottomed flask equipped with a reflux condenser and 2 ml of nitric acid added. The digestion mixture was allowed to predigest overnight at room temperature, after which the temperature was gradually increased to 150°C. The sample was digested for 2 h. The solution was transferred, with water washings, to a 10-ml volumetric flask and the pH adjusted to 6.0–6.1 with solid Na_2CO_3. Both the solid and a saturated solution of Na_2CO_3 were used with success; however, it was found that when the base was stored in glass, metals leached from the glass interfered in the analysis. A 5-ml aliquot of the digest was transferred to a 3-dram vial, 100 μl of acetylacetone was added, and the vial closed with a Miniert top (Pierce Chemical). The vials were placed in a metal canister in a 100°C oven for 1 h, allowed to cool to room temperature, and 1 ml of chloroform added to the cooled solution. The immiscible phases were mixed on a Vortex mixer for 30 min and the excess acetylacetone removed from the chloroform extract by two successive washings with 1 ml 2 *M* NaOH. The chloroform layer was separated and backwashed with water. An aliquot was then transferred to a 1-ml Reactivial. Phase separation was facilitated throughout by centrifugation. The chloroform was evaporated from the aliquot under nitrogen and ethanol used to reconstitute the sample. A portion of the ethanol solution was then injected onto the HPLC column.

RESULTS AND DISCUSSION

Previous research on HPLC separation of metal acetylacetonates has emphasized the use of polar silica gel columns[21,22].

Huber *et al.*[21] used a polar liquid phase and a non-polar mobile phase to separate acetylacetonates of beryllium, copper, aluminium, chromium, ruthenium, cobalt. The ternary system consisted of isooctane, ethanol, and water. The water-rich phase was used as a stationary phase, an immiscible water-poor phase as the eluent. Hydrolysis and other chelate reactions, however, caused severe peak distortion. These reactions were suppressed by adding a trace of acetylacetone equal to 0.008 of the mass fraction of the mobile phase, 0.002 of the stationary phase. Tollinche and Risby[22] investigated a variety of commercially available silica, alumina, bonded

phase, and open pore polyurethane columns, and found silica to be the most useful for metal chelate analysis.

Our initial screening tests employed a polar column, μPorasil, and a non-polar variety of eluents. It was found that peaks were irreproducible at the nanogram level. We believe that the chelate is being strongly bound to active silanol groups on the μPorasil column. This seems to be supported by Kutal and Sievers[31] study with chromium trifluoroacetylacetonate in which isomerism was accelerated by glass surfaces and by Dilli and Patsalides[14] study on retention of various trifluoroacetylacetonates in gas chromatography columns. Adding a trace of ligand to the eluent stream, a technique used in both gas[32] and liquid chromatography[21] of metal complexes to suppress complex disassociation proved not to be useful for our purposes, since a mass fraction of even 0.002 in the mobile phase saturated the UV detector. As we found that UV-absorbing polar substances were formed during the digestion and chelation procedure which could bond strongly to polar columns and decrease column efficiency, we abandoned further separations using polar columns.

Heat is necessary for the quantitative chelation of chromium with acetylacetone[33] so reaction vessels were placed in a metal canister and a safety shield was placed in front of the oven in the event of glass failure. No difficulty was encountered with either regular glass vials or with Reactivials as long as the oven temperature remained about 100°C.

Metal analyses were run on different days with different glassware and solution to maximize variability. The glassware used was not silanized. In our initial studies we found that if the analyses were performed on freshly chelated solutions of the digests loss of chromium to the glass surface was unimportant. The acid digests showed no loss of chromium over 48 h. However, once chelated some loss of chromium to glass container walls can occur. A 13% loss of chromium was noted from a standard solution stored for 24 h. No discernable loss occurs if the solutions are used within 3–4 h of preparation.

Though chloroform was a convenient extraction solvent for the complex[33] it forms a 2:1 adduct[34] which loses chloroform on-column, complicating the analysis. Therefore we evaporated the chloroform and substituted ethanol. No loss of chromium to the glass walls was observed.

In order to ensure that the peak observed was chromium acetylacetonate, the compound was collected from the liquid chromatograph, evaporated, and analyzed by direct probe mass spectrometry. The spectrum was identical to that of the original tris(acetylacetonato) chromium(III).

Typical chromatograms for digested orchard leaf and a blank are shown in Figs. 1 and 2. Chromium is reasonably well resolved from the other peaks, presumably other metal acetylacetonates. Data for the analysis of orchard leaf is shown in Table I. The value of 2.4 ± 0.1 μg/g is within the standard deviation reported for chromium in that NBS standard of 2.6 ± 0.3 μg/g. The reproducibility of injection is shown in Table II. Response of the detector was linear over the range 1 ng (limits of detection) to 5 μg. Recovery of chromium from standard solutions is summarized in Table III. We believe that these results demonstrate the applicability of this method to the trace determination of chromium in biological materials and we have used this procedure to determine chromium in the free living nematode *Panagrellus redivivus* to less than 1 μg/g on a 20 μg sample.

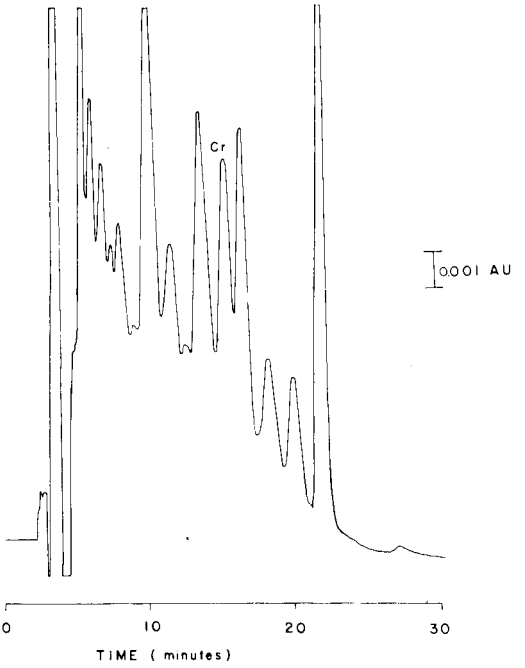

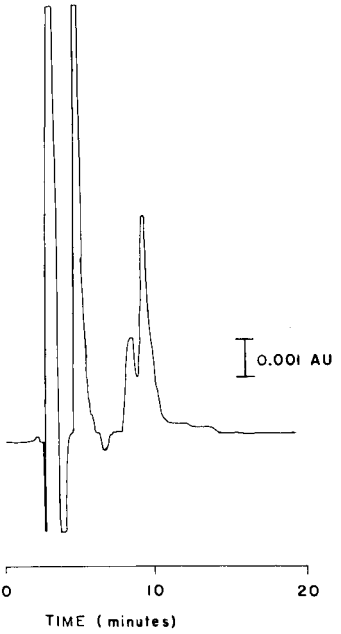

Fig. 1. Elution profile of digested orchard leaves chelated with acetylacetone. Column conditions: μBondapak C_{18} eluted with 36% acetonitrile in water at 1 ml/min.

Fig. 2. Elution profile of blank. Column conditions as in Fig. 1.

As an analysis for chromium, this method is not uniquely sensitive. Graphite furnace atomic absorption, for example, is capable of detection to 0.2 pg[35]. However, we think this system will afford rapid, single or multi-element analysis on relatively small amounts of material, depending on the exact conditions used. Acetylacetone forms well-defined chelates with over 60 metals, most of which are soluble in organic solvents and are formed under milder conditions than the chromium complex studied here[36]. We expect that conditions for extraction can be selected to optimize analysis for one metal, as in the present case, or a group of metals with minor changes in the

TABLE I

CHROMIUM IN ORCHARD LEAVES

Sample	*Weight (mg)*	*ppm*
1	250	2.3
2	250	2.5
3	250	2.3
4	250	2.5
Average		2.4 ± 0.12
Relative deviation		5%

TABLE II

REPRODUCIBILITY OF INJECTION

15 µl (15 ng)	*Peak height (mm)*
1	127
2	126
3	117
4	118
5	121
6	122
Average	122 ± 4
Relative deviation	3%

TABLE III

RECOVERY OF ADDED Cr

Added (ng)	*Found (ng)*	*Recovery (%)*
150	152.4	102
150	146.4	98
150	145.5	97
150	154.5	103
		Average 100 ± 3
		Relative deviation 3%

procedure outlined. Using standard microtechniques for enrichment by solvent extraction, trace analysis to the parts-per-bilion level is expected.

REFERENCES

1 G. Guiochon and C. Pommier, *Gas Chromatography in Inorganics and Organometallics*, Ann Arbor Science, Ann Arbor, MI, 1973.
2 R. W. Moshier and R. E. Sievers, *The Gas Chromatography of Metal Chelates*, Pergamon Press, London, 1965.
3 W. D. Ross and R. E. Sievers, *Anal. Chem.*, 41 (1969) 1109.
4 W. D. Ross, R. E. Sievers and G. Wheeler, Jr., *Anal. Chem.*, 37 (1965) 598.
5 R. E. Sievers, J. W. Connolly and W. D. Ross, *J. Gas Chromatogr.*, 5 (1967) 241.
6 G. P. Morie and T. R. Sweet, *Anal. Chem.*, 37 (1965) 1552.
7 J. Savory, M. T. Glenn and J. A. Ahlstrom, *J. Chromatogr. Sci.*, 10 (1972) 247.
8 G. M. Frame, R. E. Ford, W. G. Scribner and T. Ctvrtnicek, *Anal. Chem.*, 46 (1974) 534.
9 C. A. Burgett and J. S. Fritz, *Anal. Chem.*, 44 (1972) 1738.
10 W. R. Wolf, M. L. Taylor, B. M. Hughes, T. O. Tiernan and R. E. Sievers, *Anal. Chem.*, 44 (1972) 616.
11 R. Ross and T. Shafik, *J. Chromatogr. Sci.*, 11 (1973) 46.
12 L. C. Hansen, W. G. Scribner, T. W. Gilbert and R. W. Sievers, *Anal. Chem.*, 43 (1971) 349.
13 G. H. Booth, Jr. and W. J. Darby, *Anal. Chem.*, 43 (1971) 831.
14 S. Dilli and E. Patsalides, *J. Chromatogr.*, 176 (1979) 305–318.
15 L. R. Snyder and J. J. Kirkland, *Modern Liquid Chromatography*, Wiley-Interscience, New York, 1974.
16 O. Liška, G. Guiochon and H. Colin, *J. Chromatogr.*, 171 (1979) 145–151.
17 J. Lehotay, O. Liška, E. Brandšteterová and G. Guiochon, *J. Chromatogr.*, 172 (1979) 379–383.
18 R. Eberhardt, H. Lehner and K. Schloegl, *Mg. Chem.*, 104 (1973) 1409; *Anal. Abst.*, 27 (1974) 1998.

19 H. Veening, J. M. Greenwood, W. H. Shanks and B. R. Williford, *Chem. Commun.*, (1969) 1305.
20 C. T. Enos, G. L. Geoffrey and T. H. Risby, *Anal. Chem.*, 48 (1976) 990.
21 J. F. K. Huber, J. C. Kraak and H. Veening, *Anal. Chem.*, 44 (1972) 1554.
22 C. A. Tollinche and T. H. Risby, *J. Chromatogr. Sci.*, 161 (1978) 445-454.
23 G. E. Gaelani, C. F. Laureri, A. Mangia and G. Parolari, *Anal. Chem.*, 48 (1976) 1725.
24 P. C. Uden and F. H. Walters, *Anal. Chim. Acta*, 79 (1975) 175.
25 P. Heizmann and K. Ballschmiter, *J. Chromatogr.*, 137 (1977) 153–163.
26 M. Lohmüller, P. Heizmann and K. Ballschmiter, *J. Chromatogr.*, 137 (1977) 165–170.
27 P. Heizmann and K. Ballschmiter, *Z. Anal. Chem.*, 266 (1973) 206.
28 J. W. O'Laughlin and T. P. O'Brien, *Anal. Lett.*, A11 (1978) 823–844.
29 G. L. Wheeler and P. F. Lott, *Microchem. J.*, 19 (1974) 390; *Anal. Abstr.*, 29 (1975) 22.
30 W. L. Fernelius and J. E. Blanch, *Inorg. Snyth.*, 5 (1957) 131.
31 C. Kutal and R. E. Sievers, *Inorg. Chem.*, 13 (1974) 897.
32 T. Fujinaga and S. Murai, *Anal. Chem. Aita*, 71 (1974) 141.
33 J. P. McKavenly and H. R. Freiser, *Anal. Chem.*, 29 (1957) 290.
34 J. F. Steinbach and J. H. Burns, *J. Amer. Chem. Soc.*, 80 (1958) 1839.
35 C. Veillon, in J. D. Winefordner (Editor), *Trace Analysis: Spectroscopic Methods for Elements*, Wiley, New York, 1976, p. 164.
36 A. K. De, S. M. Khopkar and R. A. Chalmers, *Solvent Extraction of Metals*, Van Nostrand Reinhold, New York, 1970, p. 46.

Journal of Chromatography, 237 (1982) 107–113
Elsevier Scientific Publishing Company, Amsterdam — Printed in The Netherlands

CHROM. 14,473

DEVELOPMENT OF A METHOD FOR THE ANALYSIS OF T-2 TOXIN IN MAIZE BY GAS CHROMATOGRAPHY–MASS SPECTROMETRY

J. P. CHAYTOR and M. J. SAXBY*
Leatherhead Food R.A., Randalls Road, Leatherhead, Surrey KT22 7RY (Great Britain)
(First received June 29th, 1981; revised manuscript received October 13th, 1981)

SUMMARY

A ground sample is homogenised with ethyl acetate, the mixture filtered, and the extract recovered by evaporation of the solvent. The residue is defatted by partition between aqueous methanol and hexane. The aqueous phase is evaporated to dryness and the residue dissolved in dichloromethane and passed through a cartridge of silica. T-2 toxin is eluted with methanol–dichloromethane, the solvents removed and the residue silylated. O-Trimethylsilyl T-2 toxin is detected by gas chromatography–mass spectrometry with monitoring of the ions at m/z 350 and m/z 436. The quantitative detection limit is 5 ppb (μg/kg) with an average recovery of 80%.

INTRODUCTION

The trichothecenes are a family of about 40 naturally occurring sesquiterpenoids produced by various species of fungi, from the genera *Fusarium*, *Myrothecium*, *Trichoderma*, *Cephalosporium*, *Verticimonosporium*, and *Stachybotrys*. These fungi attack many agricultural and plant products. However, serious contamination of feedstuffs is probably caused primarily by species of the genera *Fusarium* and *Stachybotrys*[1]. The former has been extensively implicated in various human disorders as species of *Fusaria* commonly invade cereals. Species of the latter have been implicated in outbreaks of animal and human diseases, notably equine stachybotryotoxicosis[2].

Intoxications of both human and animal populations have been noted throughout the world in temperate regions subject to cool wet periods[3]. Haemorrhagic disease, mouldy cereal amesis, akakabibyo toxicosis, alimentary toxic aleukia, stachybotryotoxicosis, and fusariotoxicosis are a few of the diseases that can be considered primarily due to trichothecene poisoning[2]. All of these occur in populations that have consumed mouldy food, usually after exposure of the foodstuffs to prolonged cool and wet weather in the field. These conditions are ideal both for growth of the fungi responsible for the diseases and also for production by the fungi of the causative agents. Many of the symptoms can be reproduced when pure trichothecenes are fed to animals, *i.e.* dermatitis, vomiting, diarrhoea, necrosis, haemorrhage, leukopenia, and shock.

0021-9673/82/0000–0000/$02.75

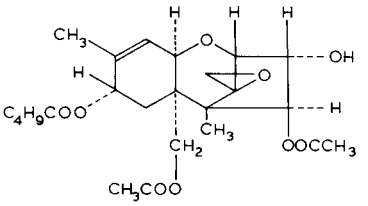

Fig. 1. Structure of T-2 toxin.

Trichothecenes are usually extracted from samples with ethyl acetate or chloroform, but more polar solvents (aqueous methanol) are required for extraction of nivalenol, fusarenone-X, and deoxynivalenol[4]. The extract is usually associated with pigmented substances and lipids which interfere with the analysis. Defatting is accomplished by partitioning the extract between a polar solvent and hexane which removes fat and pigment. The trichothecenes are retained in the polar phase. Further purification can be achieved using a silica gel column[5] or thin-layer chromatography[6]. Another approach to purification involves adsorption of the toxins on Amberlite XAD-2, followed by elution and adsorption on a florisil column[7].

Chemical analysis of the trichothecene toxins is difficult because they have no fluorescent or ultraviolet absorbing properties. They can be detected after separation on thin-layer chromatograms, by spraying with sulphuric acid and charring which causes some of the toxins to fluoresce blue under ultraviolet light. Spraying the plates with *p*-anisaldehyde reagent yields characteristic colours with some of the trichothecenes[8]. The spray reagent, 4-(*p*-nitrobenzyl) pyridine has also been used for the detection and spectrodensitometric determination of tricothecenes. The colour is based upon reaction with the 12,13-epoxy group and is sensitive for T-2 toxin (Fig. 1) to 0.1 μg per spot[9].

Even with selective detection methods, thin-layer chromatograms of natural extracts are difficult to interpret. These methods are only semi-quantitative with a detection limit of several hundred parts per billion (10^9) in foods.

Gas chromatography permits detection and quantitation of most of the trichothecenes[8] except the verrucarins and roridines. Usually acetate or trimethylsilyl derivatives are prepared and analysed on short non-polar columns (such as OV-1 phase). Detection sensitivity is better with gas chromatography, than with thin-layer chromatography, but has the disadvantage of possible incorrect identification because many components have identical retention times[6]. Separation by thin-layer chromatography prior to gas chromatographic analysis partially overcomes this problem[8].

Detection of trichothecenes has been achieved using gas chromatography fitted with an electron-capture detector[7] after preparing suitable derivatives. Although a high sensitivity is sometimes achieved, it is done at the expense of selectivity, so that further sample purification is needed. This is, however, a cheaper alternative than detection by gas chromatography–mass spectrometry (GC–MS), which has the advantage of extreme selectivity as well as sensitivity.

An alternative approach to chemical analysis is bioassay. Usually skin reactions in laboratory animals are chosen[10]. This approach only demonstrates that a skin irritant is present, which is assumed to be a trichothecene.

Two recent publications review the natural occurrence of trichothecenes[11] and the existing means for their analysis[12].

EXPERIMENTAL AND RESULTS

Gas chromatography–mass spectrometry

A Hewlett-Packard 5992A system was operated at standard autotune resolution in both the "peakfinder" mode and the "multiple ion detection" mode, unless otherwise stated. The instrument was fitted with a glass column (1 m × 2 mm I.D.) packed with 3% OV-7 on Chromosorb W AW DMCS (80–100 mesh), and programmed from 160° to 270°C at 15°C/min. Injection port temperature was 250°C. Helium was the carrier gas, at a flow-rate of 25 ml/min.

Materials and reagents

All reagents were AnalaR grade, unless otherwise stated: glass distilled water; ethyl acetate; hexane (glass distilled); methanol; chloroform; dichloromethane; sodium sulphate, anhydrous (S.L.R.); tetrachloroethylene (special for spectroscopy). N-Methyl-N-trimethylsilyl trifluoroacetamide (MSTFA) was obtained from Pierce. T-2 toxin was obtained from Makor Chemicals, Jerusalem, Israel. Stock solution made up in chloroform to concentration of 1mg/ml. Other solutions obtained by dilution.

The following equipment was used: laboratory mixer–emulsifier (heavy duty, sealed unit) fitted with a 3/4 in. tubular head (Silverson); rotary evaporator (Büchi) fitted to a vacuum water pump and used with a water bath (20°–100°C); orbital mixer; block heater (ambient to 130°C) capable of taking 0.3 ml and 1 ml Reacti-vials (supplied by Pierce); Whatman No. 1PS phase separating paper (15 cm diameter); Sep-Pak silica cartridges (Waters Assoc.); 0.3-ml and 1-ml Reacti-vials (Pierce); Pasteur pipettes, 230 mm length; 10-μl syringe (Scientific Glass Engineering).

Extraction and separation

The sample (10 g; milled in a coffee grinder), anhydrous sodium sulphate (10 g), and ethyl acetate (40 ml) were homogenised for 1.5 min in the sealed Silverson homogeniser. The mixture was filtered through Whatman 1PS paper into a round-bottomed flask and the residue washed with more ethyl acetate (2 × 15 ml), before being discarded. The filtrate was vacuum rotary evaporated at 45°–50°C just to dryness, the residue was mixed with hexane (10 ml) and 20% water in methanol (5 ml) and the mixture shaken by hand for 1 min. The hexane layer was discarded and the aqueous–methanolic phase was twice re-extracted with hexane (5 ml); the hexane extracts were discarded. The aqueous–methanolic phase was vacuum rotary evaporated at 60°–65°C to dryness.

A Sep-Pak silica cartridge was pre-washed with methanol (5 ml) and dichloromethane (10 ml). The sample residue was transferred to the syringe above the cartridge with four sequential portions of dichloromethane (4 × 0.5 ml, total volume made up to 2 ml if necessary. The solution was pumped through the cartridge, followed by dichloromethane (2 ml and then 10 ml). Eluate collection commenced and the cartridge was stripped with dichloromethane–methanol (10 ml). The eluate was vacuum rotary evaporated to dryness at 45°–50°C and the residue transferred to a 1

ml Reacti-vial with sequential portions of methanol (3 × 0.25 ml). The samples were heated at 60°C in a block heater and the solvent removed in a stream of air.

N-Methyl-N-trimethylsilyl trifluoroacetamide (25 μl) and tetrachloroethylene (50 μl) were added to the residue and the sample heated at 60°C for 30 min to form O-trimethylsilyl T-2 toxin. A 1-μl aliquot was analysed by GC–MS.

A portion of the diluted stock solution of T-2 toxin (185 ng) was mixed with tetrachloroethylene (50 μl) and N-methyl-N-trimethylsilyl trifluoroacetamide (25 μl) and heated at 60°C for 30 min. This solution was used to determine the retention time of the derivative and to calculate recovery values. Injection of an aliquot of a more concentrated solution into the GC–MS system gave the mass spectrum of O-trimethylsilyl T-2 toxin.

The mass spectrometer was operated in the selected ion detection mode for the analysis of samples and was switched on 7 min after the commencement of the gas chromatographic run. Ions *m/z* 350.0 and 436.0 (Fig. 2) were monitored with dwell times of 200 msec. O-Trimethylsilyl T-2 toxin had a retention time of 8.5 min. The sensitivity of the instrument was adjusted so that 1 ng of derivative could be detected. The response ratio between the ions was used to confirm the identity of the derivative and quantification was performed with the most sensitive ion. Typical traces obtained from maize extracts are shown in Fig. 3.

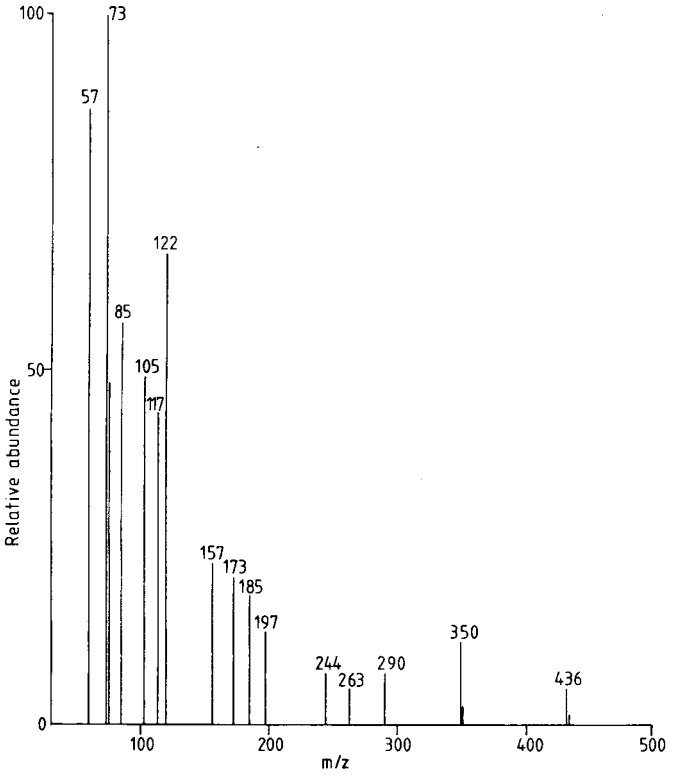

Fig. 2. Mass spectrum of O-trimethylsilyl T-2 toxin.

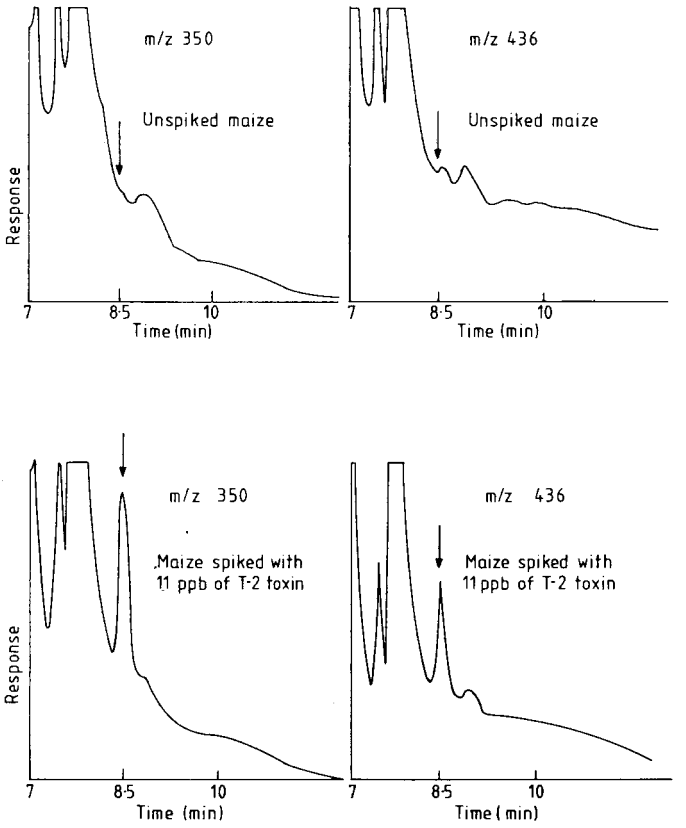

Fig. 3. Analysis of T-2 toxin as the trimethylsilyl derivative by GC–MS with selected ion monitoring. Conditions: a glass column (1 m × 2 mm I.D.) packed with 3% OV-7 in Chromosorb W AW DMCS (80–100 mesh) temperature programmed from 160°C to 270°C at 15°C/min.

Recoveries of added toxin

T-2 Toxin was added to pulverised maize at the levels shown in Table I and the samples were extracted as described. The recoveries were calculated by comparison of extracts against standards of silylated T-2 toxin, run sequentially on the gas chromatograph–mass spectrometer.

TABLE I

T-2 TOXIN IN MAIZE

Level added toxin (μg/kg)	*Recovery (%)*
368	100, 103
37	109, 97
19	70, 77
11	61, 65 60, 71

DISCUSSION

The extraction and analysis described for T-2 toxin in maize is simple and reproducible. Other workers[7] cleaned-up extracts by column or thin-layer chromatography but both of these techniques are tedious and non-reproducible.

Ethyl acetate was chosen as the extracting solvent because it was sufficiently polar to dissolve T-2 toxin but not polar enough to dissolve water-soluble materials, which could make effective separation more difficult. Most of the substituted trichothecenes, including T-2 toxin, are readily soluble in ethyl acetate or chloroform. The number of stages in the procedure was kept to a minimum to avoid undue losses of material. Separations on columns are particularly prone to cause variable recoveries when very small amounts of material are being handled. Recoveries of T-2 toxin were lower when added to samples at levels close to the detection limit than when added at the higher levels (Table I). It is likely that the defatting stage removes some T-2 toxin as it can dissolve appreciably in fat-saturated hexane, and therefore partitions between the phases rather than remaining entirely in the aqueous phase.

The extraction and separation required very selective detection to discriminate T-2 toxin from interfering material. The toxin is insufficiently volatile to pass through a gas chromatographic column but suitable derivatives like trimethylsilyl ethers or trifluoroacetyl esters may be prepared to increase its volatility. These derivatives are amenable to detection by MS which can monitor particular ions. Combined GC–MS therefore provides extremely selective detection as not only must be column retention time be correct but the ratio of responses to the monitored ions must also be correct before a peak is considered positive. The technique is also extremely sensitive as the instrument monitors only a few ions at a time. When high mass ions are examined then the chances of interference occurring are correspondingly reduced and the compound of interest can be detected in the presence of large amounts of other material. The trimethylsilyl ether of T-2 toxin was chosen as the derivative to monitor mainly because of its ease of preparation but also because of the intensity of some high mass ions in its spectrum (Fig. 2). Relatively intense ions exist at m/z 436 $(M-102)^+$, which is probably loss of the isovaleryl moiety and at m/z $(M-188)^+$. The base peak in the mass spectrum of silylated T-2 toxin is m/z 73 $(Si[CH_3]_3)^+$ which cannot be monitored as it occurs generally in any silylated compound and is therefore unselective.

Fig. 3 shows the selected ion monitor chromatograms obtained from a sample of maize and the same product spiked with T-2 toxin at a level of 11 μg/kg. The arrows on the chromatograms mark the retention time of trimethylsilyl T-2 toxin and show that the quantitation limit for this toxin is better than 5 μg/kg.

The procedure described in this report is simpler than those used by other workers[1,2] and can reach the same or lower levels of detection for T-2 toxin in maize.

ACKNOWLEDGEMENT

This work forms part of a project on Mycotoxins in raw materials and processed food undertaken for the Ministry of Agriculture, Fisheries and Food. The results are the property of the Ministry.

REFERENCES

1 J. V. Rodricks, C. W. Hesseltine and M. A. Mehlman (Editors), *Mycotoxins in Human and Animal Health*, Pathotox Publishers, Park Forest, IL 1st ed., 1977, pp. 189–340.
2 I. F. H. Purchase (Editor), "*Mycotoxins*", Elsevier, New York, 1st ed., 1974, pp. 181–281.
3 A. Ciegler, *J. Food Protect.*, 41 (1978) 399.
4 D. Forsyth, T. Yoshizawa, N. Morooka and J. Tuite, *Appl. Environ. Microbiol.*, 34 (1977) 347.
5 C. O. Ikediobi, I. C. Hsu, J. T. Bamburg and F. M. Strong, *Anal. Biochem.*, 43 (1971) 327.
6 C. J. Mirocha, S. V. Pathre and J. Behrens, *J. Ass. Offic. Anal. Chem.*, 59 (1976) 221.
7 H. Kuroda, T. Mori, C. Niskioka, H. Okasaki and M. Takagi, *J. Food Hyg. Soc. Japan.*, 20 (1979) 137.
8 T. D. Wyllie and L. G. Morehouse (Editors), *Mycotoxic Fungi, Mycotoxins, Mycotoxicoses —An Encyclopaedic Handbook*, Vol. 1, Marcel Dekker, New York, 1st ed., 1977, pp. 383–420.
9 S. Takitani, Y. Asabe, T. Kato, M. Suzuki and Y. Ueno, *J. Chromatogr.*, 172 (1979) 335.
10 C. W. Chung, M. W. Trucksess, A. L. Giles and L. Friedman, *J. Ass. Offic. Anal. Chem.*, 57 (1974) 1121.
11 S. V. Pathre and C. J. Mirocha, *J. Amer. Oil Chem. Soc.*, 56 (1979) 820.
12 R. M. Eppley, *J. Amer. Oil Chem. Soc.*, 56 (1979) 824.

Journal of Chromatography, 237 (1982) 115–125
Elsevier Scientific Publishing Company, Amsterdam — Printed in The Netherlands

CHROM. 14,444

N-ACETYL-(1-AMINO-2-NAPHTHOL-6-SULPHONIC ACID), A COMMON METABOLITE OF SUNSET YELLOW FCF, ORANGE GGN AND 1-AMINO-2-NAPHTHOL-6-SULPHONIC ACID IN RAT URINE

JACQUES O. DE BEER*, PAUL J. DIERICKX and RÉNÉE I. GRIMÉE
Instituut voor Hygiëne en Epidemiologie, J. Wytsmanstraat 14, B-1050 Brussels (Belgium)
(Received September 17th, 1981)

SUMMARY

Sunset Yellow FCF, Orange GGN and 1-amino-2-naphthol-6-sulphonic acid (ANSA) were administered to male Wistar rats by stomach intubation. Aromatic sulphonic acids excreted in 24-h urines after enzymatic cleavage of the azo link in the dyes were isolated using a thoroughly elaborated ion-pair extraction method and further separated by means of a reversed-phase ion-pair liquid chromatographic system. Blank 24-h rat urines were extracted and run at the same time under identical analytical circumstances.

In addition to the peaks corresponding to sulphanilic and metanilic acid and their N-acetylated derivatives, which are metabolites arising from Sunset Yellow FCF and Orange GGN, respectively, an important common peak appeared on the chromatograms, which was absent from the blank urine extracts. After analysis of 24-h urine of rats that had received ANSA, a peak with the same retention time as this unknown common peak could be detected under the same liquid chromatographic conditions, the retention time of which was different from that of the ANSA standard.

However, after derivatization of the ANSA standard with acetic anhydride, followed by liquid chromatographic examination of the derivatised mixture, two peaks appeared on the chromatogram, the first of which had the same retention time and the same UV-spectrum as the unknown common peak in rat urine extracts. By means of semi-preparative liquid chromatographic separation and isolation, followed by further purification over a cation-exchange resin, the compound corresponding to the unknown common peak could be identified by FT-PMR spectroscopy as N-acetyl-ANSA.

INTRODUCTION

Water-soluble azo compounds are widely used as colour additives, *e.g.*, in foods, pharmaceuticals and cosmetics. Although they have been used for at least half a century, the toxicity and metabolism of these compounds have received attention only during the last two decades. The metabolism of azo compounds has been re-

0021-9673/82/0000–0000/$02.75

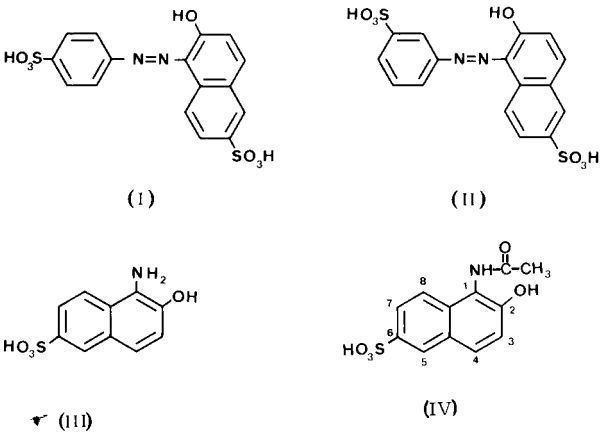

Fig. 1. Structures of Sunset Yellow FCF (I), Orange GGN (II) and 1-amino-2-naphthol-6-sulphonic acid (III).

viewed by Walker[1]. The most important metabolic reaction is cleavage of the azo link, primary amines being formed. This reaction is primarily performed by the gut flora. The mammalian hepatic azo-reductase is regarded as being of minor importance.

Acetylation of the generated primary amino groups is a common detoxification mechanism and the urinary excretion of acetylated amine metabolites has been described in many studies, including those by Bray *et al.*[2], Daniel[3], Jones *et al.*[4], Scheline and Longberg[5] and Stevenson *et al.*[6]. In some of these studies sulphanilic acid, its N-acetylated derivative and 1-amino-2-naphthol-6-sulphonic acid (ANSA) appeared to be metabolites in the urine of test animals after oral administration of Sunset Yellow FCF (I) (Fig. 1). The identification and quantification of these metabolites, however, were performed using colorimetric methods, with which the presence of the N-acetylated metabolites could not be proved directly. No results on the metabolism of Orange GGN (II) (Fig. 1) that demonstrate the formation of metanilic acid and its N-acetylated derivative have been published. For ANSA (III) (Fig. 1), its concentration in urine from test animals could only be determined colorimetrically, starting from freshly prepared standard solutions, which are very sensitive to oxidative changes, giving coloured *o*-quinoneimines. The urines had to be collected in receivers immersed in solid carbon dioxide. The presence of N-acetyl-ANSA as a urine metabolite has never been confirmed.

Larsen and Tarding[7] described the absorption and excretion of ^{35}S-labelled ANSA in rats and rabbits, measuring the radioactivity, without following the individual fates of possible different ANSA metabolites.

The combination of ion-pair extraction and reversed-phase ion-pair high-performance liquid chromatography (HPLC) offers the advantage of selective isolation and separation of the different aromatic sulphonic acids as possible urinary metabolites, so that free and N-acetylated derivatives can be distinguished and identified unambiguously. Semi-preparative HPLC isolation and purification of an unknown peak, not appearing in the blank urines, followed by spectroscopic identification can allow the detection of a new, undescribed metabolite.

EXPERIMENTAL

Instrumentation

The chromatographic separation was performed on a HPLC system consisting of two Altex Model 100A pumps, an Altex Model 421 solvent gradient programmer and a Hitachi Model 100-10 variable-wavelength UV–visible detector. Injections were made by means of an Altex Model 210 sample injection valve, supplied with loops of 20 μl and 2.0 ml. The isolation and collection of separated compounds eluting from the semi-preparative column were effected by means of an Altex automatic rotary valve (Altex, Berkeley, CA, U.S.A.).

The analytical column was a reversed-phase 10-μm Hibar LiChrosorb RP-18 25 cm × 4 mm I.D. column (Merck, Darmstadt, G.F.R.). The semi-preparative column was a reversed-phase 5-μm Ultrasphere ODS 25 cm × 10 mm I.D. column (Altex). The recorder was a single-pen Omniscribe Model 5117-2 (Houston Instruments). The UV spectra were recorded with a Beckman Model 25 UV-visible spectrophotometer, with digital reading and recorder (Beckman, Fullerton, CA, U.S.A.). Extracts were evaporated on a Büchi RE 120 Rotavapor (Büchi Laboratorium-Technik, Flawil, Switzerland).

The proton magnetic resonance (PMR) spectroscopic properties of the common metabolite were examined on a JEOL FX 100 nuclear magnetic resonance spectroscopic apparatus in the Fourier transform mode at a frequency of 99.55 MHz and a temperature of 26°C.

Reagents

All chemicals were of analytical-reagent grade unless specified otherwise.

Sulphanilic acid was supplied by Merck and metanilic acid (*m*-aminobenzenesulphonic acid, aniline-*m*-sulphonic acid) by ICN Pharmaceuticals (Plainview, NY, U.S.A.). Sunset Yellow FCF (E110, FD&C Yellow No. 6, C.I. Food Yellow 3) and Orange GGN (E111, C.I. Food Orange 2) were obtained from Chroma-Gesellschaft Schmid (Stuttgart, Untertürkheim, G.F.R.). ANSA was synthesized according to Larsen and Tarding[8]. N-Acetylsulphanilic and N-acetylmetanilic acid standards were synthesized starting from the free sulphonic acids and acetic anhydride (Merck), and recrystallized according to Daniel[3]. Tetrabutylammoniumhydrogenium sulphate (TBA^+-HSO_4^-) and tetrapentylammonium bromide (TPA^+-Br^-) were obtained from Fluka (Buchs, Switzerland).

The pH 7.0 buffer was prepared by diluting a mixture of 50 ml 0.1 *M* potassium dihydrogen orthophosphate (Merck) and 29.1 ml of 0.1 *M* sodium hydroxide to 100 ml with doubly distilled water. The pH 10.0 buffer was prepared by dilution of a mixture of 50 ml of 0.05 *M* sodium hydrogen carbonate (Merck) and 10.7 ml 0.1 *M* sodium hydroxide (Merck) to 100 ml with doubly distilled water. HPLC-grade methanol was purchased from Burdick & Jackson Labs. (Muskegon, MI, U.S.A.).

For the PMR spectroscopic examination, the purified residue of the common metabolite and the derivatized ANSA compound were disolved in 0.5 ml of ^2H_2O (Aldrich, Beerse, Belgium) containing 3-(trimethylsilyl)propionic acid-d_4 sodium salt (Uvasol, Merck) as reference.

Solvent A was a 0.01 *M* solution of sodium acetate and 0.005 *M* TPA^+–Br^- in distilled water, the pH being adjusted to 3.50 with orthophoshoric acid. Solvent B

contained the same amounts of salts, but with 50% (v/v) of methanol. Solvent A and the aqueous part of solvent B were filtered through a Millipore Type HA filter (0.45 μm). The extract solution injected for semi-preparative separation was filtered through a Millipore Type FH filter (0.5 μm) by means of a Millipore "Stainless Swinny" (13 mm) (Millipore, Bedford, MA, U.S.A.).

Dowex 50W-X8 (100–200 mesh) cation-exchange resin (Fluka), swollen for 24 h in doubly distilled water, was used to eliminate the quaternary ammonium ions from the isolated metabolite residue.

Urine samples

Male Wistar rats (*ca.* 200 g), obtained from the animal house of the KU Leuven, Belgium, were administered in duplicate by stomach intubation single doses of 20, 100, 250 and 500 mg/kg of Sunset Yellow FCF and Orange GGN and 150 and 300 mg/kg of ANSA, as an aqueous suspension. The 24-h urine samples, the volumes of which varied from 13.0 to 18.0 ml, were collected in plastic bottles without additives. They were centrifuged for 10 min at 4000 rpm and decanted.

Extraction and chromatographic procedures

For the extraction of the urinary aromatic sulphonic acid metabolites, prior to HPLC analysis on the analytical column, 1.0 ml of urine was mixed in a test-tube with 0.5 ml of 1.5 *M* orthophosphoric acid and 2.0 g of ammonium sulphate. This mixture was extracted twice with 5.0 ml of ethylacetate by vortexing for at least 2 min. After centrifugation (5 min at 3000 rpm) the ethyl acetate phases were discarded. The urine phase was neutralized to pH 7.0 adding 3–4 drops of 10 *N* sodium hydroxide solution and mixed with 1.0 ml of 0.1 *M* TBA^+–HSO_4^- in buffer solution of pH 7.0.

Some ammonium sulphate was added to maintain saturation. The urine phase was extracted further with 3.0 ml of dichloromethane by vortexing for at least 2 min and centrifuged for 10 min at 4000 rpm, the dichloromethane phase being transferred into a clean test-tube. Finally, 1.5 ml of this dichloromethane phase was extracted by vortexing for 2 min with 0.5 ml of 0.1 *M* sodium perchlorate in pH 10.0 buffer solution. After centrifugation (for 5 min at 1000 rpm, 20 μl of the aqueous layer were injected into the HPLC system.

TABLE I

HPLC GRADIENT PROGRAMME, CONTROLLED BY THE ALTEX MICROPROCESSOR, FOR THE RAT URINE EXTRACT ON THE ANALYTICAL COLUMN

Time	*Function*	*Value*	*Duration*
0.00	Flow-rate	1.25 ml/min	
0.00	%B	35%	
0.00	External flag*	1	
12.00	%B	75%	4 min
25.00	%B	100%	4 min
35.00	%B	35%	3 min
45.00	Alarm	–	0.1 min
50.00	External flag	1	0 min
50.00	Flow-rate	0 ml/min	0.2 min
50.2	End programme	–	

* External flag = apparatus that can be started by the microprocessor; *e.g.*, External flag 1 = recorder.

HPLC analysis on the analytical column was performed at two detection wavelengths (240 and 260 nm) by solvent gradient elution, controlled by the Altex solvent gradient programmer. The programme was started with 35% solvent B and increased by a two-step gradient programme to a final concentration of 100% B. This was accomplished over a 29-min period. The solvent gradient was reduced after 6 min to 35% B in 3 min and allowed to equilibrate for 15 min between two injections. The flow-rate was kept constant at 1.25 ml/min (Table I). Each extract was also submitted to an isocratic run, solvent A being 25% and solvent B being 75% at the same flow-rate.

The extraction procedure prior to the semi-preparative HPLC analysis was started with 5.0 ml of urine, the other reagents being added proportionally. The ion-pair extraction however, was performed twice with 5.0 ml of dichloromethane, which was ten evaporated at 60°C on the Büchi Rotavapor. The residue was dissolved in 2.0 ml of a mixture of solvents A and B (25:75, v/v), filtered and injected completely through the 2.0-ml loop on the semi-preparative column. This semi-preparative HPLC separation was performed by an isocratic run, the mobile phase being 25% A and 75% B, at a detector wavelength of 240 nm and a constant flow-rate of 2.25 ml/min. The column effluent, containing the probable common metabolite, was isolated and its UV spectrum was recorded. It was then evaporated to dryness at 70°C on the Büchi Rotavapor, the residue being dissolved in portions at 7–8 ml of dichloromethane which were collected and evaporated. By this means most of the dichloromethane-insoluble inorganic salts present in the column effluent were eliminated.

The salt-free residue was dissolved in 10 ml of doubly distilled water and freed from quaternary ammonium ions by passing the solution through a Dowex 50W-X8 cation-exchange column (3.0 × 1.5 cm I.D.) which was eluted with 20 ml of doubly distilled water. The aqueous effluent, free from quaternary ammonium ions, was evaporated at 70°C on the Büchi Rotavapor, the final purified extract obtained being submitted to PMR spectroscopic examination. Under identical analytical conditions, the same procedure was followed in order to isolate, purify and identify the compound with the same retention time and the same UV spectrum as the probable common metabolite obtained after injection of the concentrated mixture prepared by derivatization of 50 mg of ANSA with an excess of acetic anhydride in ethanol[3].

FT-PMR spectroscopic examination

On account of the small amount of residue of the purified metabolite, the spectra were recorded after accumulation of 1000 pulses, using the "double precision" programme. This programme improves the signal-to-noise ratio for peaks of weak intensity with respect to the intense signal of the solvent, which here is residual H_2O present in ^2H_2O. The spectra were recorded in a 1000-Hz width, using 8192 points in pulses of 45° (20 μsec) and a pulse repetition time of 5 sec. The chemical shifts are calculated in parts per million with respect to 3-(trimethylsilyl)propionic acid-d_4, sodium salt, as reference.

RESULTS

Some chromatograms of 24-h urine extracts separated on the analytical column by solvent gradient and by isocratic elution are shown in Figs. 2 and 3,

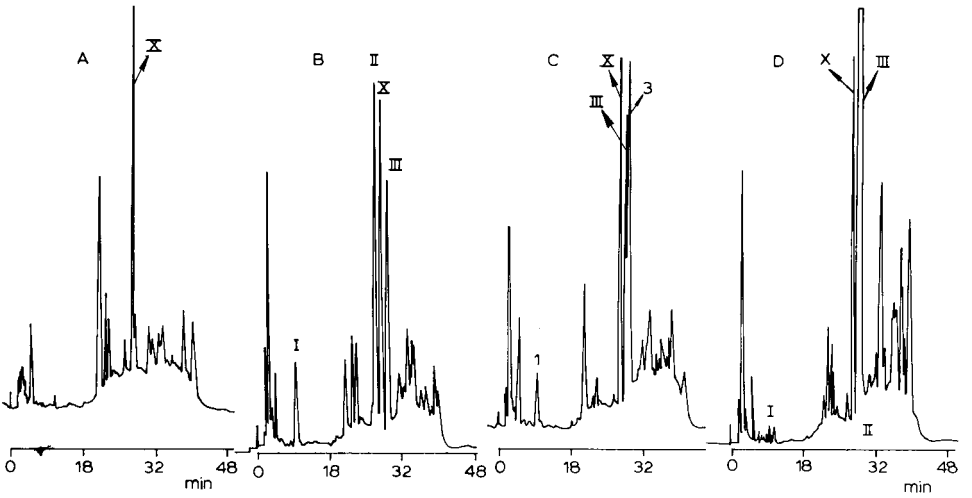

Fig. 2. Gradient-programmed HPLC chromatograms detected at 240 nm of a blank rat urine extract (A) and of 24-h rat urine extracts after administration of 100 mg/kg of Sunset Yellow FCF (B), 100 mg/kg of Orange GGN (C) and 150 mg/kg ANSA (D). I = Sulphanilic acid; II = N-acetylsulphanilic acid; III = common metabolite; 1 = metanilic acid, 3 = N-acetylmetanilic acid, X = endogenous rat urine component.

respectively. Chromatograms of a urine extract recorded at 240 and 260 nm are given in Fig. 4.

Some chromatograms of 24-h urine extracts separted on the semi-preparative column are shown in Fig. 5.

The UV spectrum of the unknown common metabolite, after administration of Sunset Yellow FCF, Orange GGN and ANSA, is given in Fig. 6.

The PMR spectrum of the purified common metabolite, which is the same as that of the derivatized ANSA compound having the same retention time and UV spectrum, is shown in Fig. 7.

DISCUSSION

Extraction procedure

In order to minimize sample work-up, direct injection of samples was attempted under various circumstances, but was unsuccessful as interfering peaks did not allow the resolution of the compounds of interest. Owing to the large difference in the physico-chemical properties between aromatic sulphonic acids, which are always ionized in water even at low pH, and most of the endogenous organic acids present in rat urine, pre-extraction of the urine with ethyl acetate at low pH seemed to be successful as a preliminary clean-up step. By adding high concentrations of ammonium sulphate, the endogenous organic acid extraction efficiency was enhanced, without the sulphonic acids leaving the aqueous phase.

The very polar aromatic sulphonic acids could be isolated from aqueous solutions by means of an ion-pair liquid–liquid extraction, this type of extraction being particularly efficient for polar and ionized compounds[9–11]. The pH, nature and concentration of the counter ion, ion strength and extraction solvent, however, must be

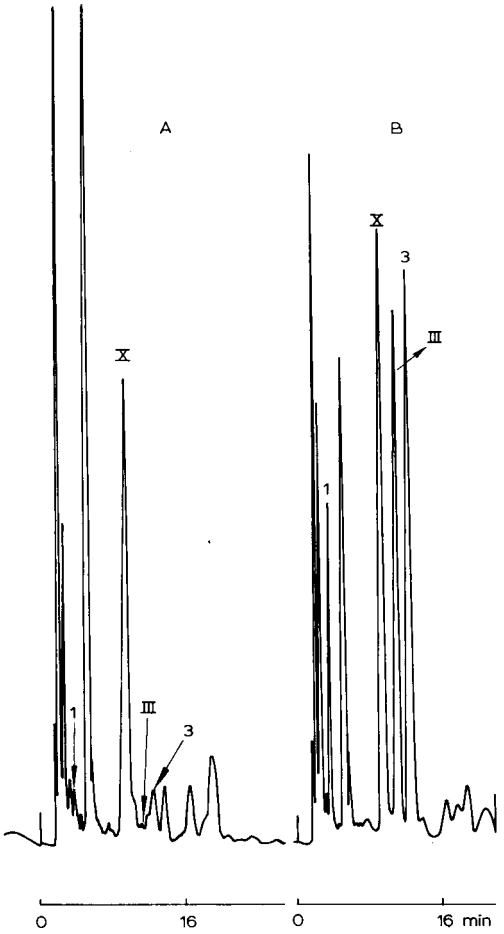

Fig. 3. Isocratic HPLC chromatogram detected at 240 nm of a 24-h blank rat urine extract (A) and a 24-h rat urine extract after administration of 100 mg/kg of Orange GGN. 1 = Metanilic acid; 3 = N-acetyl-metanilic acid; III = common metabolite; X = endogenous urine component.

optimized. A pH of 7.0–7.5 was found to be optimal in accomplishing complete extraction of Orange GGN, Sunset Yellow FCF, sulphanilic acid and metanilic acid together with their N-acetyl derivatives, TBA^+ being added as counter ion at an optimum concentration of 0.1 *M*. Lower counter-ion concentrations produced low and variable extraction efficiencies. The addition of high concentrations of ammonium sulphate to the system, producing a salting-out effect, was necessary to ensure a good extraction efficiency of sulphanilic acid, metanilic acid and their N-acetyl derivatives. Dichloromethane was preferred to chloroform as extraction solvent because also high sulphonic acid concentrations could be extracted efficiently as ion pairs. By vortexing the dichloromethane phase, containing the ion pairs, with 0.5 ml of 0.1 *M* sodium perchlorate in pH 10.0 buffer, the sulphonic acids returned to the aqueous phase, which was subsequently injected for HPLC analysis.

During the extraction procedure the probable common metabolite seemed to

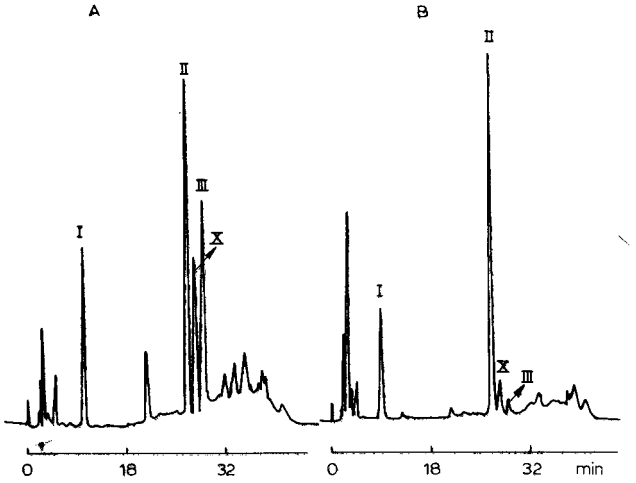

Fig. 4. Gradient-programmed HPLC chromatograms of a 24-h rat urine after administration of 100 mg/kg of Sunset Yellow FCF, detected at 240 nm (A) and 260 nm (B). I = Sulphanilic acid; II = N-acetyl-sulphanilic acid, III = common metabolite; X = endogenous urine component.

behave identically to the other aromatic sulphonic acids. In contrast, ANSA could not be recovered from spiked water and urine samples by means of this extraction method, perhaps because of its chemical instability. A partial recovery with poor reproducibility was obtained by adding ascorbic acid as an antioxidant to the sample before extraction. No peak corresponding to the ANSA standard (stable for many days in an aqueous solution with ascorbic acid as antioxidant), however, was found in real urine samples from rats given FCF, GGN or ANSA, not even when ascorbic acid was added in high concentrations before extraction.

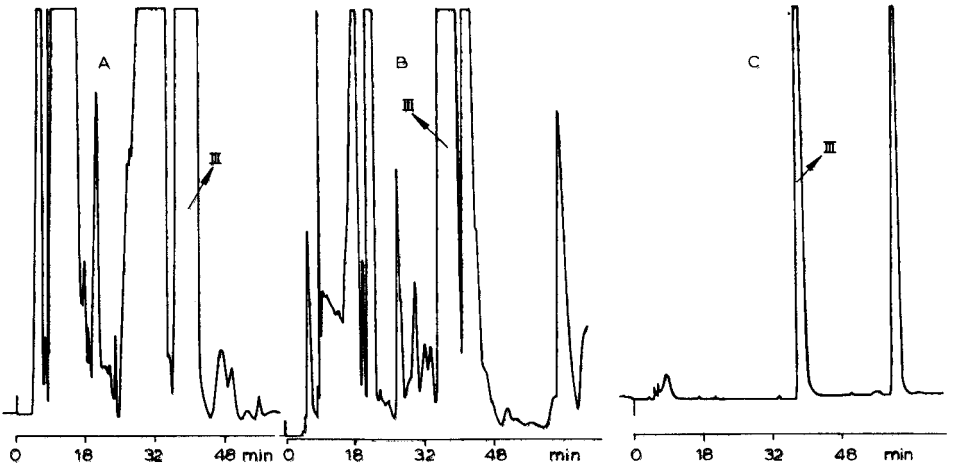

Fig. 5. Semi-preparative HPLC chromatograms of 24-h rat urine extracts after administration of 500 mg/kg of Sunset Yellow FCF (A), Orange GGN (B) and ANSA derivatized with acetic anhydride (C).

Fig. 6. UV spectrum of the common rat urine metabolite identified as N-acetyl-ANSA.

Chromatographic procedure

Without a counter ion, the retention of the standard aromatic sulphonic acids was inadequate for acceptable resolution. Addition of TPA^+ as the counter ion to the solvent system markedly increased the retention and resolution of these compounds. Small changes in pH produced marked changes in their retention times. A decrease in the pH resulted in a marked reduction of the retention time and resolution, and an increase in the pH resulted in the opposite effect. A pH of 3.50 was optimal for resolution and retention and was used in all analyses. The concentration of the TPA^+ ion was also varied at constant pH. A reduced concentration caused a small reduction in the retention times and an increased concentration produced an increased retention, although this effect was not as marked as that of the pH[12–14]. A TPA^+ counter-ion concentration of 0.005 *M* was determined to be optimal.

The chromatographic conditions were optimized with respect to the resolution and selectivity between endogenous peaks of urine blanks and the metabolites in

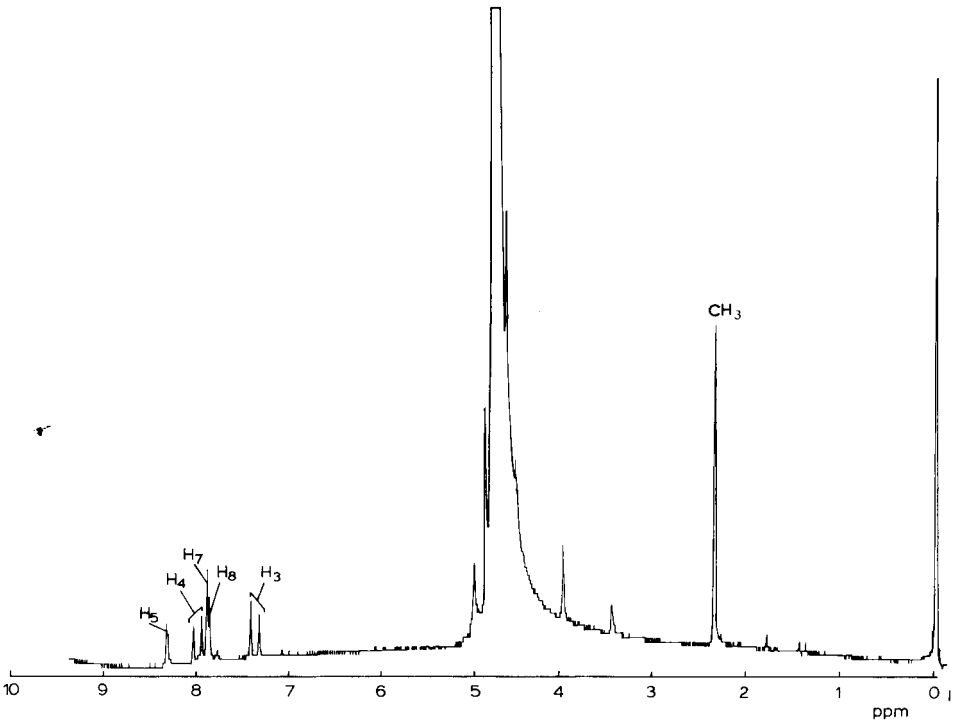

Fig. 7. PMR spectrum of the common rat urine metabolite N-acetyl-ANSA isolated after administration as well of Sunset Yellow FCF, Orange GGN and ANSA [*cf.* Fig. 1 (IV)].

urine extracts of rats that had received Orange GGN and Sunset Yellow FCF. A mixture of standard sulphanilic acid, metanilic acid and their N-acetyl derivatives was also injected under identical chromatographic conditions.

The choice of 240 and 260 nm as detection wavelengths was to check if the individual peak-height ratios of the sulphonic acid standards and the corresponding metabolites found in the urine extracts were constant (Fig. 4). At 260 nm endogenous urine peaks interfered weakly on the chromatogram, the common metabolite, however, being less sensitively detected than at 240 nm. When the dose of the administered dye was enhanced, higher peaks corresponding to the metabolites in the urine extracts were recovered. Urine extracts of rats receiving the same amounts of dyes showed metabolite peaks with nearly the same intensities.

In urine samples collected after 72 h from rats that had received the highest doses (500 mg/kg), only poor traces of the metabolites could be obtained.

PMR spectroscopic examination

Apart from the signal of H_2O, situated at 4.76 ppm, a peak at 2.35 ppm and a series of peaks in the aromatic zone are observed. Protons H_3 and H_4 (Fig. 1, IV) have chemical shifts of 7.35 (doublet) and 7.97 ppm (doublet), respectively. The coupling constant $J_{3,4}$ is 9 Hz. Proton H_5 at 8.3 ppm is weakly coupled with protons H_7 and H_8 ($J_{5,7}$ = 1.5 Hz and $J_{5,8} \approx 0.8$ Hz). Protons H_7 and H_8 have chemical shifts of 7.83 and 7.85 ppm ($J_{7,8}$ = 1 Hz), respectively. Integration of the spectrum

indicates that the peak at 2.35 ppm corresponds to a CH_3 group and its position suggests that a monoacetyl derivative of ANSA is involed. Indeed, the PMR spectrum of ANSA standard, dissolved in ^2H_2O and stabilized by addition of ascorbic acid (vitamin C), is similar to that of the isolated common metabolite, apart from the absence of the CH_3 peak at 2.35 ppm and a weak shift of proton H_8 to lower frequency. This indicates that the metabolite is acetylated at the NH_2 function and not at the OH function. Acetylation at the OH function should produce an important shift of protons H_3 and H_4.

After acetylation of the ANSA standard, followed by semi-preparative HPLC isolation and cation-exchange purification, the compound with the same HPLC retention time and the same UV spectrum as the common metabolite also has an identical PMR spectrum.

CONCLUSION

The combined system of ion-pair extraction and ion-pair reversed-phase HPLC allows the identification of sulphanilic acid and methanilic acid and their N-acetyl derivatives as metabolites in the urine of rats after administration of the dyes Sunset Yellow FCF and Orange GGN. This technique also allows the detection in rat urine of a common Orange GGN, Sunset Yellow FCF and ANSA metabolite, identified as N-acetyl-ANSA by a combination of PMR spectroscopy and semi-preparative HPLC isolation and purification of rat urine extracts and acetylated ANSA standard.

ACKNOWLEDGEMENTS

We thank Prof. Dr. A. Lafontaine and Ir. J. Gosselé for their interest in this work.

REFERENCES

1 R. Walker, *Food Cosmet. Toxicol.*, 8 (1970) 659.
2 H. G. Bray, R. C. Clowes and W. V. Thorpe, *Biochem. J.*, 49 (1951) IXV.
3 J. W. Daniel, *Toxicol. Appl. Pharmacol.*, 4 (1962) 572.
4 R. Jones, A. J. Ryan and S. E. Wright, *Food Cosmet. Toxicol.*, 2 (1964) 447.
5 R. R. Scheline and B. Longberg, *Acta Pharmacol. Toxicol.*, 23 (1965) 1.
6 E. S. Stevenson, K. Dobriner and C. P. Rhoads, *Cancer Res.*, 2 (1942) 160.
7 J. C. Larsen and F. Tarding, *Arch. Toxicol., Suppl.*, 1 (1978) 251.
8 J. C. Larsen and F. Tarding, *Acta Pharmacol. Toxicol.*, 39 (1976) 525.
9 G. Schill, *Separation Methods for Drugs and Related Organic Compounds*, Apothekarsocietetan, Stockholm, 1978.
10 C. Van Peteghem and J. Bijl, *J. Chromatogr.*, 210 (1981) 113.
11 K. T. Muir, J. H. G. Jonkman, D.-S. Tang, M. Kunitani and S. Riegelman, *J. Chromatogr.*, 221 (1980) 85.
12 J. H. Knox and G. R. Laird, *J. Chromatogr.*, 122 (1976) 17.
13 R. Gloor and E. L. Johnson, *J. Chromatogr. Sci.*, 15 (1977) 413.
14 H. U. Ehmcke, H. Kelker, K. H. König and H. Ullner, *Z. Anal. Chem.*, 294 (1979) 251.

Journal of Chromatography, 237 (1982) 127–135
Elsevier Scientific Publishing Company, Amsterdam — Printed in The Netherlands

CHROM. 14,409

CHEMICAL CHARACTERIZATION OF THE HEN EGGSHELL MATRIX: ISOLATION OF AN ALKALI-RESISTANT PEPTIDE

R. CORTIVO and I. CASTELLANI
Istituto di Istologia - Embriologia Generale, Universita di Padova, Via Falloppio 50, 35100 Padova (Italy)
M. MARTELLI
Istituto di Chimica Analytica, Università di Padova, Via Marzolo 1, 35100 Padova (Italy)
and
G. MICHELOTTO and G. ABATANGELO*
Istituto di Istologia-Embriologia Generale, Università di Padova, Via Faloppio 50, 35100 Padova (Italy)
(First received June 22nd, 1981; revised manuscript received September 28th, 1981)

SUMMARY

The eggshell matrix was obtained from hen eggshells using EDTA solutions. The water-soluble organic material was separated on a DEAE-cellulose column equilibrated with 8 *M* urea using Tris–hydrochloric acid buffer as eluent with a linear gradient of sodium chloride.

Five main fractions were obtained which differ in amino acid composition and sugar contents. As is shown from the uronic acid content, the first two fractions eluted from the column are glycoproteins, while the other three contain proteins and glycosaminoglycans.

From the alkaline hydrolysate of the eggshell matrix, a peptide was isolated which is composed of aspartic acid, threonine, serine, glutamic acid, proline, glycine and alanine in a molar ratio of 2:1:3:7:1:3:1 with a minimum molecular weight of 2158 daltons.

The calcium ion binding to this peptide was studied, at different pH values, with both free and blocked carboxyl groups, using murexide as an indicator of free Ca^{2+}. The importance of this acidic peptide in the calcification process of the eggshell matrix is discussed.

INTRODUCTION

The chicken eggshell is composed of a protein–polysaccaride and glycoprotein mixture, as already described by numerous workers[1–5]. The organic eggshell matrix represents approximately 2% (w/w) of the total calcified material in which calcium carbonate is the major inorganic component. The shell matrix, as other calcified substrates[6], seems to influence the mineral deposition, even though the binding sites in the calcifying processes are still a matter of discussion.

As far as the organic eggshell matrix of the chicken is concerned, the importance of the ionizable carboxyl groups in the calcium ion-binding processes has been demonstrated[5]. In fact, the calcium ion binding is pH dependent and rapidily decreases if the carboxyl groups of the shell matrix are previously blocked with a water-soluble carbodiimide.

Many calcifying systems, such as bone, dentine and ectopic calcifications, have

0021-9673/82/0000–0000/$02.75

been shown to contain γ-carboxyglutamic acid[7]. This calcium ion-binding amino acid seems to play an important role in the regulation of calcium salt deposition, as has been demonstrated for the process of vitamin K activation[9,10]. The presence of this particular amino acid is not obligatory, however, for the calcification process in invertebrates and in the eggshell of the chicken, as has been shown by King[11].

In our work we have separated the eggshell matrix on a DEAE-cellulose column and the fractions obtained have been chemically characterized. In addition we have investigated the presence of particular compounds such as the γ-carboxylglutamic acid, phosphoserine or similar substances, which could be involved in the calcium ion-binding process. For this purpose we have studied the amino acid composition of the eggshell matrix after alkaline and acid hydrolysis in order to observe the eventual presence of particular amino acids or peptides.

The calcium ion binding to a peptide isolated from the alkaline hydrolysate of the eggshell matrix has been also studied.

MATERIALS AND METHODS

The eggshell matrix was obtained by extraction of the broken shells with EDTA solutions as previously described[1,5]. Briefly, the broken eggs were washed with running tap water and immersed in 5% (w/v) EDTA solution adjusted at pH 7–7.5 in order to remove the cuticles. The membranes were peeled off and then the shells were crushed and decalcified with 20% EDTA solutions by stirring overnight (pH 7–7.5). The mixture was dialysed against distilled water until no salts were detectable in the tubes and then lyophilized. The organic material which represents *ca.* 2% of the starting shells was suspended in water and any precipitate was centrifuged off. Only the water-soluble material was used for the experiments.

Hexosamines were determined according to the method described by Cessi and Piliego[12]. The hydrolysis was performed 4 *M* hydrochloric and for 8 h at 110°C. Uranic acid was determined by the modified Dische procedure as described by Davidson[13] and Dische[14]. The neutral sugars were determined according to the method described by Scott and Melvin[15]. The hydrolysis was performed at 100°C in 0.5 *M* sulphuric acid for 3 h. Sialic acid was determined according to the procedure described by Warren[16].

The chromatographic separation of the eggshell matrix was performed on a DEAE-cellulose (DE 32 microgranular) column equilibrated in 8 *M* urea. Aliquots (100 mg) of the material were applied on a 30 × 2 cm column and the elution was carried out with Tris–hydrochloric acid buffer (0.05 *M*, pH 8.5) in 8 *M* urea with a sodium chloride gradient from 0 to 0.5 *M*. The column was washed with 1 *M* sodium chloride followed by 0.1 *M* sodium hydroxide.

The amino acids were determined, after hydrolysis with 6 *M* hydrochloric acid for 22 h at 110°C, on a JLC-5AH amino acid analyser.

The alkaline hydrolysis of the eggshell matrix was performed with 2 *M* sodium hydroxide at 100°C for 24 h. The hydrolysate was then neutralized with concentrated hydrochloric acid and applied on to the amino acid analyser which was provided with a split stream device in order to collect part of the effluent from the column.

For desalting, a Bio-Gel P-2 column (100 cm × 2 cm) was used with 1% acetic acid as eluent.

Calcium ion binding was determined as described elsewhere, using murexide as an indicator of free Ca^{2+} [17]. A 50-μM solution of murexide in 10 mM Tris–hydrochloric acid buffer from pH 5 to 9 was titrated with additions of $1.1 \cdot 10^{-5}$ M calcium chloride. The reaction was measured spectrophotometrically at 540–510 nm, with a dual-wavelength spectrophotometer (Johnson Research Foundation). If at the same pH value the murexide solution was titrated in the presence of 0.5–1 mg of peptide, smaller absorbance changes were initially obtained under the same experimental conditions. From the difference of the two titration curves, in the presence and in the absence of the peptide, it was possible to calculate the amount of the Ca^{2+} bound to the peptide at pH 5, 6, 7, 8 and 9 (see Results). The carboxylic groups of the protein were blocked with the glycine ethyl ester in the presence of the water-soluble carbodiimide 1-cyclohexyl-3-(2-morpholinoethyl)carbodiimide, according to the method of Hoare and Koshland[18]. The reaction was performed at pH 4.75. The pH was maintained constant by automatic titration with 0.5 M hydrochloric acid.

RESULTS

Fig. 1 shows the chromatographic separation of the eggshell matrix on DEAE-cellulose. Five main fractions are obtained. The first two peaks are eluted with the void volume, the third large fraction is eluted with the sodium chloride gradient and the last two fractions with the 1 M sodium chloride and 0.1 M sodium hydroxide washings, respectively. The five fractions represent respectively 10, 4.0, 12, 4.0 and 70.0% of the weight of the starting material.

Table I reports the amino acid composition of the eggshell matrix and its

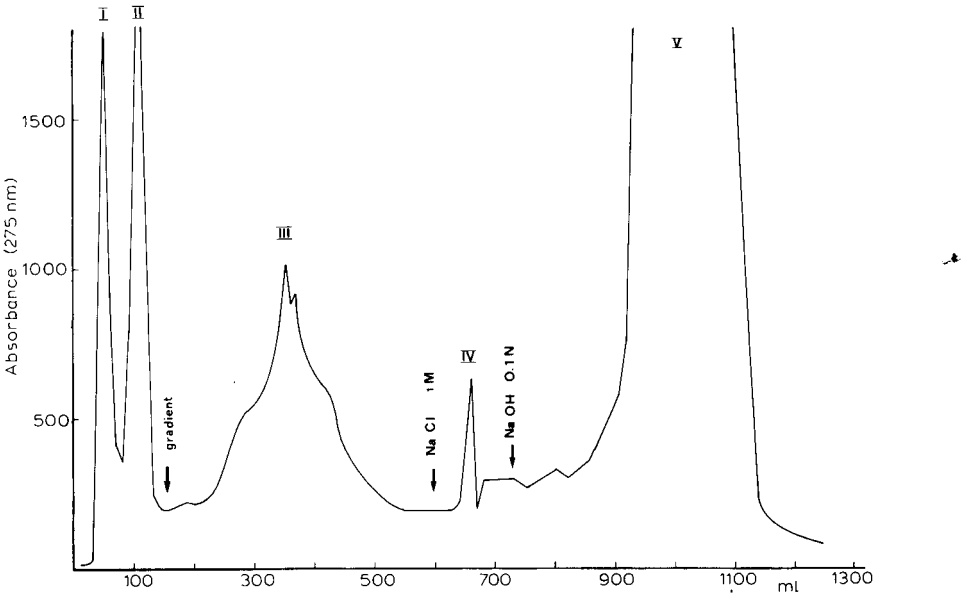

Fig. 1. Chromatographic separation of the eggshell matrix on a column (30 × 2 cm) of DE 32 DEAE-cellulose equilibrated in 8 M urea. The elution was carried out with Tris–hydrochloric acid buffer (0.05 M, pH 8.5) in 8 M urea with a sodium chloride gradient from 0 to 0.5 M. Five fractions (I–V) were collected.

TABLE I

AMINO ACID COMPOSITION OF THE EGGSHELL MATRIX AND ITS FIVE FRACTIONS

Amino acid residues per 1000 residues.

Amino acid	*Water-soluble eggshell matrix*	*Fractions isolated from the DE-cellulose column (see Fig. 1)*				
		I	*II*	*III*	*IV*	*V*
Hyl	–	–	–	–	–	–
Lys	38.7	33.5	44.6	38.3	26.9	41.0
His	22.5	9.3	–	20.9	9.6	20.6
Arg	36.1	29.2	34.1	37.5	50.0	51.3
Hyp	–	–	–	–	–	–
Asp	102.3	104.4	67.3	92.3	67.3	105.7
Thr	73.1	107.4	35.8	67.6	46.1	58.4
Ser	95.4	85.7	54.2	87.9	119.2	85.9
Glu	128.1	52.1	85.7	126.4	155.7	127.8
Pro	62.7	63.1	81.3	65.4	–	68.5
Gly	147.9	115.2	137.3	150.8	251.9	119.1
Ala	73.9	121.3	111.1	77.7	75.0	72.1
1/2 Cys	7.7	–	–	2.3	–	13.0
Val	68.8	82.2	109.3	91.9	78.8	68.7
Met	13.7	–	–	9.2	–	10.5
Ile	36.1	35.8	41.1	29.1	26.9	42.9
Leu	72.2	76.8	70.8	71.4	46.1	90.2
Tyr	7.7	25.0	70.8	10.0	46.1	9.0
Phe	12.8	58.4	55.9	20.6	–	15.6
NP/P*	1.01	1.37	2.10	1.12	1.10	1.04

* NP/P = ratio of non-polar to polar amino acids.

fractions separated on the DEAE-cellulose column. The ratio of non-polar to polar (NP/P) amino acids has been calculated for all the fractions and is expressed by the sum of the moles of proline, glycine, alanine, cystine, valine, isoleucine, leucine, methionine, tyrosine and phenylalanine, divided by that of lysine, histidine, arginine, aspartic acid, serine and glutamic acid.

Table II reports proportions of uronic acid, hexosamines and neutral sugars

TABLE II

URONIC ACID, HEXOSAMINES AND NEUTRAL SUGAR CONTENTS OF THE EGGSHELL MATRIX AND ITS FIVE FRACTIONS

Material	*Content (per 100 g of material)*		
	Uronic	*Hexosamines*	*Neutral sugar*
Water-soluble eggshell matrix	12.8	10.8	3.2
Fraction I	0.6	2.77	9.0
Fraction II	0.4	2.2	8.0
Fraction III	10.3	9.16	5.2
Fraction IV	2.2	4.4	5.1
Fraction V	7.6	8.16	3.84

for alle the fractions. No sialic acid was found in any sample. Fig. 2 shows the elution profile on the amino acid analyser of the alkaline hydrolysate of the eggshell matrix. It can be seen that just before the glutamic acid, an unknown peak is eluted. This material, referred to as GPX, was collected from many runs of the amino acid analyser with a split stream device. When this material was purified on Bio-Gel P-2 (see Fig. 3) it was resolved into two peaks, the first of which was shown on the amino acid analyser (see Fig. 4) to be the unknown substance (GPX) eluted before the glutamic acid, and the second to consist of salts and two free amino acids, serine and glutamic acid. The isolated GPX was further co-chromatographed in the presence of glutamic acid, thus confirming that its position was just before the glutamic acid.

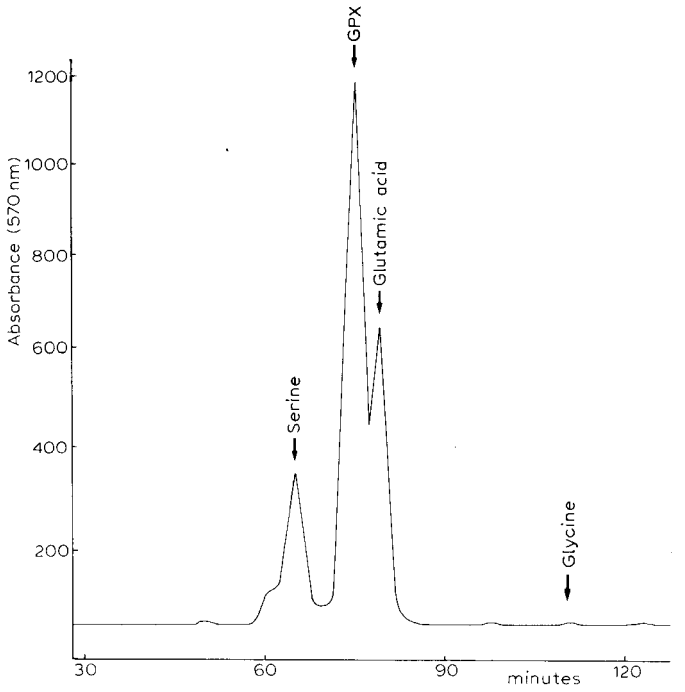

Fig. 2. Chromatographic separation of the alkaline hydrolysate of the eggshell matrix on a JLC-5AH amino acid analyser GPX is the unknown substance which is eluted just before the glutamic acid.

The unknown compound GPX, which represents 2 % of the eggshell matrix by weight, was submitted to acid hydrolysis with 6 *M* hydrochloric acid and then applied on to the amino acid analyser. The chromatographic profile (Fig. 5) shows the GPX to be composed of several amino acids; these are summarized in Table III.

The calcium ion binding to the GPX peptide at different pH values under saturation conditions is prepresented in Fig. 6. The upper curve represents the binding to the alkali-resistant peptide (GPX) in which the carboxyl functions are free, whereas the lower curve represents the calcium binding to the peptide in which the carboxyl groups are modified.

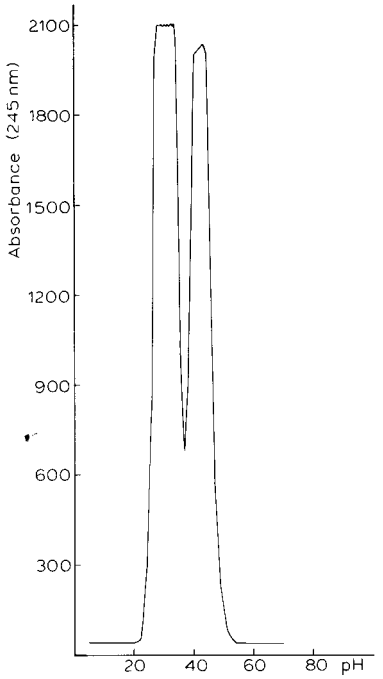

Fig. 3. Chromatographic separation of the GPX material (see Fig. 2) from the salts and amino acids on a Bio-Gel P-2 column (200 × 2 cm). The first fraction is represented by GPX.

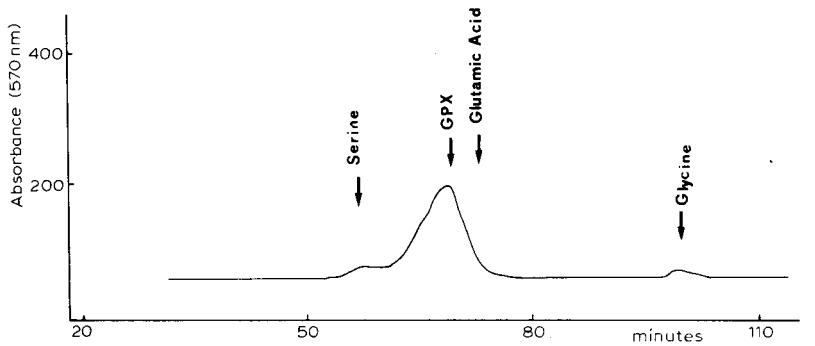

Fig. 4. Chromatographic analysis of the desalted GPX material (see Fig. 2) on a JLC-5AH amino acid analyser. The unknown substance GPX is eluted near the glutamic acid.

DISCUSSION AND CONCLUSION

The eggshell matrix, obtained by extraction of the shells with EDTA solutions, can be partially solubilized in water (*ca.* 50% of the total). When this water-soluble material is applied on to the DEAE-cellulose column, five main fractions are obtained (Fig. 1) which differ in their amino acid composition and sugar content.

From the ratio of the non-polar to polar amino acids, it can be observed that

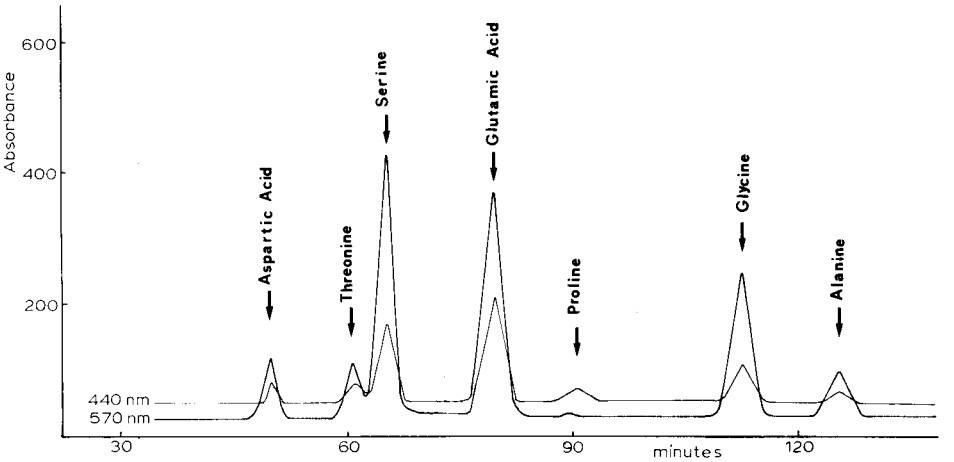

Fig. 5. Chromatographic separation of the GPX material on the amino acid analyser after acid hydrolysis with 6 *M* hydrochloric acid at 110°C for 22 h (see text).

TABLE III

AMINO ACID COMPOSITION OF THE ALKALI-RESISTANT PEPTIDE (GPX)

Amino acid	*Amino acid residues per 1000 residues*	*Molar ratio*
Asp	111.1	2
Thr	55.5	1
Ser	166.6	3
Glu	388.8	7
Pro	55.5	1
Gly	166.6	3
Ala	55.5	1

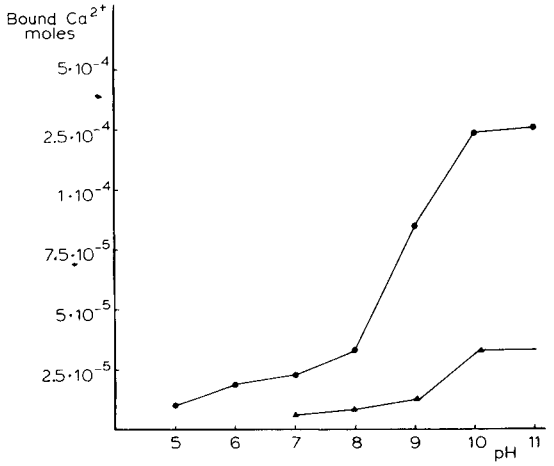

Fig. 6. Binding of Ca^{2+} to the alkali resistant peptide (GPX) under saturation conditions using murexide as indicator of free Ca^{2+}. The upper curve represents the calcium binding to the peptide with the free carboxyl groups; the lower curve represents the calcium binding to the peptide in which the carboxyl functions are modified with the glycine ethyl ester in the presence of a water-soluble carbodiimide.

the first two fractions, eluted in the void volume of the column, are richer in non-polar residues than the other fractions. The distribution of phenylalanine is different among the various fractions and it is not detectable in fraction IV. Tyrosine is more abundant in peaks I, II and IV than in peaks III and V. Only in these last two fractions are methionine and cystine present. A particular difference is also represented by the high content of glycine and glutamic acid in fraction IV. No tryptophan was detected in any of the fractions.

These observations all demonstrate that the eggshell matrix is a mixture of different proteins which possess an abundance of acidic residues (aspartic and glutamic acid). In addition, from the chemical analyses of the sugars, it must be said that the proteins are accompanied by different quantities of glycosaminoglycans (GAGs). Fractions III and V show a significant amount of glycosaminoglycans, as can be derived from the uronic acid and hexosamine content. Fractions I and II seem to be glycoprotein in nature, as shown by the high neutral sugar and hexosamine content and by the very low quantity of uronic acids. Fraction III is eluted in the region where normally hyaluronic acid appears.

The chemical analyses and the chromatographic separation clearly confirm that the eggshell matrix is composed of proteins, glyco- and proteoglycans, which show different behaviour on the DEAE-cellulose column.

From the amino acid analyses of the alkaline hydrolysate of the eggshell matrix, no compounds have been isolated which could be related to the prescence of γ-carboxyglutamic acid, which has been shown in other calcified tissues[7–11]. The unknown GPX peak observed in the region of the glutamic acid (Fig. 2) is due to a peptide resistant to the alkaline hydrolysis. A particular aspect of this peptide is represented by the amino acid composition. About 50% of the residues consists of aspartic and glutamic acid. The molar ratio of the detected amino acids aspartic acid, threonine, serine, glutamic acid, proline, glycine and alanine is 2:1:3:7:1:3:1, respectively, with a minimum molecular weight of 2158 daltons.

The peptide we have isolated from the alkaline hydrolysis represents from its chemical composition an interesting stage in the process of the calcium ion binding. The study of the calcium ion binding to the peptide GPX demonstrates the importance of the ionized side chain carboxyl groups. In fact more calcium ion binding occurs with increasing pH values (Fig. 6). The ionic nature of the calcium binding is confirmed also by the absence of calcium bound to the peptide in which the carboxyl groups have been previously blocked with the glycine ethyl ester in the presence of water-soluble carbodiimide. This study confirms the previous observations made on eggshell matrix[5] and on elastin[17,19] which have demonstrated the importance of the carboxyl groups in the calcium ion binding. In the particular case of this alkali-resistant peptide the abundance of the aspartic and glutamic acid residues makes this molecule extremely rich in ionizable acidic groups which in turn are responsible for the binding with calcium.

REFERENCES

1 J. R. Baker and D. A. Balch, *Biochem. J.*, 82 (1962) 352–361.
2 R. K. Heaney and D. S. Robinson, *Biochim. Biophys. Acta*, 451 (1976) 133–142.
3 A. S. Cooke and D. A. Balch, *Brit. Poult. Sci.*, 11 (1970) 353–365.

4 G. Von Krampitz, J. Engels, I. Heindl, A. Heinrich, M. Hamm and R. Faust, *Arch. Geflügelkunde*, 6 (1974) 197–205.
5 G. Abatangelo, D. Daga-Gordini, I. Castellani and R. Cortivo, *Calc. Tiss. Res.*, 26 (1978) 247–252.
6 V. R. Meenakshi, G. Donnay, P. L. Blackwelded and K. M. Wilbua, *Calc. Tiss. Res.*, 15 (1974) 31–44.
7 P. V. Hauscka, J. B. Liah and P. M. Gallop, *Proc. Nat. Acad. Sci. U.S.*, 72 (1975) 3925–3929.
8 P. A. Price, J. W. Poser and M. Raman, *Proc. Nat. Acad. Sci., U.S.*, 73 (1976) 3374–3375.
9 J. Stenflo and P. O. Ganrot, *Biochem. Biophys. Res. Commun.*, 50 (1973) 98–104.
10 G. L. Nelsestuen, T. H. Zytkovicz and J. B. Howard, *J. Biol. Chem.*, 249 (1974) 6347–6350.
11 K. King, Jr., *Biochem. Biophys. Acta*, 542 (1978) 542–546.
12 C. Cessi and F. Piliego, *Biochem. J.*, 77 (1960) 508–512.
13 E. A. Davidson, *Methods Enzymol.*, 8 (1966) 55–56.
14 Z. Dische, *J. Biol. Chem.*, 167 (1947) 199–206.
15 T. A. Scott and E. H. Melvin, *Anal. Chem.*, 25 (1953) 1656–1661.
16 L. Warren, *J. Biol. Chem.*, 234 (1959) 1971–1973.
17 G. Abatangelo and D. Daga-Gordini, *Biochem. Biophys. Acta*, 342 (1974) 281–289.
18 D. G. Hoare and D. E. Koshland, *J. Biol. Chem.*, 242 (1967) 2447–2453.
19 G. Abatangelo, D. Daga-Gordini, G. Garbin and R. Cortivo, *Biochim. Biophys. Acta*, 371 (1974) 526–533.

Journal of Chromatography, 237 (1982) 137–143
Elsevier Scientific Publishing Company, Amsterdam — Printed in The Netherlands

CHROM. 14,426

QUANTITATIVE ANALYSIS OF CHENODEOXYCHOLIC ACID AND RELATED COMPOUNDS BY A DENSITOMETRIC THIN-LAYER CHROMATOGRAPHIC METHOD

G. SZEPESI*, K. DUDÁS, A. PAP and Z. VÉGH
Chemical Works of Gedeon Richter, Ltd., Gyömröi u. 19, H-1475 Budapest (Hungary)
and
E. MINCSOVICS and T. TYIHÁK
Research Institute for Medical Plants, Budakalász (Hungary)
(First received July 28th, 1981; revised manuscript received October 1st, 1981)

SUMMARY

A new thin-layer chromatographic (TLC) method was developed for the isolation and determination of chenodeoxycholic acid and related compounds. The separation was performed on pre-coated Kieselgel 60 chromatoplates with chloroform–ethyl acetate–glacial acetic acid–2-methoxyethanol (9:9:2:1). The separated spots were evaluated by densitometry after treatment with *p*-toluenesulphonic acid. The separation of lithocholic, chenodeoxycholic, deoxycholic and cholic acid and their glycine and taurine conjugates was achieved with two chromatographic developments. Overpressured TLC gave a satisfactory separation of bile acids and related compounds by development of a high-performance TLC Kieselgel 60 chromatoplate with a four-component solvent mixture.

INTRODUCTION

Many different thin-layer chromatographic (TLC) systems have been developed for the analysis of bile acids and related compounds (see refs. 1–6 for comprehensive reviews), but the resolution of so-called "critical" pairs is difficult by the methods published earlier[7–11]. The successful separation of deoxycholic and chenodeoxycholic acid and their glycine and taurine conjugates was achieved by Goswami and Frey[12] with six successive chromatographic developments and similar results were subsequently obtained by other authors[13–16]. Reversed-phase partition TLC on octadecyl-bonded silica gel chromatoplates has been successfully applied by Raedsch *et al.*[11] to the separation of individual sulphated bile acid conjugates, but this method cannot be used for the analysis of other conjugates and non-conjugated bile acids. Gas–liquid chromatography (GLC) and high-performance liquid chromatography (HPLC) are less useful for the analysis of bile acids and their conjugates than TLC. The highly polar conjugates are not sufficiently volatile for GLC and the sensitivity of detection is too low for HPLC.

0021-9673/82/0000–0000/$02.75

One of the aims of our work was to develop a TLC method suitable for the analysis of chenodeoxycholic acid in the presence of other bile acids in pharmaceutical raw materials, where the problem is to determine the impurities occurring in low concentrations. The second objective was the separation of bile acids and their glycine and tuarine conjugates, a problem which has not yet been adequately solved. Our third aim was to test the potential of overpressured TLC (OPTLC), a technique which has been recently introduced[17].

Further improvement in separation can be expected from application of the OPTLC technique, which has been recently introduced in the practice of TLC by Tyihák *et al.*[17]. The technique is based on a concept similar to column liquid chromatography; the solvents are passed through an ultramicro chamber by an appropriate pump system and the sorbent layer is completely covered in the chamber with a flexible membrane under an external pressure. In this manner the vapour space over the layer can be excluded, resulting in more reproducible retention, better resolution and faster development compared with classical TLC systems.

EXPERIMENTAL

TLC was performed on pre-coated Kieselgel 60 F_{254} (Merck, Darmstadt, G.F.R.) chromatoplates. For the analysis of chenodeoxycholic acid, chloroform–ethyl acetate–glacial acetic acid–2-methoxyethanol (9:9:2:1) was used as mobile phase.

For the separation of bile acids and conjugates two chromatographic developments were needed. The sample solutions, prepared from the reference substances listed in Table I, were applied twice in 1-cm streaks to the chromatoplate, and solvent A [isooctane–ethyl acetate–glacial acetic acid (5:4:1)] was used for the first development to separate the critical pairs of non-conjugated bile acids. The plate was then dried in a stream of air at room temperature and a narrow channel was cut into the silica gel around the compounds separated by the first development (see Fig. 3). The plate was developed a second time with solvent B [chloroform–*n*-butanol–glacial acetic acid–water (2:16:1:1)].

OPTLC was performed in a Labor MIM (Esztergom-Budapest, Hungary) pressurized ultramicro chamber, the solvents being introduced into the chamber under the flexible membrane by a Micropump Type S13 (Labor MIM). Linear migration of the solvent front in the ultramicro chamber was ensured by impregnating the sides of the layer and by placing a narrow plastic sheet on the layer behind starting line.

The separation was performed on a high-performance TLC (HPTLC) Kieselgel 60 F_{254} chromatoplate with solvent B as the mobile phase.

The separated spots were evaluated by densitometry after spraying with 20% *p*-toluenesulphonic acid, dissolved in sulphuric acid–ethanol (1:1) in the case of chenodeoxycholic acid and 20% aqueous sulphuric acid in the case of bile acids conjugates. The spots were developed by heating the sprayed plates at 120°C for 20 min. For the analysis, a Zeiss PMQ III chromatogram spectrophotometer (Opton, G.F.R.) was used.

All solvents and reagents were of analytical-reagent grade (Reanal, Budapest, Hungary). The non-conjugated bile acids were prepared at the Chemical Works of Gedeon Richter (Budapest, Hungary), and the glycine and taurine conjugates of bile acids were supplied by T. Fehér.

TABLE I

COMPOUNDS INVESTIGATED

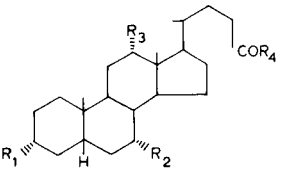

No.	*Compound*	R_1	R_2	R_3	R_4*
I	Lithocholic acid	OH	H	H	OH
II	Deoxycholic acid	OH	H	OH	OH
III	Chenodeoxycholic acid	OH	OH	H	OH
IV	Cholic acid	OH	OH	OH	OH
V	Glycolithocholic acid	OH	H	H	Gly
VI	Glycochenodeoxycholic acid	OH	OH	H	Gly
VII	Glycodeoxycholic acid	OH	H	OH	Gly
VIII	Taurolithocholic acid	OH	H	H	Tau
IX	Glycocholic acid	OH	OH	OH	Gly
X	Taurochenodeoxycholic acid	OH	OH	H	Tau
XI	Taurodeoxycholic acid	OH	H	OH	Tau
XII	Taurocholic acid	OH	OH	OH	Tau

* Gly = $-NH-CH_2-COOH$; Tau = $-NH-CH_2-CH_2-SO_3H$.

RESULTS AND DISCUSSION

The compounds investigated are listed in Table I.

For the detection of other bile acids in chenodeoxycholic acid, various solvent systems were tried. The chromatograms obtained with three different solvents are shown in Fig. 1.

Chloroform–ethyl acetate–glacial acetic acid–2-methoxyethanol (9:9:2:1) provides the best overall separation, although better resolution can be obtained for deoxycholic acid and chenodeoxycholic acid by using solvent A, previously reported by Fehér and Kazik[7]. Fig. 1 shows that one of the unknown impurities (X_3) is separated satisfactorily from cholic acid only by solvent C (Fig. 2). Fig. 2 shows that a satisfactory separation of the impurities occurring in low concentrations can be achieved when 1 mg of the sample is applied to the plate.

None of the three eluent systems mentioned above can be used for the separation of different conjugates of bile acids because these compounds stay in the neighbourhood of the origin. The less polar non-conjugated bile acids and their more polar glycine and taurine conjugates can be resolved when two eluent systems of different polarities are used. The basic concept is illustrated in Fig. 3 where chromatograms obtained for a model mixture of all the compounds listed in Table I are shown.

The sample solution is applied twice to the same chromatoplate. For the first chromatographic development solvent A is used. This solvent system permits the separation of compounds I–V, while the other compounds stay near the origin. After this development the compounds separated are isolated from the solvents to be used

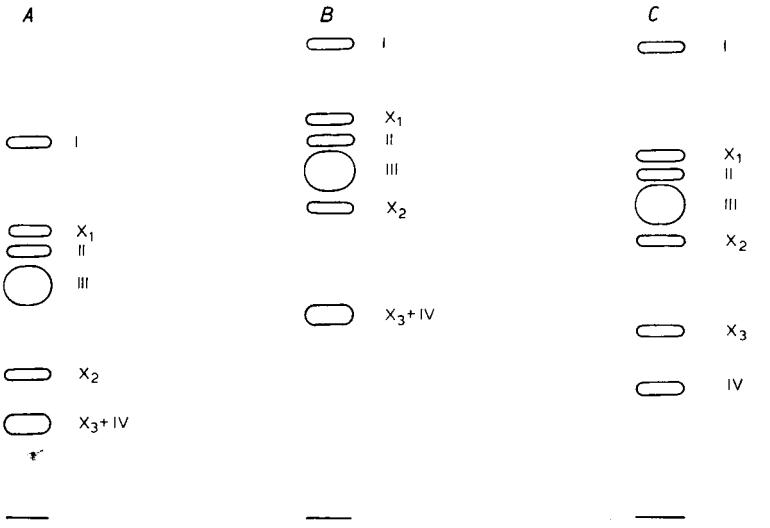

Fig. 1. Separation of chenodeoxycholic acid and related compounds. Plate: Kieselgel 60 F_{254}. Solvent A, isooctane–ethyl acetate–glacial acetic acid (5:4:1); solvent B, dichloromethane–ethyl acetate–glacial acetic acid–2-methoxyethanol (9:9:2:1); solvent C, chloroform–ethyl acetate–glacial acetic acid–2-methoxyethanol (9:9:2:1). Application: 1000–1000 μg of the sample in 1-cm streaks. Detection: 20% *p*-toluenesulphonic acid in sulphuric acid–ethanol (1:1), heated at 120°C for 20 min. Compounds I–IV, see Table I; X_1, X_2, X_3, unknown.

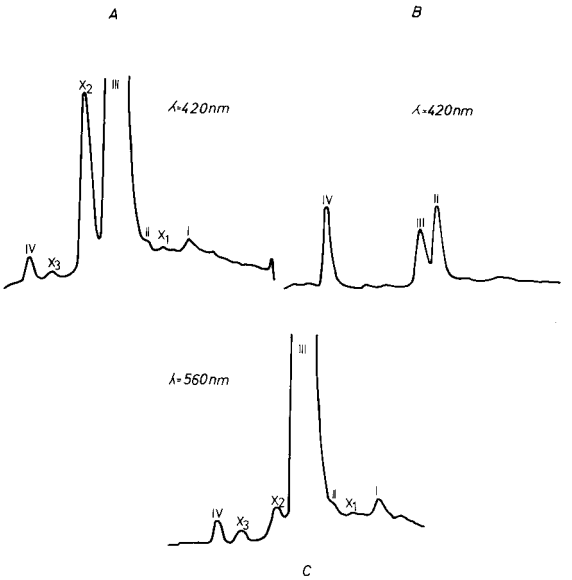

Fig. 2. Densitogram of the separated compounds. Developed with solvent C and assayed with a Zeiss PMQ III chromatogram spectrophotometer at 420 nm (A, B) and 560 nm (C). Application: 1000–1000 μg of the sample (Fig. 2A and 2C) and 10–10 μg of reference compounds (Fig. 2B). For other conditions see Fig. 1.

in the second development by cutting a narrow channel into the silica gel. The more polar compounds (VI–XII) are then separated by a second development with solvent B. No separation of compounds II and III, however, can be achieved owing to the more polar solvent system used.

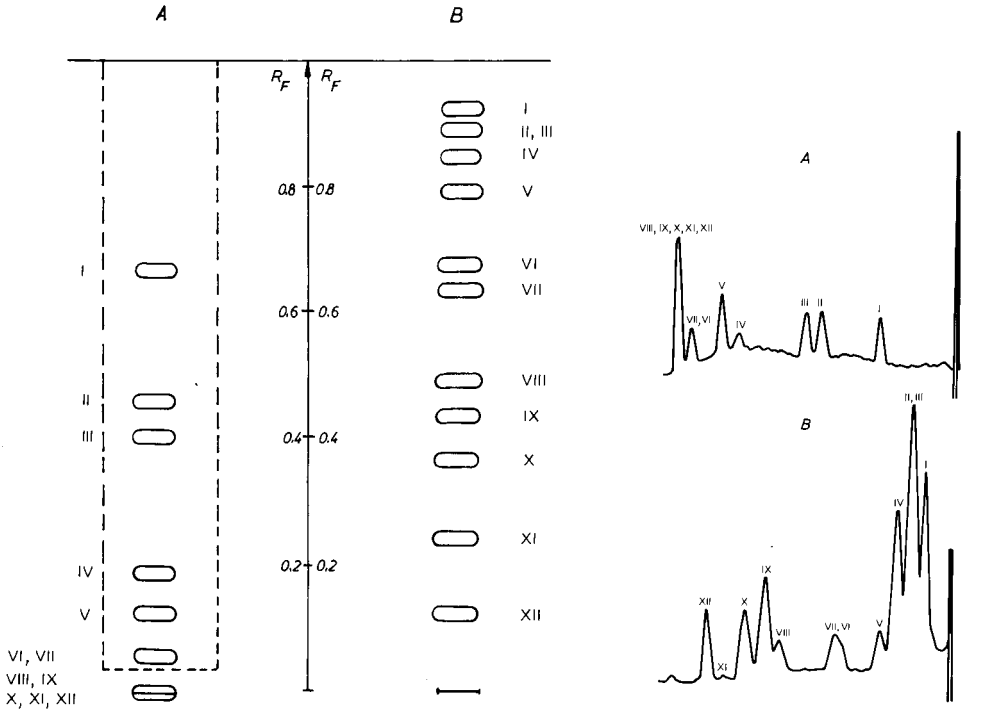

Fig. 3. Chromatogram of bile acids and their conjugates. Solvent A, isooctane–ethyl acetate–glacial acetic acid (5:4:1); solvent B, chloroform–1-butanol–glacial acetic acid–water (2:16:1:1) after first development with solvent A. Detection: 20% sulphuric acid, heated at 120°C for 20 min. For other conditions see Fig. 1. For compounds see Table I.

Fig. 4. Densitogram of bile acid conjugates. Densitometer, Zeiss PMQ III chromatogram spectrophotometer at 366 nm. For other conditions see Fig. 3.

Fig. 4 shows the densitogram of the separated compounds. In Fig. 4B the peaks of compounds VI and VII as well as those of compounds X and XI are not resolved, but these compounds can be distinguished at 366 nm. The separation of compounds investigated by OPTLC using solvent B is shown in Fig. 5.

Comparing the densitograms in Figs. 3 and 5, it can be concluded that the separation efficiency is improved by using OPTLC and that a satisfactory separation is achieved for the "critical" pairs of conjugates. The R_F values of the compounds obtained in different solvent systems are summarized in Table II.

CONCLUSIONS

The separation of chenodeoxycholic acid and related compounds has been studied by TLC. For detecting the presence of impurities in bulk chenodeoxycholic

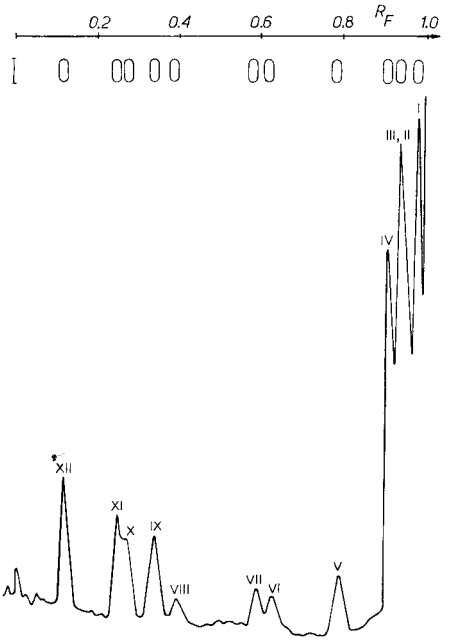

Fig. 5. Separation of bile acids and their conjugates by OPTLC. Labor MIM pressurized ultramicro chamber with Micropump S13, Zeiss PMQ III chromatogram spectrophotometer at 366 nm. Mobile phase, chloroform–1-butanol–glacial acetic acid–water (2:16:1:1); flow-rate 26 ml/h; pressure 1.2 MPa; 16 cm development in 28 min; plate, HPTLC silica gel 60 F_{254} with impregnated edges. For compounds see Table I.

TABLE II

R_F VALUES OF THE COMPOUNDS INVESTIGATED

Plates: 1–4, Kieselgel 60 F_{254}; 5, HPTLC silica gel 60 F_{254}. Solvents: 1, dichloromethane–ethyl acetate–glacial acetic acid–2-methoxyethanol (9:9:2:1); 2, chloroform–ethyl acetate–glacial acetic acid–2-methoxyethanol (9:9:2:1); 3, isooctane–ethyl acetate–glacial acetic acid (5:4:1); 4 and 5, solvent D, chloroform–1-butanol–glacial acetic acid–water (2:16:1:1). Other conditions: 1–3, see Fig. 1; 4, see Fig. 3; 5, see Fig. 5. Compounds I–XII, see Table I; X_1, X_2, X_3, unknown.

No.	*1*	*2*	*3**	*4***	*5****
I	0.84	0.83	0.66	0.92	0.98
X_1	0.70	0.71	0.50		
II	0.66	0.64	0.46	0.89	0.94
III	0.62	0.59	0.41	0.89	0.94
X_2	0.54	0.40	0.24		
X_3	0.35	0.26	0.16		
IV	0.35	0.16	0.16	0.84	0.90
V			0.13	0.79	0.78
VI			0.05	0.67	0.61
VII			0.05	0.63	0.58
VIII			0	0.48	0.38
IX			0	0.43	0.33
X			0	0.36	0.26
XI			0	0.25	0.23
XII			0	0.15	0.11

* TLC, after first development.
** TLC, after second development.
*** OPTLC.

acid, solvent C was found to be optimal. For the separation of bile acids and their glycine and taurine conjugates, the OPTLC technique with a HPTLC silica gel chromatoplate and solvent D was found to be optimal. The use of classical TLC can also resolve the conjugated and non-conjugated bile acids, but the "critical" pairs of conjugated bile acids (glycochenodeoxycholic acid–glycodeoxycholic acid and taurochenodeoxycholic acid–taurodeoxycholic acid) can be distinguished only at 366 nm. The proposed method seems to be promising for clinical and biological analysis because a satisfactory separation for non-conjugated and conjugated bile acids was obtained.

ACKNOWLEDGEMENT

We are grateful to Dr. T. Fehér (Department of Medicine, Semmelweis Medical University, Budapest, Hungary) for placing the glycine and taurine conjugates at our disposal.

REFERENCES

1 A. F. Hofmann, in A. T. James and L. J. Morris (Editors), *New Biochemical Separations*, Van Nostrand, New York, 1964, pp. 261–282.
2 P. Eneroth, in G. V. Marinetti (Editor), *Lipid Chromatographic Analysis*, Vol. 2, Marcel Dekker, New York, 1969, pp. 146–186.
3 R. Neher, in E. Stahl (Editor), *Thin Layer Chromatography*, Springer, Berlin, 1969. pp. 351–354.
4 R. H. Palmer, *Methods Enzymol.*, 15 (1969) 280.
5 E. Heftmann, *Chromatography of Steroids*, Elsevier, Amsterdam, 1976, pp. 71–77.
6 S. Görög, *Quantitative Analysis of Steroids*, Elsevier, Amsterdam, and Akadémiai Kiadó, Budapest, in press.
7 T. Fehér and M. Kazik, *Magyar Kém. Foly.*, 78 (1972) 186.
8 T. Fehér, J. Papp and M. Kazik, *Z. Klin. Chem. Klin. Biochem.*, 11 (1973) 376.
9 T.-L. Huang and B. L. Nichols, *J. Chromatogr.*, 101 (1974) 235.
10 M. N. Chavez, *J. Chromatogr.*, 162 (1979) 71.
11 R. Raedsch, A. F. Hofmann and K. Tserng, *J. Lipid Res.*, 20 (1979) 796.
12 S. K. Goswami and C. F. Frey, *J. Chromatogr.*, 145 (1978) 147.
13 P. Back, *Z. Klin. Chem. Klin. Biochem.*, 7 (1969) 365.
14 G. Parmentier and H. Eyssen, *J. Chromatogr.*, 152 (1978) 285.
15 A. K. Batta, G. Salen and S. Shefer, *J. Chromatogr.*, 168 (1979) 557.
16 W. A. Taylor, K. G. Blass and C. S. Ho, *J. Chromatogr.*, 168 (1979) 501.
17 E. Tyihák, E. Mincsovics and H. Kalász, *J. Chromatogr.*, 174 (1979) 75.

Journal of Chromatography, 237 (1982) 144–147
Elsevier Scientific Publishing Company, Amsterdam – Printed in The Netherlands

CHROM. 14,459

Note

Separation of aromatic compounds on phenyl-bonded silica

ROGER M. SMITH
Department of Chemistry, University of Technology, Loughborough, Leicestershire LE11 3TU (Great Britain)
(Received October 23rd, 1981)

Many bonded phases have been synthesised for use in liquid chromatography and a number are available commercially. Of these C_{18} (ODS), C_2, C_6, C_8 and CN-silica are the most widely used. A number of suppliers also offer phenyl bonded phases[1] but these have attracted little attention. The majority of applications have been in the separation of peptides (for example ref. 2) and some work has been carried out on pharmaceuticals such as propanolol[3]. Generally phenyl phases have been regarded as being more polar than ODS-silica.

As part of a study into the use of alkylarylketones as retention index standards[4] and of their application to determining retention constants for stationary phases[5], it was found that the indices of a set of standards varied markedly between alkyl-bonded and phenyl-bonded phases. In particular toluene appeared to be repelled from the stationary phase. As this was contrary to the anticipated affinity of phenyl phases for aryl-hydrocarbons the present study was undertaken to examine the interaction of alkylbenzenes in greater detail.

EXPERIMENTAL

Conditions were as described in ref. 4. Alkylbenzene standards were as described in ref. 7.

RESULTS AND DISCUSSION

In gas–liquid chromatography (GLC), stationary phases incorporating phenyl groups such as OV-17 or SE-52 are frequently chosen for the analysis of aromatic compounds, because they are considered to be more compatible with the samples than dimethyl-silicones such as OV-1 or SE-30. It was therefore expected that similar behaviour might be expected on high-performance liquid chromatography (HPLC), with neutral aromatic compounds being strongly retained on phenyl-bonded silica columns. However, in the recent retention index study the opposite seemed to be found, toluene having a lower retention index on Spherisorb phenyl than on ODS Hypersil[4] (Table I). Thus, compared to the alkylarylketones used as a reference scale, toluene appears to be less soluble in a phenyl-bonded phase than in a hydrocarbon phase. There were also differences in the indices of the other test compounds particu-

0021-9673/82/0000–0000/$02.75

larly of the more polar compounds *p*-cresol and benzyl alcohol which was ascribed to the increased polarity of the phase. Except for phenetole the non-polar compounds showed only small changes.

TABLE I

RETENTION INDICES OF STANDARD COMPOUNDS ON ODS-HYPERSIL AND SPHERISORB PHENYL*

Compound	*Retention index***	
	ODS-Hypersil (methanol–water, 70:30)	*Spherisorb phenyl (methanol–water, 30:70)*
Toluene	1047 (k' = 2.31)	745 (k' = 2.08)
Hexan-2-one	849	711
Benzylalcohol	735	543
2-Phenylethanol	795	625
p-Cresol	818	618
Nitrobenzene	869	802
Methylbenzoate	926	848
Phenetole	1022	809

* From ref. 4, mobile phases selected so that k' of toluene are similar.
** Alkylarylketone scale.

This marked relative change in the retention of arylhydrocarbons had also been noted in a study of nitro-aromatic compounds on phenyl ether-, phenyl- and ODS-bonded phases[6]. On ODS-silica, benzene (capacity factor, k' = 8.18) was eluted after the mono- to trinitrobenzenes, (k' = 6.95–3.13) whereas on phenyl-silica benzene (k' = 1.28) was eluted before the mono- to trinitrobenzenes (k' = 3.48–1.77). On the aryl-ether phase the order of elution was reversed compared to ODS-silica and a charge-transfer interaction was thought to be present between the column and the nitrobenzenes.

In the present study the high eluent polarity needed to retain toluene on the phenyl phase was also unexpected as it was similar to that required for a C_2 (SAS-Hypersil) column[4].

In order to study the interaction further an earlier study of the alkylbenzenes on alkyl-bonded silicas[7] was extended to the phenyl-bonded phase (Table II).

Using methanol–water (30:70) as eluent gave results similar to those obtained previously[4], toluene retention index = 739. The *n*-alkylbenzenes showed a good correlation between carbon number and log k' with a similar slope to the reference scale (Table III). Similar results were obtained for acetonitrile–water (10:90) as eluent except that the retention indices were all higher. They increased further if acetonitrile–water (20:80) was used. These changes in indices were much greater than those found previously for the test compounds when the solvent was changed from 20–80% methanol in water[4]. However in their study using an alkan-2-one scale, Baker and Ma[8] found a marked decrease for andesterone of about 100 units between 10 and 20% acetonitrile in water on μBondapak CN.

Thus, although retention indices are apparently not very sensitive to solvent

TABLE II

CAPACITY FACTORS AND RETENTION INDICES (I) OF ARYLHYDROCARBONS ON A SPHERISORB PHENYL COLUMN USING DIFFERENT SOLVENTS

Compound	*Solvent*					
	Methanol–water (30:70)		*Acetonitrile–water (10:90)*		*Acetonitrile–water (20:80)*	
	k'	I	k'	I	k'	I
Benzene	1.08	634	1.69	668	1.69	776
Toluene	1.69	734	3.23	785	2.85	881
Ethylbenzene	2.69	833	5.92	895	4.77	986
o-Xylene	2.54	821			4.38	967
m-Xylene	2.69	833			4.54	976
p-Xylene	2.69	833			4.38	967
Propylbenzene	4.69	952	12.5	1030	8.54	1103
Isopropylbenzene	4.00	918			7.54	1078
1,2,3-Trimethylbenzene	3.92	914			6.54	1049
1,2,4-Trimethylbenzene	3.92	914			7.00	1064
1,3,5-Trimethylbenzene	4.08	922			7.54	1078
n-Butylbenzene	8.54	1079	28.2	1177	15.6	1225
Isobutylbenzene	7.62	1054			14.1	1205
sec.-Butylbenzene	7.23	1043			13.1	1190
tert.-Butylbenzene	5.92	1001			11.0	1155
1,2,3,4-Tetramethylbenzene	5.85	999			9.92	1134

composition changes, when the solvent polarity changes markedly as it does at the ends of the composition scale, quite large index shifts can be found, particularly if the sample functional group is different to that in the standard.

Although it was hoped that the phenyl phase interactions would lead to a greater discrimination between the alkylbenzenes, the order of elution and the resolutions of isomeric compounds were similar to those obtained previously on alkyl bonded silica[7].

TABLE III

CORRELATION OF LOG k' WITH CARBON NUMBER (C_n) FOR ALKYLARYLKETONE STANDARDS AND *n*-ALKYLBENZENES ON SPHERISORB PHENYL

Compounds	*Eluents*		
	Methanol–water (30:70)	*Acetonitrile–water (10:90)*	*Acetonitrile–water (20:80)*
Alkylarylketones			
Correlation*	0.9997	0.9993	0.9998
Slope	$2.042 \cdot 10^{-3}$	$2.403 \cdot 10^{-3}$	$2.152 \cdot 10^{-3}$
n-Alkylbenzenes			
Correlation	0.9978	0.9981	0.9994
Slope	$2.24 \cdot 10^{-3}$	$3.033 \cdot 10^{-3}$	$2.409 \cdot 10^{-3}$

* For $\log k' = a\,(C_n \times 100) + b$. Using values from Table II.

ACKNOWLEDGEMENT

I thank the S.E.R.C. for financial assistance.

REFERENCES

1 R. E. Majors, *J. Chromatogr. Sci.*, 18 (1980) 488.
2 W. S. Hancock, C. A. Bishop, L. J. Meyer, D. R. K. Harding and M. T. W. Hearn, *J. Chromatogr.*, 161 (1978) 291.
3 R. L. Nation, G. W. Peng and W. L. Chiou, *J. Chromatogr.*, 145 (1978) 429.
4 R. M. Smith, *J. Chromatogr.*, 236 (1982) 313.
5 R. M. Smith, *J. Chromatogr.*, 236 (1982) 321.
6 T. H. Mourey and S. Siggia, *Anal. Chem.*, 51 (1979) 763.
7 R. M. Smith, *J. Chromatogr.*, 209 (1981) 1.
8 J. K. Baker and C.-Y. Ma, *J. Chromatogr.*, 169 (1979) 107.

Journal of Chromatography, 237 (1982) 148–150
Elsevier Scientific Publishing Company, Amsterdam — Printed in The Netherlands

CHROM. 14,495

Note

Adsorption of chlorinated phenols on Sephadex LH-20

DAN JOHNELS*, ULF EDLUND and SVANTE WOLD
Department of Organic Chemistry, Institute of Chemistry, Umeå University, S-901 87 Umeå (Sweden)
and
CARL-AXEL NILSSON
National Board of Occupational Safety and Health, Department of Occupational Health, S-901 85 Umeå (Sweden)
(Received October 27th, 1981)

This study of the retention behaviour of chlorophenols was stimulated by our interest in multivariate structure–activity relationships of hazardous environmental compounds and a search for appropriate molecular descriptors in these studies.

Using Sephadex as adsorbent several investigations have been undertaken, eluting phenols and other aromatic compounds, in order to assess a valid retention mechanism. Determann and Walter suggested that the ether linkage between the dextran chains is the preferred site of adsorption[1]. However, a complete understanding of the retention mechanism of these compounds on dextran gels is still lacking.

Brook and Housley, and later Brook and Munday, proposed that hydrogen bonding is the preferred mode of interaction, except for halogenated phenols, where the adsorption is governed by direct interaction between the halogen substituents and the dextran chains[2,3].

A contradictory proposal has been advanced by Streuli and Orloff, who claimed that phenols are adsorbed through π-bonding and hydrogen bonding[4]. De Ligny states that the adsorption of phenols is controlled not by hydrogen bonding, but by a phenol–dextran π-bonding[5].

On several occasions deviating behaviour of chlorophenols has been noted[3]. However, so far only a limited number of chlorophenols have been studied. Therefore, in the present study we have included all possible isomers of chlorophenols and they were all studied on Sephadex LH-20, using chloroform as eluent.

MATERIALS AND METHODS

The chlorophenols were eluted through a 14.2 × 2.45 cm column packed with Sephadex LH-20, using chloroform as eluent. The flow-rate was 0.75 ml/min. A LKB 2089 UVICORD III was used as detector (275 nm). A 100-μl volume of the chlorophenol was injected on to the column, and the concentration was 0.3 M except for pentachlorophenol where the concentration was 0.24 M owing to restricted solubility. The retention was characterized by the retention volume V_R. The reported V_R values are calculated means from three independent runs.

0021-9673/82/0000–0000/$02.75

The chlorophenols were commercially available. The chloroform was obtained from May & Baker (Dagenham, Great Britain) and redistilled before use. Sephadex LH-20 (Batch No 2167) was purchased from Pharmacia (Uppsala, Sweden).

The IR measurements have been reported previously by Perelygin and Akhunov[6]. They used carbon tetrachloride as solvent and acetonitrile as hydrogen acceptor.

RESULTS AND DISCUSSION

V_R and IR data ($\Delta\nu/\nu$) are listed in Table I. The correlation between V_R and $\Delta\nu/\nu$ is further illustrated in Fig. 1.

TABLE I

RETENTION VOLUMES (V_R) AND PROTON-DONATING ABILITIES ($\Delta\nu/\nu$) OF THE CHLOROPHENOLS

Chlorine substitution	*No.*	V_R/ml	$\Delta\nu/\nu$*
2,6	1	87	0.0594
2,4,6	2	113	0.0642
2,3,6	3	113	0.0651
2,3,4,6	4	137	0.0696
2,3,5,6	5	138	–
2,3,4,5,6	6	163	0.0752
2	7	122	0.0538
2,3	8	166	–
2,4	9	175	0.0589
2,5	10	196	0.0609
2,3,4	11	218	0.0647
2,3,5	12	257	–
2,4,5	13	266	0.0652
2,3,4,5	14	309	–
–	15	368	0.0463
4	16	494	0.0507
3	17	544	0.0533
3,4	18	652	0.0572
3,5	19	683	0.0603
3,4,5	20	757	0.0634

* Ref. 6.

A separation into three distinct classes is quite obvious and caused by the actual type of *ortho* substitution (an identical correlation was observed if we used the $\Delta\delta_{OH,dil}$ NMR differentials, as expected)[7]. A correlation with $\Delta\nu/\nu$ is observed in each class, *i.e.* increasing proton-donating ability of the phenol causes a larger V_R value. Any other physical interaction correlated with $\Delta\nu/\nu$ is of course possible, but we have chosen the proton-donating ability of the phenol.

If the retention was dominated by a π-bonding interaction, we would observe lower V_R values by increasing the degree of chlorine substitituion, because the π-bonding ability is expected to decrease if electron-accepting substituents are intro-

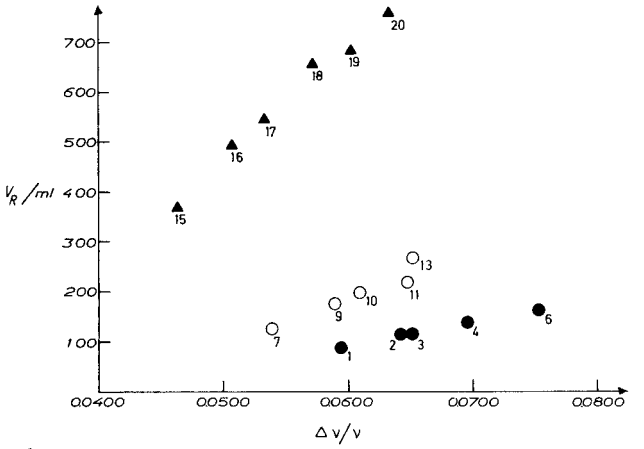

Fig. 1. Retention volume V_R as a function of the proton-donating ability $\Delta\nu/\nu$. ▲, no *ortho* chlorines; ○, one *ortho* chlorine; ●, two *ortho* chlorines.

duced[8]. As is evident from Fig. 1 this is not the case. Thus π-bonding or variation in π-bonding is hardly important in our chromatographic system.

If we consider direct gel–substituent interactions, as earlier proposed[3], this could possibly account for the behaviour in each class, but the dependence of *ortho* substitution would not be so dramatic.

However, the correlation between V_R and the proton-donating ability is not necessarily valid under other conditions. It has recently been observed[9] that by changing the system to silica gel/dichloromethane–hexane (40:60) one obtains a reasonable correlation with a parameter inversely proportional to $\Delta\nu/\nu$. This observation supports Streuli's idea that several retention mechanisms can be operative for a given compound and the relative importance of each is determined by the actual experimental conditions[10].

For the general case of substituted phenols at least two mechanisms exist, a proposal that is supported by the data of Haglund[11], but this conclusion is not reached in her work. If direct gel–substituent and/or gel–π interactions are excluded, the retention behaviour is closely correlated with the hydrogen-bonding ability[11].

REFERENCES

1 H. Determann and I. Walter, Nature (London), 219 (1968) 604.
2 A. J. W. Brook and S. Housley, J. Chromatogr., 41 (1969) 200.
3 A. J. W. Brook and K. C. Munday, J. Chromatogr., 47 (1970) 1.
4 C. A. Streuli and M. Orloff, J. Chromatogr., 62 (1971) 73.
5 C. L. De Ligny, J. Chromatogr., 172 (1979) 397.
6 I. S. Perelygin and T. F. Akhunov, Opt. Spectrosc., 30 (1971) 367.
7 D. P. Eyman and R. S. Drago, J. Amer. Chem. Soc., 88 (1966) 1617.
8 I. S. Perelygin and T. F. Akhunov, Opt. Spectrosc., 33 (1972) 132.
9 A. Bjørseth and K. Ugland Sogn, personal communication.
10 C. A. Streuli, J. Chromatogr., 56 (1971) 225.
11 Å. Ch. Haglund, J. Chromatogr., 156 (1978) 317.

Journal of Chromatography, 237 (1982) 151–154
Elsevier Scientific Publishing Company, Amsterdam — Printed in The Netherlands

CHROM. 14,470

Note

Infrared detection of organometallic compounds separated by high-performance liquid chromatography

MICHAEL COOKE* and NORMAN R. GODFREY
The Department of Inorganic Chemistry, The University of Bristol, Bristol BS8 1TS (Great Britain)
(Received October 15th, 1981)

Although high-performance liquid chromatography (HPLC) has been used to separate metal carbonyl compounds for a number of years this technique is still not widely used by synthetic chemists. Preparative HPLC has been used to isolate new compounds[1] containing the tricarbonylchromium moiety. Analytical HPLC has been used to monitor the progress of reactions of tricarbonyl(diene)iron compounds[2]. The technique has proved capable of rapidly separating *cis/trans* and *endo/exo* isomers[3]. Both normal-phase[3] and reversed-phase[4] modes of chromatography have been employed. For all these studies detection of column eluates was by absorption in the ultraviolet (UV) region.

Of the many types of detector available to detect column eluates from HPLC separations those based on the absorption of radiation receive the most widespread use and the commonest of these is the UV detector. Providing that a compound possesses a reasonably good chromophore ($\varepsilon > 10^3$ l mol^{-1} cm^{-1}) detection by monitoring a specific wavelength ($\lambda_{max.}$) in the UV region is possible. However, the broadness of absorption bands in the UV effectively precludes the selective or specific detection of compounds of interest. Thus, for example, the isolation of a component of interest from a mixture by selectively detecting it in a preparative LC system is difficult to achieve if detection in the UV is used. The lack of specificity of UV spectra is clearly demonstrated in Table I which lists details of the UV spectra of several ruthenium carbonyl compounds. There is little variation in $\lambda_{max.}$ between these compounds and the broadness of the bands means that all compounds would respond to detection anywhere in the range 210 to 260 nm. (Note: the values of $\lambda_{max.}$ quoted are those associated with the polynuclear ruthenium moiety and not those which may be attributed to the organic fragment.)

In contrast infrared (IR) spectroscopy offers considerable potential as a selective detection technique because of the relatively narrow band width of IR absorption bands. This particularly applies to functional groups which are characterised by strong bands, for example $\gamma_{C\equiv O}$, $\gamma_{C\equiv N}$ and γ_{B-X}. Thus monitoring of column eluates in the IR region at a selected frequency characteristic of a particular compound or functional group allows detection of that compound and discrimination against other components present in the mixture. We now report briefly on our studies using an IR spectrophotometer for the selective detection of organometallic compounds separated by HPLC.

0021-9673/82/0000–0000/$02.75

TABLE I

UV SPECTRAL DATA OF POLYNUCLEAR RUTHENIUM CARBONYL COMPOUNDS

Compound No.	*Compound*	$\lambda_{max.}$ *(nm)*	$\varepsilon_{max.}$ *(l mol^{-1} cm^{-1})*
1	$Ru_3(CO)_{12}$	238	14,230
2	$[(CH_3)_3Si]_3C_8H_3Ru_3(CO)_8$	222	19,150
3	1-$[(CH_3)_3Si]C_8H_5Ru_3(CO)_8$	222	17,250
4	2-$[(CH_3)_3Si]C_8H_5Ru_3(CO)_8$	222	19,050
5	$(CH_3)_3SiC_8H_7Ru_2(CO)_5$	234	6,540

Compounds were chromatographed on a silica (10 μm) column (25 cm × 4 mm I.D.) and eluted with hexane at 2 ml min^{-1}. The detection wavelength was 240 nm. A typical separation is shown in Fig. 1. The column contained approximately 2700 effective theoretical plates.

To detect compounds by IR spectroscopy the sample cell of a conventional IR spectrophotometer was modified to reduce its volume to *ca.* 100 μl and to permit the column eluate to flow through the cell whilst it was located in the spectrophotometer. The instrument was operated in the single-beam mode at a series of a pre-selected frequencies. Unfortunately the modified cell permitted only a low energy transmis-

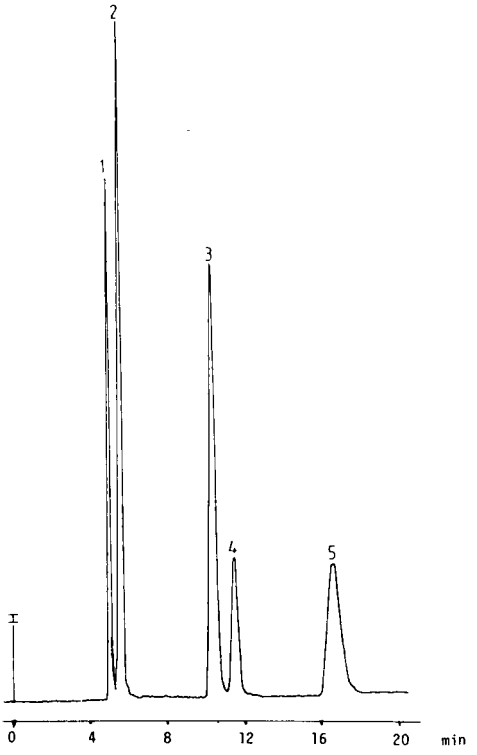

Fig. 1. Separation of ruthenium carbonyl compounds on 10-μm silica. Eluent: hexane, 2 ml min^{-1}. Detector wavelength 240 nm. For peak identification see Table I.

TABLE II

DETECTOR FREQUENCIES FOR IR MONITORING OF COLUMN ELUATES

*Chromatogram code**	*Wavenumber (cm^{-1})*	*Associated compounds*
A	1975	5
B	2010	2, 3, 4, 5
C	2030	1, 2, 3, 4
D	2060	1
E	2080	2, 3, 4

* F = 240 nm, UV detection.

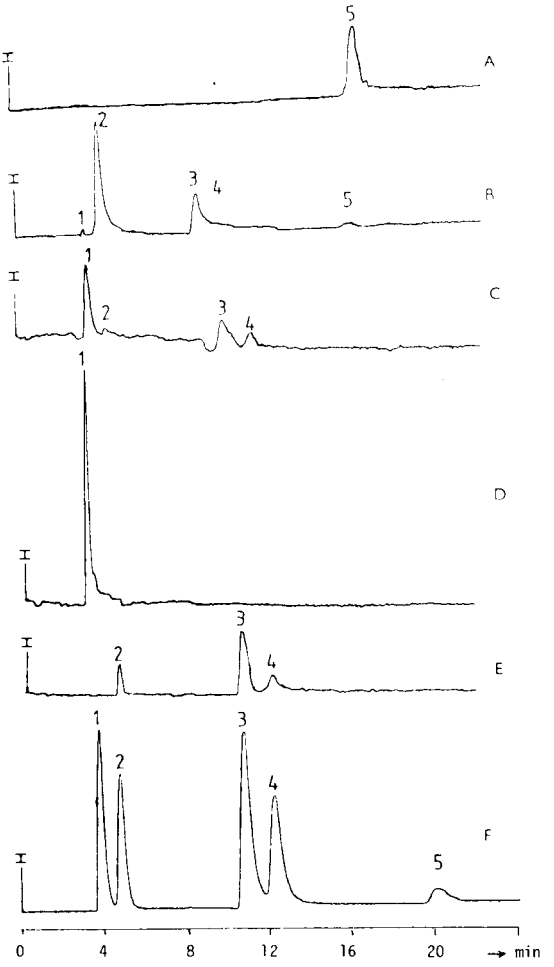

Fig. 2. IR detector response (A–E) for various frequencies and UV detector response (F) to polynuclear ruthenium carbonyl compounds separated by HPLC.

sion and therefore a low signal-to-noise ratio resulted. This modified IR detector was placed in series after the UV detector. Column eluates were thus detected firstly in the UV region and secondly in the IR region. A dual-pen recorder allowed the simultaneous monitoring of both responses.

Table II lists the pre-selected frequencies used together with the compounds which are associated with absorption at the particular wavelength. Fig. 2 summarises the results obtained when a mixture of the five carbonyl compounds was chromatographed and detected at various points in the IR spectrum.

In spite of the poor performance of the IR detector discrimination between the compounds was achieved. For example, monitoring the column eluate at 1975 cm^{-1} (trace A), detects only the compound 5 [$(CH_3)_3SiC_8H_7Ru_2(CO)_5$]. This absorption is associated with the bridging carbonyl group present in this compound. In contrast, monitoring at 2080 detects only trimethylsilyl-substituted pentalene compounds (2, 3 and 4) bonded to an $-Ru_3(CO)_8$ fragment. Perhaps the clearest example of selective detection occurs when the column eluate is monitored at 2060 cm^{-1} (trace D). For this case only $Ru_3(CO)_{12}$ (compound 1) is detected. Thus is clear that IR detection in LC although less sensitive than UV detection, can be used to selectively detect discrete components in a complex mixture. For a situation where detector sensitivity is not important IR detection provides a powerful tool for the isolation of specific compounds from complex mixtures by preparative or sem-preparative HPLC. By this technique interference from other, unwanted, compounds present in the mixture can be avoided.

ACKNOWLEDGEMENT

We thank Dr. S. A. R. Knox, University of Bristol, for the gift of pentalene complexes.

REFERENCES

1 S. A. Gardner, R. J. Seyler, H. Veening and B. R. Willeford, *J. Organomet. Chem.*, 60 (1973) 271.
2 R. E. Graf and C. P. Lillya, *J. Organomet. Chem.*, 47 (1973) 413.
3 D. G. Gresham, C. P. Lillya, P. C. Uden and F. H. Walters, *J. Organomet. Chem.*, 142 (1977) 123.
4 C. H. Gast, F. Nooitgedacht and J. C. Kroak, *J. Organomet. Chem.*, 184 (1980) 221.

Journal of Chromatography, 237 (1982) 155–158
Elsevier Scientific Publishing Company, Amsterdam — Printed in The Netherlands

CHROM. 14,574

Note

Studies of barbiturate degradation following methylation with dimethyl sulfate

ROBERT D. BUDD
L.A. County Medical Examiner-Coroner, Los Angeles, CA 90033 (U.S.A.) and Rancho Los Amigos Hospital, Downey, CA 90242 (U.S.A.)*
(Received November 24th, 1981)

Barbiturates are frequently converted to their dimethyl derivatives for either more ready and improved gas chromatographic analyses[1] or as part of a gas chromatographic confirmation procedure[2–9]. Methylation with dimethyl sulfate has been found to be easily done and to yield quite clean chromatograms, making it superior to other methylating reagents and techniques[2].

In our laboratory, methylation is done by adding 1 ml of carbonate buffer and 0.1 ml of dimethyl sulfate to barbiturate extraction residues. The mixture is heated in a 75–85°C water bath in an open tube, which is occasionally vortexed until the dimethyl sulfate layer has disappeared, signalling completion of the methylation. The tube is then removed from the water bath and allowed to cool in a cold water bath. The solution is then extracted with carbon tetrachloride and an aliquot of the extract is injected into a gas chromatograph to confirm the presence of barbiturates found in our free barbiturate screening procedure[8–9].

This methylation procedure is performed on 20–50 samples per day. Occasionally we have found that quality-control samples that screened positive as free barbiturates for short- and intermediate-acting barbiturates, gave negative or very weak results as methylated derivatives; the internal standard was present but not the barbiturate(s) that was originally found and supposed to be there. When this had happened, it has been found that the tubes had been left in the water bath for a period of time after methylation was completed. This result has prompted us to intiate this study of the methylation procedure. We have sought to ascertain the extent of the adverse affects of over-heating upon barbiturate solutions left sitting in the hot water bath after methylation has been completed.

EXPERIMENTAL

Reagents

Dimethyl sulfate and carbon tetrachloride were used as received. The barbiturate solution consisted of 1 *N* sodium carbonate solution containing 15 μg/ml of each barbiturate: amobarbital, butabarbital, ibomal, pentobarbital, phenobarbital, and secobarbital.

0021-9673/82/0000–0000/$02.75

Chromatography

Gas chromatographic determinations were performed on a Hewlett-Packard Model 1500 gas chromatograph equipped with a flame ionization detector and a 1.83 m × 2 mm I.D. glass column packed with 3% OV-1 on Chromosorb W run at 170°C.

Methylation

Open-tube methylation. A 1-ml volume of barbiturate solution and 0.1 ml of dimethyl sulfate were added to a conical centrifuge tube. The tube was then placed in a 75°C water bath, and vortexed every few seconds until the dimethyl sulfate layer disappeared (completion of methylation). At that point the time was noted. The tube was left in the water bath for the desired amount of time (0, 10, 25, 45, or 60 min), after which it was removed, placed in an ice–water bath for 3 min, and then extracted with 0.1 ml of carbon tetrachloride. An aliquot of the organic layer was then chromatographed and the barbiturate peak heights measured.

Closed-tube methylation. The reagents were added to a centrifuge tube as above, then the tube was sealed with a screw cap. The tube was heated and vortexed until the dimethyl sulfate layer disappeared, then the tube was allowed to stand in the water bath for an additional 60 min. The tube was removed from the water bath and cooled; then the solution was extracted and chromatographed as above.

RESULTS AND DISCUSSION

The results (Table I) indicate that for open-tube methylation carried out under the conditions described (using dimethyl sulfate and aqueous alkaline barbiturate solutions, heated at 75°C) that short- and intermediate-acting barbiturates which have a shorter retention time than ibomal (the internal standard) such as amobarbital, butabarbital, pentobarbital, and secobarbital are rapidly lost as time passes following the completion of methylation (disappearance of the dimethyl sulfate layer). The losses for these barbiturates become significant after as little as 10 min of continued heating (24–31% for several of the barbiturates), reach nearly 30% for all the barbiturates after 25 min, and reach at least 45% for all the barbiturates after 45

TABLE I

CONCENTRATION CHANGES *VERSUS* TIME LEFT IN WATER BATH

Based on ibomal internal standard.

Barbiturate	*Minutes left in water bath*					
	Without cap					*Capped: 60*
	0	*10*	*25*	*45*	*60*	
Butabarbital	0%	−18.2%	−29.4%	−47.2%	−52.4%	− 8.2%
Amibarbital	0%	−29.8%	−51.0%	−67.3%	−77.9%	−21.6%
Pentobarbital	0%	−24.3%	−46.2%	−66.9%	−72.8%	−17.2%
Secobarbital	0%	−30.7%	−53.6%	−62.9%	−79.3%	−21.4%
Ibomal	0%	0%	0%	0%	0%	0%
Phenobarbital	0%	+ 7.2%	+10.3%	+20.1%	+20.6%	+ 0.5%

min. The losses are clearly great enough that quantitations will be seriously lowered and some positive specimens may give negative (too small) results.

Phenobarbital, a long-acting barbiturate with a longer retention time than ibomal, was found to increase slightly in concentration under the described methylation conditions (Table I). This can only reflect a slight loss in ibomal, rather than an actual increase in phenobarbital concentration. The fact that ibomal slightly decreased during the study means that the short- and intermediate-acting barbiturates actually decreased more than is indicated in Table I. The results in Table II illustrate the losses based on phenobarbital and more closely reflect the actual barbiturate losses during overheating. (Note that since even phenobarbital may be lost relative to a barbiturate with an even longer retention time that the loss values in Table II represent a lower limit for the percent loss).

TABLE II

CONCENTRATION CHANGES *VERSUS* TIME LEFT IN WATER BATH

Based on phenobarbital.

Barbiturate	*Minutes left in waterbath*					
	Without cap					*Capped: 60*
	0	*10*	*25*	*45*	*60*	
Butabarbital	0%	−23.5%	−36.1%	−55.5%	−60.5%	− 8.4%
Amobarbital	0%	−35.2%	−55.6%	−73.1%	−81.5%	−22.2%
Pentobarbital	0%	−29.9%	−50.6%	−72.4%	−77.0%	−17.3%
Secobarbital	0%	−34.7%	−56.9%	−69.4%	−83.3%	−22.2%
Ibomal	0%	− 7.7%	− 9.6%	−17.3%	−19.2%	− 1.9%
Phenobarbital	0%	0%	0%	0%	0%	0%

The results for methylation carried out with dimethyl sulfate at 75°C using closed tubes show that all barbiturates experience a slight loss with respect to phenobarbital as time passes following continued heating after the completion of methylation. This loss, however, is only about 1/4 or less than that for open-tube methylation.

The reason(s) behind the loss of the barbiturates during overheating is not completely understood. We suspect that it may be due largely to the fact that methylated barbiturates are more volatile than free acid barbiturates and may boil away as they stand in the hot water bath after methylation is completed. This factor is supported by the fact that the barbiturate losses increase with time and the fact that closed-tube methylation, which limited the amount of barbiturate that could be lost via boil-away, yielded much less of a barbiturate loss than open-tube methylation. Another possible factor for the barbiturate loss is demethylation and/or barbiturate breakdown due to the heat. Demethylation seems unlikely since the overheated solutions did not contain peaks on the chromatogram for free barbiturates. Breakdown seems more likely and is supported by the fact that closed-tube methylation at 85°C carried out in strong acid and in strong base both lead to complete destruction of all the barbiturates after only 20 min, while methylation of a neutral solution under these conditions lead to only partial destruction.

The results of this study indicate that while methylation with dimethyl sulfate may be faster and lead to cleaner chromatograms than other methylation agents, that steps must be taken to prevent barbiturate loss that may yield false negative or falsely lowered results. Several steps can be taken to minimize possible barbiturate degradation: (1) remove the tubes from the heated water bath as soon as methylation is completed; (2) use closed-tube rather than open-tube methylation; (3) methylate a calibration standard to be used for quantitation with each batch of samples methylated.

REFERENCES

1 N. C. Jain and R. H. Cravey, *J. Chromatogr. Sci.*, 12 (1974) 228–236.
2 E. A. Fiereck and N. W. Tietz, *Clin. Chem.*, 17 (1971) 1024–1027.
3 S. Dilli and A. Weekley, *J. Chromatogr.*, 195 (1980) 349–358.
4 J. MacGee, *Clin. Chem.*, 17 (1971) 587–591.
5 H. F. Martin and J. L. Driscoll, *Anal. Chem.*, 38 (1966) 345.
6 E. Brochmann-Hansen and T. O. Oke, *J. Pharm. Sci.*, 58 (1969) 370–371.
7 K. D. Parker, J. A. Wright, A. F. Halpern and C. H. Hine, *J. Forensic Sci. Soc.*, 8 (1968) 125–140.
8 N. C. Jain, R. D. Budd, T. C. Sneath, D. M. Chinn and W. J. Leung, *Clin. Tox.*, 9 (1976) 221–233.
9 R. D. Budd and D. F. Mathis, *Clin. Tox.*, (1982) in press.

Journal of Chromatography, 237 (1982) 159–163
Elsevier Scientific Publishing Company, Amsterdam — Printed in The Netherlands

CHROM. 14,454

Note

Pyridoxine O-methylether cyclic *n*-butane boronate: a new derivative for gas chromatography of pyridoxine

M. S. CHAUHAN and K. DAKSHINAMURTI*
Department of Biochemistry, Faculty of Medicine, University of Manitoba, Winnipeg R3E OW3 (Canada)
(First received April 6th, 1981; revised manuscript received October 20th, 1981)

Several chemical, microbiological and enzymatic methods are available for the assay of pyridoxal and its phosphorylated form. They have been listed in a recent review[1]. However, there is only one fluorometric method, *i.e.*, the "lactone method" available for the determination of pyridoxine[2]. This method involves oxidation of pyridoxine with potassium permanganate to 4-pyridoxic acid which subsequently is converted into its lactone with hydrochloric acid. This method is very unsatisfactory since the yields are low (30–32%) and inconsistent[3,4]. Furthermore, as the reagents are non-specific, pyridoxal also is oxidized and converted into the lactone under the reaction conditions[4]. Thus, prior separation of pyridoxine from pyridoxal is necessary for differential assay.

Several investigators have examined the gas chromatographic (GC) behaviour of acetyl, benzyl, isopropylidine, trimethylsilyl, trifluoroacetyl and heptafluorobutyryl derivatives of B_6 vitamers[5]. Some of these methods employ the more conventional flame ionization detector which has low sensitivity (*i.e.* in the μg range). Trifluoracetyl and heptafluorobutyryl derivatives, although more sensitive, require the use of a electron-capture detector instead of the more routinely available flame ionization detector. In fact, alkylating or silylating agents such as those mentioned above are single protecting group donors and they do not exploit the distinctive moieties of polyfunctional compounds which could allow the use of more specific reagents involving proximal groups[6]. The use of *n*-butylboronic acid can be very rewarding in this respect as this reagent can form a cyclic boronate with the 1,4-diol group of pyridoxine. In this communication, we have exploited this reaction to develop a new, simple, very specific and highly sensitive GC method for the determination of pyridoxine.

MATERIALS AND METHODS

Chemicals

2,2-Dimethoxypropane, *n*-butylboronic acid and pyridoxine were purchased from Sigma (St. Louis, MO, U.S.A.). Diethyl ether and methanol were obtained from Fisher Scientific (Fair Lawn, NJ, U.S.A.) and were 99.9 mole% pure and used without further purification. Diazald, 99% (N-methyl-N-nitroso-*p*-toluenesulfonamide) was purchased from Aldrich (Milwaukee, WI, U.S.A.). 3% OV-101 on 100–200 mesh

0021-9673/82/0000–0000/$02.75

Gas-Chrom Q and methyl caprate were obtained from Applied Science Labs. (State College, PA, U.S.A.).

The infrared (IR) spectra were obtained on a Perkin-Elmer Model 337 spectrophotometer as Nujol mulls or neat film. Nuclear magnetic resonance (NMR) spectra were recorded with a Varian Model 56/60A spectrometer in C^2HCl_3 using tetramethylsilane as an internal standard. Mass spectra were obtained on a Finnegan 1015 quadruple mass spectrometer. Melting points were determined on a precalibrated "Thermopan" apparatus. Thin-layer chromatography (TLC) was performed on 0.1 mm thick silica gel plates purchased from Eastman-Kodak (Rochester, NY, U.S.A.).

Preparation of 4,5-dihydroxymethyl-3-methoxy-2-methylpyridine (A)

Pyridoxine (100 mg) was dissolved in anhydrous methanol (3 ml) and diazomethane in dry ether was added in small lots till no discoloration of diazomethane was observed. The solution was allowed to stand at room temperature for 1 h. Excess diazomethane and organic solvent were removed on a rotary evaporator under reduced pressure and the residue gave 104 mg of the desired ether in 96% yield. It was crystallized from a mixture of chloroform and ether, m.p. 89–90%. It gave a single spot on TLC plate in chloroform containing 5% methanol. It also gave a single peak in gas–liquid chromatography (GLC) when injected with *n*-butyl boronic acid in dimethoxy propane. The spectral properties of the methyl ether are as follows: IR, 3265 cm^{-1}, OH; 3360 cm^{-1}, OH; NMR, δ 3.8, OCH_3; δ 2.5, CH_3; δ 4.7, CH_2; δ 8.08, H (ring); δ 5.2, OH; the hydroxyl signal disappeared when the compound was shaken with ^2H_2O; mass spectrum, calculated for $C_9H_{13}NO_3$ 183; found M^+ 183.

Preparation of n-butylboronate of 4,5-dihydroxymethyl-3-methoxy-2-methylpyridine (B)

4,5-Dihydroxymethyl-3-methoxy-2-methylpyridine (36.4 mg) and chloroform (0.5 ml) were warmed in a 5-ml test tube provided with a rubber septum and a nitrogen in-let. *n*-Butane boronic acid (20.2 mg/molar proportion) was added and the mixture was warmed under nitrogen atmosphere for 30 min. The reaction solution was then transferred to a sublimation apparatus and the organic solvent removed by flushing nitrogen through the solution. Sublimation of the residue at 125–130°C/0.6 mm pressure yielded 47.0 mg of the pure cyclic boronate (94.4% yield) as a viscous liquid. NMR, δ 3.68, s, OCH_3; δ 2.57, s, CH_3; δ 0.4-1.5, m, C_4H_9; δ 5.0, s, CH_2; δ 5.1, s, CH_2; δ 8.2, s, H; mass spectrum, calculated for $C_{13}H_{20}BNO_3$ 249; found M^+ 249.

4,5-Dihydroxymethyl-3-methoxy-2-methylpyridine (1 mg) was also dissolved in dimethoxypropane (1 ml) and *n*-butylboronic acid (3 mg) was added. The reaction mixture was allowed to stand at room temperature for 30 min and then, 1 μl of the reaction mixture was injected into the gas chromatograph. A single peak of the cyclic boronate (B) was observed.

Similar results were observed when the methyl ether of pyridoxine and *n*-butylboronic acid were injected into the gas chromatograph directly.

Gas–liquid chromatography

This was accomplished with a Beckman GC-65 gas chromatograph provided with a flame-ionization detector. A U-shaped glass column (1.8 m × 2.0 mm I.D.) packed with 3% OV-101 on 100–200 mesh Gas-Chrom Q was used. The injector, inlet

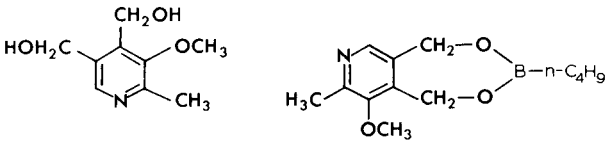

A B

Fig. 1. Formulae of pyridoxine derivatives.

and detector temperatures were 200, 225 and 250°C, respectively. The column temperature was maintained at 160°C. The carrier gas (nitrogen), hydrogen and air flow-rates were 30, 45 and 280 ml/min, respectively. The attenuation range used was 100 × 2.

RESULTS

Diazomethane reacted with pyridoxine to give 4,5-dihydroxy-3-methoxy-2-methylpyridine (A) (Fig. 1). The reaction was complete in 1 h as followed by GLC of the reaction mixture. The presence of excess diazomethane did not affect the nature of the end product.

The reaction of 4,5-dihydroxymethyl-3-methoxy-2-methylpyridine with *n*-butylboronic acid was also quantitative. The mass spectrum of the cyclic boronate showed the molecular ion at 249. The peak at 149, which also is the base peak, represents loss of $C_4H_9BO_2$ from the molecular ion and thus is consistent with the cyclic ester structure (B). The other major peaks observed were at *m/e* 192, 178, 162, 119 and 83. The NMR spectrum lends further support to the structure assigned to the ester. In the ester the methylene protons are shifted δ 0.3 down field when compared to the methyl ether of pyridoxine. Furthermore, the IR and NMR spectra of the ester did not show any hydroxyl absorptions. Such addition of *n*-butane boronic acid to hydroxy and amino functions has been reported by other workers[7,8].

We have applied this procedure for the determination of pyridoxine. To ascertain the linearity of the reaction 10, 20, 30 and 40 μg, respectively of pyridoxine was treated separately with diazomethane as described under Materials and methods. The residue from each of these reactions was dissolved in 100 μl of dimethoxypropane containing 300 μg of methyl caprate as internal standard. An aliquot (1 μl) containing 100, 200, 300 or 400 ng of A from these reactions was injected into the gas chromatograph along with 3 μg of *n*-butylboronic acid in 0.5 μl of dimethoxypropane and the internal standard. The total volume of each injection was 1.5 μl. The reaction was linear and a plot of the peak areas *vs.* concentration is shown in Fig. 2. The retention time was 5.24 min measured from the appearance of the internal standard.

The sensitivity of this procedure was determined by running aliquots of standard containing 10–80 ng of B with 1 μg of *n*-butylboronic acid in a total volume of 1.0 μl of dimethoxypropane. A plot of the peak areas vs concentration is given in Fig. 2 (inset).

DISCUSSION

GC methods based on derivatization with alkylating or silylating agents lack

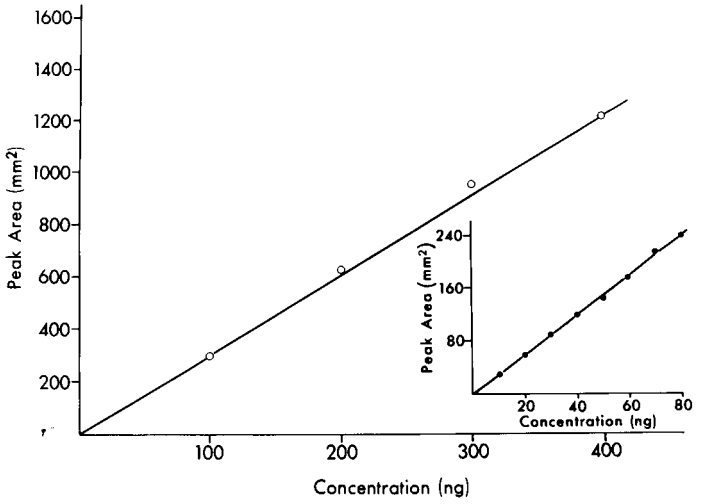

Fig. 2. Plot of peak areas (mm^2) *versus* concentration (ng/1.5 μl) to show linearity of reaction. Each dot represents the mean area from 10 experiments. Inset, plot of peak areas (mm^2) *versus* concentration (ng/1.5 μl) to show the lower response range of the pyridoxine boronate. Each dot represents mean area from 10 experiments.

specificity. The recovery of the target compound is low due to multiple product formation and consequent extraction procedures.

Brooks and Watson[9] introduced the use of boronic acids for the GC analysis of compounds bearing 1,2-diol group in the molecule to achieve specificity of the reaction[6,10,11]. These reagents form highly volatile cyclic boronates which have been used for the GC analysis of 3,4-dihydroxyphenylethyleneglycol, its methoxy derivative and 3,4-dihydroxyphenylacetic acid[6,10–13]. The presence of 1,4-diol group in pyridoxine makes it amenable to such derivitization. The phenolic group of pyridoxine was protected by ether formation with diazomethane prior to boronation.

The method reported here is free of complications since highly specific reagents such as *n*-butylboronic acid and diazomethane have been used for the preparation of the volatile derivative of pyridoxine. Diazomethane reacts only with the phenolic functionality while *n*-butylboronic acid forms cyclic boronates only in the presence of 1,4-diol group. No side products were observed in the presence of large excess of these reagents. Furthermore, organic solvent extraction operations, which reduce the yield of the target compounds, are not needed in this procedure. Therefore the yields are quantitative. Furthermore, the conventional flame ionization detectors are adequate to detect up to 10 ng of pyridoxine. This procedure, therefore has a great potential as a routine assay procedure for pyridoxine. Since pyridoxal and pyridoxamine can be converted into pyridoxine[2,13] these vitamers can also be determined with this method.

ACKNOWLEDGEMENTS

This work was supported by a grant from the Children's Hospital of Winnipeg Research Foundation Inc. and the Medical Research Council of Canada.

REFERENCES

1 K. Dakshinamurti and M. S. Chauhan, in R. Reynolds and J. Leklem (Editors), *Vitamin B_6-analytical Methodology and Criteria for Assessing Nutritional Status*, Plenum Press, New York, 1981, p. 99.
2 S. Udenfriend, *Fluorescence Assay in Biology and Medicine*, Academic Press, New York, 1962, p. 253.
3 E. W. Toepfer and M. M. Polansky, *Vitamins Hormones*, 22 (1964) 825.
4 D. Heyl, *J. Amer. Chem. Soc.*, 70 (1948) 3434.
5 A. J. Sheppard and A. R. Prosser, *Methods Enzymol.*, 18 (1970) 494.
6 M. Cagnasso and P. A. Biondi, *Anal. Chem.*, 71 (1976) 597.
7 G. M. Anthony, C. J. W. Brooks, I. Maclean and I. Sangster, *J. Chromatogr. Sci.*, 7 (1969) 623.
8 H. C. Brown and G. Zweifel, *J. Org. Chem.*, 27 (1962) 4708.
9 C. J. W. Brooks and J. Watson, *Chem. Comm.*, (1967) 952.
10 P. A. Biondi, M. Cagnasso and C. Secchi, *J. Chromatogr.*, 143 (1977) 513.
11 P. A. Biondi, G. Fedelle, A. Motta and C. Secchi, *Clin. Chim. Acta*, 94 (1979) 155.
12 M. S. Chauhan and K. Dakshinamurti, *J. Chromatogr.*, 227 (1982) 323.
13 W. Korytnyk, G. Fricke and B. Paul, *Anal. Biochem.*, 17 (1966) 66.

Journal of Chromatography, 237 (1982) 164–168
Elsevier Scientific Publishing Company, Amsterdam – Printed in The Netherlands

CHROM. 14,497

Note

Gas–liquid chromatographic determination of pyridazinones in waste waters. I.

E. MATISOVÁ*, J. LEHOTAY and J. GARAJ
Department of Analytical Chemistry, Faculty of Chemical Technology, Slovak Technical University, Jánska 1, 880 37 Bratislava (Czechoslovakia)
and
A. VIOLOVÁ
Environment Protection, CHZJD, 811 00 Bratislava (Czechoslovakia)
(Received October 26th, 1981)

Pyridazinones are currently used because of their biological properties as active ingredients in pharmaceutical preparations[1] and as pre- and post-emergent herbicides[2,3]. 5-Amino-4-chloro-2-phenyl-3(2*H*)-pyridazinone (PCA, common name pyrazon) is the active ingredient of herbicide formulations known under the trade names Burex, Chlorazine, Pyramin and Phenazon, which are used for weed control, particularly for sugar beet and beet crops. The main impurities in the technical products and formulations are 4-amino-5-chloro-2-phenyl-3(2*H*)-pyridazinone (i-PCA), the non-active pyrazon isomer, and 4,5-dichloro-2-phenyl-3(2*H*)-pyridazinone, the unreacted derivative (PCC), which is significant from the point of view of toxicology.

Several methods of analysis for the substances in technical products have been reported in literature: potentiometry[4], polarography[5] and spectrometry[6]. However, none selectively determines all components of the above mixture. A thin-layer chromatographic (TLC) method[7] was used to separate every component for subsequent quantitation by UV spectrophotometry, but results have not proved satisfactory because of the photolability of pyridazinones adsorbed on silica gel[8]. A gas–liquid chromatographic (GLC) method was also introduced[9]. Simultaneous determination[10] of the active ingredient and of by-products in technical and formulated pyridazinones was rapidly performed. A semi-quantitative method[11] has been proposed for the determination of PCA in water, which involves extraction with chloroform–ethyl acetate, separation by TLC and a visual estimation of the level of pyrazon by comparison with reference plates. We have developed a specific analytical method for determination of the active ingradient in the waste water used in the technological processes in the presence of many impurities.

EXPERIMENTAL

Chemicals

The pyridazinones listed in Table I were analytical grade standard materials obtained from Research Institute of Agrochemical Technology, Bratislava, Czechoslovakia.

0021-9673/82/0000–0000/$02.75

TABLE I

PYRIDAZINONES

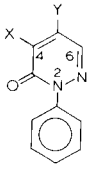

Substance	*Substituents*	
	X	*Y*
PCA	Cl	NH_2
i-PCA	NH_2	Cl
PCC	Cl	Cl

The solvents used were of analytical-reagent grade and were distilled prior to use.

Apparatus

A Carlo Erba Model 2350 gas chromatograph equipped with a flame-ionization detector (FID) was used. The thermostat was maintained at 473°K and 493°K, respectively; an injection block temperature of 498°K was used.

A glass column (0.6 m × 3.5 mm I.D.) packed with 2% OV-17 (Chrompack, The Netherlands) on 60–70 mesh Chromaton N AW DMCS (Lachema, Brno, Czechoslovakia) was employed. The carrier gas was nitrogen at a pressure of 20.3 kPa and 25.3 kPa, respectively.

A 350 rotary evaporator (Unipan, Warsaw, Poland) was used.

Procedure

Extraction was performed in a round-bottomed flask using a shaking machine.

Water samples, 100 or 500 ml, were extracted three times for 15 min with 25- and 100-ml portions of chloroform, respectively. Chloroform extracts were separated in a separating funnel. The extracts were combined and evaporated to dryness using a rotary evaporator. The residues were dissolved in a suitable defined volume of chloroform. A 1–5-μl volume of the solution was injected into the column with a 10-μl Hamilton syringe.

The recovery determination was performed in the same way using model samples of PCA and PCC of 1 mg/l concentration in distilled water.

Calibration graphs

Calibration graphs were prepared from standard solutions containing 0.5–10.0 mg of solid substance in 10 ml of chloroform. Solutions of lower concentration were prepared by dilution.

RESULTS AND DISCUSSION

Since PCA, i-PCA and PCC differ in polarity, the choice of the stationary

TABLE II

RECOVERY OF PCA AND PCC EXTRACTION, AVERAGE RECOVERY AND STANDARD DEVIATION

Substance	*Recovery (%)*	*Average recovery (%)*	*Standard deviation*
PCA	91.27 90.56 95.83	92.55	3.10
PCC	96.90 96.16 100.60	97.89	2.62

phase is significant for the efficiency of analysis. Cellerino and Re[10] tested several stationary phases. For substances of high boiling point they considered polyglycols and polyesters to be unsuitable, and silicones of lower polarity (SE-30, OV-1, OV-101, OV-7) gave unsymmetrical peaks. The OV-17 column had excellent reproducibility and column life, but the shape of PCA peak was not quite symmetrical. As the peak symmetry at the residue level is very important, we tried to prepare a column that would give perfect symmetry of all peaks. The first essential was an inert support material. Higher stationary phase loading, which diminishes the influence of support material active sites, resulted in long analysis times.

We tested several columns and achieved excellent results with a Carbowax 20M column and non-polar stationary phases of the silicone type with Carbowax 20M deactivated support material[12] in the analysis of standard solutions of PCA, i-PCA and PCC in chloroform. However, after repeated injection of water extracts of these substances very unsymmetrical peaks of PCA were observed. Unlike i-PCA, which preferentially forms intramolecular hydrogen bonds owing to the acidic hydrogen atom in the amino group, PCA forms intermolecular hydrogen bonds, which is the reason for the peak tailing.

Thus all further determinations of the above-mentioned substances in water extracts were performed on a Chromaton N AW DMCS column with 2% OV-17.

Recovery values of extraction were determined by adding known amounts of the individual pyridazinones to untreated samples (distilled water) before the extraction procedure. The average recoveries of three different samples and standard deviations were calculated and are given in Table II. These values are acceptable for residue analysis.

In the quantitative analysis we studied the linear response range of the FID, limit of detection and the reproducibility of measurements. It was found that in the studied range of 0.05–5.00 μg of injected PCA and 0.01–2.00 μg of PCC the response of the detector was linear. For peak area measurement, the methods of height multiplied by width at half height (determined by a calibrated magnifying glass with readout precision ± 0.05 mm) was used. An analytical curve was constructed from values of the peak area and height, respectively, and the dependence on the injected amount of pyridazinones. The sample was injected by the washed-out plug of solvent technique. The results of the analytical curves ($n \geq 15$) were statistically evaluated by linear regression. We have tested the calculated value b of straight lines $y = ax + b$,

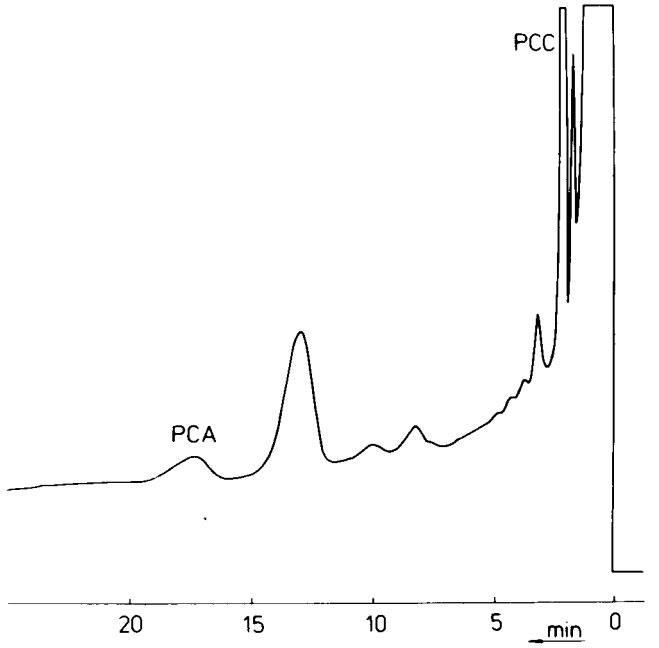

Fig. 1. Gas chromatogram of water extract of pyridazinones (1.69 mg of PCA per litre) on the column with 2% OV-17 on Chromaton N AW DMCS at 473 K and nitrogen pressure of 25.33 kPa; 500 ml of water sample was taken for extraction; 1.1 μl was injected from the final volume of 5 ml.

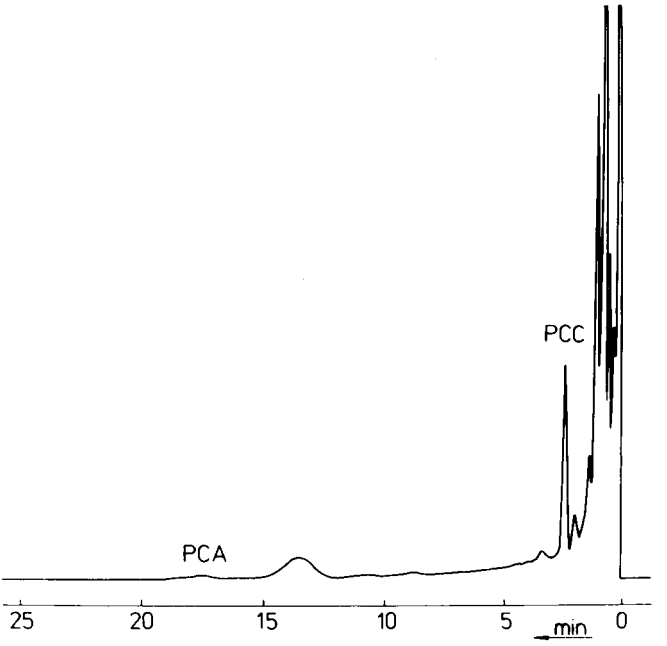

Fig. 2. Gas chromatogram of water extract of pyridazinones (4.37 mg of PCC per litre); 1.7 μl was injected from the final volume of 5 ml. The conditions were the same as in Fig. 1.

TABLE III

DETERMINED AMOUNTS OF PCA AND PCC IN WASTE WATERS

Sample	*PCA (mg/l)*	*PCC (mg/l)*
I	1.69 ± 0.18	4.37 ± 0.33
II	0.79 ± 0.09	4.49 ± 0.34

to determine whether there is a random or systematic error[13]. The limit of detection (3 × noise) of injected standard was found to be 30 ng of PCA and 1 ng of PCC; values of 6.6 μg of PCA per litre and 0.2 μg of PCC per litre were found when 1 l of water sample was extracted to a final volume of 0.2 ml.

The analysis of a practical sample of pyridazinones water extract is shown in Figs. 1 and 2. The amounts of PCC and PCA in waste waters, which represent the average values of three measurements, are given in Table III. In the quantitative analysis of practical samples, where besides the substances of interest there were many other compounds, the peak position was checked by the standard addition method. The GLC method was compared with high-performance liquid chromatographic method, where the possibility of the overlapping of a peak of interest was excluded by using many mobile phases of different polarity. The results of this part of the work are to be published elsewhere[13]. The results gained by both methods are in good agreement.

REFERENCES

1 D. T. Mowry, *J. Amer. Chem. Soc.*, 75 (1953) 1909.
2 A. Fisher, *Weed Res.*, 2 (1962) 177.
3 H. Maier-Bode, *Herbicide und ihre Ruckstände*, Eugen Ulmer, Stuttgart, 1971.
4 J. Missala and C. Czulinska, *Chem. Anal. (Warsaw)*, 13 (1968) 23.
5 M. Gruca, Z. Janko, J. Kanty and A. Kotarski, *Chem. Anal. (Warsaw)*, 12 (1967) 1331.
6 A. Lineberga, *Gig. Sanit.*, 34 (1969) 69.
7 K. Ďulák, J. Kováč and P. Rapoš, *J. Chromatogr.*, 31 (1967) 354.
8 J. D. Rosen and M. Siewierski, *J. Agr. Food Chem.*, 20 (1972) 434.
9 P. Výboh, M. Michálek, J. Šustek and V. Bátora, *Pestic. Sci.*, 5 (1974) 171.
10 G. Cellerino and M. Re, *J. Ass. Offic. Anal. Chem.*, 61 (1978) 161.
11 O. Palušová, M. Sackmauerová and A. Madarič, *J. Chromatogr.*, 106 (1975) 405.
12 W. A. Aue, C. R. Hastings and S. Kapila, *J. Chromatogr.*, 77 (1973) 299.
13 J. Lehotay, E. Matisová, J. Garaj and A. Violová, *J. Chromatogr.*, in press.

Journal of Chromatography, 237 (1982) 169–173
Elsevier Scientific Publishing Company, Amsterdam — Printed in The Netherlands

CHROM. 14,481

Note

Simultaneous determination of benztropine mesylate and benzophenone by high-performance liquid chromatography

STEPHEN BIFFAR* and DONALD TIBBETTS
Merck, Sharp & Dohme, West Point, PA 19486 (U.S.A.)
(Received October 13th, 1981)

Benztropine mesylate is an anticholinergic drug used in the therapy of parkinsonism. It may be administered orally or by intramuscular injection. Ion-exchange[1] or colorimetric[2] methods have been reported in the literature. Spectrophotometric[3] analyses are currently used for the analysis of benztropine mesylate tablets and injectables.

The compendial method[3] for benztropine mesylate injection specifies an extraction into ether and a back-extraction into dilute hydrochloric acid. The aqueous solution is read at 258 nm.

The compendial method[3] for tablets involves a dichromate oxidation solution of benztropine mesylate in acid solution. The resulting benzophenone is read at 247 nm.

This paper describes a high-performance liquid chromatographic (HPLC) procedure for the simultaneous determination of benztropine mesylate and benzophenone.

The mobile phase contains octylamine phosphate at a pH equal to 3.0. The *n*-octylamine then acts as a competing base by adsorbing to the unreacted silanol groups[4] or as an ion-repelling agent[5] by adsorbing to the octylsilane groups bonded to the base silica. A reduction in the octylamine concentration greatly increases the retention time of the benztropine mesylate.

The method is rapid, accurate, and precise. A comparison of the HPLC method with the current official method[3] indicates that the methods are equivalent for tablets and injectable solutions.

EXPERIMENTAL

Reagents and chemicals

USP reference standard benztropine mesylate and reagent-grade benzophenone (MCB, Plainfield, NJ, U.S.A.) were used in the standard solutions. HPLC acetonitrile, *n*-octylamine (Aldrich, Milwaukee, WI, U.S.A.) and reagent-grade phosphoric acid (85%) (Fisher Scientific, Fair Lawn, NJ, U.S.A.) were used in the mobile phase. Isopropanol and methanol (Fisher Scientific) were reagent-grade.

Octylamine phosphate buffer was prepared by adding 0.84 ml of *n*-octylamine to 1.0 l of deionized-distilled water. While stirring, phosphoric acid was added until the pH was equal to 3.0.

0021-9673/82/0000–0000/$02.75

Aqueous phosphoric acid–isopropanol solution was prepared by mixing 600 ml of deionized-distilled water, 400 ml of isopropanol, and 1.0 ml of phosphoric acid.

Mobile phase

The mobile phase was prepared by mixing 650 ml of HPLC acetonitrile with 350 ml of octylamine phosphate buffer. This solution was degassed by vacuum filtration through a 0.45-μm membrane filter (HVLPO4700; Millipore, Bedford, MA, U.S.A.).

Assay for tablets

Standard preparation. The standard solution contains both benztropine mesylate and benzophenone.

A solution of benzophenone was prepared by dissolving 25 mg of benzophenone in 1.0 l of methanol.

The standard solution was prepared by dissolving 50 mg of benztropine mesylate USP reference standard in 100 ml of deionized-distilled water in a 200-ml volumetric flask. A 5-ml volume of the benzophenone solution was added to the 200-ml volumetric flask, and the solution was diluted to volume with deionized-distilled water.

Assay preparation. Weigh and finely powder not less than 20 tablets (Merck, Sharp & Dohme, West Point, PA, U.S.A.). Transfer an accurately weighed portion of the powder equivalent to about 10 mg of benztropine mesylate to a 50-ml stoppered centrifuge tube. Pipet 40.0 ml of aqueous phosphoric acid–isopropanol solution, into the centrifuge tube. Shake by mechanical means for not less than 60 min. Centrifuge for 5 min. Filter each sample through a 0.45-μm membrane filter (HVLP01300, Millipore).

Assay for injectables

Standard preparation. Dissolve 100 mg of benztropine mesylate reference standard in 50 ml of deionized-distilled water in a 100-ml volumetric flask. Dilute to volume with deionized-distilled water.

Assay preparation. 1.0 mg/ml benztropine mesylate injection samples (Merck, Sharp & Dohme) were assayed with no sample preparation.

Solutions for linearity and precision. Standard solutions were prepared by adding 20 mg, 25 mg, 35 mg, 50 mg, 100 mg, and 150 mg of benztropine mesylate USP reference standard into separate 100-ml volumetric flasks. Each flask was diluted to volume with deionized-distilled water. These solutions were used to test the linearity and precision of the HPLC method.

Conditions for chromatographic quantification. The Varian Model 5060 liquid chromatograph was equipped with a loop-injector, a variable-wavelength detector (Spectromonitor III, Model 1204, LDC Instrument Co), and an octylsilane column (Ultrasphere Octyl (5 μm), 25 cm × 4.6 mm column; Altrex Co., Berkely, CA, U.S.A.). The mobile phase was pumped at a flow rate of 1.3 ml/min, at approximately 25°C. An injection volume of 25 μl was used for both the tablets and injectables. The peaks were detected at 239 nm.

RESULTS AND DISCUSSION

Benztropine mesylate tablets and injectables were assayed by this method. The benztropine mesylate is separated from its degradation product, benzophenone. When injected into the chromatograph, benzophenone is eluted first followed by benztropine mesylate at retention times of 5.20 and 7.60 min, respectively (Fig. 1).

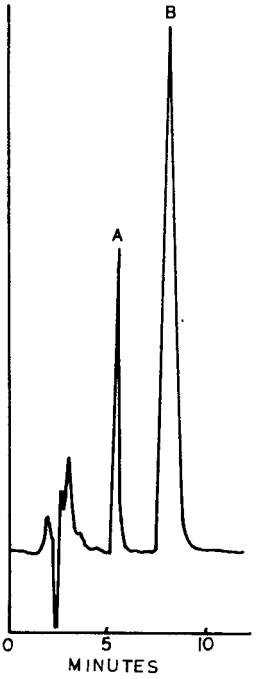

Fig. 1. The separation of benzophenone from benztropine mesylate. Peaks: A = benzophenone; B = benztropine mesylate.

TABLE I

LINEARITY AND PRECISION OF THE HPLC METHOD

Actual weighed concentration benztropine mesylate (mg/ml)	*Observed HPLC results (mg/ml)**	*Recovery (%)*	*Slope*	*Intercept*	*r***
0.202	0.203 ± 0.001	100.4	0.996	0.003	1.00
0.253	0.253 ± 0.001	100.1			
0.353	0.353 ± 0.001	99.9			
0.500	0.508 ± 0.001	101.7			
0.998	0.996 ± 0.002	99.9			
1.498	1.495 ± 0.002	99.8			

* Results based on six replicate injections. The value given is the mean ± S.D.

** Correlation coefficient between the actual and observed concentrations as determined by linear regression analysis.

Standard solutions of benztropine mesylate were chromatographed using the reversed-phase C_8 column. The concentration of each solution was calculated using a Spectra-Physics SP4100 programmable integrator.

A linear regression analysis of the data for the six concentration levels of benztropine mesylate is shown in Table I. This data shows that the benztropine mesylate response is linear from 0.0 to 1.50 mg/ml.

Three lots each of 0.5 mg, 1.0 mg, and 2.0 mg tablets were assayed by this method and the official procedure (USP XX). The results are shown in Table II. The

TABLE II

BENZTROPINE MESYLATE TABLETS COMPARISON OF THE HPLC AND OFFICIAL METHODS

Tablet strength (mg)	*Benztropine mesylate observed results*				*Benzophenone HPLC result*	
	*HPLC**		*USP*			
	mg/tablet	*% claim*	*mg/tablet*	*% claim*	*mg/tablet*	*% Benztropine mesylate equivalent*
0.50	0.486 ± 0.001	97.1	0.490	98.0	0.0007	0.31
	0.491 ± 0.003	98.1	0.491	98.2	0.0005	0.22
	0.499 ± 0.005	99.7	0.509	101.8	0.0001	0.04
1.0	1.007 ± 0.010	100.7	1.02	102.0	0.0012	0.27
	0.970 ± 0.007	97.0	0.985	98.5	0.0037	0.82
	1.003 ± 0.003	100.3	0.988	98.8	0.0020	0.44
2.0	2.036 ± 0.010	101.8	1.95	97.5	0.0039	0.43
	1.974 ± 0.004	98.7	1.92	96.0	0.0078	0.86
	2.040 ± 0.008	102.0	2.03	101.5	0.0017	0.19

* Result is based on two replicate injections. The value given is the mean ± S.D.

TABLE III

BENZTROPINE MESYLATE INJECTION COMPARISON OF THE HPLC AND OFFICIAL METHODS

Sample No.	*Benztropine mesylate observed results*				*Benzophenone HPLC result*	
	*HPLC**		*USP*			
	mg/ml	*% claim*	*mg/ml*	*% claim*	*mg/ml*	*% Benztropine mesylate equivalence*
1	1.009 ± 0.002	100.9	0.998	99.8	$<2.0 \cdot 10^{-5}$	≤0.01
2	1.014 ± 0.001	101.4	1.01	101.0	$<2.0 \cdot 10^{-5}$	≤0.01
3	1.005 ± 0.003	100.5	0.993	99.3	$<2.0 \cdot 10^{-5}$	≤0.01

* Result is based on four replicate injections. The value given is the mean ± S.D.

assay methods are comparable and the HPLC method indicates less than 1.0% degradation of the benztropine mesylate in any lot.

Three lots of 1.0 mg/ml injection were assayed by the HPLC method and the official procedure (USP XX) as shown in Table III. The injection samples all have less than $2.0 \cdot 10^{-5}$ mg/ml of benzophenone, indicating excellent stability in aqueous solution.

This HPLC method is rapid, quantitative, and can simultaneously assay benztropine mesylate and low levels of benzophenone in tablets and injectables.

REFERENCES

1 M. C. Stricklin and D. J. Smith, *J. Ass. Offic. Anal. Chem.*, 54 (1971) 893.
2 M. C. Stricklin, *J. Ass. Offic. Anal. Chem.*, 56 (1973) 681.
3 *The United States Pharmacopeia*, Mack Publishing Co., Easton, PA, 20th Rev., 1980, p. 78.
4 A. Sokolowski and K.-G. Wahlund, *J. Chromatogr.*, 189 (1980) 299.
5 B. A. Bidlingmeyer, *J. Chromatogr. Sci.*, 18 (1980) 525.

Journal of Chromatography, 237 (1982) 174–177
Elsevier Scientific Publishing Company, Amsterdam Printed in The Netherlands

CHROM. 14,531

Note

High-performance liquid chromatographic method for separation of dinucleotides

EBERHARD HAGEMEIER, SIEGMAR BORNEMANN, KARL-SIEGFRIED BOOS and ECKHARD SCHLIMME*

Laboratorium für Biologische Chemie der Universität (GH) Paderborn, Warburger Strasse 100, D-4790 Paderborn (G.F.R.)

(Received November 9th, 1981)

During the last decade, dinucleotides linked via a 5′,5″-phosphate bridge have become of particular interest, as nucleotides of this unusual type were found to function as 5′-terminal cap structures in the majority of eucaryotic and viral messenger RNA[1,2] and on the monomer level as regulators in the biosynthesis of macromolecules[3].

For analytical investigations in the biochemical field and for reaction and purity control monitoring in chemical synthesis work with 5′,5″-bridged dinucleotides and structurally related compounds highly efficient chromatographic separation techniques are required. In this paper we report three aspects of the high-performance liquid chromatographic (HPLC) analysis of nucleotides and dinucleotides: (1) efficient separation of cap-structured dinucleotides and related compounds with respect to resolution, sensitivity and shortness of separation time; (2) monitoring of the time-dependent progress of dinucleotide synthesis; and (3) purity control of naturally occurring and synthesized compounds.

EXPERIMENTAL

Equipment

HPLC separations were carried out on two different systems, as follows, with a column temperature of 24°C in each instance.

(A) A Serva two-piston pump, a home-made separating column[4] (300 × 2.3 mm I.D.) packed with Nucleosil 10 SB (10 μm) (Macherey & Nagel, Düren, G.F.R.) with a diaphragm-sealed injection system was used. The effluent was monitored continuously with an ISCO Model UA 5 absorbance detector (Instrumentation Specialties, Lincoln NE, U.S.A.) at 254 nm.

(B) Two Altex Model 110 A pumps (Altex, CA, U.S.A.) controlled by a Model 420 microprocessor, a Rheodyne Model 7125 loop injector for sample introduction and a Kontron Uvicon Model 725 spectrophotometer (Kontron, Eching, G.F.R.) to monitor the UV absorbance of the effluent at 266 nm throughout the study were used. The column was an Altex Partisil PAC (10 μm) (250 × 3.2 mm I.D.).

0021-9673/82/0000–0000/$02.75

Mobile phases

The mobile phase for system A was a 0.1 *M* KNO_3 potassium nitrate–0.02 *M* potassium dihydrogen orthophosphate buffer adjusted to pH 2.6 with dilute orthophosphoric acid. The flow-rate of the mobile phase was constant at 8 ml h^{-1} and the inlet pressure was 500 p.s.i. The mobile phases for system B were alternatively (B1) 0.8 *M* ammonium formate buffer; (B2) 0.4 *M* ammonium formate buffer; both buffers were adjusted to pH 4.1 with 85% formic acid; (B3) a 6-min linear gradient from water up to 0.8 *M* ammonium formate, pH 4.1. The flow-rate of the mobile phase in each instance was 2 ml min^{-1} at an inlet pressure of 2000 p.s.i. All buffers were prepared with doubly distilled water and degassed in an ultrasonic bath.

Materials

5′-AMP, 5′-ADP, 5′-ATP, 5′-GMP, 5′-GDP, 5′-GTP, 5′-IMP, 5′-IDP and 5′-ITP were purchased from Boehringer (Mannheim, G.F.R.). [^{14}C]5′-AMP$(NH_4)_2$ was a product from New England Nuclear (Boston, MA, U.S.A.). All other dinucleotides investigated were prepared in micromolar amounts[5].

RESULTS AND DISCUSSION

Separation of 5′,5″-phosphate-bridged dinucleotides

5′,5″-Phosphate-bridged dinucleotides represent groups of similar compounds as there are dinucleotide 5′,5″-di-, -tri-, -tetra- and -pentaphosphates which differ in anionic charge with respect to the length of the intramolecular phosphate chain and, in addition, to their heterocyclic bases. Depending on these molecular differences, especially due to anionic charges, it was possible to find a suitable anion exchanger and a mobile phase for the analysis of such similar groups of compounds under both isocratic and gradient elution conditions.

Under isocratic separation conditions it was possible to separate completely up to eighteen 5′,5″-linked dinucleotides. Although the separation was efficient with respect to resolution and sensitivity, dinucleotides bearing a tri-, tetra- and pentaphosphate bridge could not be eluted from the column in a reasonable time with system A (Table I).

Concerning the retention times of the different groups of dinucleotides, systems B1 and B2 are more convenient. The resolution of compounds of the same group, on the other hand, is not as efficient as that obtained with system A. However, with systems B1 and B2 a complete separation of the different groups of dinucleoside di-, tri-, tetra- and pentaphosphates is possible (Table I).

A very rapid and selective separation, however, of all nucleotides investigated in the course of this work was achieved by the use of system B with linear gradient elution (B3). This was done by programming a 6-min linear gradient from water up to 0.8 *M* ammonium formate (pH 4.1), followed by a "hold" at the final concentration of 0.8 *M* ammonium formate until all nucleotides were completely eluted (Table I).

Fig. 1 shows the separation of a synthetic mixture of chemically synthesized dinucleotides with system B3.

HPLC monitoring of dinucleotide synthesis

Fig. 2 shows schematically the HPLC monitored reaction course of a Gp_3A

TABLE I

RETENTION TIMES OF 5′,5″-PHOSPHATE-BRIDGED DINUCLEOTIDES

Type of compound	*Compound*	*Retention time (min)*			
		A	*B1*	*B2*	*B3*
Nucleotides	5′-AMP	12	0.92	1.02	3.12
	5′-ADP	22	1.06	1.64	5.17
	5′-ATP	58	1.33	3.46	6.82
	5′-GMP	18	0.88	1.01	3.25
	5′-GDP	42	1.02	1.54	5.61
	5′-GTP	–	1.24	3.15	7.39
	5′-IMP	21	0.86	0.96	3.14
	5′-IDP	–	0.98	1.43	5.34
	5′-ITP	–	1.16	2.33	7.12
Dinucleoside diphosphates	Ap_2A	19	0.99	1.25	4.17
	$rroAp_2rroA$	14	1.28	1.53	4.66
	Gp_2A	25	0.96	1.24	3.90
	Ip_2A	30	–	–	–
	$2'dGp_2A$	31	–	–	–
	$2',3'ddGp_2A$	42	–	–	–
	Ip_2I	74	–	–	–
Dinucleoside triphosphates	$rroGp_3rroA$	29	1.19	2.26	6.58
	Gp_3A	96	1.15	2.17	6.16
	$2'dGp_3A$	108	1.26	2.64	6.75
	$2'-O-mGp_3A$	109	1.26	2.42	6.97
	$2',3'ddGp_3A$	117	1.93	4.68	7.99
	$2'dGp_32'dG$	152	1.35	3.34	7.13
	Gp_3G	160	.–	.–	.–
	Ip_3G	146	1.04	2.10	5.44
	Ip_3A	160	1.10	2.14	5.96
	m^7-Gp_3A	–	1.01	1.46	5.13
Dinucleoside tetra- and pentaphosphates	Gp_4G	360	1.43	6.36	8.07
	$2'dGp_42'dG$	304	1.76	7.81	9.20
	Ap_5A	–	2.00	.–	10.23
	Ip_5I	–	1.60	.–	9.71
	$2'dGp_52'dG$	–	2.53	.–	11.92

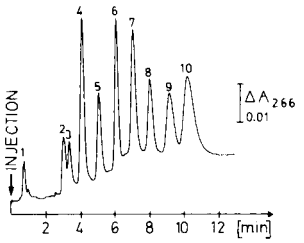

Fig. 1. HPLC separation of a synthetic mixture of chemically synthesized dinucleotides. Peaks: 1 = adenosine, guanosine; 2 = AMP; 3 = GMP; 4 = Ap_2A; 5 = m^7-Gp_3A; 7 = $2'dGp_32'dG$; 8 = Gp_4G; 9 = $2'dGp_42'dG$; 10 = Ap_5A.

synthesis. This application allows convenient reaction control by analysing the time-dependent decrease of the starting material AMP, the increase of the side-product Gp_2A and the increase of the desired product Gp_3A. Ap_2A turned out to be constant over the monitored time range owing to its generation in a preceding reaction step[5].

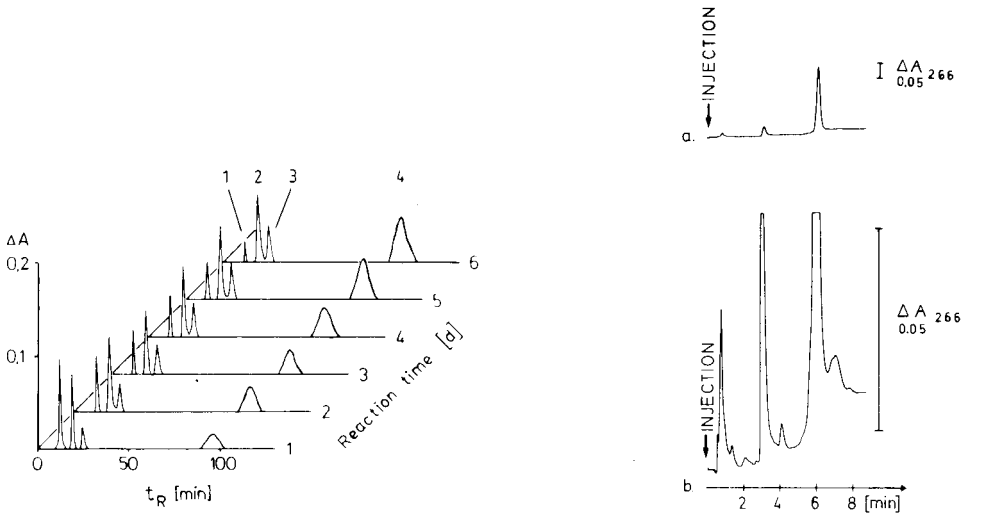

Fig. 2. Results of HPLC analysis of 5-μl aliquots of a Gp_3A synthesis reaction mixture (17 ml) with system A. Peaks: 1 = AMP (retention time, t_R = 12 min); 2 = Ap_2A (t_R = 19 min); 3 = Gp_2A (t_R = 25 min); 4 = Gp_3A (t_R = 96 min). GDP (t_R = 42 min) is present in excess and not shown for graphical reasons.

Fig. 3. Analysis of an aliquot of a homogeneous product peak (Gp_3A), obtained by DEAE-cellulose chromatography, using two different detector sensitivities with system B3.

Purity control

A homogeneous product peak of a Gp_3A synthesis eluted from DEAE-cellulose was analysed for purity and yield (Fig. 3). A 75-fold increase in sensitivity leads to the appearance of five additional impurities and decreases the overall yield by 10%. This comparison shows that the highest available detector sensitivity should be used in order to obtain reasonable purity and yield.

ACKNOWLEDGEMENT

Financial support from the government of Landes Nordrhein-Westfalen is gratefully acknowledged.

REFERENCES

1 A. J. Shatkin, *Cell*, 9 (1976) 645.
2 A. K. Banerjee, *Microbiol. Rev.*, 44 (1980) 175.
3 A. Travers, *Nature (London)*, 283 (1980) 16.
4 K.-W. Stahl, E. Schlimme and D. Bojanowski, *J. Chromatogr.*, 83 (1973) 395.
5 S. Bornemann and E. Schlimme, *Z. Naturforsch. C*, 36 (1981) 135.

Journal of Chromatography, 237 (1982) 178–182
Elsevier Scientific Publishing Company, Amsterdam – Printed in The Netherlands

CHROM. 14,507

Note

Separation of farnesol isomers by liquid chromatography

HISAYA SATO*, AKIRA KAGEYU, KIYOSHI MIYASHITA and YASUYUKI TANAKA
Department of Textiles and Polymer Science, Faculty of Technology, Tokyo University of Agriculture and Technology, Koganei, Tokyo 184 (Japan)
(Received November 2nd, 1981)

Farnesol (3,7,11-trimethyldodeca-2,6,10-triene-1-ol) is a linear sesquiterpene having four geometric isomers due to the double bonds at the C-2 and C-6 positions: 2-*cis*,6-*cis* (2c-6c), 2-*cis*,6-*trans* (2c-6t), 2-*trans*,6-*cis* (2t-6c) and 2-*trans*,6-*trans* (2t-6t) isomers. The widespread occurrence of the 2t-6t isomer has been recognized in many higher plants, and the presence of the 2c-6t isomer accompanied by the 2t-6t isomer has been reported in petigrain and some other plant oils[1]. On the other hand, a commercially obtained synthetic farnesol contained all of four isomers.

The separation of farnesol isomers has been investigated by gas and liquid chromatography. Using gas chromatography only small amounts of the pure isomers are collected[2]. The liquid chromatographic separation of farnesol isomers has been carried out using silica gel as the stationary phase; the four isomers have been separated into two fractions consisting of 2c-6c + 2c-6t and 2t-6c + 2t-6t isomers[3].

In this work a farnesol mixture was separated into the four isomers by liquid chromatography using styrene–divinylbenzene copolymer gel as the stationary phase. The separation mechanism is discussed in terms of the solvent polarity.

EXPERIMENTAL

Materials

Farnesol containing all four isomers was obtained commercially (Aldrich, Milwaukee, WI, U.S.A.) and was used without further purification. All the eluents were obtained commercially and were used without further purification.

Gas chromatography

Gas chromatography was carried out using a Hitachi 163 gas chromatograph equipped with a 30-m glass capillary column coated with free fatty acid polyester (FFAP).

Liquid chromatography

Liquid chromatography was carried out using a JASCO Trirotar II as a high-pressure pump and a Waters R 401 differential refractometer as a detector. For analytical purposes a 500 × 10 mm I.D. stainless-steel column was used and for preparative purposes a 600 × 21 mm I.D. column. The columns were packed with

0021-9673/82/0000–0000/$02.75

styrene–divinylbenzene copolymer gel having an exclusion limit of 3000 in gel permeation chromatography, which was prepared by conventional suspension polymerization[4]. The flow-rate was controlled at 1 and 6 ml/min in analytical and preparative work, respectively.

RESULTS AND DISCUSSION

Elution behaviour of farnesol

The separation of farnesol was examined with an analytical column using seven eluents. The elution volumes of farnesol are given in Table I together with the solvent strengths on alumina and the solbility parameter for each eluent[5]. Using chloroform as the eluent farnesol was eluted at an elution volume of 16 ml, earlier than with any other eluent. This finding indicates the absence of adsorption of farnesol on the gel in chloroform. Acetone and diisopropyl ether eluted farnesol at an elution volume of *ca.* 33 ml, indicating weak adsorption of farnesol on the gel. With these three eluents separation due to geometric isomerism was not observed.

TABLE I

ELUTION VOLUMES OF FARNESOL

Measured with a 500 × 10 mm I.D. column at a flow-rate of 1.0 ml/min.

Eluent	*Solvent strength on alumina*[5], ε^0	*Solubility parameter*[5], δ	*Elution volume of farnesol (ml)*
2,2,4-Trimethylpentane	0.01	7.1	78.0, 86.5
Cyclohexane	0.04	8.2	55.1, 58.2
Diisopropyl ether	0.20	7.3	33.6
Chloroform	0.40	9.1	15.3
Acetone	0.56	9.4	32.6
Acetonitrile	0.65	11.8	53.2, 54.0, 55.2
Methanol	0.95	12.9	61.3, 65.2, 69.9

Cyclohexane, 2,2,4-trimethylpentane, acetonitrile and methanol eluted farnesol at elution volumes of 50–90 ml, indicating strong adsorption. With these eluents farnesol was separated into two or three peaks, as shown in Fig. 1. In methanol and acetonitrile farnesol was separated into three peaks, which were identified by gas chromatography of the collected fractions as 2c-6c, 2t-6c + 2c-6t and 2t-6t isomers, in order of increasing elution volume. On the other hand, cyclohexane and 2,2,4-trimethylpentane provided only two peaks; 2c-6c and 2c-6t isomers eluted earlier than 2t-6c and 2t-6t isomers.

The different separation patterns of these eluents can be explained as follows. In methanol and acetonitrile farnesol was adsorbed on the gel by the alkenyl part of the molecule, because these eluents are more polar than the gel, as can be seen from their solubility parameters. Therefore, the separation was governed by the total number of *cis* or *trans* double bonds in the isomers, as illustrated in Fig. 2a. On the other hand, in cyclohexane and 2,2,4-trimethylpentane, which are less polar than the gel, farnesol was adsorbed on the gel by the terminal hydroxyl group. This means that

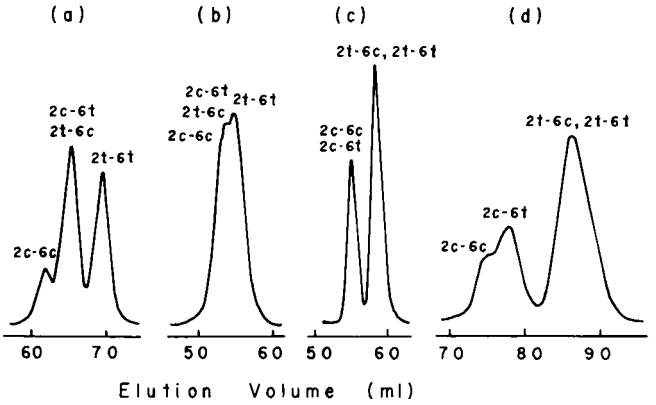

Fig. 1. Liquid chromatograms of farnesol. Eluent: (a) methanol; (b) acetonitrile; (c) cyclohexane; (d) 2,2,4-trimethylpentane.

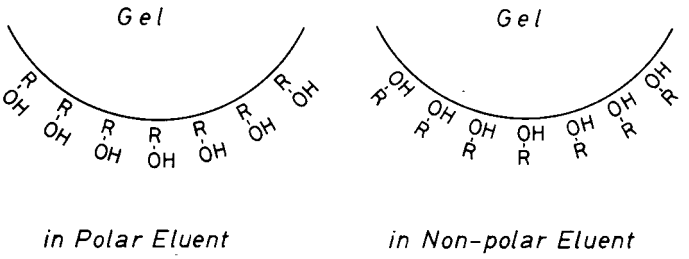

Fig. 2. Schematic representation of the adsorption of farnesol on the polymer gel.

the separation was carried out mainly according to the *cis* or *trans* configuration of the double bond at the C-2 position, as illustrated in Fig. 2b.

From these findings the eluents can be classified into three groups: (1) polar eluents, providing three peaks; (2) eluents with medium polarity, providing no separation due to geometric isomerism; and (3) non-polar eluents, providing two peaks. With styrene oligomers the solubility parameter was demonstrated to be a good indicator of the polarity of eluents[6]. However, with farnesol the solubility parameter is not a good indicator, because diisopropyl ether is classified as an eluent of medium polarity, although it has a small solubility parameter. This can be explained by the presence of a hydrogen bond between the hydroxyl group in farnesol and the ether oxygen atom in the eluent. In such a case the solvent strength on alumina is a better indicator of the polarity of the eluents, as shown in Table I.

Preparative separation of farnesol

The preparative separation of farnesol was carried out using methanol and cyclohexane as eluents, because these eluents provided columns with a high number of theoretical plates and good resolution for farnesol isomers. With a sample size of 120 mg in 1 ml almost pure 2c-6c and 2t-6t isomers were obtained after six recyclings (*ca.* 4 h) with methanol as the eluent (Fig. 3a). The 2c-6t and 2t-6c isomers overlapped with each other and displayed only one peak, even after seventeen recyclings. How-

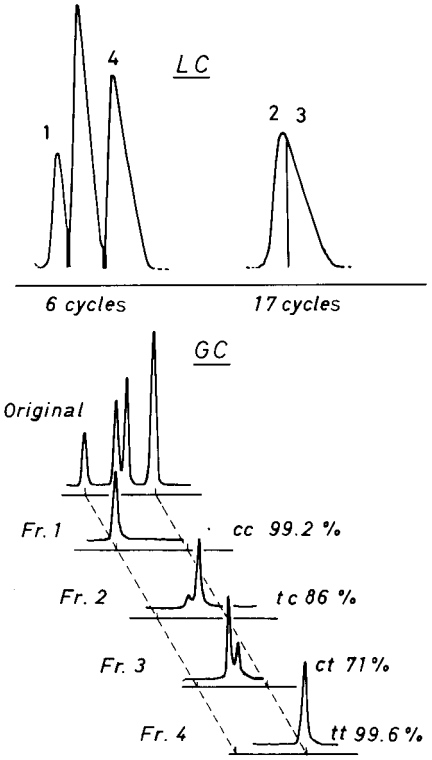

Fig. 3. Preparative-scale fractionation of fornesol isomers using methanol as eluent, and the composition of each fraction analysed by gas chromatography.

ever, the first half of the peak contained 86 % of the 2t-6c isomer and in the latter half the 2c-6t isomer was enriched up to 71 %, which was detected by gas chromatography (Fig. 3b).

The sample size was increased from 120 mg to 200, 400 and 600 mg in 1 ml. With a 200-mg injection the separation was almost the same as with a sample size of 120 mg. With further increases in sample size each peak became broader. By removing a portion of the first and the last peak several times in the course of recycling, which is called the "shaving" method, almost pure 2c-6c and 2t-6t fractions and a mixture of 2t-6c and 2c-6t isomers were collected after eight or nine recyclings (Fig. 4).

The second fraction obtained by fractionation with methanol as the eluent, which contained 2c-6t and 2t-6c isomers, was separated into almost pure isomers with cyclohexane as the eluent after eight recyclings, as shown in Fig. 5.

The purities of the four fractions obtained above were shown by gas chromatography to be more than 98 %. Thus, by combination of the two eluents, methanol and cyclohexane, synthetic farnesol was separated into four almost pure isomers.

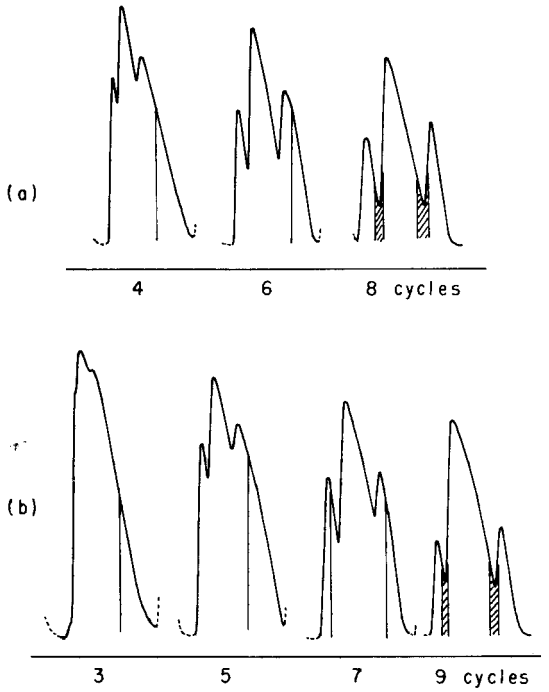

Fig. 4. Preparative-scale fractionation of farnesol isomers using methanol as eluent with sample sizes of (a) 400 mg and (b) 600 mg.

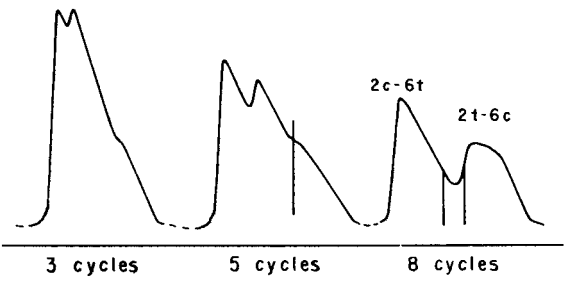

Fig. 5. Separation of the 2c-6t and 2t-6c isomers with cyclohexane as eluent with a sample size of 450 mg.

REFERENCES

1 M. Windholz, *The Merck Index*, Merck, Rahway, NJ, 9th ed., 1976, p. 516.
2 R. B. Bates, D. M. Gale, B. J. Gruner and P. P. Nicholas, *Chem. Ind. (London)*, (1961) 1907.
3 M. J. Pettei, F. G. Pilkiewicz and K. Nakanishi, *Tetrahedron Lett.*, (1977) 2083.
4 Y. Tanaka, J. Takeda and K. Noguchi, *Jap. Pat.*, 48211 (1980); *C.A.*, 93 (1980) 27444e.
5 D. L. Saunders, in E. Heftmann (Editor), *Chromatography*, Van Nostrand-Reinhold, Princeton, NJ, 3rd ed., 1975, p. 96.
6 H. Sato, K. Saito, K. Miyashita and Y. Tanaka, *Makromol. Chem.*, 182 (1981) 2259.

Journal of Chromatography, 237 (1982) 183
Elsevier Scientific Publishing Company, Amsterdam — Printed in The Netherlands

CHROM. 14,435

Book Review

Two biographies:

Maria Skłodowska-Curie und ihre Familie, by O. Wołczek, BSB B.G. Teubner Verlagsgesellschaft, Sternwartenstrasse 8, DDR-701 Leipzig, 3rd ed., 1980, 136 pp., 28 figs., price M 6.50, VLN 294-375/38/80. LSV 1108;

and

Otto Warburg, cell physiologist, biochemist and eccentric, by H. Krebs (translated by H. Krebs and A. Martin) Clarendon Press (Oxford University Press), Oxford, 141 pp., 22 figs., ISBN 0-19-858171-8.

To write a book on Madame Curie should be relatively easy as both she and her daughter, Irène, had written accounts of the lives of Pierre Curie and Marie Curie, respectively. Nevertheless, the English translations of both of those books abound in errors of scientific and academic terms. The German book under review is a welcome exception to this rule. It quotes the French texts extensively, without the usual mistranslations. Two examples were noted, nevertheless: "das Tal Valleé de Chevreuse", which is rather like saying "der Wald Wienerwald", and on p. 125, "1933 gelang es im Curie-Laboratorium eine Aktiniumquelle zu erschliessen"; evidently the author misunderstood "une source d'Actinium".

A final chapter is devoted to general (mainly political) comments on nuclear energy today, which seems irrelevant. However, on the whole, the biography is readable and well illustrated (28 figs.) and can be warmly recommended. Its low price (M 6.50) should make it available to every reader.

The biography of Otto Warburg by his former student, Sir Hans Krebs, should be considered one of the important chapters of the history of biochemistry, written perhaps by the only living person capable of telling it correctly.

It is not only a biography but also a scientifically written treatise complete with references and an annotated list of "people mentioned in the book", as well as a list of publications by Otto Warburg and his collaborators.

The actual text is only 83 pp. long and it is impressive how much information it imparts and how clearly it is written. This book is a must for every biochemist.

M. LEDERER

Journal of Chromatography, 237 (1982) 184
Elsevier Scientific Publishing Company, Amsterdam — Printed in The Netherlands

CHROM. 14,438

Book Review

Gmelin Handbook of inorganic chemistry: Sc, Y, La–Lu —Rare earth elements, Part D3, Coordination compounds, by E. R. Birnbaum, J. H. Forsberg and Y. Marcus, Springer, Berlin, Heidelberg, New York, 8th ed., 1979, XIV + 324 pp., price DM 793.00, *ca.* US$ 467.90, system No. 39, ISBN 3-540-93432-4 (Berlin, Heidelberg), 0-387-93432-4 (New York).

This volume should be of considerable interest to chromatographers as it surveys complexes that can be used for both liquid and gas chromatography.

There is a short chapter by Y. Marcus on complexes with water, quoting 109 references, followed by chapters on compounds with alcohols, aromatic hydroxy compounds, aldehydes and monoketones (50 papers).

The longest chapter deals, of course, with compounds with 1,3-diketones (by J. H. Forsberg), giving a wealth of physico-chemical data, but mentioning chromatography only briefly.

The last chapters deal with quinones (mainly triphenylmethane dyes, etc.), ethers (including crown ethers), pyranone derivatives (kojic acid!), coumarin, hydroxyflavones and hematein.

The great quality of this volume is the breadth of its treatment of the compounds; unfortunately, much of it is not critical and it is left to the reader to assess the relevance of the published information.

Lausanne (Switzerland) M. JANOVSKY

PUBLICATION SCHEDULE FOR 1982

Journal of Chromatography (incorporating *Chromatographic Reviews*) and *Journal of Chromatography, Biomedical Applications*

MONTH		J	F	M	A	M	J	J	A	S	O	N	D
Journal of Chromatography		234/1 234/2 235/1 235/2	236/1 236/2	237/1 237/2 237/3	238/1 238/2 239	240/1 240/2 241/1	The publication schedule for further issues will be published later.						
Chromatographic Reviews			251/1		251/2								
Biomedical Applications		227/1	227/2	228	229/1	229/2							

INFORMATION FOR AUTHORS

(Detailed *Instructions to Authors* were published in Vol. 209, No. 3, pp. 501–504. A free reprint can be obtained by application to the publisher.)

Types of Contributions. The following types of papers are published in the *Journal of Chromatography* and the section on *Biomedical Applications:* Regular research papers (Full-length papers), Short communications and Notes. Short communications are preliminary announcements of important new developments and will, whenever possible, be published with maximum speed. Notes are usually descriptions of short investigations and reflect the same quality of research as Full-length papers, but should preferably not exceed four printed pages. For reviews, see page 2 of cover under Submission of Papers.

Submission. Every paper must be accompanied by a letter from the senior author, stating that he is submitting the paper for publication in the *Journal of Chromatography*. Please do not send a letter signed by the director of the institute or the professor unless he is one of the authors.

Manuscripts. Manuscripts should be typed in double spacing on consecutively numbered pages of uniform size. The manuscript should be preceded by a sheet of manuscript paper carrying the title of the paper and the name and full postal address of the person to whom the proofs are to be sent. Authors of papers in French or German are requested to supply an English translation of the title of the paper. As a rule, papers should be divided into sections, headed by a caption (e.g., Summary, Introduction, Experimental, Results, Discussion, etc.). All illustrations, photographs, tables, etc., should be on separate sheets.

Introduction. Every paper must have a concise introduction mentioning what has been done before on the topic described, and stating clearly what is new in the paper now submitted.

Summary. Full-length papers and Review articles should have a summary of 50–100 words which clearly and briefly indicates what is new, different and significant. In the case of French or German articles an additional summary in English, headed by an English translation of the title, should also be provided. (Short communications and Notes are published without a summary.)

Illustrations. The figures should be submitted in a form suitable for reproduction, drawn in Indian ink on drawing or tracing paper. Each illustration should have a legend, all the *legends* being typed (with double spacing) together on a *separate sheet*. If structures are given in the text, the original drawings should be supplied. Coloured illustrations are reproduced at the author's expense, the cost being determined by the number of pages and by the number of colours needed. The written permission of the author and publisher must be obtained for the use of any figure already published. Its source must be indicated in the legend.

References. References should be numbered in the order in which they are cited in the text, and listed in numerical sequence on a separate sheet at the end of the article. Please check a recent issue for the lay-out of the reference list. Abbreviations for the titles of journals should follow the system used by *Chemical Abstracts*. Articles not yet published should be given as "in press", "submitted for publication", "in preparation" or "personal communication".

Proofs. One set of proofs will be sent to the author to be carefully checked for printer's errors. Corrections must be restricted to instances in which the proof is at variance with the manuscript. "Extra corrections" will be inserted at the author's expense.

Reprints. Fifty reprints of Full-length papers, Short communications and Notes will be supplied free of charge. Additional reprints can be ordered by the authors. An order form containing price quotations will be sent to the authors together with the proofs of their article.

News. News releases of new products and developments, and information leaflets of meetings should be addressed to: The Editor of the News Section, Journal of Chromatography/Journal of Chromatography, Biomedical Applications, Elsevier Scientific Publishing Company, P.O. Box 330, 1000 AH Amsterdam, The Netherlands.

Advertisements. Advertisement rates are available from the publisher on request. The Editors of the journal accept no responsibility for the contents of the advertisements.

from ELSEVIER your partner in successful CHEMICAL ANALYSIS

Structural Analysis of Organic Compounds
by Combined Application of Spectroscopic Methods

J. T. Clerc, E. Pretsch and J. Seibl, Zürich, Switzerland.

Studies in Analytical Chemistry, 1

Spectroscopic methods have certainly captured the lion's share of organic analysis with at least one such method in current use in all chemical laboratories. Now at last a concise and logically structured reference work details how their combined application substantially increases overall effectiveness. By giving examples which demonstrate different methods of approach and reasoning, and supplementing these with comments and hints on previously neglected analytical aspects, the authors have produced a work to cover the widest possible variety of chemical structures and spectroscopic capabilities.

1981 280 pages
0-444-99748-2
US $66.00/Dfl. 135.00

Evaluation and Optimization of Laboratory Methods and Analytical Procedures

D. L. Massart, L. Kaufman and A. Dijkstra

Techniques and Instrumentation in Analytical Chemistry, 1

Acclaimed as ... "a valuable addition to the analytical literature" by *Analytical Chemistry*, "a comprehensive and practical handbook... all aspects of optimization are discussed" by *Laboratory Equipment* and "... a real aid to postgraduate students following taught courses" by *Chromatographia*. The authors provide in a single volume, a discussion of all aspects of optimization from the simple evaluation of procedures to the organization of laboratories and the selection of optimal complex analytical programmes. No laboratory or library can afford to be without this book.

1978. 1st reprint 1980
612 pages 0-444-41743-5
US $68.25/Dfl. 140.00

Chemical Derivatization in Gas Chromatography

J. Drozd, Brno, Czechoslovakia.

Journal of Chromatography Library, 19.

The novice will find here explanatory coverage of the entire range of problems, will become acquainted with all types of derivatives and methods, and will be able to apply the information without recourse to original sources. For proficient workers it will be a valuable information source, a guide to the most recent research results and an indication of future trends.

1981 244 pages
0-444-41917-9
US $58.50/Dfl. 120.00

Analytical Isotachophoresis

Proceedings of the 2nd International Symposium on Isotachophoresis, Eindhoven, September 9-11, 1980.

F. M. Everaerts, Eindhoven The Netherlands (Editor).

Analytical Chemistry Symposia Series, 6

"A new twig on the tree of differential separation methods": Thus has isotachophoresis been described. It is proving a valuable technique in clinical (bio)chemistry, pharmacy, physical and inorganic chemistry, as well as in the industrial and environmental field.

Theoretical and practical aspects of the method, new developments in isotachophoretic equipment and applications are presented clearly.

1981 246 pages
0-444-41957-8
US $58.50/Dfl. 120.00

Send your order with your payment to one of the addresses below and receive the book(s) ordered postfree.
For further details on these titles and our Spring list of analytical chemistry publications check number 3 on the reader enquiry card.

ELSEVIER

P.O. Box 211
1000 AE Amsterdam
The Netherlands

52 Vanderbilt Ave
New York, N.Y. 10017
U.S.A.